

**Synthesis and biophysical studies of 2'-5'*iso*DNA
analogues locked in N-type or S-type sugar ring
conformations**

**THESIS SUBMITTED TO
THE UNIVERSITY OF PUNE FOR THE DEGREE OF**

DOCTOR OF PHILOSOPHY

**IN
CHEMISTRY**

BY

Mrs. ANITA D. GUNJAL

RESEARCH SUPERVISOR

Dr. VAIJAYANTI A. KUMAR

**DIVISION OF ORGANIC CHEMISTRY
NATIONAL CHEMICAL LABORATORY**

PUNE 411008

SEPTEMBER 2013



सीएसआयआर-राष्ट्रीय रासायनिक प्रयोगशाला

(वैज्ञानिक तथा औद्योगिक अनुसंधान परिषद)

डॉ. होमी भाभा मार्ग, पुणे - 411 008. भारत

CSIR-NATIONAL CHEMICAL LABORATORY

(Council of Scientific & Industrial Research)

Dr. Homi Bhabha Road, Pune - 411008. India



CERTIFICATE

This is to certify that the work presented in the thesis entitled “ **Synthesis and biophysical studies of 2'-5'isoDNA analogues locked in N-type or S-type sugar ring conformations**” submitted by Mrs. Anita D. Gunjal was carried out by the candidate at the National Chemical Laboratory Pune, under my supervision. Such materials as obtained from other sources have been duly acknowledged in the thesis.

Dr. Vaijayanti A. Kumar

September 2013


(Research Supervisor)

Division of Organic Chemistry

National Chemical Laboratory

Pune 411008.

Communication Channels


NCL Level DID : 2590
NCL Board No. : +91-20-25902000
EPABX : +91-20-25893300
: +91-20-25893400

FAX

Director's Office : +91-20-25902601
COA's Office : +91-20-25902660
COS&P's Office : +91-20-25902664

WEBSITE

www.ncl-india.org

CANDIDATE'S DECLARATION

I hereby declare that the thesis entitled “ **Synthesis and biophysical studies of 2'-5'isoDNA analogues locked in N-type or S-type sugar ring conformations**” submitted for the award of the degree of *Doctor of Philosophy* in Chemistry to the University of Pune has not been submitted by me to any other University or Institution . This work was carried out by me at the National Chemical Laboratory, Pune, India. Such materials as obtained from other sources have been duly acknowledged in the thesis.



Mrs. Anita D. Gunjal

September 2013

National Chemical Laboratory

Pune 411008.

*Dedicated to
my beloved mother, my guru
forever*





Reflections

*“ I have no sense of success
on any large scale in things achieved
but have the sense of having worked
and of having found happiness in doing so.”*

Sir P. C. Ray

Acknowledgements

I sincerely thank my research supervisor, Dr. Vaijayanti Kumar for her patient guidance, enthusiastic encouragement and valuable and constructive suggestions during the planning and development of this research project. Her confidence and positive approach has been the source of my energy to step ahead and achieve my research goal in the form of this thesis. I also wish to thank her for giving me this great opportunity and guiding me into this wonderful area of research in Organic Biomolecular Chemistry.

I also offer my thanks to Dr. Moneesha Fernandes for her encouragement, valuable suggestions and unconditional support. She has been with me through every phase of this research and has made an enormous contribution towards the completion of this thesis.

I deeply appreciate and thank Dr. Seema Bagmare for her meticulous and constant help throughout the course of this work,

My special thanks to Namrata Erande for her efforts and unceasing co-operation in helping me in all possible ways during the course of this work,

I wish to especially thank Mrs. Meena Mane for helping me in the HPLC and LCMS data required for this work,

I acknowledge and thank all the MALDI –TOF mass group and the NMR facility especially Dr. Rajamohanan for the NMR experiments done by him.

All the research fellows in my lab: Namrata, Kiran, Venu, Manoj, Anjan, Tanaya, Amit, Govind deserve a special word of thanks for all their help and support. I am also grateful to them for always making my work atmosphere lively and vibrant.

I wish to acknowledge and thank specially Dr. Vandana Pore, for her continuous backing and help rendered during the course of this work,

I also appreciate and acknowledge the encouragement and support given by Dr Anil Kumar during the course of this research work,

A special thanks to Dr. Dinesh Kamath for making the Dedication and Reflections images realistic and beautiful.

All my friends and colleagues (present and past) at NCL have always encouraged me, which has definitely helped me in the completion of this thesis. My wholehearted thanks to you all for your best wishes.

I owe a lot to my mother, Mrs Pratibha Jadhav nee Indira Bagwe, my father, Mr. L.V.Jadhav, my sisters Monali and Ela who encouraged and helped me at every stage of my personal and academic life, and longed to see this achievement come true. I deeply miss my mother, who has always been an eternal source of inspiration, is no longer with me to share this joy.

I owe my deepest gratitude to my family, my husband Dr. Dinkar who has given me a strong support, his encouragement and patience has given me the strength to accomplish this goal. My son, Indraneel made me venture into this doctoral degree project. I thank him for making my dream come true.

I wish to thank all the Gunjal family members for their encouragement, appreciation and well wishes for the completion of my Ph.D thesis.

Finally, I wish to thank Dr. Sourav Pal, Director, National Chemical Laboratory, for encouraging me and giving me permission to work for my Doctoral degree.

Anita Gunjal

Contents

Publication /Symposia	i
Abbreviations	ii
Abstract	vi

Chapter 1

1	Introduction: Nucleic acids in therapeutics	
1.1	Introduction	1
1.2	Nucleic Acid structure	2
1.2.1	Basic structure of DNA/RNA	2
1.2.2	H-bonding patterns- Watson-Crick and Hoogsteen	3
1.2.3	Higher order structures-duplex, triplex, quadruplex	3
1.3	<i>Iso</i> Nucleic Acids	4
1.4	Sugar ring conformations in 3'5' Vs 2'5' linked oligomers	6
1.4.1	Pseudorotation cycle, north type, south type, RNA, DNA.	7
1.4.2	Stereoelectronic effects and the ribo/deoxyribofuranose conformation	9
1.4.3	Base-stacking	10
1.4.4	Steric effects	11
1.4.5	The double helix conformations	11
1.5	Conformational restriction/ pre-organization	12
1.6	Antisense approach	13
1.6.1	Antisense mechanism	14
1.6.2	Antisense Oligonucleotides	15
1.7	Quadruplex-forming DNA and applications in therapeutics	17
1.7.1	Quadruplex DNA-the beginning	17
1.7.2	Types of quadruplex structures	18
1.7.3	Structural polymorphism in G-quadruplexes	20
1.7.4	Influence of sugar, base conformations on the topology and stability of G-quadruplexes	21
1.7.5	The G-quadruplex in aptamers	22
1.7.6	Thrombin-binding aptamer	23
1.8	Tools and techniques for structural studies of nucleic acid complexes, and higher ordered G-quadruplexes	24
1.8.1	UV-spectroscopy	24
1.8.2	Circular Dichroism (CD)	26

1.8.3	Stoichiometry of binding	27
1.8.4	Fluorescence spectroscopy	28
1.8.5	Polyacrylamide gel electrophoresis (PAGE)	28
1.8.6	Nuclear Magnetic Resonance (NMR)	29
1.8.7	MALDI TOF Mass Spectroscopy	29
1.8.8	HPLC	30
1.9	Present work	30
1.10	References	32

Chapter 2

2	Conformationally locked <i>iso</i>DNA	40
	Section A: Synthesis, characterization and conformational analysis of N-type and S-type locked monomer building blocks	41
2.1	Introduction to present work	41
2.1.1	2'-5'-linked <i>iso</i> DNA /RNA and relevant conformational restriction	41
2.1.2	Unmodified single stranded <i>iso</i> RNA/ <i>iso</i> DNA and <i>iso</i> RNA/ <i>iso</i> DNA:RNA duplexes	42
2.2	Present work	44
2.2.1	Synthesis of N-type locked monomer	45
2.2.2	Synthesis of S-type locked monomer	47
2.2.3	Conformational analysis of the nucleoside analogues	48
	Section B :Synthesis, characterization and biophysical studies of the 2'-5'- linked <i>iso</i>DNA and modified <i>iso</i>DNA and their stability towards snake venom phosphodiesterase	51
2.3	Solid Phase oligonucleotide synthesis using the phosphoramidite chemistry	51
2.4	Synthesis, purification and characterization of modified <i>iso</i> DNA sequences	53
2.5	UV melting studies of the modified <i>iso</i> DNA sequences	57
2.6	CD spectroscopy of the duplexes	61
2.7	Stability of the modified and unmodified 2'-5'-linked oligonucleotides towards snake venom phosphodiesterase (SVPD)	61
2.8	Summary	63
2.9	Conclusion	63
2.10	Experimental	64
2.10.1	Synthesis of compounds/monomers	65
2.10.2	Synthesis of buffers	77

2.10.3	Synthesis of oligonucleotides	78
2.10.4	Purification and characterization	78
2.10.5	Biophysical techniques	79
2.11	Appendix	81
2.12	References	104

Chapter 3

3	Synthesis, characterization and biophysical studies of 2'-<i>O</i>-allyl/ 3'-<i>O</i>-allyl derived DNA and <i>iso</i>DNA oligonucleotides	107
	Section A: Synthesis of 2'-<i>O</i>-allyl/3'-<i>O</i>-allyluridine monomers and conversion of 2'-<i>O</i>-allyl/3'-<i>O</i>-allyluridine derivatives to the respective cytidine monomers	108
3.1	Introduction to present work	108
3.1.1	Present work	110
3.1.2	Synthesis of 2'- <i>O</i> -allyl and 3'- <i>O</i> -allyl-uridine monomers	111
3.1.3	Conversion of the 2'- <i>O</i> -allyl and 3'- <i>O</i> -allyluridine to the respective cytidine monomers	111
3.1.4	2'- <i>O</i> -allyl and the 3'- <i>O</i> -allyl isomers differentiation using ¹³ C NMR	113
	Section B: Synthesis of 2'-<i>O</i>-allyl and 3'-<i>O</i>-allyl modified DNA and <i>iso</i>DNA sequences and their biophysical study	114
3.2	Synthesis, purification and characterization of modified DNA and <i>iso</i> DNA sequences	114
3.3	A comparative study of the thermal stability of modified 2'-5' DNA:RNA duplexes and the modified 3'-5' DNA:DNA, DNA:RNA duplexes by UV melting experiments	118
3.3.1	Thermal stability of 2'- <i>O</i> -allyluridine modified sequences	118
3.3.2	Thermal stability of 2'- <i>O</i> -allylcytidine modified sequences	120
3.3.3	Thermal stability of 3'- <i>O</i> -allyluridine modified sequences	123
3.3.4	Thermal stability of 3'- <i>O</i> -allylcytidine modified sequences	125
3.3.5	Summary	126
3.3.6	Conclusions	127
3.4	Experimental	127
3.4.1	Synthesis of compounds/monomers	128
3.4.2	Synthesis of buffers	137
3.4.3	Synthesis of oligonucleotides	137
3.4.4	Purification and characterization	138
3.4.5	Biophysical techniques	139

3.5	Appendix	140
3.6	References	166

Chapter 4

4	2'-5'-linked thrombin binding aptamer (<i>iso</i>TBA), its quadruplex formation, and application as a thrombin inhibitor	169
4.1	Introduction to present work	170
4.1.1	G-quadruplex formation, structure and topology	170
4.1.2	Quadruplex stability dependence on metal ions	172
4.1.3	Molecular crowding conditions	172
4.1.4	Aptamers or Decoy oligonucleotides: An emerging class of therapeutics	174
4.1.5	Spiegelmers	175
4.1.6	Thrombin-binding aptamer-TBA: Discovery, structural features, function, modifications with effect on structure and function	176
4.1.6.1	Modifications in TBA	177
4.2	Present Work	180
4.2.1	Chemical synthesis of a 2'-5'-linked, non-genetic, regioisomeric thrombin binding aptamer (<i>iso</i> TBA) and a modified <i>iso</i> TBA	182
4.2.2	G-tetraplex formation in the presence of monovalent cations using CD, UV and fluorescence spectroscopy	183
4.2.3	Thermal Difference Spectra (TDS)	186
4.2.4	Molecular crowding effects on TBA-1 and <i>iso</i> TBA-2	187
4.2.5	Imino proton NMR spectra of TBA-1 and <i>iso</i> TBA-2.	188
4.2.6	G-tetraplex formation in the presence of thrombin without added monovalent cations	189
4.2.7	Anti-thrombin activity measurements	191
4.2.8	Stability of aptamers to SVPD	193
4.2.9	Non-denaturing Gel electrophoresis study	194
4.2.10	Summary	195
4.2.11	Conclusion	196
4.3	Experimental	196
4.4	Appendix	201
4.5	References	204

List of Research Publications:

1. Probing the furanose conformation in the 2'-5' strand of isoDNA:RNA duplexes by freezing the nucleoside conformations. Namrata Erande, **Anita D. Gunjal**, Moneesha Fernandes and Vaijayanti A. Kumar* *Chem. Commun.*, 2011, 47, 4007–4009.
2. Synthesis and structural studies of S-type/N-type locked/ frozen nucleoside analogues and their incorporation in RNA-selective, nuclease resistant 2'-5' linked oligonucleotides. Namrata Erande, **Anita D. Gunjal**, Moneesha Fernandes, Rajesh Gonnade and Vaijayanti A. Kumar* *Org. Biomol. Chem.*, 2013, 11, 746.
3. Introduction of S/N-type frozen 3'-fluorinated nucleoside in to nongenetic nucleic acid enhance the duplex stability as well as resistance to exonuclease. Namrata Erande, **Anita D. Gunjal**, Moneesha Fernandes and Vaijayanti A. Kumar* (manuscript under preparation).
4. Synthesis, characterization and biophysical studies of 2'-O-allyl/ 3'-O-allyl derived DNA and isoDNA oligonucleotides. **Anita D. Gunjal** and Vaijayanti A. Kumar* (manuscript under preparation).
5. A non-genetic 2'-5'-linked isoDNA folds into unimolecular G-quadruplex and retains molecular recognition properties of the 3'-5'-linked genetic congener. **Anita D. Gunjal**, Moneesha Fernandes, Namrata D. Erande, P. R. Rajamohan and Vaijayanti A. Kumar* (submitted for publication)

Symposia Attended/Poster/Oral Presentations:

1. Attended 4th INSA-KOSEF Symposium in Organic Chemistry. Contemporary Organic Chemistry and its future directions. National Chemical Laboratory, Pune India, January 12-13, 2009.
2. Attended 11th CRSI National Symposium in Chemistry. National Chemical Laboratory, Pune India, February 5-8, 2009.
3. National Science Day, NCL Research Foundation, National chemical Laboratory, Pune. February 28, 2010. Poster Presentation on "Preferred S-type sugar conformation in 2'-5'-isoDNA:RNA duplexes" Namrata Erande, **Anita Gunjal**, Moneesha D'Costa and Vaijayanti A. Kumar.
4. National Science Day, NCL Research Foundation, National chemical Laboratory, Pune. February 24-25, 2013. Poster Presentation on "Comparative Conformational Analysis of Nucleosides by NMR, X-ray, and MATLAB Pseudorotation GUI Program" Namrata Erande, **Anita D. Gunjal**, Moneesha Fernandes, Rajesh Gonnade and Vaijayanti A. Kumar*
5. Attended International Meeting on Chemical Biology. The 60th Anniversary of DNA Double Helix. Indian Institute of Science Education and Research (IISER) Pune. May 26-28, 2013.

ABBREVIATIONS

A	Absorbance
A	Adenine
Å	Angstrom
Ac	Acetate
ADA	Allose-diacetonide
Ac ₂ O	Acetic anhydride
ACN	Acetonitrile
AcOH	Acetic acid
ap	Antiparallel
aq.	Aqueous
BNA	Bridged Nucleic Acid
Bz	Benzoyl
BSA	N,O-Bis(trimethylsilyl)acetamide
C	Cytidine
C	Cytosine
Calcd.	Calculated
Cat.	Catalytic/catalyst
CD	Circular Dichroism
Conc.	Concentrated
CPG	Controlled pore glass
COSY	Correlation spectroscopy
DBTO	Dibutyltin oxide
DCA	Dichloroacetic acid
DCM	Dichloromethane
DEPT	Distortionless Enhancement by Polarization Transfer
DMT-Chloride	4,4'-Dimethoxytritylchloride
DIPEA/DIEA	Diisopropylethylamine

DMAP	4',4'-Dimethylaminopyridine
DMF	<i>N,N</i> -dimethylformamide
DMSO	<i>N,N</i> -Dimethyl sulfoxide
DNA	2'-deoxyribonucleic acid
ds	double stranded DNA
DI	Deionized
EDTA	Ethylenediaminetetraacetic acid
EtOH	Ethanol
EtOAc	Ethyl acetate
ENA	Ethylene bridged Nucleic Acid
US-FDA	United States-Food and Drug Administration
GDA	Glucose-diacetonide.
g	gram
G	Guanine
h	Hours
HIV	Human Immunodeficiency Virus
HPLC	High Performance Liquid Chromatography
HRMS	High Resolution Mass Spectrometry
Hz	Hertz
HSQC-COSY	Heteronuclear single-quantum correlation spectroscopy
IBX	2-iodoxybenzoic acid
IGF-II	Insulin- like growth factor 2
IR	Infra red
L	litre
LC-MS	Liquid Chromatography-Mass Spectrometry
LNA	Locked Nucleic Acids
MeOH	Methanol
MALDI-TOF	Matrix Assisted Laser Desorption Ionisation-Time of Flight

MF	Molecular formula
mg	milligram
MHz	MegaHertz
min	minutes
M	Mole
μL	Microliter
μM	Micromolar
mL	milliliter
mM	millimolar
mmol	millimoles
MS	Mass spectrometry
MW	Molecular weight
N	Normal
N-type	North-type
nm	Nanometer
NMR	Nuclear Magnetic Resonance
NOE/NOESY	Nuclear Overhauser Effect(Spectroscopy)
Obsd.	Observed
PAGE	Polyacrylamide gel electrophoresis
ppm	Parts per million
PO-oligo	Phosphodiester-oligo
PS-oligo	Phosphorothioate-oligo
Py	Pyridine
PNA	Peptide Nucleic Acid
Pet-ether	Petroleum ether
RNA	Ribose Nucleic Acid
RNase H	Ribonuclease H
RNase L	Ribonuclease L

R _f	Retention factor
RP-HPLC	Reversed Phase-HPLC
rt	Room temperature
s	second
SELEX	S ystematic <i>E</i> volution of <i>L</i> igands by <i>E</i> xponential Enrichment
S-type	South-type
ss	single stranded DNA
STAT3	Signal transducer & activator of transcription3
SVPD	Snake venom phosphodiesterase
T	Thymine
T	Thymidine
TBA	Thrombin binding aptamer
TBAB	Tetrabutylammonium bromide
Tc-DNA	Tricyclo-DNA
TINA	Twisted intercalating nucleic acids
t _R	Retention time (HPLC)
TMSOTf	Trimethylsilyltrifluoromethanesulfonate
TEAA	Triethyl ammonium acetate
TEA/Et ₃ N	Triethylamine
TFA	Trifluoroacetic acid
THAP	2', 4', 6'-trihydroxyacetophenone
THF	Tetrahydrofuran
TLC	Thin layer chromatography
T _m	Melting temperature
TOCSY	Total Correlation Spectroscopy
U	Uracil
U	Uridine
UV-Vis	Ultraviolet-Visible

Abstract

The Thesis Title: “**Synthesis and biophysical studies of 2’-5’*iso*DNA analogues locked in N-type or S-type sugar ring conformations**”

Chapter 1: **Introduction: Nucleic acids in therapeutics**

Chapter 2 : **Conformationally locked *iso*DNA**

Section A: Synthesis, characterization and conformational analysis of the N-type and S- type locked monomer building blocks

Section B: Synthesis, characterization and biophysical studies of the 2’-5’- linked *iso*DNA, modified *iso*DNA and their stability towards snake venom phosphodiesterase

Chapter 3: **Synthesis, characterization and biophysical studies of 2’-*O*-allyl/ 3’-*O*-allyl derived DNA and *iso*DNA oligonucleotides**

Section A: Synthesis of 2’-*O*-allyl / 3’-*O*-allyl uridine monomers and conversion of 2’-*O*-allyl / 3’-*O*-allyl-uridine derivatives to the respective cytidine monomers

Section B: Synthesis of 2’-*O*-allyl / 3’-*O*-allyl modified DNA and *iso*DNA sequences and their biophysical study

Chapter 4: **2’-5’-linked thrombin binding aptamer (*iso*TBA), its quadruplex formation, and application as a thrombin inhibitor**

Chapter 1: Introduction: Nucleic acids in therapeutics

The recent past has witnessed intense research in the field of antisense technology, owing mainly to the discovery of naturally-existing antisense-based regulatory mechanisms, such as the RNA interference (RNAi), induced by short interfering RNA (siRNA) or micro RNA (miRNA). A second antisense drug (ASO), Mipovirsen from ISIS pharmaceuticals, by the US FDA, was also approved recently. The target-specific hybridization *via* Watson-Crick hydrogen-bonding of complementary nucleobase sequence and regulation of target gene expression is the basis of antisense therapy. The inherent drawbacks of natural DNA or RNA oligonucleotides (ONs), *viz.*, cellular delivery and short half-life limit their *in vivo* application. This has in turn, spawned a large area of research in the field of chemical modifications of nucleosides, nucleotides and their derivatives. This chapter briefly reviews the important developments for chemical modifications of these agents, directed towards improving RNA-specific selectivity, cellular delivery and stability

in biological systems. Exclusive RNA binding features of 2'-5'- linked *iso*DNA/RNA are presented in this chapter from the literature. The sugar ring conformations and their correlation with 3'-5' DNA *versus* 2'-5' *iso*DNA linked oligomers with respect to this feature are discussed. The recently discovered and biologically important quadruplex forming ONs are reviewed describing their important applications in therapeutics.

Chapter 2: Conformationally locked *iso*DNA

The 2'-5' linked ONs are a unique class of oligonucleotides for therapeutic applications because, (1) They exhibit a remarkable preference for duplex formation with complementary 3'-5'-linked natural RNA, (2) These hetero duplexes are less stable than the normal 3'-5'-linked RNA:RNA duplexes allowing exploration of chemical modifications, (3) The 2'-5'-linked nucleic acids show high resistance to nuclease digestion.

Section A: Synthesis, characterization and conformational analysis of N-type and S-type locked monomer building blocks

We planned the synthesis of conformationally locked nucleosides and their incorporation in 3'-deoxy-2'-5'-ONs (*iso*DNA) in order to improve the binding strength of these *iso*DNA ONs. As there is no conclusive experimental evidence in literature for the preferred sugar geometries in *iso*DNA strands, we selected in this work to study both nucleoside analogues that would be N-type and S-type locked.

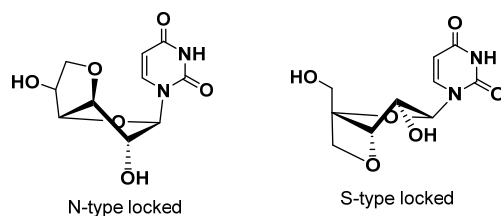
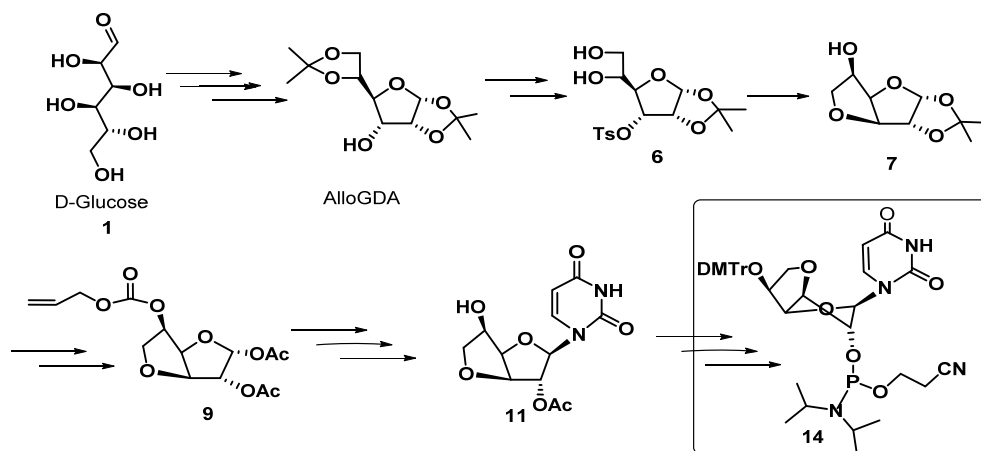


Figure 1. N-type I and S-type II locked nucleosides.

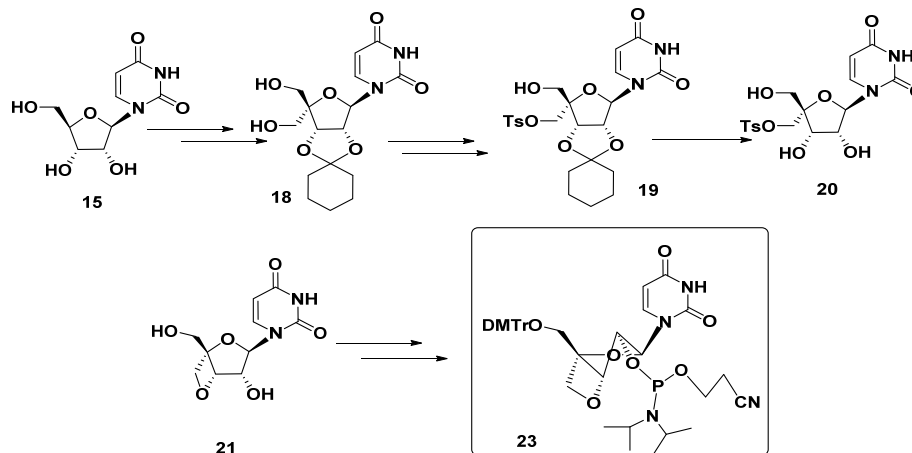
Herein, we report for the first time, a study of the effects of incorporation of these monomers in locked N-type I and S-type II sugar conformation in *iso*DNA:RNA duplexes (Figure 1). The locked N-type conformations of DNA oligomers are known to have entropic advantage while binding to RNA. By applying such locks on the *iso*DNA strand, the structural preferences of sugars in the *iso*DNA strand of the chimeric duplex could be understood and that would provide important leads to design therapeutically useful synthetic *iso*DNA.

Synthesis of N-type locked monomer: Synthesis of N-typed locked monomer is briefly outlined in Scheme 1 starting from D-Glucose indicating important intermediates.



Scheme 1. Synthesis of N-type locked monomer.

Synthesis of S-type locked monomer: Using uridine as starting material, the S-type locked amidite monomer was synthesized in 8 steps according to literature procedure (Scheme 2).



Scheme 2. Synthesis of S-type locked monomer

All the compounds were purified by column chromatography and the pure compounds were characterized using ^1H , ^{13}C , ^{31}P NMR and LCMS mass analysis.

Conformational analysis of the nucleoside analogues: The sugar conformations of 3'-deoxyuridine and the N-type/S-type locked nucleosides (Figure 2b, c **I**, **II**) were compared based on the $^3J_{\text{H1}'\text{-H2}'}$. The 3'-deoxyuridine is 97% N-type, *i.e.* C3'-*endo* sugar pucker, which is consistent with the O4'-C1'-C2'-O2' *gauche* effect as well as the anomeric effect which brings the nucleobase in pseudoaxial orientation. The xylo-3'-O-5'-C-methylene-linked uridine (U^{N} , **I** Figure 2b) and the 3'-O-4'-C-methylene-linked uridine (U^{S} , **II** Figure 2c) would lock the nucleoside in N-type and S-type conformations respectively. The 2-D NOE NMR experiments were performed to further study the orientation of nucleobase and

the 5'-OH groups. The results suggested *anti* conformation of the uracil nucleobase in either case. Two forms of sugar conformations for **I** could be possible, in which the C5'-carbon is fixed in *R* configuration as depicted in (Figure 2a). Predominantly 3'-*endo* sugar pucker (N-type) and 2'-*endo* sugar pucker (S-type) were also confirmed by these studies for compound **I** and **II**, respectively.

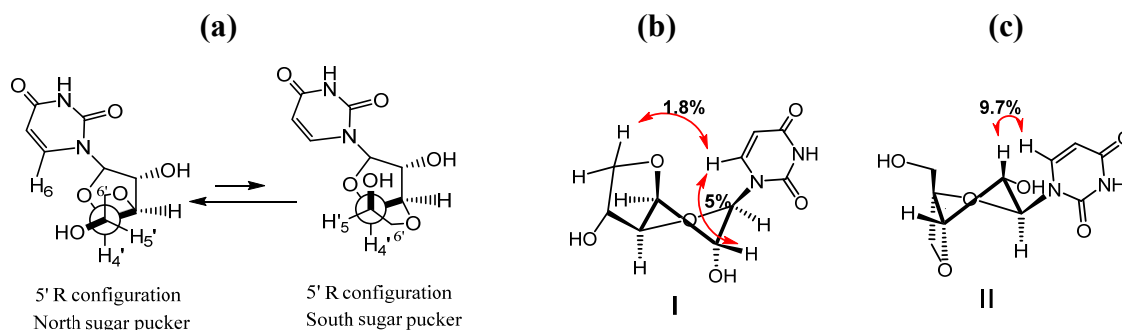


Figure 2. (a) Two possible conformers for N-type locked due to flexible 5-membered locked ring in **I**. (b) NOESY U^N **I**; (c) NOESY U^S **II**

Section B: Synthesis, characterization and biophysical studies of the 2'-5'- linked *iso*DNA, modified *iso*DNA and their enzymatic stability

Solid Phase synthesis (SPS) of isoDNA and modified isoDNA ONs using phosphoramidite chemistry, purification and characterization:

The SPS of 2'-5' *iso*DNA ONs was accomplished using universal support (Scheme 3). Commercially available universal solid support and protected 3'-deoxy phosphoramidite building blocks (Figure 3) were used for the synthesis of unmodified *iso*DNA ONs. Two 18mer sequences of biological relevance were selected. **DNA-1** is used for miRNA down-regulation and **DNA-2** is used in the splice-correction assay developed by Kole *et al.* The control, modified and complementary DNA ONs were also synthesized. All the synthesized ONs were cleaved from solid support, purified and characterized by MALDI-TOF mass analysis and used for the UV T_m experiments.

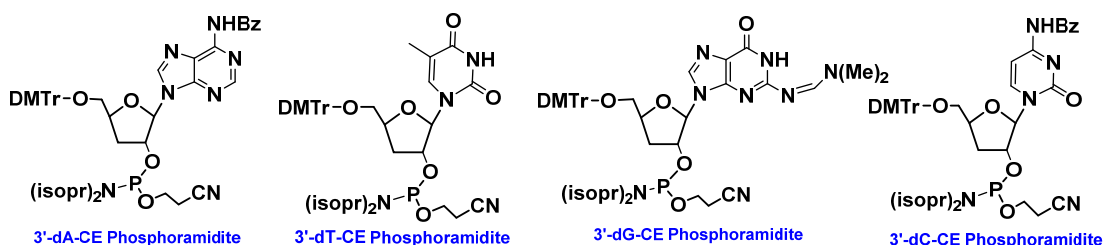
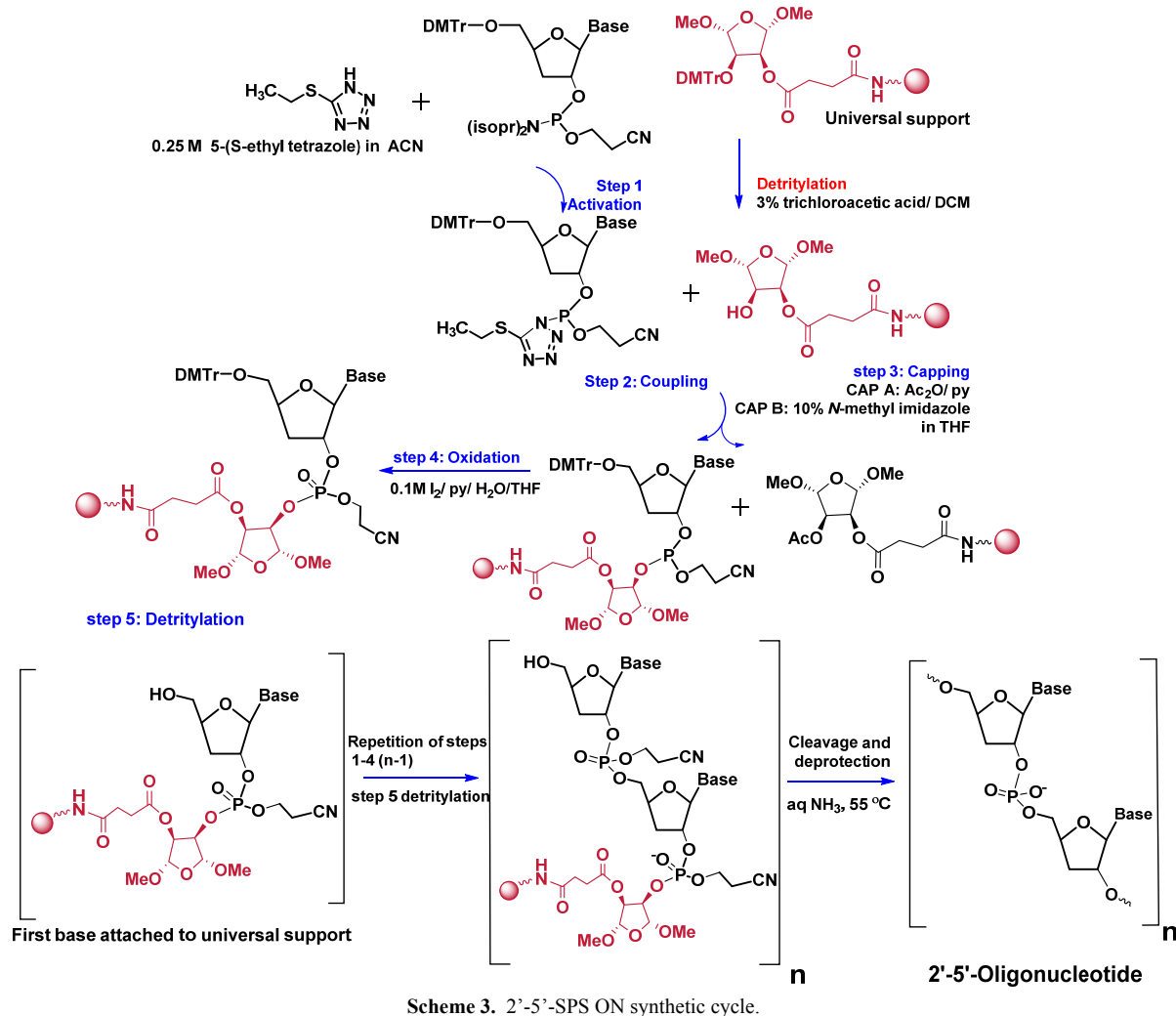


Figure 3. 3'-deoxy phosphoramidite monomers



The N-type and S-type phosphoramidite monomers (Scheme 1, **14** and Scheme 2, **23**) characterized by ^{31}P NMR were used for incorporation of modified monomer units into *iso*DNA oligonucleotides at defined positions (Table 1).

UV melting studies of the modified *iso*DNA sequences: The UV T_m determination was carried out by monitoring the absorbance at 260nm wavelength by heating the annealed samples from 10°C to 85°C. The T_m were obtained from the maxima of the first derivatives of the melting curves ($A_{260 \text{ nm}}$ versus temperature). The results obtained for the *iso*DNA:RNA complexes are summarised in Table 1. Sharp, well-defined sigmoidal melting curves were observed for the complexes with complementary RNA with a 10-20% hyperchromicity at 260 nm As seen from the entries in Table 1 and the UV T_m plots (Figure 4) for the complexes containing modified 2'DNA-1 and 2'DNA-2, the **S-type locked units** were found to favour stable duplex formation with the complementary RNA (Figure 4a).

The N-type locked units, on the other hand, caused destabilization of the complexes with RNA (Figure 4b). The *iso*DNA sequences in this study did not bind to complementary DNA, thus confirming specific binding to cRNA as earlier reported.

Table 1. Comparative UV T_m values of the N-type (U^N) and S-type (U^S) modified sequences. (ΔT_m gives the difference in T_m between the control and modified sequence). Complementary RNA oligonucleotides used: RNA-15'UGGAGUGUGACAAUGGUG3' RNA-2 5'UGUACUGAGGUAAGAGG3'

Sr. No.	Code No.	Sequence	RNA UV T_m (°C)	ΔT_m
1.	2'DNA-1	5' CACCATTGTCACACTCCA ^{2'}	50.5	0.0
2.	2'DNA-N-1s	5' CACCATTGTCACAC U^N CCA ^{2'}	49.4	-1.1
3.	2'DNA-N-1d	5' CACCATTG U^N CACAC U^N CCA ^{2'}	42.8	-7.7
4.	2'DNA-N-1t	5' CACCA U^N TG U^N CACAC U^N CCA ^{2'}	42.3	-8.3
5.	2'DNA-S-1s	5' CACCATTGTCACAC U^S CCA ^{2'}	51.0	+0.5
6.	2'DNA-S-1d	5' CACCATTG U^S CACAC U^S CCA ^{2'}	52.8	+2.3
7.	2'DNA-S-1t	5' CACCA U^S TG U^S CACAC U^S CCA ^{2'}	50.3	-0.2
8.	2'DNA-2	5' CCTCTTACCTCAGTTACA ^{2'}	46.0	0.0
9.	2'DNA-N-2s	5' CCTCTTACCTCAGT U^N ACA ^{2'}	46.4	+0.4
10.	2'DNA-N-2d	5' CCTCTTACC U^N CAGT U^N ACA ^{2'}	41.9	-4.1
11.	2'DNA-N-2t	5' CCTCT U^N ACC U^N CAGT U^N ACA ^{2'}	41.9	-4.1
12.	2'DNA-S-2s	5' CCTCTTACCTCAGT U^S ACA ^{2'}	47.0	+1.0
13.	2'DNA-S-2d	5' CCTCTTACC U^S CAGT U^S ACA ^{2'}	46.7	+0.7
14.	2'DNA-S-2t	5' CCTCT U^S ACC U^S CAGT U^S ACA ^{2'}	47.2	+1.2

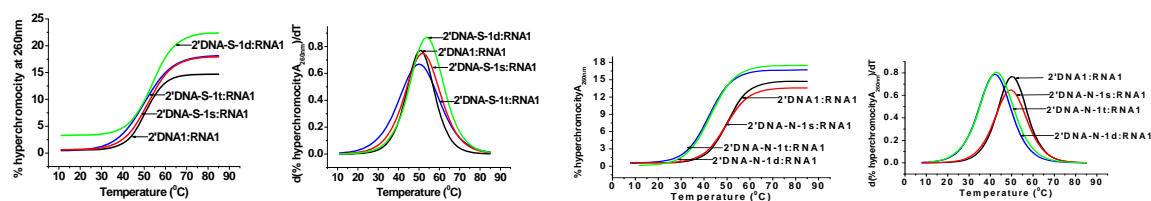


Figure 4. UV-melting plots and the respective first derivative curves of modified 2'DNA-1 (a) of the S-type locked duplexes and (b) of the N-type locked duplexes.

CD spectroscopy of the duplexes: CD spectra of the duplexes were similar for all complexes and resembled the A-type DNA:RNA duplex spectra, when compared to the CD spectrum of 3'-5'-linked DNA1:cDNA-1 duplex- B-type, although the thermal stability was affected.

Stability of the modified and unmodified 2'-5'-linked oligonucleotides towards snake venom phosphodiesterase (SVPD): The stability of unmodified and modified 2'-5'-linked oligonucleotides towards the 3'-exonuclease, snake venom phosphodiesterase (SVPD) was examined and compared with the natural DNA. The natural 3'-5'-ssDNA was completely digested within thirty minutes. The 2'-5'-linked 3'-deoxy-oligonucleotides were found to be stable under these conditions (Figure 5).

Conclusion: The results obtained provide for the first time an experimental proof that in *iso*DNA:RNA complexes, the *iso*DNA strand prefers to assume S-type geometry that is

complemented by the furanose ring locked in S-type geometry, resulting in A-type duplexes with more stability. Also, these ONs are more stable towards SVPD than the natural 3'-5'-phosphodiester linked ONs.

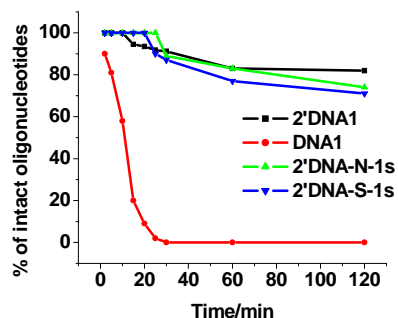


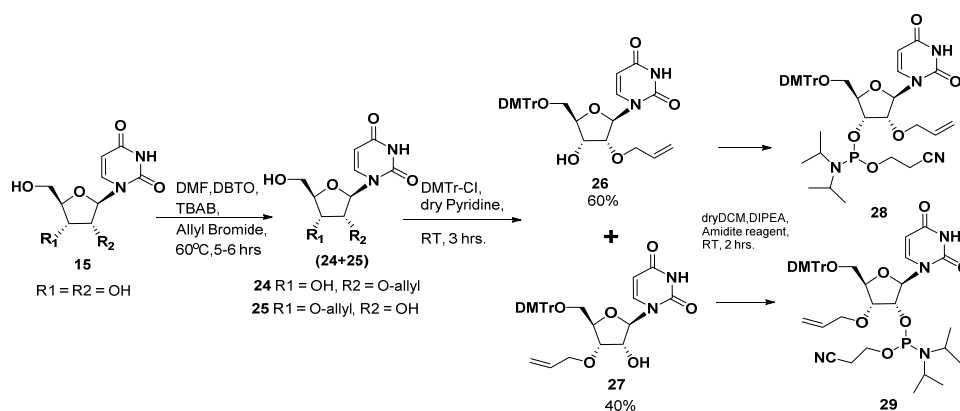
Figure 5. Stability of the 2'-5' oligonucleotides towards degradation by SVPD.

Chapter 3: Synthesis, characterization and biophysical studies of 2'-*O*-allyl/ 3'-*O*-allyl derived DNA and *iso*DNA oligonucleotides.

The encouraging literature reports of 2'-*O*-allyl oligoribonucleotides as effective ASOs and in continuation of the theme of synthesis and biophysical study of 2'-5'-linked *iso*DNA analogues, the synthesis of 2'-*O*-allyl and 3'-*O*-allylribonucleotides was undertaken.

Section A: Synthesis of 2'-*O*-allyl and 3'-*O*-allyl uridine monomers and conversion of 2'-*O*-allyl and 3'-*O*-allyl-uridine derivatives to the respective cytidine monomers.

Synthesis of 2'-*O*-allyl and 3'-*O*-allyl-uridine monomers: A short and convenient method for the synthesis of 2'-*O*-allyluridine and 3'-*O*-allyluridine phosphoramidite monomers is given in (Scheme 4).

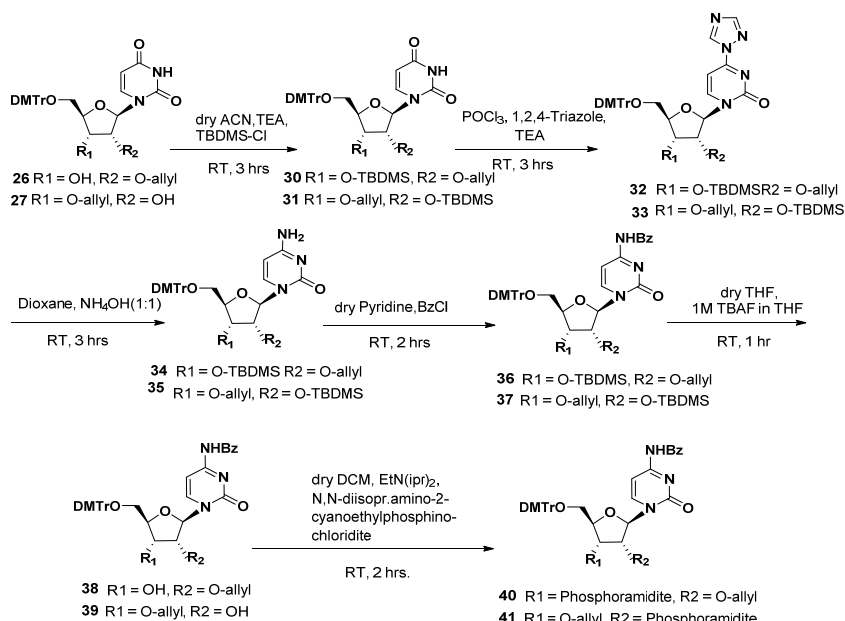


Scheme 4. Synthesis of 2'-*O*-allyl and 3'-*O*-allyl Uridine monomers

Conversion of the 2'-*O*-allyl /3'-*O*-allyluridine to the respective cytidine monomers:

The isomeric 2'-*O*-allyl/3'-*O*-allyluridine nucleosides were converted to the respective cytidine derivatives using reported procedure for conversion of uridine to cytosine. The N-

benzoyl protected cytidine isomers were then converted into their respective amidite monomers (Scheme 5). All the compounds were characterised by ^1H and ^{13}C NMR spectroscopy and LCMS mass. The 2'-*O*-allyl and the 3'-*O*-allyl isomers could be differentiated on the basis of assignments of ^{13}C NMR shifts of the sugar carbons as reported in the literature.



Scheme 5. Synthesis of 2'-*O*-allyl, 3'-*O*-allyl Cytidine monomer

SectionB: Synthesis of 2'-*O*-allyl and 3'-*O*-allyl modified DNA and *iso*DNA sequences and their biophysical study

Synthesis, purification and characterization of modified DNA and *iso*DNA sequences: The four phosphoramidite monomers 2'-*O*-allyl-uridine monomer **28**, 2'-*O*-allyl-cytidine monomer **40**, and the 3'-*O*-allyl-uridine monomer **29**, 3'-*O*-allyl-cytidine monomer **41** (Schemes 4 and 5) were characterized by ^{31}P NMR and incorporated into DNA and *iso*DNA ONs (DNA 1 and DNA 2) at the modified sites and as described in Chapter 2. The RP-HPLC purified sequences were characterized by MALDI-TOF mass spectrometry. The control and complementary DNA, *iso*DNA oligonucleotides were synthesized in-house and used for the UV melting studies.

A comparative study of the thermal stability of modified 2'-5' DNA:RNA duplexes and the modified 3'-5' DNA:DNA, DNA:RNA duplexes by UV melting experiments: For the UV melting (T_m) experiments the HPLC pure ONs were annealed with the complementary DNA /RNA oligonucleotides and experiments were carried out as described in Chapter 2.

Thermal stability of 2'-O-allyluridine modified sequences: The 2'-O-allyl uridine modified DNA-1 (sequences 2-6) and DNA-2 (sequences 8-10) exhibited marginal stabilization (Table 2, Figure 6), when complexed with the complementary RNA, whereas, the modified DNA:DNA duplexes were destabilised.

Table 2. The UV T_m of the 3'-5'-linked 2'-O-allyluridine modified complexes with complementary DNA and RNA respectively. (The values in parentheses with + or - sign gives ΔT_m , the difference in T_m between the control and modified sequence).

Seq No.	Code No	Name	Sequence	UV T_m °C	
				cDNA1	RNA1
1	3'DNA1	DNA-1	5' CACCATTGTCACACTCCA 3'	60.0	59.0
2	3'DNA1-1	DNA2'allU-1s	5'CACCATTGTCACAC UCCA 3'	59.2	59.4
				(-0.8)	(+0.4)
3	3'DNA1-2	DNA2'allU-1d	5'CACCATTG UCACACUCCA 3'	54.9	59.2
				(-6.1)	(+0.2)
4	3'DNA1-3	DNA2'allU-1t	5'CACCA UTGUCACACUCCA 3'	53.0	58.1
				(-7.0)	(-0.9)
5	3'DNA1-4	DNA2'allU-1S ^{5'}	5'CACCA UTGTCACACTCCA 3'	57.2	58.4
				(-2.8)	(-0.6)
6	3'DNA1-5	DNA2'allU-1D ^{5'}	5'CACCA UUGTCACACTCCA 3'	57.6	59.6
				(-2.4)	(+0.6)
7	3'DNA2	DNA-2	5' CCTCTTACCTCAGTTACA 3'	54.0	56.0
8	3'DNA2-1	DNA2'allU-2s	5'CCTCTTACCTCAGT UACA 3'	51.8	57.6
				(-2.2)	(+1.6)
9	3'DNA2-2	DNA2'allU-2d	5'CCTCTTACC UCAGTUACA 3'	48.6	57.6
				(-5.4)	(+1.6)
10	3'DNA2-3	DNA2'allU-2t	5'CCTCT UACCUCAGTUACA 3'	46.1	56.8
				(-7.9)	(+0.8)

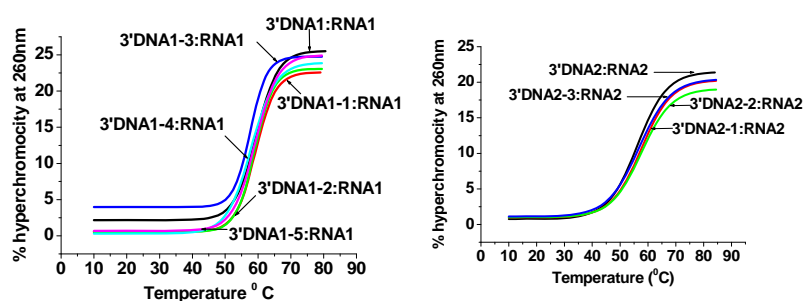


Figure 6. UV- T_m studies of the complexes of sequences 1-6 with RNA1 and of sequences 7-10 with RNA2

Thermal stability of 2'-O-allylcytidine modified sequences: The 2'-O-allylcytidine-incorporated 3'-5' linked DNA-1 and DNA-2 oligomers 11-16 (Table 3) showed a trend similar to the 2'-O-allyl uridine oligomers of destabilization when forming DNA:DNA duplexes ($\Delta T_m = -0.8$ to -4.8°C). The DNA:RNA duplexes containing 2'-O-allylcytidine

resulted in a modest stabilization for single (Sequences **11**, **14**), double (Sequences **12**, **15**) and triple (Sequences **13**, **16**) modifications, especially the DNA-2:RNA complexes (sequences **14**, **15**, **16**; $\Delta T_m = +2.2$, $+1.4$ and $+2.3^\circ\text{C}$ respectively; Figure 7b) Thus, the 2'-*O*-allylcytidine modification resulted in a better stabilization for the DNA:RNA duplexes as compared to the 2'-*O*-allyluridine containing DNA:RNA duplexes.

Table 3. The UV T_m of the 3'-5'-linked 2'-*O*-allylcytidine modified complexes with complementary DNA and RNA respectively. (The values in parentheses with + or - sign gives ΔT_m , the difference in T_m between the control and modified sequence).

Seq No	Code No	Name	Sequence	UV T_m °C	
				DNA	RNA
1	3'DNA1	DNA-1	5' CACCAT TGTCACACTCCA ^{3'}	60.0	59.0
11	3'DNA1-6	DNA 2'allC-1s	5' CACCAT TGTCACACT CCA ^{3'}	59.2	60.6
				(-0.8)	(+1.6)
12	3'DNA1-7	DNA 2'allC-1d	5' CACCAT TGT CACACT CCA ^{3'}	55.9	60.1
				(-4.1)	(+1.1)
13	3'DNA1-8	DNA 2'allC-1t	5' CA C ATTGT CACACT CCA ^{3'}	53.9	59.9
				(-6.1)	(+0.9)
2	3'DNA2	DNA-2	5' CCTCTT ACCTCAGTTACA ^{3'}	54.0	56.0
14	3'DNA2-4	DNA 2'allC-2s	5' CCTCTT ACCTCAGTTA CA ^{3'}	51.8	58.2
				(-2.2)	(+2.2)
15	3'DNA2-5	DNA 2'allC-2d	5' CCTCTT AC CT CAGTTA CA ^{3'}	49.2	57.4
				(-4.8)	(+1.4)
16	3'DNA2-6	DNA 2'allC-2t	5' CT CTTAC CT CAGTTA CA ^{3'}	-	58.3
					(+2.3)

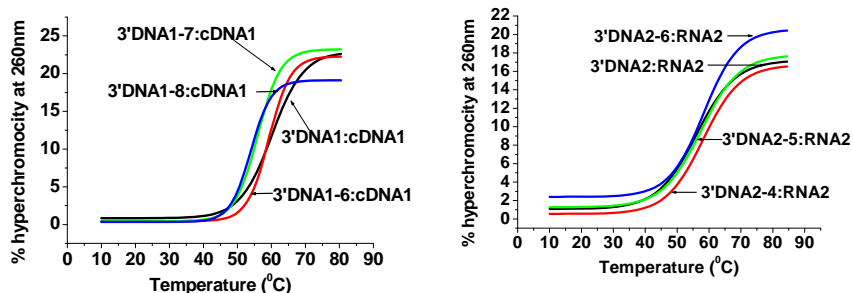


Figure 7. UV-melting plots of complexes of sequences (a) 11-13; (b) 14-16 with complementary RNA1 and RNA2 respectively

Thermal stability of 3'-*O*-allyluridine modified sequences: The 2'-5' *iso*DNA oligonucleotides do not show complex formation with 3'-5' DNA as reported earlier. Therefore, the thermal stability of only *iso*DNA:RNA duplexes were determined (Table 4). Introduction of 3'-*O*-allyluridine unit in the 2'-5'-linked *iso*DNA oligonucleotides resulted in stabilization of all the 2'DNA-1 oligonucleotides **18**, **19** and **20** with increasing modifications ($\Delta T_m = +0.5$, $+1.8$ and $+1.4^\circ\text{C}$ respectively; Figure 8). Surprisingly, however, all the 2'DNA-2 modified sequences **22**, **23** and **24** resulted in destabilization ($\Delta T_m = -1.1$, -1.7 and -2.3°C respectively)

Table 4. The UV T_m values of the 2'-5'-linked 2'-*O*-allyluridine modified complexes with complementary RNA. The 2'-5'-linked *iso*DNA did not complex with DNA as reported in literature. (The values in parentheses with + or - sign gives ΔT_m , the difference in T_m between the control and modified sequence).

Seq No	Code No	Name	Sequence	UV T_m °C	
				DNA	RNA
17	2'DNA1	2'DNA-1	5' CACCATTGTCACACTCCA ^{2'}	ND	50.5
18	2'DNA1-1	2'DNA3'allU-1s	5' CACCATTGTCACACUCCA ^{2'}	ND	51.0 (+0.5)
19	2'DNA1-2	2'DNA3'allU-1d	5' CACCATTGUCACACUCCA ^{2'}	ND	52.3 (+1.8)
20	2'DNA1-3	2'DNA3'allU-1t	5' CACCAUTGUCACACUCCA ^{2'}	ND	51.9 (+1.4)
21	2'DNA2	2'DNA-2	5' CCTCTTACCTCAGTTACA ^{2'}	ND	46.0
22	2'DNA2-1	2'DNA3'allU-2s	5' CCTCTTACCTCAGTUACA ^{2'}	ND	44.9 (-1.1)
23	2'DNA2-2	2'DNA3'allU-2d	5' CCTCTTACCUCAGTUACA ^{2'}	ND	44.3 (-1.7)
24	2'DNA2-3	2'DNA3'allU-2t	5' CCTCTUACCUCAGTUACA ^{2'}	ND	43.7 (-2.3)

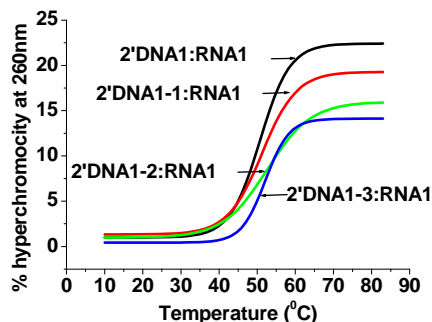


Figure 8. UV-melting plot for complexes of sequences 18-20 with complementary RNA1.

Thermal stability of 3'-*O*-allylcytidine modified sequences: In the case of 3'-*O*-allylcytidine containing 2'DNA-1 modified oligonucleotides (Table 5), only the sequence **25** with single modification stabilized the *iso*DNA:RNA duplex ($\Delta T_m = +0.8^\circ\text{C}$). Sequences **26** and **27** caused considerable destabilization ($\Delta T_m = -2.4$ and -8.1°C respectively).

Table 5. The UV T_m values of the 2'-5'-linked 2'-*O*-allyluridine modified complexes with complementary RNA. (The bracketed values with + or - sign gives ΔT_m , the difference in T_m between the control and modified sequence).

Seq No	Sr No	Code No	Sequence	UV T_m °C	
				DNA	RNA
17	2'DNA1	2'DNA-1	5' CACCATTGTCACACTCCA ^{2'}	ND	50.5
25	2'DNA1-4	2'DNA3'allC-1s	5' CACCATTGTCACACTCCA ^{2'}	ND	51.3 (+0.8)
26	2'DNA1-5	2'DNA3'allC-1d	5' CACCATTGTCACACTCCA ^{2'}	ND	48.1 (-2.4)
27	2'DNA1-6	2'DNA3'allC-1t	5' CACCATTGTCACACTCCA ^{2'}	ND	42.4 (-8.1)
21	2'DNA2	2'DNA-2	5' CCTCTTACCTCAGTTACA ^{2'}	ND	46.0
28	2'DNA2-4	2'DNA3'allC-2s	5' CCTCTTACCTCAGTTACA ^{2'}	ND	47.6 (+1.6)
29	2'DNA2-5	2'DNA3'allC-2d	5' CCTCTTACCTCAGTTACA ^{2'}	ND	47.3 (+1.3)
30	2'DNA2-6	2'DNA3'allC-2t	5' CCTCTTACCTCAGTTACA ^{2'}	ND	44.6 (-1.4)

On the other hand, the 2'-DNA-2 modifications containing 3'-*O*-allylcytidine stabilized the single and double modified sequences **28** ($\Delta T_m = +1.6^\circ\text{C}$) and **29** ($\Delta T_m = +1.3^\circ\text{C}$)(Figure 9). The pattern of stabilization and destabilization observed for the modified *iso*DNA oligonucleotides with the introduction of the 3'-*O*-allyluridine or 3'-*O*-allylcytidine modification in these sequences seems to be sequence dependent.

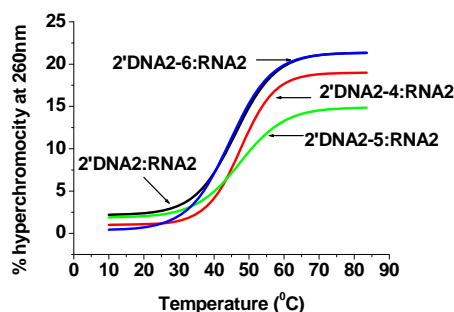


Figure 9. UV-melting plot of complexes of sequences 28-30 with complementary RNA2

Conclusions: Introduction of the 2'-*O*-allyluridine and 2'-*O*-allylcytidine modifications in 3'-5'DNA, stabilized the resulting DNA:RNA complexes. Alkylation at the 3' position of uridine did not result in uniform stabilization in the 2'-5'-linked *iso*DNA:RNA duplexes containing 3'-*O*-allyluridine/cytidine as was seen in the 3'-5'DNA:RNA duplexes containing 2'-*O*-allyluridine/cytidine modifications. It is unclear at this point to comment upon the nucleobase and sequence dependence of the modifications and more work would be necessary to understand the results in the context of sequence, nucleobase and site of modification.

Chapter 4: Synthesis of 2'-5'-linked thrombin binding aptamer (*iso*TBA), its quadruplex formation, and application as a thrombin inhibitor

Introduction:

G-quadruplexes are formed when four G-rich oligonucleotide strands associate through hydrogen-bonding by means of G-tetrad formation resulting in a right-handed helical motif (parallel quadruplex) or by folding of the single G-rich strand to form stacked G-tetrads

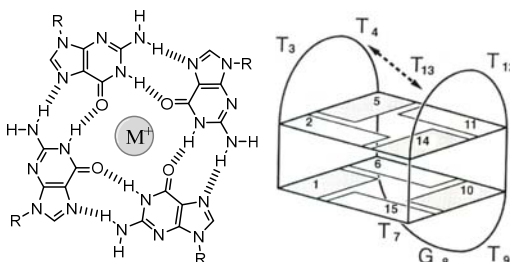


Figure 10. The G-tetrad motif and the structure of Thrombin binding aptamer(TBA).

(antiparallel quadruplex, Figure10). The stacked tetrads are stabilized by sandwiched monovalent cations co-ordinated to the O6 oxygen atoms of the guanines.

Present work: A 15-mer DNA oligonucleotide, 5'-GGTTGGTGTGGTTGG3' thrombin binding aptamer (TBA), obtained by SELEX, was found to inhibit fibrin-clot formation by binding to the thrombin protein with high selectivity and affinity. The RNA binding selectivity and stability of regioisomeric 2'-5'linked *iso*DNA towards endonucleases as seen in the earlier work (Chapters 2, 3) prompted the synthesis of isomeric TBA oligonucleotides aptamers, to examine their quadruplex forming possibility and consequent anti-thrombin activity which remains unexplored. The stability and structural topology of the quadruplex using 2',5'-backbone (*iso*TBA) and its effect on anti-clotting ability was studied with reference to the control 3',5'-linked TBA. The effect of riboU units in the loop region of *iso*TBA oligomer was also investigated.

Chemical synthesis of TBA, 2'-5'-linked TBA(*iso*TBA) and a modified *iso*TBA:

Two sequences, *iso*-TBA-2 and a modified *iso*-TBA-3 were synthesized using SPS methodology described in Chapter 2. Replacement of 3'-deoxythymidine in the TGT loop (T7 and T9 in *iso*-TBA-2) by uridine gave UGU loop-modified sequence *iso*-TBA-3. Longer coupling times were used to ensure efficient coupling. The 3'-5'-linked TBA-1 was synthesized for control experiments (Table 6). The sugar residues in the TT loop involved in interactions with thrombin and the guanine nucleosides involved in the G-quartet formation, were not changed in our design.

Table 6. Oligomers synthesized, MALDI-ToF mass spectrometric characterization and HPLC retention time and thermal stability in presence of cations

Sequence code	Sequence	MALDI-ToF Mass		HPLC t_R (min)	T_m °C		
		$M_{calcd.}$	$M_{obsd.}$		Na ⁺	K ⁺	Thrombin (K ⁺)
TBA-1	5'-dGGTTGGTGTGGTTGG-3'	4726	4728	10.05	22.2	52.0	22.2 (52)
<i>iso</i> -TBA-2	5'-dGGTTGGTGTGGTTGG-2'	4726	4731	8.45	24.9	37.1	<10.0 (37)
<i>iso</i> -TBA-3	5'-dGGTTGGUGUGGTTGG-2'	4730	4739	8.74	nd	42.5	13.2 (42.5)

G-tetraplex formation in the presence of monovalent cations using CD, UV and fluorescence spectroscopy:

CD spectroscopy and T_m measurement of the TBA sequences: The G-quadruplex formation for the synthesized sequences was studied by CD spectroscopy in the presence of

added monovalent cations such as K^+ and Na^+ and their stability was determined as a function of temperature-dependent change in CD amplitude at 295nm (Figure 11, Table 6). The 2'-5'-linked *isoTBA-2* and *isoTBA-3* and control sequence **TBA-1** were found to exhibit intense maxima at 295nm in the CD spectra in presence of K^+ ions (Figure 11A) which corresponds to antiparallel G-quadruplex topology for 3'-5'-DNA. The stability of the G-quadruplexes was followed by the change in the amplitude of the CD signal at 295nm with temperature (Figure 15B). The monovalent cations Na^+ and K^+ were necessary for the for the stability of the quadruplex structure, K^+ being most favoured(Figure 11C,D).

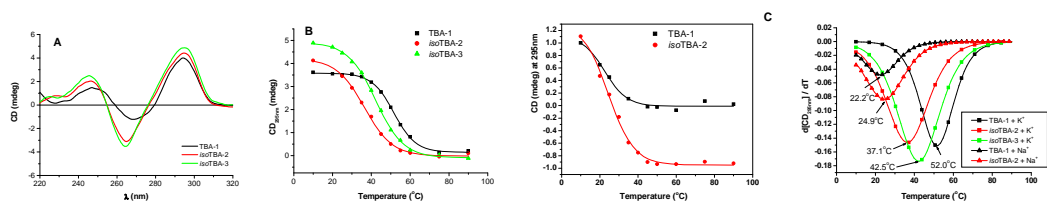


Figure 11. A CD spectra of oligomers **TBA-1**, *isoTBA-2* and *isoTBA-3* in K^+ buffer, **B** Temperature-dependent changes in CD amplitude at 295nm plotted against temperature. **C** CD- T_m of oligomers **TBA-1**, *isoTBA-2* having a strand concentration of $5\mu M$ in 10mM Na-phosphate buffer (pH 7.5) containing 100mM NaCl **D** The first derivative curves of **TBA-1**, *isoTBA-2* and *isoTBA-3* in K-phosphate and Na-phosphate buffers.

The CD and UV hysteresis between the heating and cooling curves (data not shown) was found to be negligible in all the cases indicating unimolecular folding into G-quadruplex form.

Comparison of TBA-1 and isoTBA-2 quadruplexes in the presence of different monovalent ions:

The CD spectra of **TBA-1** and *isoTBA-2* in the presence of different monovalent ions is shown in Figure 13. In contrast to **TBA-1**, which exhibited characteristic CD signatures of stable quadruplexes in the presence of all the monovalent ions under study, *isoTBA-2* showed the characteristic maximum at 295nm for antiparallel quadruplex formation only in the presence of Na^+ and K^+ ions indicating a subtle difference in the quadruplex structure of the *isoTBA-2*.

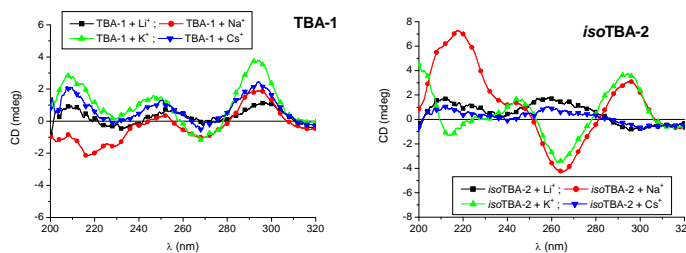


Figure 12. CD spectra of **TBA-1** and *isoTBA-2* at $10^\circ C$, in the presence of different cations (Li^+ , Na^+ , K^+ , Cs^+).

Intrinsic Fluorescence of G-quadruplexes: The intrinsic fluorescence of G-quadruplexes was also used to confirm the formation of G-quadruplexes, in addition to the CD and UV

spectroscopic studies discussed above. Accordingly, a significant increase in fluorescence emission was observed at ~330nm to 340nm for **TBA-1** and *isoTBA-2* in the presence of cations, which was minimal with **TBA-1**, and absent with *isoTBA-2*, in the absence of any added cations (Figure 13a).

Thermal Difference Spectra (TDS): The characterization of G-quadruplexes can be done by the thermal difference spectra (TDS), obtained by subtracting the spectra of the folded state from that of the unfolded state at temperatures below and above the melting temperatures (T_m s). TDS has a specific shape that is unique for each type of nucleic acid structure. UV TDS complements CD spectroscopy as a tool for the structural characterization of nucleic acids in solution. The TDS of *isoTBA-2* and **TBA-1** (Figure 13b) clearly illustrate the formation of G-quadruplexes in buffer containing K^+ ions. Fluorescence TDS is also similarly useful in characterization of G-quadruplexes (Figure 13c).

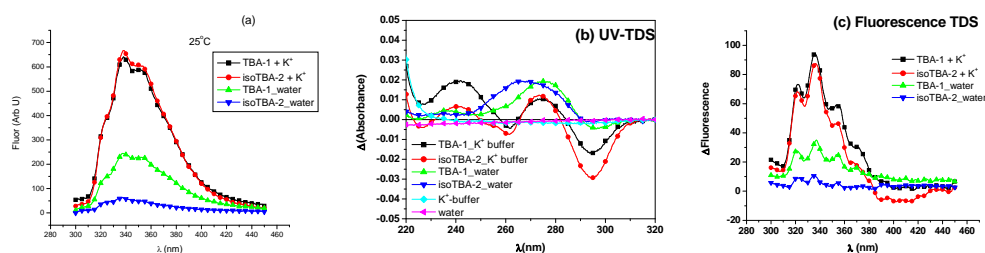


Figure 13. (a) Fluorescence emission spectra, (b) UV-TDS and (c) Fluorescence-TDS of **TBA-1** and *isoTBA-2* in the presence and absence of added cations (K^+) at 25°C.

Imino proton NMR spectra of TBA-1 and isoTBA-2: The characteristic chemical shifts of imino proton signals of the eight H-bonds formed between the guanines of each G-quartet of a quadruplex structure were observed between 11.5ppm and 12.5ppm range in the 1H NMR spectrum. The imino proton chemical shifts for *isoTBA-2* are comparable with the control **TBA-1** and indicate the hydrogen-bonded quadruplex formation (Figure 14). In the temperature-dependent 1H NMR, the 1H NMR signals between 11.5ppm and 12.5ppm slowly disappeared with increasing temperature due to the loss of quadruplex structure near T_m . The appearance of characteristic H-bonded imino protons supports the fact that *isoTBA-2* does form a G-quadruplex structure, although less stable (Table 6, T_m 37°C) compared to the 3'-5'-linked **TBA-1** (Table 6, T_m 52°C) quadruplex structure. It is evident from the 1H NMR signals at 4°C between 11.5ppm and 12.5ppm that **TBA-1** has significant quadruplex structure even in the absence of K^+ whereas *isoTBA-2* is not structured without monovalent cations such as K^+ (Figure 14 Inset).

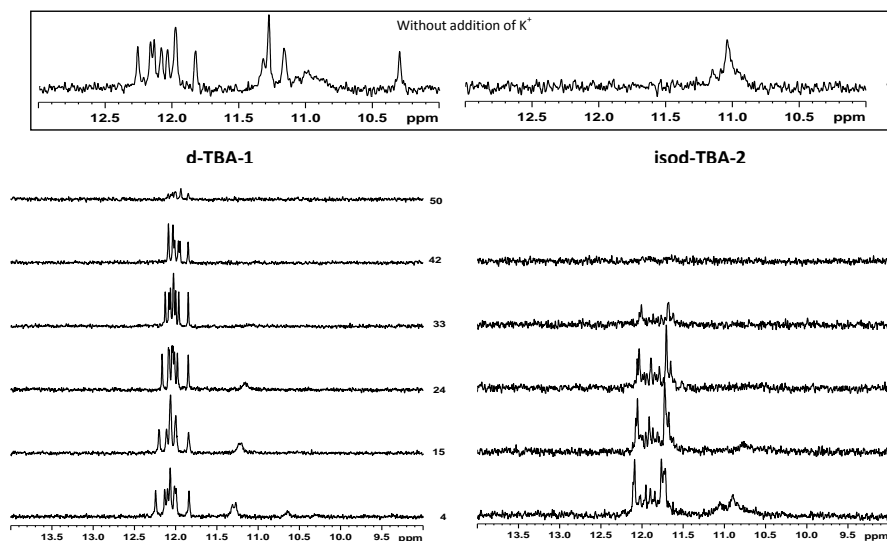


Figure 14. Quadruplex imino proton spectral region for **TBA-1** and *isoTBA-2* in the presence of K^+ from 4°C to 50°C. Inset shows the imino proton spectral region in the absence of K^+ at 4°C.

G-tetraplex formation in the presence of thrombin without added monovalent cations

It has been earlier demonstrated that thrombin can act as a molecular chaperone for the folding of **TBA-1**. At low temperature, the quadruplex structure necessary for thrombin-binding was formed, even in the absence of K^+ , but as the temperature was increased, the presence of K^+ was needed to preserve the quadruplex integrity. CD experiments were done with **TBA-1**, *isoTBA-2* and *isoTBA-3* in the presence of increasing concentrations of thrombin at low temperature.

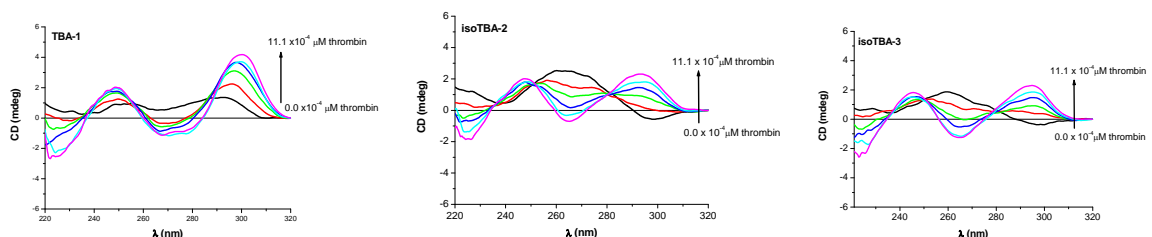


Figure 15. Changes in CD signal at upon addition of thrombin to (a) **TBA-1**, (b) *isoTBA-2*, and (c) *isoTBA-3*

Thrombin was indeed found to display its chaperone effect on the folding of the G-quadruplex. In the case of control **TBA-1**, (Figure 15a) a CD maximum at 295nm was observed even in the absence of either thrombin or K^+ , revealing the preference of G-quadruplex structure. In the case of *isoTBA-2* and *isoTBA-3*, the CD band at 295nm and G-quadruplex structure was not evident in the absence of either thrombin or K^+ , a fact also supported by 1H NMR. Upon incremental addition of thrombin, however, the characteristic CD maximum at 295nm emerged for *isoTBA-2* (Figure 16b) and *isoTBA-3* (Figure 16c). Changes in CD spectral amplitudes were not observed when serum albumin was used

instead of thrombin in these experiments confirming the specific role of thrombin in inducing quadruplex structures.

Anti-thrombin activity measurements: The inhibitory activity of the aptamers on thrombin-catalyzed conversion of fibrinogen to fibrin (clotting) was investigated by measuring the percent transmittance with time. **TBA-1** slowed down the coagulation with an increased induction time (t_i as coagulation parameter), confirming its reported inhibitory activity (Figure 16).

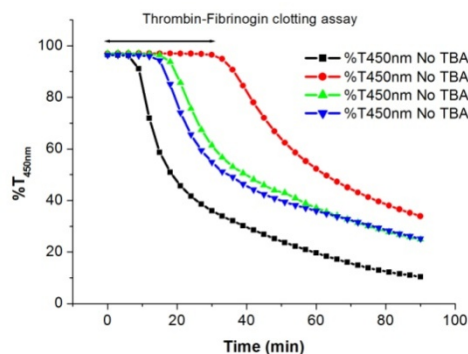


Figure 16. Antithrombin activity measured by % transmittance at 450nm in the presence of **TBA-1**, *isoTBA-2* and *isoTBA-3*. \leftrightarrow indicates induction time as coagulation parameter (t_i).

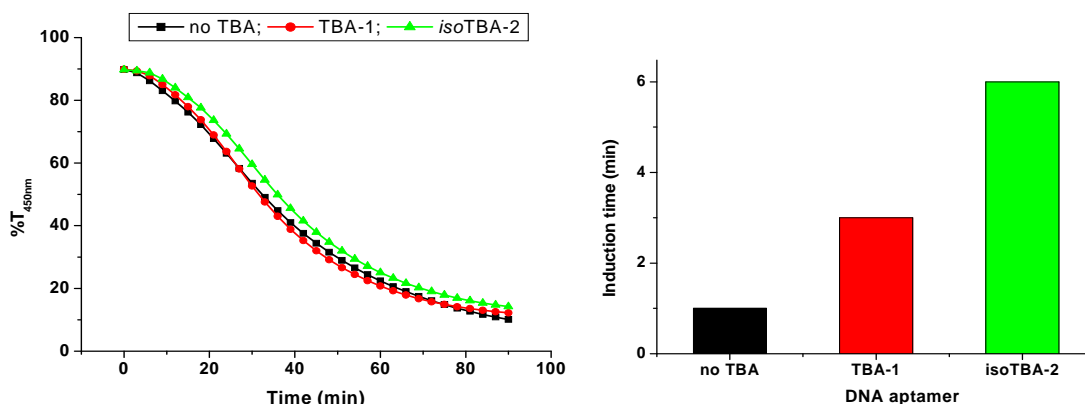


Figure 17. Antithrombin activity measured by % transmittance at 450nm with **TBA-1** and *isoTBA-2* in the presence of SVPD and the corresponding induction time plots.

The induction time for the *isoDNA* oligomers *isoTBA-2* and *isoTBA-3* was considerably less than for **TBA-1**, but more than that in the absence of any aptamer. The thrombin-fibrinogen clotting assay when carried out in presence of SVPD brought down the anti-thrombin activity of **TBA-1** as it is less stable to SVPD than *isoTBA-2* as shown in Figure17. These experiments provide conclusive evidence that the *isoTBA* oligomers are indeed capable of not only forming G-quadruplex structures but also hold similarity in structural topology capable of taking active part in the assigned function of the **TBA-1**, though less efficiently.

Stability of aptamers to snake venom phosphodiesterase(SVPD): The enzymatic stability towards SVPD of the 2'-5' *iso*DNA quadruplex as compared to the 3'-5'-DNA quadruplex aptamers was tested (Figure18a). The 2'-5'-linked *iso*DNA oligomer ***iso*TBA-2** was found to be digested much slower compared to the control **TBA-1**. The observed higher stability of the *iso*DNA oligomer offers obvious advantages for applications in biological systems, where the control unmodified oligomer has a relatively low half-life.

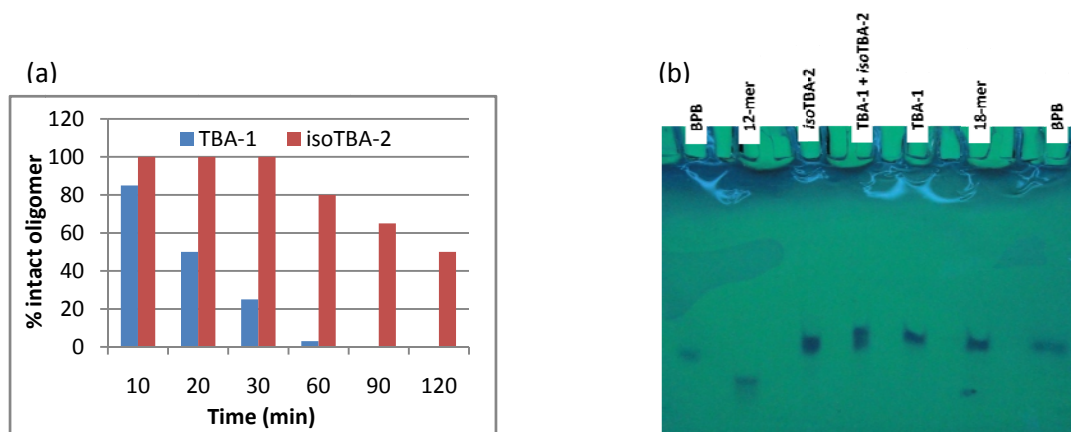


Figure 18. (a) Stability of the aptamers :TBA-1 and *iso*TBA-2 (7.5 μ M) towards Snake venom phosphodiesterase (SVPD) enzyme (5mg/mL). (b) Non-denaturing PAGE analysis :showing the relative mobilities of TBA-1 and *iso*TBA-2, visualized by UV shadowing.

Non-denaturing Gel electrophoresis study.

The quadruplex-forming ability of the synthesized oligomers was assessed by non-denaturing polyacrylamide gel electrophoresis. As reference oligonucleotides, two oligomers of differing lengths, viz., 5'-dAACCGATTCAG-3' (12-mer) and 5'-dCACCATTGTCACACTCCA-3' (18-mer) were used. PAGE analysis indicated similar complex formation in the case of **TBA-1** and ***iso*TBA-2**, evident from their similar mobilities in the gel (Figure18b).

Conclusions: The new findings prove that the 2'-5'-*iso*DNA aptamers, ***iso*TBA-2** and ***iso*TBA-3** form quadruplex structures similar to the natural DNA aptamer (**TBA-1**) and are functionally active, though their functional efficiency is lower compared to the **TBA-1** but with an additional property of stability towards nuclease enzyme can function as a better anticoagulant than **TBA-1**.

Chapter 1

Introduction

Nucleic acids in therapeutics

Chapter 1

Nucleic acids in therapeutics

1.1 Introduction

The recent past has witnessed a revival of interest and intense research in the field of antisense technology, owing mainly to the discovery of naturally-existing antisense-based regulatory mechanisms, such as the RNA interference¹ (RNAi), induced by short interfering RNA² (siRNA) or micro RNA³ (miRNA). The beginning of the year 2013 also saw the approval of only the second antisense drug, Mipovirsen⁴ from ISIS pharmaceuticals, by the US FDA, spurring on further research in this interesting area.

The antisense activity of the agents used in this technology arises mainly as a result of target-specific hybridization *via* Watson-Crick hydrogen-bonding of sequence-complementary nucleobases. It is thus, useful in regulation of target gene expression at the translation level. The activity of the antisense agent may be realized by various mechanisms⁵ such as by splice correction of the pre-mRNA, by steric blocking of the translation machinery, by activation of ribozymes, by increasing the susceptibility to nuclease degradation, such as by induction of RNase H and as seen in the RNAi pathways involving siRNA or miRNA. As suggested by the mechanisms listed above, the antisense action may downregulate the target gene or effect a correction in its expression. Owing to the inherent drawbacks of natural DNA or RNA oligonucleotides, *viz.*, mainly their cellular delivery and short half-life as a result of low stability in biological systems, their application as antisense agents is limited. This has in turn, spawned a large area of research in the field of chemical modifications of nucleosides, nucleotides and their derivatives. This research is directed towards improving not only the cellular delivery and stability of these agents in biological systems, but also their hybridization to target sequences and RNA-specific selectivity, coupled with the ease of synthesis and scale-up, while at the same time, minimizing toxicity.

1.2 Nucleic acid structure

1.2.1 Basic structure of DNA/RNA

The natural nucleic acids (DNA and RNA) are polymers of nucleotide units that are joined by phosphodiester linkages between the 3'-OH group of one unit and the 5'-OH group of the neighbouring unit. Each nucleotide unit in turn, is composed of a pentose sugar (D-ribose in RNA and 2-deoxyribose in DNA) that is linked to a nitrogenous base (nucleobase) by a β -glycosidic linkage (Figure 1).

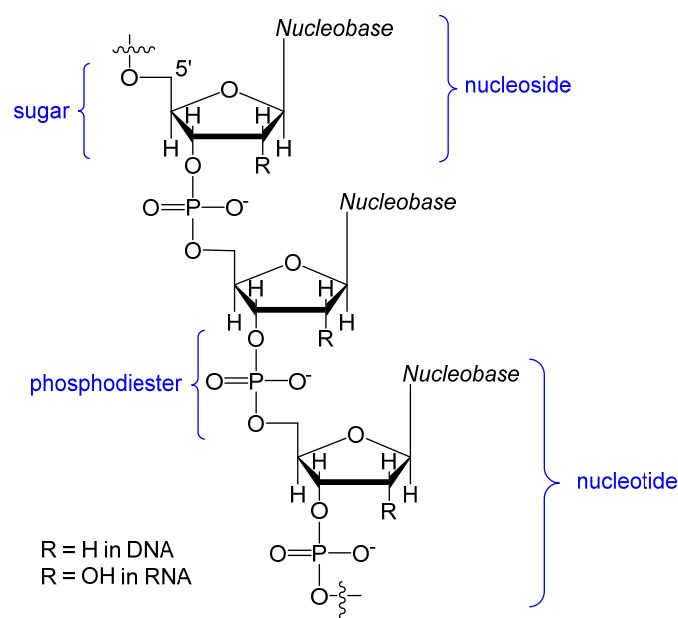


Figure 1. Basic structure of natural DNA and RNA

The nucleobase may be a purine (adenine and guanine) or a pyrimidine (cytosine and thymine in DNA or uracil in RNA). Other than these, several modified nucleobases or pseudo-nucleobases are known to be present in tRNA. The presence or absence of the 2'-OH group that serves to chemically differentiate the structures of DNA and RNA is also responsible for the structural differences between the two. For example, DNA is predominantly double-stranded, while RNA is mainly single-stranded, with a high tendency to form secondary structures such as hairpins, loops, bulges, etc. Some RNAs can function as enzymes. The 2'-OH group also makes RNA chemically more susceptible to hydrolysis than DNA, because of neighbouring group participation.

1.2.2 H-bonding patterns- Watson-Crick and Hoogsteen

Duplex formation generally involves hydrogen bonding between complementary nucleobases on facing strands that run in antiparallel directions. Thus, adenine binds to thymine/uracil by two hydrogen bonds, while guanine forms three hydrogen bonds with cytosine. This hydrogen-bonding pattern was first proposed by J. D. Watson and F. H. Crick in their model of the DNA double-helix in 1953.⁶ As the purine of one strand binds to the pyrimidine in the facing strand, the width of the A-T and G-C base-pairs, of the resulting double helix, remains the same (Figure 2).

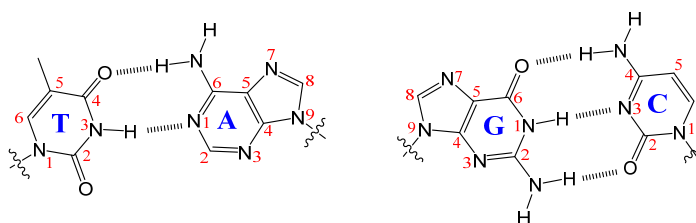


Figure 2. Watson-Crick hydrogen bonding

In addition to these *Watson-Crick* hydrogen bonds, the N7-face of the purines is also open to hydrogen bonding by the *Hoogsteen* mode, where another strand of DNA/RNA can potentially bind.

1.2.3 Higher order structures-duplex, triplex, quadruplex

Hydrogen bonding in the *Hoogsteen* mode is observed during the formation of higher order structures such as triplexes and quadruplexes. Non-canonical base-pairing is also observed in some cases, known as *Wobble* base-pairing, for example, the hydrogen-bonding between guanine and uracil/thymine. In some triplexes, where the third strand is purine-rich, *reverse-Hoogsteen* hydrogen-bonding is observed (Figure 3). Quadruplexes are four-stranded structures and are mainly of two types, depending upon the nucleobases involved in their formation. These are the G-quadruplexes that involve G-tetrad formation by guanine nucleobases and the i-motif quadruplexes, that are formed by inter-digitating hydrogen bonds between cytosine and protonated cytosine nucleobases of opposite strands of the tetraplex.⁷ (Figure 4).

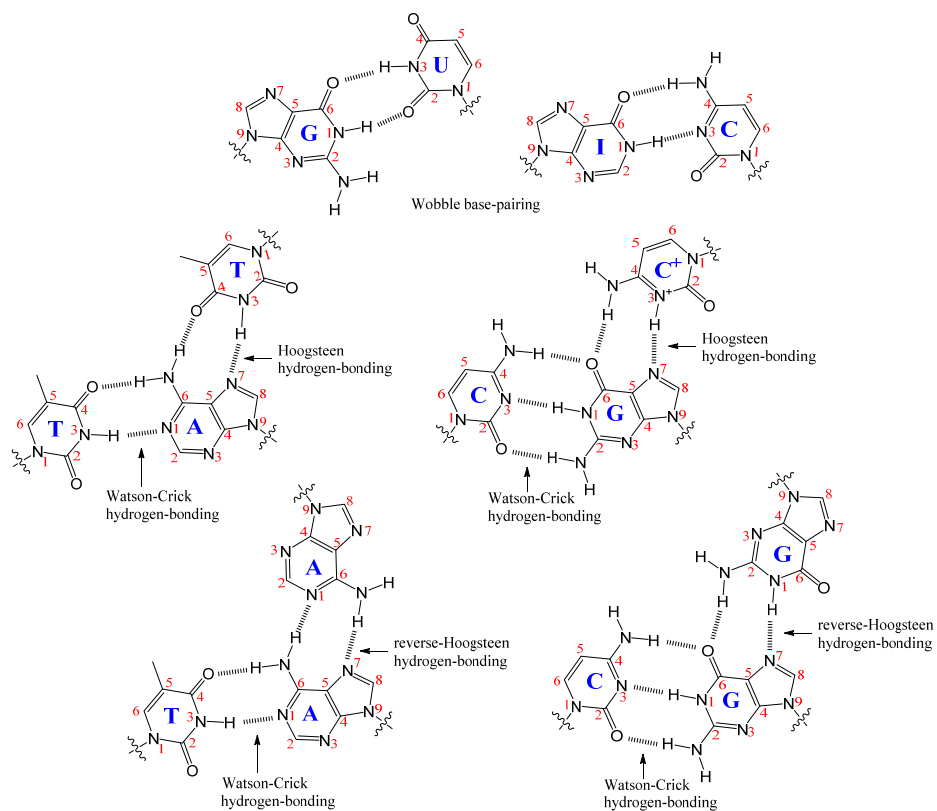


Figure 3 Wobble, Hoogsteen, and reverse-Hoogsteen base pairs

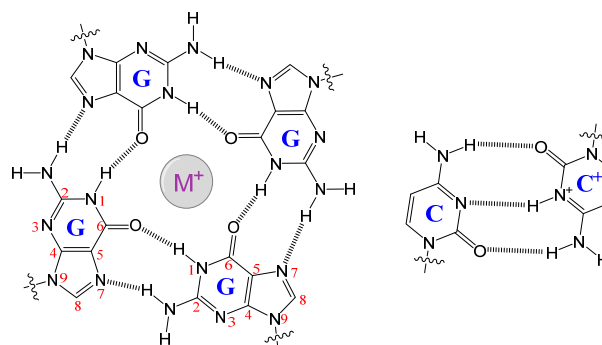


Figure 4. G-tetrads of G-quadruplexes and C-C⁺ hydrogen-bonding of i-motif tetraplexes

1.3 *Iso*Nucleic Acids

*Iso*DNA or *iso*RNA differs from the native DNA or RNA in having regioisomeric 2'-5'-phosphodiester-linkages instead of 3'-5'-phosphodiester-linkages (Figure 5). The 2'-

5'-linkage is the major product of many non-enzymatic oligomerizations of nucleotide monomers, depending on the conditions. The 2'-OH group is more reactive than the 3'-OH group and consequently, the 2'-5'-linkage is formed more readily than the 3'-5'-linkage in non-enzymatic oligomerizations.⁸ Thus, the 2'-5'-linkage could have been a primary substitute of the natural 3'-5'-linkage in evolution. The lower rates of hydrolysis of the 3'-5'-linkage, coupled with the low helix-forming ability of the 2'-5'-linked oligonucleotides could be the reasons for the evolutionary selection of the 3'-5'-phosphodiester as the linkage in the carriers of genetic information-DNA and RNA. However, *isoDNA/isoRNA* are not used to encode genetic information, and are therefore, sometimes referred to as non-genetic nucleic acids.

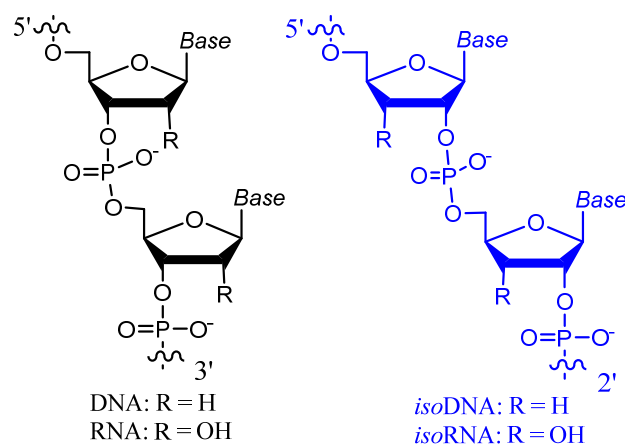


Figure 5. The natural 3'-5'-linkage and the isomeric 2'-5'-linkage.

IsoRNA does occur naturally,⁹ mainly as 2'-5'-linked oligoadenylate sequences and forms a part of what is known as the 2-5A system that is believed to mediate certain actions of interferon, and supposedly plays some role in the regulation of cell growth and differentiation. Such 2'-5'-linked oligoadenylates have been reported to be able to activate the enzyme RNaseL, an enzyme that is known to degrade the selected RNA. This property has been exploited in the literature by the synthesis of chimeras of 2-5A with 3'-5'-linked oligonucleotides for antisense applications.¹⁰

In 1993, Giannaris and Damha¹¹ reported the chemical synthesis of 2'-5'-linked oligoadenylate and mixed base sequence RNA (*isoRNA*) oligomers, including

phosphorothioate backbones. Binding studies with complementary nucleic acids revealed a marked selectivity for single-stranded RNA over DNA. While the complexes with complementary RNA were observed with all the sequences studied, the complexes with complementary DNA were either not observed at all, or were found to be highly unstable, could be observed only at high salt conditions, and that too, with very low melting temperatures. The complexes formed with complementary RNA were further found to be thermally less stable than the complexes formed by the natural 3'-5'-linked DNA or RNA. This higher stability of the duplexes formed by natural RNA was a probable factor in the favourable evolutionary selection of 3'-5'-linkages over the 2'-5'-linkages in *isoRNA*.¹² The lower stability of the complexes formed by 2'-5'-linked oligomers is a result of a less favourable enthalpy change for association, rather than a more favourable entropy change for the association. Modeling studies carried out by Yathindra *et al.*¹³ show that duplex formation by the *isoDNA/isoRNA* oligomers mandates a displacement of the base-pairs from the helix axis, which is a direct consequence of the lateral shift of the sugar-phosphate backbone from the periphery (as in 3'-5'-linked oligomers) towards the interior of the helix (in 2'-5'-linked oligomers). Similar to the duplexes, *isoDNA* triplexes are also found to be thermodynamically less stable than the corresponding DNA triplexes, owing to lower enthalpy, which could result from the lower base-stacking in the *isoDNA* duplexes.

Complex formation by *isoDNA* was independently reported by Breslow *et al.*¹⁴ and by Hashimoto and Switzer.¹⁵ Duplex formation was found to be enthalpically driven. *IsoDNA* was found to form either a triplex, or no complex at all, in contrast to DNA, when either a duplex or triplex was formed, depending on the salt concentration.¹⁶ The stability of the duplexes formed by *isoDNA* with complementary RNA was reported to be comparable to that of the duplexes formed by DNA.¹⁷

All these studies together seemed to suggest that the 2'-5'-linkage was a co-runner in evolution, but eventually lost the race to the 3'-5'-linkage.

1.4 Sugar ring conformations in 3'5' Vs 2'5' linked oligomers

The furanose ring forms the central part of the sugar phosphate chain of nucleic acids. From X-ray studies it is known that this five-membered ring occurs in two

conformations, usually referred to as C(2')-endo and C(3')-endo forms. Bringing about a changeover from one conformer of the furanose ring to the other conformer causes major structural changes in the naturally occurring nucleic acids (e.g. B-DNA has a C(2')-endo and RNA C(3')-endo) and has important bearing in their biological function. Several important factors that govern the ultimate structure assumed by a natural 3'-5'DNA and a 2'-5' isomeric DNA are described in the following paragraphs.

1.4.1 Pseudorotation cycle, north type, south type, RNA, DNA

The pentafuranose sugar ring in DNA/RNA is puckered in order to attain an energetically more favourable conformation, where the substituents on the ring carbon atoms are as far from each other as possible. On the other hand, the planar ring conformation is energetically unfavourable because all the substituents on the ring carbons are eclipsed. Puckering reduces the energy of the system. The conformation of the sugar ring is dynamic and is often described using the pseudorotation concept.¹⁸ The concept of pseudorotation was first applied to furanose by Hall *et al.*¹⁹, which considers the influence of the endocyclic oxygen atom in inducing the ring pucker. It is defined by mainly two parameters, *viz.*, the pseudorotation phase angle, P [$\tan(P) = (v_4 + v_1) - (v_3 + v_0) / 2v_2 (\sin 36^\circ + \sin 72^\circ)$], which represents the part of the sugar ring that is mostly puckered, and the maximum amplitude of puckering,²⁰ v_{\max} or Ψ_m ($v_{\max} = v_2 / \cos P$), which represents the extent of puckering. These are derived from the endocyclic torsion angles that are obtained from the experimentally measured proton-proton coupling constants. The torsion angles in the furanose ring, v_0 through v_4 , along with those in the phosphate backbone, α , β , γ , δ , ϵ and ζ , and of the glycosidic bond, χ , together define the conformation of the nucleotide. These torsion angles are as defined in Figure 6.

The torsion angle χ , about the glycosidic bond, can adopt two main conformations-*syn* ($-90^\circ \leq \chi \leq 90^\circ$) and *anti* ($90^\circ \leq \chi \leq 180^\circ$).²¹ The *anti* conformation is usually preferred because of the lower steric penalty in this instance, between the sugar and the nucleobase. However, the *syn* conformation may be observed with some substituted nucleobases or depending on the sugar pucker. The six backbone sugar-phosphate torsion angles are often roughly described as being in a conformational hyperspace as *cis* (c) = $0 \pm 30^\circ$, + *gauche*

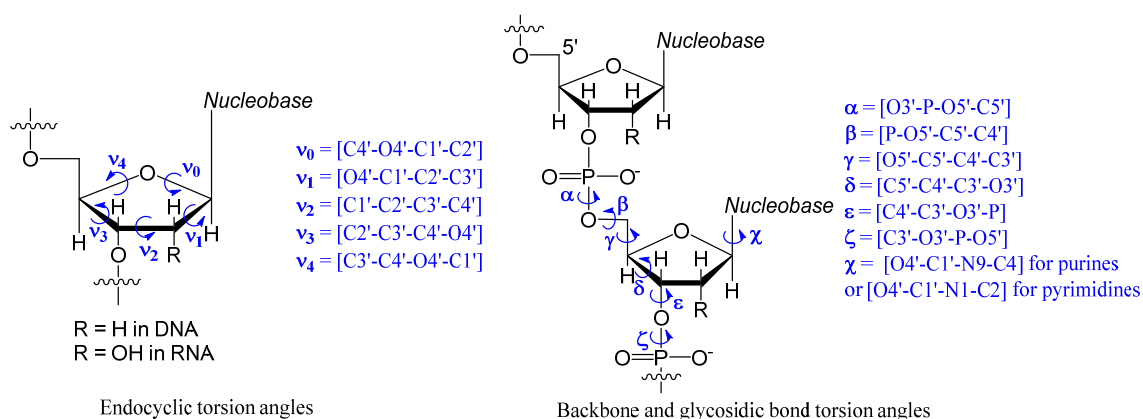


Figure 6. The torsion angles in the furanose ring, the phosphate backbone, and the glycosidic bond.

$(g^+) = 60 \pm 30^\circ$, + *anticlinal* (a^+) = $120 \pm 30^\circ$, *trans* (t) = $180 \pm 30^\circ$, - *anticlinal* (a^-) = $240 \pm 30^\circ$ and - *gauche* (g^-) = $300 \pm 30^\circ$. The sugar pucker is described by considering the major displacement of mainly the C2' or C3' atoms from the median plane of C1'-O4'-C4'. The *endo* face of the sugar ring is on the same side as C5' and the nucleobase, while the *exo* face is on the opposite side to the base.

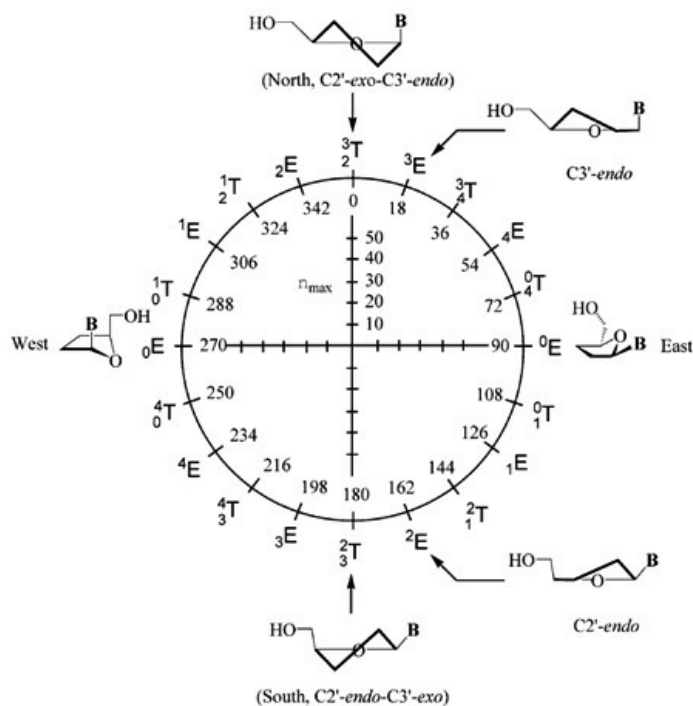


Figure 7. Pseudorotational cycle for nucleosides showing the characteristic North, South, East and West conformations. The radius of the cycle corresponds to v_{\max} . The units of ϕ and v_{\max} values are degrees. Envelope (E) and twist (T) forms alternate every 18° . (Mathé, C., Périgaud, C. *Eur. J. Org. Chem.*, **2008**, 1489-1505.)

In the furanose ring, the unsymmetrical substitution (e.g., $-\text{CH}_2\text{OH}$, $-\text{OH}$, $-\text{H}$ and the nucleobase) leads to the generation of potential energy thresholds limiting the pseudorotation to preferred sugar pucker, The major puckers being the North-type and the South-type puckers, that are involved in a two-state equilibrium in solution. The pseudorotation cycle²² is depicted in Figure 7. In DNA, the deoxyribose sugar adopts preferentially the 2'-*endo*, 3'-*exo* twist that is commonly referred to the South- or S-type conformation, while the ribose sugar in RNA exists predominantly in the North- or N-type conformation that is characterized by a 3'-*endo*, 2'-*exo* twist. Although these two conformations exist in dynamic equilibrium in solution, the placement of different substituents on the sugar ring, and the aromatic nature of the nucleobase can influence the predominance of one conformation. The two conformations have profound effects on the overall DNA/RNA conformation in that they specify different phosphate-phosphate distances along each strand ($\sim 7\text{\AA}$ for C2'-*endo* and $\sim 6\text{\AA}$ for C3'-*endo*).

1.4.2 Stereoelectronic effects and the ribo/deoxyribofuranose conformation

The conformation adopted by the sugar is governed by stereoelectronic effects which include mainly the *anomeric* and *gauche* effects.²³ The *anomeric* and *gauche* effects influence the conformational equilibrium of nucleosides and nucleotides. The *anomeric* effect in nucleosides is induced by the presence of the nucleobase at C1' position and it is maximum when the conformation of the furanose sugar is in the East position of the pseudorotation cycle, as in this case, one of the lone pairs of the endocyclic oxygen of the sugar ring is fully antiperiplanar to the exocyclic glycosidic C-N bond. However, due to the large steric hindrance generated by the exocyclic 5'CH₂OH and the nucleobase substituents in these conformations, the existence of E-type pseudorotamers are prevented. The *anomeric* effect thus, is strongest in N-type pseudorotamers. The *gauche* effects, in turn, exhibit their influence on the sugar pseudorotation. Thus, the [O3'-C3'-C4'-O4'] *gauche* effect favours the S-type conformation in 2'-deoxyribonucleosides. In ribonucleosides the [O2'-C2'-C1'-O4'] *gauche* effect favours the N-type conformation and the [O3'-C3'-C4'-O4'] *gauche* effect, in turn, favours the S-type conformation. The anomeric effect in ribonucleosides along with the [O2'-C2'-C1'-O4'] *gauche* effect allows the favoured N-

type conformation. These stereoelectronic effects can be quantified by using the PSEUROT programme developed by de Leeuw and Altona,²⁴ which translates the experimentally measured temperature-dependent proton-proton coupling constants for the furanose ring to determine the relative populations of the N- and S-type pseudorotamers.

1.4.3 Base-stacking

The stability of the DNA double helix is due to mainly two factors, these being base-pairing between complementary strands and the stacking between adjacent nucleobases.²⁵ Base-stacking is a significant stabilizing interaction in DNA and RNA 3-D structures, such as duplexes, stem-loop structures, etc., playing an important role in their folding and complexation. Stacking occurs more often between adjacent nucleobases, but also between non-adjacent nucleotides. Since the nucleobases are aromatic and therefore, mainly hydrophobic, stacking minimizes the solvent exposure of the base surfaces, leading to the face-to-face stacking of bases and base-pairs. This π - π -stacking refers to attractive, non-covalent interactions between aromatic rings. It has been found that differential contribution of base-stacking in A:T and G:C-containing contacts is responsible for 50% of the dependence of DNA stability on its G:C content.²⁶ The specific orientation of stacked base-pairs contributes to the conformational stability of the DNA duplex. The sugar pucker has been shown to exert an effect on the base-stacking propensity, since it influences the orientation of the nucleobase. Studies have implied that the North-type sugar conformation (C3'-*endo*) causes the nucleobase to be pseudoaxially oriented,^{20a} which leads to more efficient base-stacking, as opposed to the case in sugars with the South-type conformation (C2'-*endo*), where the nucleobase is pseudoequatorial.²⁷ Van der Waals forces, electrostatic interactions and solvent effects also define the geometry and associated energies of stacked bases.

It has been reported that the 2'-5'-linked nucleotides show a much stronger tendency to stack than the 3'-5'-linked nucleotides.²⁸ The mode of stacking is different from the 3'-5'-linked ribonucleotides, where the sugar rings predominantly adopt an N-type conformation. For example, A2'-5'U displays an A(S)2'-5'U(N) stacked state.

1.4.4 Steric effects

Steric effect considerations alone for β -D-nucleosides energetically favour the S-type ($C2'$ -endo) sugar pucker, since the pseudoequatorially-oriented nucleobase exerts less steric repulsion from the other sugar ring substituents. On the other hand, in the N-type ($C3'$ -endo) sugar pucker, the nucleobase is pseudoaxially-oriented, leading to steric clashes between the nucleobase and the sugar ring substituents. However, the energetics of the North \longleftrightarrow South conformational equilibrium (Figure 8) is mainly determined by the relative *gauche* and *anomeric* effects.

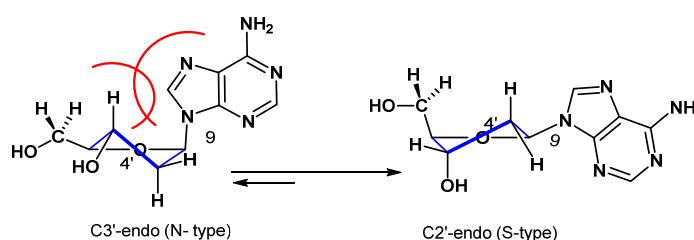


Figure 8. The steric interactions of nucleobase in the North \longleftrightarrow South equilibrium in DNA.

Therefore, as described above, the sugar pucker defines the intrastrand phosphate-phosphate distance, the base-stacking defines the nucleobase-nucleobase distance, the base-pairs define the radius of the double helix and all these combine to decide, as a rough approximation, how the double helix twists into a specific conformation.

1.4.5 The double helix conformations

In single stranded RNA or the A-form helices (DNA:RNA and RNA:RNA), the *anomeric* and *gauche* effects lead to predominantly N-type or $C3'$ -endo conformations of the sugar ring. In the B-form of DNA (DNA:DNA) under physiological conditions, the sugars adopt the $C2'$ -endo or the S-type conformations. Both A- and B-form helices are antiparallel right-handed helices²⁹ that differ mainly in the sugar pucker as mentioned above, which contributes to the other differences between the two forms, such as, (i) the number of base-pairs per helical turn (10 in B-DNA Vs. 11 in A-DNA), (ii) the plane of the nucleobases (perpendicular to the helix axis in B-DNA Vs. slightly tilted in A-DNA), (iii) the major and minor grooves (the major groove is wide and deep in B-DNA Vs. narrow and

deep in A-DNA; the minor groove is deep and narrow in B-DNA Vs. wide and shallow in A-DNA). With increased nucleobase stacking and hydrogen bonding interactions in pseudoaxial base orientation in N-type sugars, the RNA:RNA/DNA duplexes are more stable than the DNA:DNA duplexes.

1.5 Conformational restriction/ pre-organization

Nucleosides locked in the N-type (3'-*endo*) sugar conformation by the introduction of a methylene link between the 2'-O and 4'-C were reported independently by Imanishi *et*

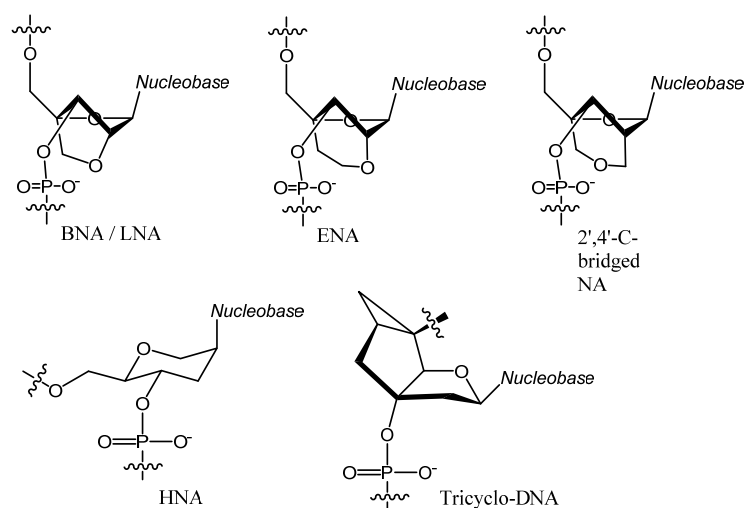


Figure 9. Constrained/preorganised modifications for enhanced stability.

*al.*³⁰ (BNA, Bridged Nucleic Acids) and Wengel *et al.*³¹ (LNA, Locked Nucleic Acids). The conformational locks in these systems lead to local organization of the phosphate backbone, which increases the strength of base-stacking interactions (Figure 9). These nucleic acids were found to bind with high affinity to complementary DNA and RNA, specially with RNA, mainly as a consequence of entropic advantage. The LNA bases within a mixed DNA-LNA strand of a complex with RNA induce flanking DNA bases to adopt an A-type conformation. The A-type conformation of DNA affects the ability to activate RNase-H-induced cleavage of bound RNA, detrimental to antisense applications. Novel 2'-4' conformationally restricted nucleosides were designed that combined the structural elements of 2'-*O*-methoxyethyl (MOE) residues and locked nucleic acids.

LNA (or 2'-4'BNA) is essentially a 2'-*O*-Me nucleoside where the methyl group is constrained back to the 4'- position of the furanose ring system (Figure 10).

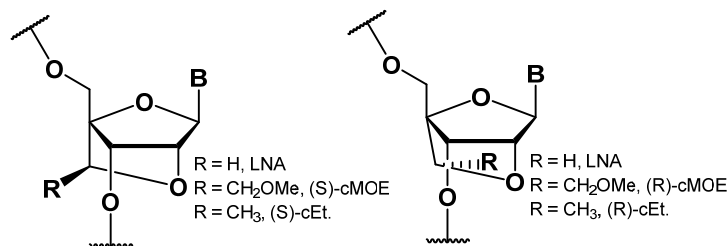


Figure 10. Novel constrained cMOE and constrained cEt nucleosides.

Similarly constraining the ethyl chain in the MOE residue back to the 4'-position, the cMOE and cEt modifications³² were introduced leading to improved hybridisation and steric and hydration attributes of MOE and thereby improve the safety profile of the antisense oligonucleotides containing these modifications. Some other constrained analogues, the 2',4'-C-bridged 2'-deoxynucleosides³³ and the 2'-*O*,4'-C-ethylene-bridged nucleic acids (ENA)³⁴ were reported. These nucleic acids are also locked in the N-type (3'-*endo*) sugar conformation and exhibit enhanced binding to complementary RNA. They also have dramatically increased resistance to exonucleases, enhancing their applicability as antisense agents. 1',5'-anhydrohexitol nucleic acids (HNA)³⁵ are completely stable towards 3'-exonucleases and form very stable self-complementary duplexes as well as sequence-selective duplexes with complementary DNA and RNA. The complexes involving LNA/BNA, DNA-HNA closely resemble the A-form structure of dsRNA, as evident from CD studies. Tricyclo-DNA was developed by Leumann *et al.*³⁶ to explore the effect of further conformational restriction on the association mode and affinity to complementary nucleic acids. In comparison to bicyclo-DNA, there is additional conformational stabilization of the carbocyclic five-membered ring and also a partial correction of the torsional angle γ toward the anticlinal range. These NAs exhibit no self-pairing, but form stable duplexes with complementary NAs. They are also stable to enzyme degradation.

1.6 Antisense approach

In the antisense approach, an antisense drug works at the genetic level to interrupt the process by which disease-causing proteins are produced. While traditional drugs only

work with protein molecules that sustain or induce some disease, the antisense drugs have the ability to inhibit the production of the disease-causing proteins. The antisense molecule can control different types of diseases in a selective manner. This technology has become a powerful tool to modulate gene expression in animals and represents an innovative platform for therapeutics.³⁷ The targets for antisense drugs are RNA molecules and the antisense oligonucleotide binds to messenger RNA (mRNA) and inhibits the production of disease-causing proteins. A significant advantage of the antisense approaches to traditional small molecule-based drug development is the possibility of targeting mRNA from any gene. There are multiple mechanisms that can be exploited to interfere in the function of RNA.³⁸

1.6.1 Antisense mechanism

A natural enzyme called RNase H is frequently used to degrade the target mRNA. When the antisense oligonucleotide binds to the target RNA, this enzyme cleaves the RNA strand of an RNA-DNA hetero duplex thus preventing the translation process³⁹ (Figure 11).

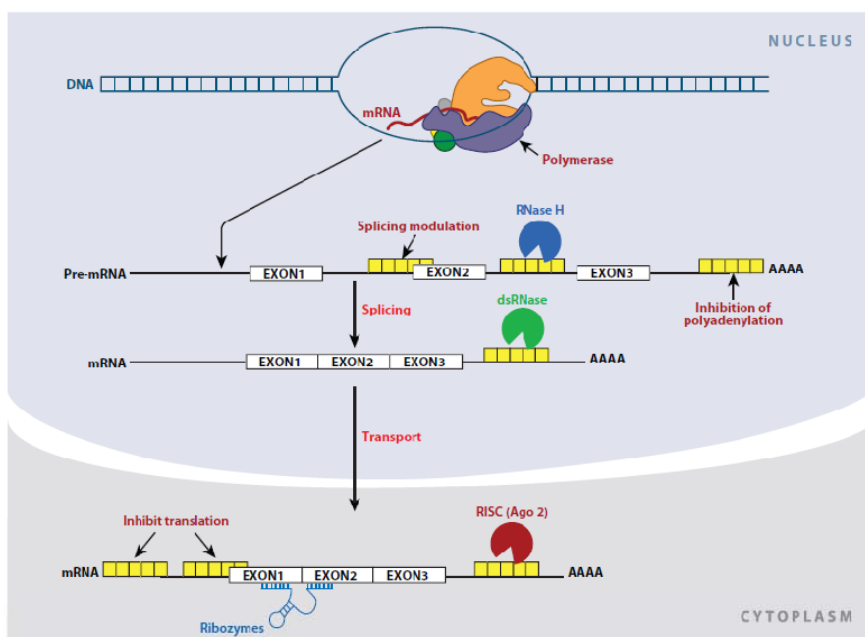


Figure 11. Different antisense mechanisms: different steps of maturation of mRNA where ASOs are known to interact and block the function of the mRNA. **Nondegradative mechanisms** (modulation of RNA splicing, modulation of polyadenylation, inhibition of translation.) and **mechanisms that promote degradation of the RNA** (RNase H, RNA interference(Ago2), ribozymes, and double-stranded RNases (dsRNase) (Bennett, F.C. and Swayze, E.E., *Annu. Rev. Pharmacol. Toxicol.* **2010**,50, 259-293.)

Another antisense mechanism is RNA interference¹ or RNAi. This mechanism involves using small interfering RNA or siRNA to target a mRNA sequence. The siRNA molecules bind to a protein complex termed RNA-induced silencing complex (RISC), which unwinds the two RNA strands allowing the antisense strand to bind to the target RNA.¹ Further the RISC also contains an endonuclease activity which hydrolyses the target RNA.^{40,2b} RNase L is also used in antisense applications.⁴¹ RNase L is a ribonuclease activated by 2'-5'linked oligoadenylates generated in response to interferon activation. Linkage of 2'-5' oligoadenylates to an antisense oligonucleotide has been reported to promote selective cleavage of the target mRNA.⁴² In addition to utilising the cellular nucleases to cleave the target RNA, oligonucleotides have been designed to chemically cleave the target RNA after hybridization. These are ribozymes and DNAzymes.⁴³ A translational arrest mechanism can be employed by sterically blocking certain sites in the 5'-untranslated region of an mRNA with an antisense oligonucleotide. The 5'-terminus of a transcript is a good target site for oligonucleotides as the occupancy of this region prevents the assembly of ribosome on the RNA.⁴⁴ Regulation of RNA processing or RNA splice correction is another efficient mechanism in which oligonucleotides can be utilised to regulate gene expression.⁴⁵ Dean and Bennett⁴⁶ have compared many of the antisense mechanisms in cell-based assays and have found that once optimized, oligonucleotides that work by each mechanism can be potent and selective inhibitors of gene expression and it also shows that no single mechanism is vastly superior to the other mechanisms. Thus, there is always a need to tailor the mechanism for a specific biological application.

1.6.2 Antisense Oligonucleotides

To enhance the properties of antisense oligonucleotides chemical modifications are a necessity. The key issues to be addressed are: increase the stability, increase the nuclease resistance, enhance potency and decrease toxicity. Among the first generation antisense oligonucleotides are the phosphorothioates,⁴⁷ in which the non bridging oxygen atom in the phosphodiester linkage is substituted by a sulfur atom (Figure 12). Phosphorothioates are commercially available, easy to synthesize, support the RNase H activity and exhibit acceptable pharmacokinetics for systemic and local delivery. The first antisense

oligonucleotide drug in clinical use is Vitravene⁴⁸ which acts by blocking translation of viral mRNA. Vitravene is a phosphorothioate oligonucleotide, this synthetic modification is one of that has been shown to confer greater resistance to nuclease degradation. The morpholino modification is a replacement of the furanose ring by the morpholine ring with a neutral phosphorodiamidate linkage.⁴⁹ They exhibit a binding affinity similar to DNA-DNA duplexes and are nuclease stable but they do not support RNase H activity. They have been reviewed in detail and show promising results for modulated splicing and translational arrest.⁵⁰ Peptide nucleic acid (PNA) is unique in which the sugar phosphate backbone is completely replaced with a peptide-based backbone.⁵¹ This modification resulted in higher affinity for complementary nucleic acids and completely resistant to nucleases and peptidases. Poor solubility and cell penetration were the main drawbacks in using them as antisense agents.⁵² The increase in binding affinity with 2'-sugar modifications is energetically driven by the electronegative 2'-fluoro group (Figure 12). This has been

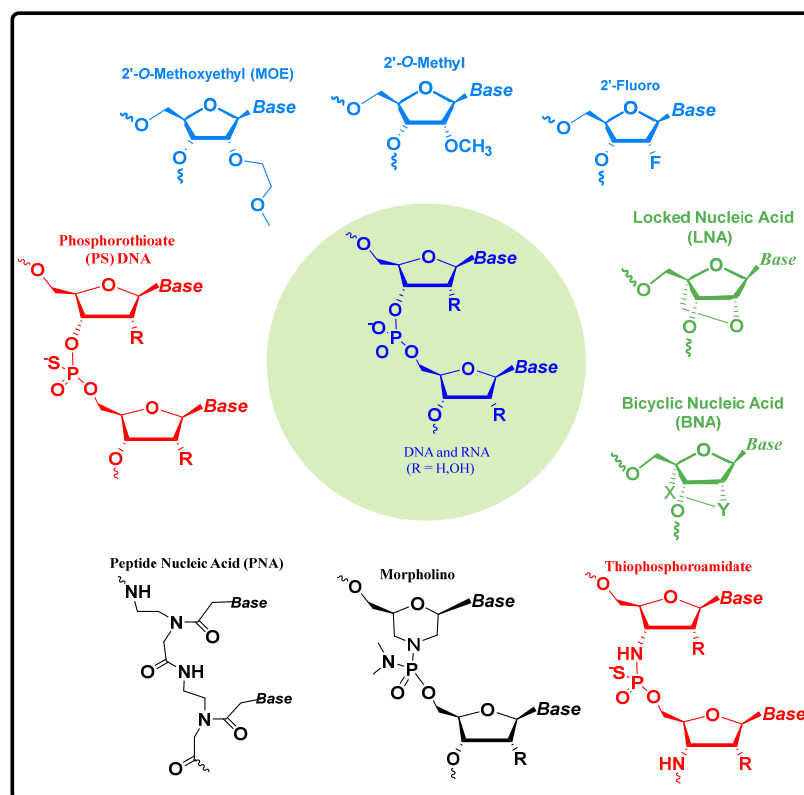


Figure 12. Representation of three generations of nucleotide modifications for use in antisense oligonucleotides. (Bennett, F.C. and Swayze, E.E., *Annu.Rev. Pharmacol. Toxicol.* **2010**,*50*, 259-293.)

employed in the design of siRNA oligonucleotides.⁵³ The most advanced sugar modifications 2'-*O*-methyl and 2'-*O*-methoxyethyl (MOE) resulted in a 3-10 fold increase in potency in cell-based assays compared to phosphorothioate oligonucleotides, an increase in nuclease resistance and decreased cytotoxicity.^{37,42,54} Since the 2'-*O*-modified oligonucleotides do not support RNase H mechanism, a chimeric strategy was developed that focused on the design of high affinity, nuclease resistance oligonucleotides which contain a 'gap' of continuous phosphorothioate modified oligonucleotides. Introducing constraint in sugar modification gives rise to large entropic gains in binding affinity. The 2',4' bicyclic nucleic acid BNA/LNA^{30a,31b,55} showed dramatically improved hybridization properties and nuclease resistance.

1.7 Quadruplex-forming DNA and applications in therapeutics

1.7.1 Quadruplex DNA-the beginning

The quadruplex DNA has attracted a lot of attention recently.⁵⁶ The ability of guanosine -rich DNA to form unusual structures characterized by the ready formation of polycrystalline gels was observed much earlier by a medical doctor/ clinical laboratory scientist Ivar Christian Bang (1869-1918).^{57,58} In 1962, after almost five decades it was proposed that short guanine rich stretches of DNA could assume unusual structure.⁵⁹ On the basis of diffraction studies and the UV melting experiments of polyguanylic acid gels, it was concluded that if four guanines were close enough, together they could form planar hydrogen-bonded arrangements, now called guanine quartets (Figure 13) The existence of

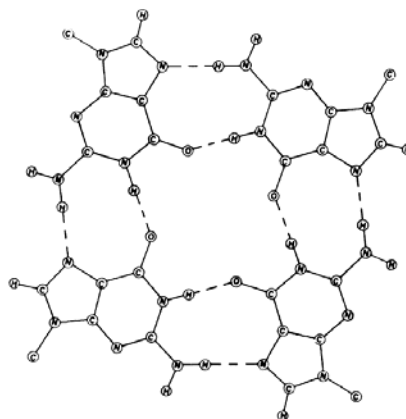


Figure13. Proposed arrangement of bases in GMP gels.

such planar tetramers in solution was found to result in the formation of linear aggregates formed by the stacking of tetramers as the large planar surfaces would result in strong van der Waals attractions. Such aggregates are now called G-quadruplexes.

The significance of DNA and RNA G-rich sequences having the ability to self-associate and form novel higher ordered structures assumed importance when guanine-rich repeat sequences were identified at the ends of human chromosomes.⁶⁰ The d(TTAGGG) repeat sequences, termed telomeres, were shown to play a major structural and regulatory role in chromosomal maintenance, and crucially ended in an extended single stranded G-rich 30 DNA overhang⁶¹ ideal for G-quadruplex formation. The enzyme telomerase, that is involved in extending 30 telomeric repeats has recently received a lot of attention, when in 2009 the Nobel prize in physiology or medicine was awarded (Blackburn E.H., Greider, C.W. Szostak, J.W.) with their focus on this vital enzyme and telomere maintenance. The exploitation of DNA and RNA quadruplexes as therapeutic targets was first developed for telomeric DNA. The formation of quadruplexes in telomeres decreases the activity of telomerase. The recent findings⁶² of abundant G-quadruplexes sprinkled throughout the human genome and their ability in controlling gene expression through regulating transcription and translation has given quadruplex cancer therapeutics an uplift beyond the ends of chromosomes and telomerase inhibition.

1.7.2 Types of quadruplex structures

The three main structures of this type are the **Holliday junction**,⁶³ the **G-quadruplex**⁶⁴ and the **i-motif tetraplex**⁶⁵ (Figure 14). These show very different and unique helical forms, starting with a conformation that is most similar to B-DNA, and leading through forms that differ dramatically from the original Watson-Crick model.

Holliday junctions are four-stranded junctions that are formed as intermediates during recombination of two homologous DNA duplexes, to enable the reciprocal exchange of genetic information. These DNA junctions were shown to adopt either an extended open-X form under low-salt conditions, or a more compact stacked-X conformation as the negatively-charged phosphate backbone becomes shielded under high salt conditions.

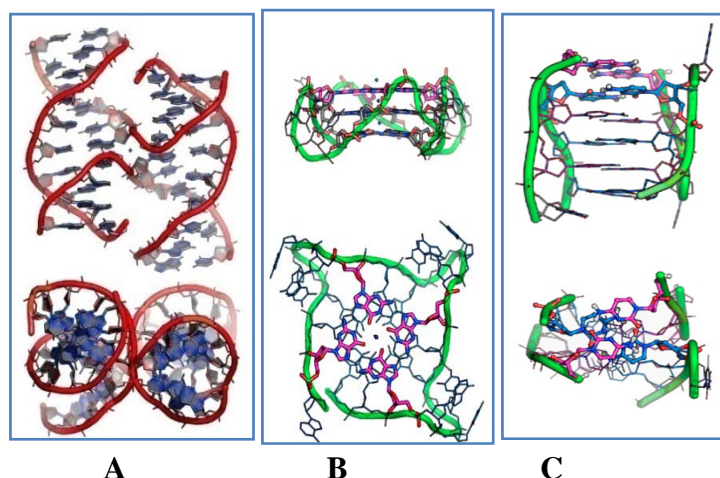


Figure 14. Structure Holliday Junction **A**; G-Quadruplex **B**; i-Motif **C** (Ho, P. S.; Carter, M. in *DNA replication-Current Advances*, 2011, Ed. Seligmann, H., ISBN 978-953-307-593-8.

i-motif tetraplexes are formed by C-rich sequences, and involve intercalation between two parallel C-strands in head-to-tail fashion.⁶⁶ The two duplexes are stabilized by base-pairing the Watson-Crick edges of two cytosines to form hemi-protonated C:C⁺ pairs.

G-quadruplexes comprise four-stranded structures that are formed from guanine-rich sequences. They are held together by hydrogen-bonding between the Watson-Crick face of each guanine with the Hoogsteen face of an adjacent guanine, creating a cyclic arrangement of four guanines in a G-tetrad (Figure 15a). These tetrads are stacked in a right-handed helical motif,⁵⁹ with a helical twist of 30° and a diameter of 25Å, and are stabilized by monovalent cations co-ordinated to the O6 oxygen atoms of the guanines, and sandwiched between the base-stacks. These cations neutralize the electrostatic repulsion between the guanine O6 atoms and thus stabilize the overall structure (Figure 15b).

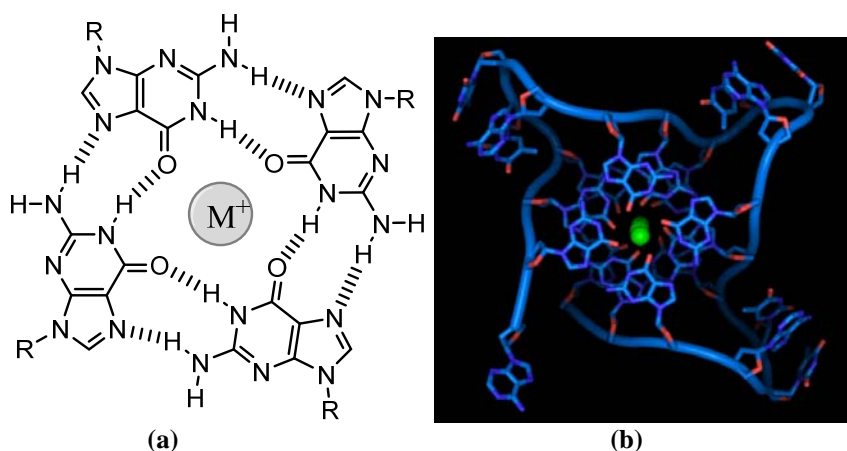


Figure 15 (a) The G-tetrad, (b) The G-quadruplex stacked structure arising from G-rich sequences. (<http://www.molecularstation.com/molecular-biology-images/>)

1.7.3 Structural polymorphism in G-quadruplexes

G-quartets can be formed from the association of one or more G-rich strands of DNA, (Figure 16) i.e., they may be intra- or inter-molecular, and can display a wide variety of topologies, based on strand polarity, loop length and geometry, the presence of metal ions, the oligonucleotide concentration in the solution, etc.⁶⁷

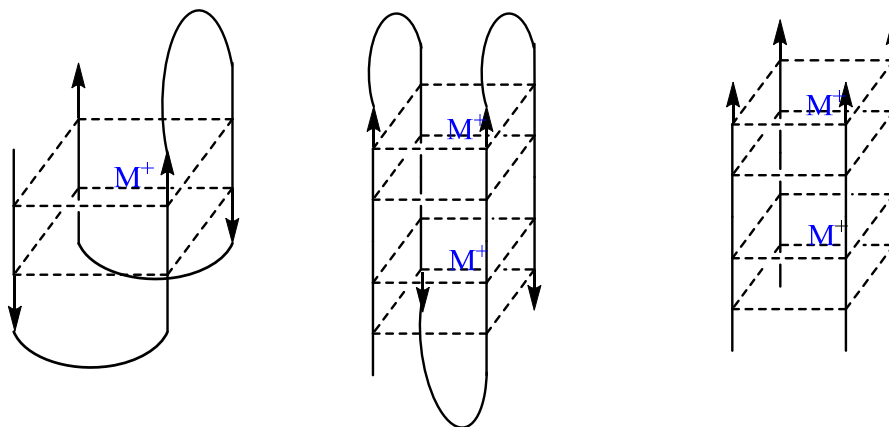


Figure 16. Schematic representation of G-quartets, antiparallel, unimolecular and multimolecular parallel DNA G-quadruplex.

The central charged cavity can accommodate a variety of different cations of differing radii, that strongly influences not only the final folded topology of the quadruplex, but also its stability. Potassium is generally found to be optimal and leads to increased G-quadruplex stability. The phosphate backbone generates four grooves that accommodate well-defined networks of ordered water molecules. In RNA and DNA G-quadruplexes, the G-tetrad stacks remain planar with a similar rise and twist, but the direction of the phosphodiester backbone may vary. Unlike in DNA/RNA duplexes, where an antiparallel strand orientation is predominant, in G-quadruplexes, the strands may exist in any combination of parallel and antiparallel orientations. The linkers between the G-stretches forming the tetrads generally make three different types of connections in stacked G-quadruplexes, viz., (i) lateral loops, which join adjacent antiparallel phosphate backbones on the same quadruplex surface, (ii) cross-diagonal, which link opposite antiparallel strands on the same surface and (iii) propeller loops, which link adjacent parallel strands on opposite surfaces (Figure 17)

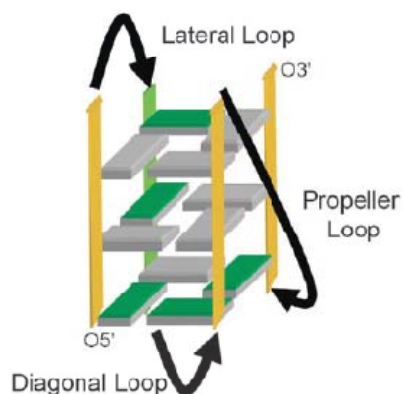


Figure 17. G-quadruplex linker orientations. Linking loop motifs (black arrows). Backbone strand polarity: parallel (yellow) and antiparallel (green). Glycosidic torsion angles: anti-conformation (grey) and syn-conformation (dark green). (Collie, G. W., Parkinson, G. N., *Chem. Soc. Rev.*, **2011**, *40*, 5867-5869).

The linker length is instrumental in defining the final topology and stability of the quadruplex, and also determines if the resulting quadruplex will be intra- or inter-molecular⁶⁸. A detail study on the influence of loop length on the stability and folding topology of intramolecular DNA G-quadruplexes has been reported. Balasubramanian *et al.*⁶² have designed G-rich DNA libraries (Figure 18) and used UV T_m and CD to examine and compare the properties of 21 DNA quadruplex libraries. This study provided a framework to identify or classify biologically relevant G-quadruplex forming sequence.

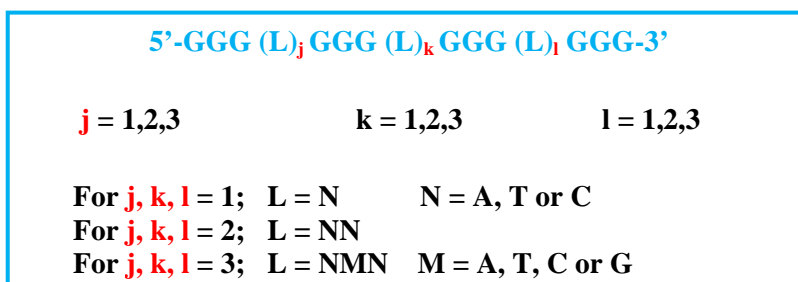


Figure 18. G-rich DNA libraries designed to determine the stability and folding topology of G-quadruplexes.

1.7.4 Influence of sugar, base conformations on the topology and stability of G-quadruplexes

In G-quadruplexes, the sugar can assume both C2'- and C3'-*endo* conformations and the guanine bases can be found in either *anti* or *syn* positions respectively. The relationship between backbone strand orientation (+/-), glycosidic torsion angles (syn/anti) and groove widths (w/m/n) is based on simple geometric relationships and structural

constraints imposed by the guanines held in the stacked G-tetrads, and together impact the quadruplex structure.⁶⁹ All parallel stranded quadruplexes have the nucleobases either all *syn* or all *anti* oriented, while in antiparallel stranded quadruplexes, mixed *syn*- and *anti*-oriented nucleobases are observed. The groove widths are equal when all the strands are aligned parallel (all *syn* or all *anti*) and antiparallel arrangement generates both wide and narrow grooves (mixed *syn*, *anti*).^{67b} The sugar pucker (N-/S-type) influences the nucleobase orientation and can be used at predetermined positions, depending upon the requirement, in order to stabilize the resulting quadruplex, e.g., LNA, which has the sugar locked in the C3'-*endo* pucker, promotes a *anti* orientation of the nucleobase because the *syn* orientation is prohibited due to a steric clash between H3' and N3.⁷⁰ Stabilization could also be achieved by addition of large aromatic chromophores, intercalating nucleic acids (INA),⁷¹ or twisted intercalating nucleic acids (TINA).⁷² The differences between RNA and DNA quadruplexes occur mainly due to the absence of the C5-methyl group in RNA and the presence of the C2'-hydroxyl group in the ribose sugar of RNA, the hydroxyl group having a larger effect. This -OH group influences the sugar pucker to be predominantly in the C3'-*endo* or the N-type and favours *anti* conformation about the glycosidic bond. However, the RNA quadruplex displays a mixture of C2'-*endo* and C3'-*endo* sugar puckers, similar to the DNA quadruplex. Additionally, the -OH group offers additional sites for hydrogen-bonding interactions. The methyl group at the C5 position of thymine, that is absent in uracil, is likely to affect the hydration structure within the loop around the grooves.

1.7.5 The G-quadruplex in aptamers

Aptamers are single-stranded DNA or RNA or modified nucleic acids that can fold into specific three-dimensional structures that can bind to specific targets with selectivity, specificity and affinity equal or superior to those of antibodies. In 1990 Joyce,⁷³ Szostak⁷⁴ and Gold⁷⁵ independently reported on the development of an *in vitro* selection and amplification technique for the isolation of oligonucleotides able to bind non-nucleic acid targets with high affinity and specificity. Several of these aptamers were found to be G-rich with an ability to form G-quadruplex structures. The enhanced resistance to nuclease

degradation and increased cellular uptake are advantageous in the development of **G-quadruplex aptamers as drug candidates**.⁷⁶ Structural information is critical to the development of G-quadruplex aptamers in order to enable modifications that enhance their function. One of the most extensively studied G-quadruplex aptamer is the **thrombin-binding aptamer**⁷⁷ (TBA), where the rational design could lead to several chemical modifications to allow improvements. Besides TBA, several other G-quadruplex-based aptamers have been designed successfully to target a number of **HIV protein targets**,⁷⁸ **bovine prion proteins**⁷⁹ (RNA aptamers), **anticancer targets such as nucleolin**⁸⁰ and **STAT3**.⁸¹ In addition to targeting protein binding and function regulation, G-quadruplex aptamers have also been reported in **DNAzyme-based detection of drug molecules**,⁸² **protein and hormone detection**,⁸³ **drug delivery**,⁸⁴ **affinity capture of insulin and IGF-II**.⁸⁵

1.7.6 Thrombin-binding aptamer

The thrombin-binding aptamer was first discovered in 1992⁷⁷ as a 14-17 nucleotide consensus sequence within artificially selected thrombin-binding single-stranded DNA sequences which were able to inhibit clot formation. NMR and X-ray structural studies⁸⁶ showed this sequence [d(GGTTGGTGTGGTTGG)] to be an intramolecular antiparallel G-quadruplex, with two G-quartets stacked on each other and linked by edge-wise two TT loops and one TGT loop (Figure19). The quadruplex forming, Thrombin binding aptamer TBA has been innovatively used as a DNA based nano machine that can cyclically bind and release thrombin. In a communication Dittermer *et al*⁸⁷ have used DNA-fuelled system based on quadruplex– duplex transition to control the concentration of the human blood-

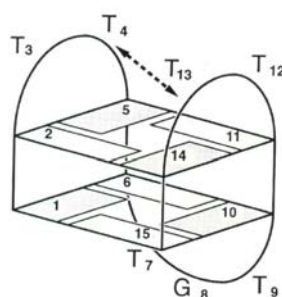


Figure 19 Thrombin binding aptamer. (Schultze, P., Macaya, R. F., Feigon, J., *J. Mol. Biol.* **1994**, 235, 1532).

clotting a thrombin in solution. The core sequence is the aptamer TBA that, when folded in a quadruplex structure, strongly binds to thrombin; switching between a quadruplex and a duplex conformation leads to trapping and releasing of thrombin, respectively (Figure 20). This approach may be extended to regulate other biological processes too.

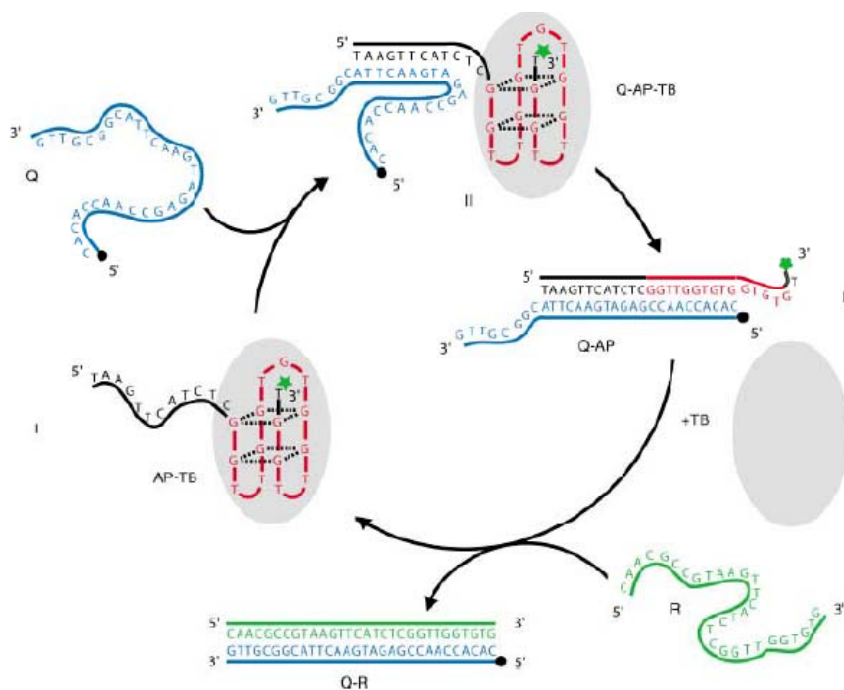


Figure 20. Schematic of the operation cycle of the aptamer –based molecular machine in the presence of thrombin. (Dittmer, W.U., Reuter and Simmel, F.C., *Angew.Chem. Int.Ed.*,**2004**, *43*,3550-3553).

1.8 Tools and techniques for structural studies of nucleic acid complexes, and higher ordered G-quadruplexes

1.8.1 UV-spectroscopy

The absorbance of polynucleotide depends on the sum of the absorbance of all the nucleotides and the effect of the interacting nucleotides. The interactions cause a single strand to absorb less than the sum of its nucleotides and a double strand absorbs less than its two component single strand. The effect is called hypochromicity which results from the coupling of the transition dipoles between neighboring stacked bases and is larger in amplitude for A-U and A-T pairs.⁸⁸ Conversely, hyperchromicity refers to the increase in absorption when a double stranded nucleic acid is dissociated into single strands. The UV

absorption of a DNA duplex increases typically by 10-20% when it is denatured. This transition from a stacked, hydrogen bonded double helix to an unstacked, strand-separated coil has a strong entropic component and is temperature dependent. The mid-point of this thermal transition is known as the **melting temperature** (T_m). The converse of melting is the renaturation of two separated complementary strands to reform the duplex.

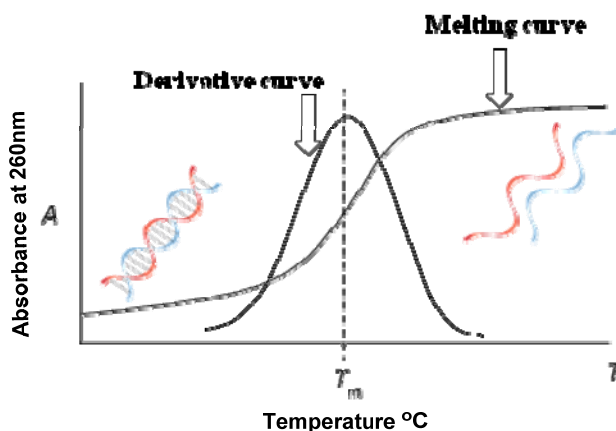


Figure 21. An oligonucleotide duplex melting curve and derivative curve

Duplex melting: According to the ‘all or none model’⁸⁹, the UV absorbance value at any given temperature is an average of the absorbance of duplex and single strands. A plot of absorbance at 260 nm against temperature gives a sigmoidal curve in case of duplexes and the midpoint of the sigmoidal curve (Figure 21) called as the ‘melting temperature’ (T_m) (equilibrium point) at which the duplex and the single strands exist in equal proportions.

Triplex melting: In the case of triplexes, the first dissociation leads to melting of triplex generating the duplex (*WC* duplex) and third strand (*Hoogsteen* strand), followed by the duplex dissociation to form two single strands. The DNA triplex melting monitored at 260 nm shows characteristic double sigmoidal transition and UV melting temperature for each transition is obtained from the first derivative plots. The lower melting temperature (T_{m1}) corresponds to triplex to duplex transition while the second higher melting temperature (T_{m2}) corresponds to the transition of duplex to single strands.⁹⁰

Quadruplex melting: Monitoring of melting for G-quadruplexes⁹¹ with increasing temperature is carried out at 295 nm. This wavelength maximises hyper/hypochromic shift

between the folded and unfolded states. The refolding of the DNA/RNA during the cooling process can also like-wise, be monitored. Analysis of the UV-melting graphs can provide information of the thermodynamics of the system, which can be combined with CD and calorimetry data such as DSC or ITC to generate a fuller picture of the formation of the stacked complexes.

1.8.2 Circular Dichroism (CD)

Circular dichroism is a spectroscopic technique that has been widely used for the secondary structure elucidation of chiral molecules, including biomolecules. It has thus been instrumental in the confirmation of the B- and A-form duplex of DNA/RNA. Circular dichroism (CD) spectroscopy measures differences in the absorption of left-handed polarized light versus right-handed polarized light which arise due to structural asymmetry. The absence of regular structure results in zero CD intensity, while an ordered structure results in a spectrum which can contain both positive and negative signals. CD is particularly useful for studying chiral molecules and has very special significance in the characterization of biomolecules (including the secondary structure of proteins and the handedness of DNA). The commonly used units in current literature are the mean residue ellipticity ($\text{degree cm}^2 \text{dmol}^{-1}$) and the difference in molar extinction coefficients called as molar circular dichroism or $\Delta\epsilon$ ($\text{liter mol}^{-1}\text{cm}^{-1}$). The molar ellipticity $[\theta]$ is related to the difference in molar extinction coefficients by $[\theta] = 3298 (\Delta\epsilon)$. In the nucleic acid, the heterocyclic bases are principal chromophores. As these bases are planar, they do not have any intrinsic CD. CD arises from the asymmetry induced by linked sugar group. CD spectra from the dinucleotide exhibit hyperchromicity, being more intense by roughly an order of magnitude than those from monomers. It is when the bases are linked together in polynucleotides, giving rise to many degenerate interactions that they gain additional characteristics associated with the asymmetric feature of secondary structure such as in proteins and nucleic acids.⁹²

The simplest application of CD to DNA structure determination is for identification of polymorphs present in the sample.⁹³ The CD signature of the B-form DNA as read from

longer to shorter wavelength is a positive band centered at 275 nm, a negative band at 240 nm, with cross over around 258 nm.

These two bands arise not from a simple degenerate exciton coupling, but as a result of superimposition of all coupling transitions from all the bases. A-DNA is characterized by a positive CD band centered at 260 nm that is larger than the corresponding B-DNA band, a fairly intense negative band at 210 nm and a very intense positive band at 190 nm (Figure 22). The 250-230 nm region is also usually fairly flat though not necessarily zero. Naturally occurring RNAs adopt the A-form if they are duplex. CD denaturation (melting) and CD-Job's plots are equally important as they give T_m and binding stoichiometry of DNA/RNA complexes respectively.

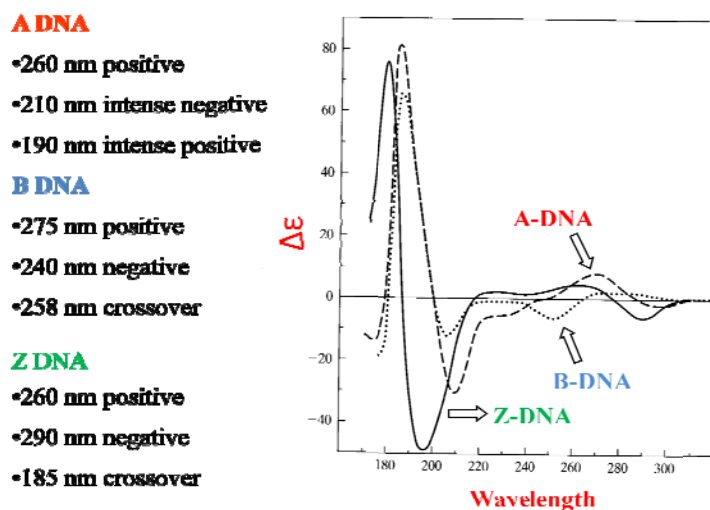


Figure 22. CD spectra of DNA secondary structure

1.8.3 Stoichiometry of binding

The binding *stoichiometry* of oligonucleotide to target DNA/RNA by UV-titration (mixing) can be derived from Job's plot.⁹⁴ The two components of the complex are mixed in different molar ratios, so that the total concentration of each mixture should be constant, i.e., as the concentration of one strand decreases, concentration of the second strand increases and the UV-absorbance of each mixture is recorded. The absorbance decreases in the beginning to a minimum and then again increases. The molar ratio of the two strands at which absorbance reached minimum indicates the stoichiometry of complexation. CD has been used to detect the primary structure of a G-quadruplex for a given sequence. In

addition to the detection of G-quadruplex existence, CD is also able to provide some information as to the relative nucleobase orientations *anti* or *syn*, exhibiting unique spectra from which topological arrangements of either parallel (240nm_{min}/260nm_{max}) or mixed parallel-antiparallel or antiparallel (260nm_{min}/290nm_{max}) strand orientations can be inferred, though not guaranteed.⁹⁵ CD spectra vary with ligand/salt binding, allowing these conditions to be easily studied. Both DNA and RNA G-quadruplexes have been studied by CD, which is an exceptionally useful tool in this area.⁹⁶ However, care should be taken while drawing conclusions regarding topology, since out of the 26 theoretically available loop arrangements for a sequence containing four G-runs, 25 will be antiparallel, while one will be parallel.⁶⁹

1.8.4 Fluorescence spectroscopy

Molecules of DNA rich in guanine, exhibit significantly higher fluorescence (quantum yield of polyG at room temperature in aqueous solution is 4.7×10^{-4}) than homologous sequences without consecutive guanines.⁹⁷ G-quadruplexes have been shown to be intrinsically fluorescent,⁹⁸ which makes fluorescence spectroscopy a very convenient tool to monitor their formation, circumventing the necessity for any additional fluorescent labels.

1.8.5 Polyacrylamide gel electrophoresis (PAGE)

Polyacrylamide gel electrophoresis has long been used to study and prove complex formation in DNA/RNA, ranging from duplex to triplex and even quadruplex formation. The stability of the complexes to enzyme digestion is also conveniently monitored by PAGE, which can be used to prove the stability/susceptibility of native or modified complexes and also the single strands. Footprinting studies afford information about binding sequences. Native PAGE can be used to differentiate structural changes too, such as caused by nicks, bends, or by the formation of folded and compact structures as in the case of G-quadruplexes. Thus, folded G-quadruplexes migrate faster within the gel matrix than the equivalent unfolded structure. Moreover, the addition of specific ions to the running buffer/gel allows the formation of G-quadruplexes in response to ionic conditions to

be investigated. Further association of the G-quadruplexes, such as dimers and higher multimers can also be demonstrated by PAGE.⁹⁹ Here again, care must be exercised when interpreting band patterns, as molecular species cannot always be unambiguously assigned, as the exact size of each species will not be known.

1.8.6 Nuclear Magnetic Resonance (NMR)

NMR spectroscopy is a powerful experimental technique that is useful for confirmation of the formation and topology of complexes of DNA and RNA such as duplexes, triplexes and quadruplexes. It also can be used to study hydrogen-bonding between the nucleobases. The information obtainable includes sugar pucker characterization, backbone conformations and also local architecture. In the case of G-tetrad formation, 1D proton NMR spectra provides characteristic imino, amino and aromatic peaks, indicating the presence of Hoogsteen and Watson-Crick base-pairing. Further structure elucidation, of course, necessitates the use of more specialized techniques such as NOESY, TOCSY, HSQC-COSY, etc. The introduction of high field NMR and cryoprobes have in turn, reduced the need for higher concentrations of sample and made the analysis more affordable. This technique has clearly dominated the structure elucidation research of quadruplex folding and topology.

1.8.7 MALDI TOF Mass Spectroscopy

Matrix-assisted laser desorption/ionization time-of-flight (MALDI TOF) is a soft ionization technique¹⁰⁰ used in the analysis of biomolecules (biopolymers such as DNA¹⁰¹, proteins, peptides and sugars) and large organic molecules (such as polymers, dendrimers and other macromolecules), where these large ions obtain in gas phase producing many fewer multiply charged ions. MALDI is a two step process. First, desorption is triggered by a UV laser (nitrogen lasers 337 nm) beam. Matrix material heavily absorbs UV laser light, leading to the ablation of upper layer (~micron) of the matrix material. The hot plume produced during ablation contains many species: neutral and ionized matrix molecules, protonated and deprotonated matrix molecules, matrix clusters and nanodroplets. Second, the analyte molecules are ionized (more

accurately protonated or deprotonated) in the hot plume. The time-of-flight (TOF) analyzer uses an electric field to accelerate the ions through the same potential, and then measures the time they take to reach the detector. If the particles all have the same charge, the kinetic energies will be identical, and their velocities will depend only on their masses. Lighter ions will reach the detector first. Their time-of-flight is proportional to their $(MW)^{1/2}$.

The matrix is the crystalline, a low molecular weight compound with several conjugated double bonds. The some basic properties are that they should not evaporate during standing in spectrometer, often acidic for acting as a proton source to encourage ionization of the analyte molecules, strong optical absorption in either the UV or IR range. Most commonly used matrices are 3, 5-dimethoxy-4-hydroxycinnamic acid (sinapinic acid, SA), α -cyano-4-hydroxycinnamic acid (alpha-cyano or alpha-matrix, CHCA) and 2, 5-dihydroxybenzoic acid (DHB). 2', 4', 6' trihydroxy acetophenone (THAP). A solution of one of these molecules is made, often in a mixture of highly purified water and an organic solvent (normally acetonitrile (ACN) or ethanol). Trifluoroacetic acid (TFA) or Ammonium citrate may also be added.

1.8.8 HPLC

HPLC is a chromatographic technique that has been used traditionally for separation of mixtures and also quantification of the components. When coupled to other analytical techniques, such as mass spectrometry, it is a powerful analytical technique. In the present work of this thesis, this technique has been successfully employed to study the degradation of single-stranded nucleic acid oligomers (both modified and unmodified) by analysing the elution profile of the digestion mixture at different time-points by reverse-phase HPLC. Accordingly, the area under the peak can be used to quantify the amount of intact oligonucleotide. When plotted against time, this gives an idea of the half-life of the oligonucleotide under the given test conditions.

1.9 Present work

Chapter 1 comprises literature overview regarding nucleic acids (DNA/RNA) with respect to their conformations in basic and higher ordered structures. The exclusive RNA binding features of 2'-5'- linked *iso*DNA/RNA have been reviewed. The pre-organization or

conformational restriction which gives greater stability to the natural DNA:RNA duplexes for applications in antisense therapeutics designing was also surveyed. The recently discovered and biologically important quadruplex forming DNA oligonucleotides have been reviewed describing their important applications in therapeutics. With these recent advances in chemical and structural biology, vast opportunities have opened up to design novel DNA/RNA oligomers, both as antisense oligonucleotides and as aptamers, leading to applications in therapeutics.

Chapter 2 Conformationally constrained and RNA-selective 2'-5' *iso*DNA oligonucleotides exhibit preferred S-type sugar conformations over the N-type sugar geometry in 2'-5' *iso*DNA : RNA duplexes.

The synthesis and biophysical studies of a unique class of 2'-5' linked *iso*DNA oligonucleotides containing nucleoside analogues locked in N-type or S-type sugar ring conformations, selective binding to RNA and nuclease resistance of the 2'-5'linked *iso*DNA oligomers and biophysical studies of these modified oligomers with target DNA/RNA sequences is presented.

The chapter consists of two sections

Section A: The synthesis and structural studies of N-type- and S-type- conformationally locked uridine nucleosides is described in this chapter.

Section B: Synthesis of 2'-5' linked DNA oligonucleotides containing the N-type and S-type modified units and their biophysical studies to determine the effects of these modifications on the stability of duplexes with target DNA/RNA. Also the nuclease resistance of the modified *iso*DNA oligomers in comparison with unmodified DNA and *iso*DNA to snake venom phosphodiesterase (SVPD) is described.

Chapter 3. Synthesis, characterization and biophysical studies of 2'-*O*-allyl/ 3'-*O*-allyl derived DNA and *iso*DNA oligonucleotides.

As a part of antisense therapeutic approach the synthesis and incorporation of 2'-*O*-allyl and 3'-*O*-allyl nucleoside analogues into DNA and *iso*DNA oligonucleotides for their

comparative biophysical studies was undertaken and is presented. This chapter has two sections

Section A: Synthesis of 2'-*O*-allyl and 3'-*O*-allyl-uridine monomers and conversion of 2'-*O*-allyl and 3'-*O*-allyl-uridine to the respective cytidine monomers.

Section B: Incorporation of the 2'-*O*-allyl-uridine and 2'-*O*-allyl-cytidine monomers into 3'-5'DNA oligomers . and that of the 3'-*O*-allyl-Uridine and 3'-*O*-allyl-cytidine monomers into 2'-5'DNA oligomers respectively. A comparative study of the stability of modified 2'-5' DNA:RNA duplexes and the modified 3'-5' DNA :DNA, DNA:RNA duplexes was determined by conducting UV melting experiments.

Chapter 4 Synthesis of a 2'-5'-linked, non-genetic, regioisomeric thrombin binding aptamer (*iso*TBA) , its quadruplex formation, and application as a thrombin inhibitor.

The application of 2'-5'linked *iso*DNA as an aptamer, wherein a 2'-5'linked thrombin binding aptamer (*iso*TBA) is synthesized that folds into a quadruplex structure and binds to thrombin is demonstrated using various spectroscopic techniques in Chapter 4.

This chapter describes the chemical synthesis of a 2'-5'linked thrombin binding aptamer (*iso*TBA) and modified *iso*TBA, and the biophysical studies of *iso*TBA using CD, UV, NMR, fluorescence and gel electrophoresis. A fibrinogen clotting assay using percent transmittance at 495nm was employed to study the inhibition activity of the thrombin binding aptamers. Enzymatic stability of *iso*TBA aptamer sequences to exonuclease enzyme SVPD was also determined.

1.10 References

1. (a) Fire, A., Xu, S., Montgomery, M.K., Kostas, S.A., Driver, S.E. and Mello, C.C., *Nature*, **1998**, *391*, 806-811,(b) Zamore, P.D., *Science*, **2002**, *296*, 1265-1269. (c) Caplan, N. J.; Parrish, S.; Imani, F.; Fire, A.; Morgan, R. A. *Proc. Natl. Acad. Sci. USA*, **2001**, *98*, 9742-9747.

2. (a) Hamilton, A., Baulcombe, D., *Science* **1999**, 286, 950-952, (b) Elbashir, S., Harborth, J., Lendeckel, W., Yalcin, A., Tuschl, T. *Nature* **2001**, 411, 494-988.
3. (a) Chen, K., Rajewsky, N. *Nat. Rev. Gen.*, **2007**, 8, 93-103, (b) Bartel, D. P. *Cell* **2009**, 136, 215-233.
4. (a) Merki, E., Graham, M. J., Mullick, A. E., Miller, E. R., Crooke, R. M., Pitas, R. E., Witzum, J. L.; Tsimikas, S. *Circulation* **2008**, 118, 743-753. (b) El Harchaoui, K.; Akdim, F.; Stroes, E. S.; Trip, M. D.; Kastelein, J. J. *Am. J. Cardiovasc. Drugs* **2008**, 8, 233-242. (c) Athyros, V. G., Kakafika, A., Tziomalos, K., Karagiannis, A., Mikhailidis, D. P. *Expert Opin. Investig. Drugs* **2008**, 17, 969-972.
5. Bennett, F.C. and Swayze, E.E., *Annu.Rev. Pharmacol. Toxicol.* **2010**, 50, 259-293.
6. Watson, J.D. and Crick, F.H.C., *Nature*, 1953, 171, 737-738.
7. Hannon, M. J. *Chem. Soc. Rev.*, **2007**, 36, 280-295.
8. Orgel, L. E., Lohrmann, R., *Acc. Chem. Res.*, **1973**, 7, 368-377.
9. (a) Wallace, J.C. and Edmons, M., *Proc. Natl. Acad. Sci. U. S. A.*, **1983**, 80, 950-954; (b) Kerr, I.M. and Brown, R.E., *Proc. Natl. Acad. Sci. U. S. A.*, **1978**, 75, 256-260.
10. Li, G.; Xiao, W., Torrence, P. J., *J. Med. Chem.*, **1997**, 40, 2959-2966.
11. Giannaris, P. A., Damha, M. J., *Nucleic Acids Res.*, **1993**, 21, 4742-4749.
12. Kierzek, R., He, L., Turner, D. H., *Nucleic Acids Res.*, **1992**, 20, 1685-1690.
13. Premraj, B. J., Raja, S., Yathindra, N., *Biophys. Chem.*, **2002**, 95, 253-272.
14. Dougherty, J. P. Rizzo, C. J., Breslow, R., *J. Am. Chem. Soc.*, **1992**, 114, 6254.
15. Hashimoto, H., Switzer, C., *J. Am. Chem. Soc.*, **1992**, 114, 6255.
16. Jin, R., Chapman, Jr., W. H., Srinivasan, A. R., Olson, W. K., Breslow, R., Breslauer, K., *J. Proc. Natl. Acad. Sci. USA.*, **1993**, 90, 10568-10572.
17. Prakash, T. P., Jung, K. -E., Switzer, C., *Chem. Commun.*, **1996**, 1793-1794.
18. Altona, C., Sundarlingam, M., *J. Am. Chem. Soc.*, **1972**, 94, 8205-8212.
19. Hall, L. D.; Steiner, P. R.; Pedersen, C. *Can. J. Chem.*, **1970**, 48, 1155.
20. (a) W. Saenger, Principles of Nucleic Acid Structure, Springer- Verlag; New York, 1984. (b) Lescrinier, E., Froeyen, M., Herdewijn, P., *Nucleic Acids Research*, **2003**, 31, (12), 2975-2989.
21. IUPAC-IUB Joint Commission on Biochemical Nomenclature *Eur. J. Biochem.*, **1983**, 131, 9-15.

22. Mathé, C.; Périgaud, C. *Eur. J. Org. Chem.*, **2008**, 1489-1505.
23. Plavec, J., Tong, W. M., Chattopadhyaya, J., *J. Am. Chem. Soc.*, **1993**, *115*, 9734-9746.
24. de Leeuw, F.; Altona, C. *J. Comput. Chem.*, **1983**, *4*, 428.
25. Yakovchuk, P.; Protozanova, E.; Frank-Kamenetskii, M. D. *Nucleic Acids Res.*, **2006**, *34*, 564-574
26. Kool, E. T. *Annu. Rev. Biophys. Biomol. Struct.*, **2001**, *30*, 122.
27. Wodak, S. Y.; Liu, M. Y.; Wyckoff, H. W. *J. Mol. Biol.*, **1977**, *116*, 855.
28. Doornbos, J.; Den Hartog, J. A. J.; van Boom, J. H.; Altona, C. *Eur. J. Biochem.*, **1981**, *116*, 403-412.
29. (a) Richmond, T. J., Davey, C. A., *Nature*, **2003**, *423*, (6936), 145-150. (b) Leslie, A. G. W., Arnott, S., Chandrasekaran, R., Ratliff, R. L. *Journal of Molecular Biology*, **1980**, *143*, (1), 49-72. (c) Wahl, M. C., Sundaralingam, M., *Biopolymers*, **1997**, *44*, (1), 45-63. (d) Ghosh, A., Bansal, M., *Acta Crystallographica Section D-Biological Crystallography*, **2003**, *59*, 620-626. (e) Herbert, A., Rich, A., *Genetica*, **1999**, *106*, (1-2), 37-47.
30. (a) Obika, S., Nanbu, D., Hari, Y., Andoh, J-i, Morio, K-i, Doi, T. and Imanishi, T., *Tetrahedron Lett.*, **1998**, *39*, 5401, (b) Imanishi, T.; Obika, S. *Chem. Commun.*, **2002**, 1653-1659.
31. (a) Singh, S. K.; Nielsen, P.; Koshkin, A. A.; Wengel, J. *Chem. Commun.*, **1998**, 455-456, (b) Koshkin, A. A., Singh, S. K., Nielsen, P., Rajwanshi, V. K., Kumar, R., Meldgaard, M., Olsen, C. E. and Wengel, J., *Tetrahedron*, **1998**, *54*, 3607-3630, (c) Braasch, D. A. and Corey, D. R., *Chem. Biol.* **2001**, *8*, 1; (d) Vester, B. and Wengel, J., *Biochemistry*, **2004**, *43*, 13233, (e) Jespen, J. S., Sorensen, M. D., Wengel, J. *Oligonucleotides*, **2004**, *14*, 130-146.
32. (a) Seth, P. P., Siwkowski, A., Allerson, C. R., Vasquez, G., Lee, S., Prakash, T. P., Wanciwicz, E. V., Witchell, D. and Swayze, E. E., *J. Med. Chem.*, **2009**, *52* (1), 10-13, (b) Seth, P. P., Vasquez, G., Allerson, C. R., Berdeja, A., Gauss, H., Kinberger, G. A., Prakash, T. P., Migawa, M. T., Bhat, B. and Swayze, E. E., *J. Org. Chem.*, **2010**, *75*, 1569-1581, (c) Pallan, P. S., Allerson, C. R., Berdeja, A., Seth, P. P., Swayze, E. E., Prakash, T. P., Egli, M., *Chem. Commun.*, **2012**, *48* (66), 8195-8197.

33. Wang, G., Gunic, E., Girardet, J.-L., Stoisavljevic, V., *Bioorg. Med. Chem. Lett.*, **1999**, 9, 1147-1150.
34. Koizumi, M., *Biol. Pharm. Bull.*, **2004**, 27, 453-456.
- 35.(a) Hendrix, C., Rosemeyer, H., Verheggen, I., Seela, F., Van Aerschot, A. and Herdewijn, P., *Chem. Eur. J.*, **1997**, 3, 110, (b) Van Aerschot, A., Verheggen, I., Hendrix, C. and Herdewijn, P., *Angew. Chem. Int. Ed. Engl.*, **1995**, 34, 1338.
- 36.(a) Steffens, R. and Leumann, C.J., *J. Am. Chem. Soc.*, **1997**, 119, 11548, (b) Steffens, R. and Leumann, C.J., *J. Am. Chem. Soc.*, **1999**, 121, 3249, (c) D. Renneberg, D. and C. J. Leumann, C.J., *J. Am. Chem. Soc.*, **2002**, 124, 5993.
37. Crooke, S.T.; *Antisense Drug Technology: Principles, Strategies and Applications*; 2nd ed.; CRC Press Boca Raton, FL, **2007**, p 799.
38. Crooke, S.T., *Biochim. Biophys. Acta.*, **1999**, 1489, 30-42.
- 39.(a) Monia, B.P., Lesnik, E.A., Gonzalez, C. Lima, W.F., McGee, D., Guinasso, C.J., Kawasaki, A.M., Cook, P.D. and Frier, S.M., *J. Biol. Chem.*, **1993**, 268, 14514-14522, (b) Wu, H., Lima, W.F. and Crooke, S.T. *J. Biol. Chem.*, **1999**, 274, 28270-28278.
- 40.(a) Caplan, N.J., Parrish, S., Imani, F., Fire, A., Morgan, R.A., *Proc. Natl. Acad. Sci. USA*, **2001**, 98, 9742-9747, (b) Elbashir, S.M., Harborth, J., Lendeckel, W., Yalcin, A., Weber, K. And Tuschl, T., *Nature*, **2001**, 411, 494-498.
41. Torrence, P.F., Maitra, R.K., Lesaik, K., Khamnei, S., Zhou, A. And Silverman, R.H., *Proc. Natl. Acad. Sci. USA*, **1993**, 90, 1300-1304.
42. Leaman, D.W., Longano, F.J., Okicki, J.R., Soike, K.F., Torrance, P.F. Silverman, R.H. and Cramer, H., *Virology*, **2002**, 292, 70-77.
- 43.(a) Breaker, R.R. and Joyce, G.F., *Chem. Biol.*, **1994**, 1, 223-229, (b) Cech, T.R. and Uhlenbeck, O.C., *Nature*, **1994**, 372, 39-40.
44. Baker, B.F., Lot, S.S., Condon, T.P., Cheng-Flournoy, S., Lesnik, E.A., Sasmor, H.M. and Bennett, C.F., *J. Biol. Chem.*, **1997**, 272, 11994-12000.
- 45.(a) Dominiski, Z. and Kole, R., *Proc. Natl. Acad. Sci. USA*, **1993**, 90, 8673-8677, (b) Taylor, J., Zang, Q., Wyatt, J. And Dean, N., *Nat. Biotech.*, **1999**, 17, 1097-1100, (c) Sazani, P., Kang, S.H., Maier, M.A., Wei, C., Dillman, J., Summerton, J., Manoharan, M., and Kole, R., *Nucleic Acids Res.*, **2001**, 29, 3965-3974
46. Bennett, F.C. and Dean N.M., *Oncogene*, **2003**, 22, 9087-9096.

- 47.(a)Eckstein, F., *Antisense Nucleic Acid Drug Dev.*,**2000**, *10*, 117-121, (b) Stein, C.A., Subasinghe, C., Shinozuka, K., Cohen, J.S., *Nucleic Acids res.*, 1988, *16*,3209-3221.
- 48.Roehr, B., *J. Int. Assoc.Physicians AIDS Care*, 1998, *4*, 14-16.
- 49.Summerton, J., *Biochim. Biophys. Acta.*,1999, *1489*, 141-158.
- 50.(a)Alter,J., Lou, F., Rabiniwitz, A., Yin, H., Rosenfeld, J.,et al, *Nat.Med.*,2006,*12*, 175-177, (b) Wu, B., Moulton, H.M., Iverson, P.L., Jiang, J.,Li, J., et al, *Proc.Natl.Acad.Sci. USA*, 2008, *105*, 14814-14819.
- 51.Nielsen, P. E.; Egholm, M.; Berg, R. H.; Buchardt, O. *Science* **1991**, *254*, 1497-1500.
- 52.Mcmahon, B.M., Mays, D., Lipsky, J., Stewart, J.A., Fauq, A. and Richelson, E., *Antisense Nucleic Acid Drug Dev.*,**2002**,*12*, 65-73.
- 53.(a)Chiu,Y.L.,Rana,T.M., *RNA*, **2003**, *9*,1034-1048, (b) Morrissey,D.V.,Lockridge,J.A., Shaw,L.,Blanchard,K.,Jensen,K et al, *Nat.Biotech.*, **2005**, *23*, 1002-1007.
- 54.(a)Zang,R. Lu, Z. Zhao, H., Zhang, X., Diasio, R.B., Habus, I. Jiang, Z., Iyer, R.P., Yu, D. and Agarwal, S., *Biochem. Pharm.*, **1995**,*50*, 545-556, (b) Zhao, Q., Temsamani, J., Iadarola, P.L., Jiang,Z. and Agarwal, S., *Biochem. Pharm.*, **1995**, *51*,173-182, (c) Henry, S., Stecker, K., Brooks, D., Montieth, D., Conklin, B. and Bennett, C.F., *J.Pharm. Exp. Ther.*,**2000**, *292*, 468-479, (d) Geary, R.S., Watanabe, T.A., Truong, I.,Freier, S., Lesnik, E.A., Sioufi, N.B., Sasmor, H., Manoharan, M. and Levin, A.A., *J.Pharm. Exp. Ther.*, **2001**, *296*, 890-897.
- 55.Wengel, J., *Acc. Chem. Res.*,**1999**, *32*, 301-310.
- 56.Biffi, G., Tannahill, D., McCafferty, J. and Balasuramanian, S., *Nat.Chem*, **2013**, *5*, 182-186.
- 57.Bang, I., *Z. Physiol. Chem.*, **1898**, *26*, 133-159.
- 58.Bang, I., *Biochem. Z.*, **1910**, *26*,293-311
- 59.Gellert, M., Lipsett, M.N. and Davies, D.R.,*Proc.Natl.Acad.Sci.*,**1962**, *48*, 2013-2018.
- 60.R. K. Moyzis, J. M. Buckingham, L. S. Cram, M. Dani, L. L. Deaven, M. D. Jones, J. Meyne, R. L. Ratliff and J. R. Wu, *Proc. Natl. Acad. Sci. U. S. A.*, **1988**, *85*, 6622–6626
- 61.W. E. Wright, V. M. Tesmer, K. E. Huffman, S. D. Levene and J. W. Shay, *Genes Dev.*, **1997**, *11*, 2801–2809
- 62.Bugaut, A. and Balasubramanian, S., *Biochemistry*, **2008**, *47*, 689.

- 63.(a) Holliday, R. *Genet. Res.*, **1964**, 5, 282-304, (b) Eichman, B. F., Ortiz-Lombardia, M., Aymami, J., Coll, M., Ho, P. S., *J. Mol. Biol.*, **2002**, 320, 1037-1051.
- 64.Parkinson, G. N., Lee, M. P., Neidle, S., *Nature*, **2002**, 417, 876-880.
- 65.Weil, J., Min, T., Yang, C., Wang, S., Sutherland, C., Sinha, N., Kang, C., *Acta Crystallogr. D Biol. Crystallogr.*, **1999**, 55, 422-429.
- 66.Mills, M., Lacroix, L., Arimondo, P. B., Leroy, J. L., François, J. C., Klump, H., Mergny, J. L., *Curr.Med.Chem. Anticancer Agents*, **2002**, 2, 627-644.
- 67.(a) Burge, S., Parkinson, G. N., Hazel, P.; Todd, A. K., Neidle, S. *Nucleic Acids Res.*, **2006**, 34, 5402., (b) Collie, G. W., Parkinson, G. N., *Chem. Soc. Rev.*, **2011**, 40, 5867., (c) Mirkin, S. M. *Front Biosci.* **2008**, 13, 1064-1071.
- 68.Todd, A. K., Johnston, M., Neidle, S., *Nucleic Acids Res.*, **2005**, 33, 2901-2907.
- 69.Webba da Silva, M., *Chemistry*, **2007**, 13, 9738-9745.
- 70.Nielsen, J. T., Arar, K., Petersen, M., *Nucleic Acids Res.*, **2006**, 34, 2006-2014.
- 71.Cogoi, S., Paramasivam, M., Filichev, V., Géci, I., Pedersen, E. B., Xodo, L. E., *J. Med. Chem.*, **2009**, 52, 564-568.
- 72.Pedersen, E. B., Nielsen, J. T., Nielsen, C., Filichev, V. V., *Nucleic Acids Res.*, **2010**, 39, 2470-2481.
- 73.Robertson, D.L., Joyce, J.F., *Nature*, **1990**, 344, 467-468.
- 74.Ellington, A.D., Szostak, J.W., *Nature*, **1990**, 346, 818-822.
- 75.Tuerk, C., Gold, L., *Science*, **1990**, 249, 505-510.
- 76.Gatto, B.; Palumbo, M.; Sissi, C. *Curr. Med. Chem.* **2009**, 16, 1248-1265.; Bates, P. J.; Laber, D. A.; Miller, D. M.; Thomas, S. D.; Trent, J. O. *Exp. Mol. Pathol.*, **2009**, 86, 151-164.
- 77.Bock, L. C.; Griffin, L. C.; Latham, J. A.; Vermaas, E. H.; Toole, J. J. *Nature* **1992**, 355, 564-566.
- 78.(a) Schneider, D. J., Feigon, J., Hostomsky, Z., Gold, L., *Biochemistry*, **1995**, 34, 9599-9610, (b) Michalowski, D., Chitima-Matsiga, R., Held, D. M., Burke, D. H., *Nucleic Acids Res.*, **2008**, 36, 7124-7135, (c) Andreola, M. L., Pileur, F., Calmels, C., Ventura, M., Tarrago-Litvak, L., Toulmé, J. J., Litvak, S., *Biochemistry*, **2001**, 40, 10087-10094.
- 79.Murakami, K., Nishikawa, F., Noda, K., Yokoyama, T., Nishikawa, S., *Prion*, **2008**, 2, 73-80 .

80. Bates, P. J., Laber, D. A., Miller, D. M., Thomas, S. D., Trent, J. O., *Exp. Mol. Pathol.*, **2009**, *86*, 151-164.
- 81.(a) Jing, N., Zhu, Q., Yuan, P., Li, Y., Mao, L., Tweardy, D. J., *Mol. Cancer Ther.*, **2006**, *5*, 279-286. (b) Weersinghe, P., Li, Y., Guan, Y., Zhang, R., Tweardy, D. J., Jing, N., *Prostate*, **2008**, *68*, 1430-1442.
82. Du, Y., Li, B., Guo, S., Zhou, Z., Zhou, M., Wang, E., Dong, S., *Analyst*, **2010**, *136*, 493-497.
- 83.(a) Li, T., Shi, L., Wang, E., Dong, E., *Chemistry*, **2009**, *15*, 1036-1042, (b) Lévesque, D., Beaudoin, J.-D., Roy, S., Perreault, J.-P., *Biochem. J.*, **2007**, *403*, 129-138.
84. Shieh, Y.-A., Yang, S.-J., Wei, M.-F., Shieh, M.-J., *ACS Nano*, **2010**, *4*, 1433-1442.
85. Xiao, J., Carter, J. A., Frederick, K. A., McGown, L. B., *J. Sep. Sci.*, **2009**, *32*, 1654-1664.
- 86.(a) Macaya, R. F., Schultze, P., Smith, F.W., Roe, J.A. and Feigon, J., *Proc. Natl. Acad. Sci., USA*, **1993**, *90*, 3745-3749, (b) Schultze, P., Macaya, R. F., Feigon, J., *J. Mol. Biol.*, **1994**, *235*, 1532-1547, (c) Kelly, J.A., Feigon, J. and Yeates, T.O., *J. Mol. Biol.*, **1996**, *256*, 417-422.
87. Dittmer, W.U., Reuter, A. and Simmel, F.C., *Angew. Chem. Int. Ed.*, **2004**, *43*, 3550-3553.
88. Blackburn, G. M.; Gait, M. J.; Loakes, D.; Williams, D. M., *Nucleic acids in Chemistry and Biology.*, **2006**, RSC publication 3rd edition.
89. Cantor, C. R.; Schimmel, P. R. (Eds), *Biophysical Chemistry part III* W. H. Freeman and Company **1971**, New York.
90. Plum, G. E., Park, Y.-H., Singleton, S. F., Dervan, P. B., Breslauer, K. J., *Proc. Nat. Acad. Sci. USA*, **1990**, *87*, 9436.
91. Mergny, J.-L.; Lacroix, L. *Curr. Protoc. Nucleic Acid Chem.*, **2009**, Ch.17, Unit 17.1.
92. Vanholde, K. E.; Brahm, J.; Michelson, A., *Journal of Molecular Biology*, **1965**, *12*, (3), 726.
- 93.(a) Stryer, L., *Biochemistry*, **1988**, 3rd ed.; New York: W. H. Freeman and Company., (b) Egli, M.; Williams, L. D.; Gao, Q.; Rich, A. *Biochemistry* **1991**, *30*, (48), 11388-11402. (c) Calladine, C. R.; Drew, H. R., *Understanding DNA, The molecule and how it works.*, **1992**, Cambridge: Academic Press Ltd. (d) Beveridge, D. L.; Jorgensen, W. L.,

- Ann. NY Acad. Sci.*, **1986**, 482. (e) Gessner, R. V.; Frederick, C. A.; Quigley, G. J.; Rich, A.; Wang, A. H. J., *J. Biol. Chem.* **1989**, *264*, (14), 7921-7935.
- 94.(a) Job, P. *Ann. Chim. Appl.* **1928**, *9*, 113. (b) Huang, C. Y., *Methods in Enzymology* **1982**, *87*, 509-525.
- 95.Masiero, S.; Trotta, R.; Pieraccini, S.; De Tito, S.; Perone, R.; Randazzo, A.; Spada, G. *P. Org. Biomol. Chem.* **2010**, *8*, 2683-2692.
- 96.(a) Paramasivan, S.; Rujan, I.; Bolton, P. H. *Methods* **2007**, *43*, 324-331.; (b) Arora, A.; Maiti, S. *J. Phys. Chem. B.* **2009**, *113*, 10515-10520.; (c) Joachimi, A.; Benz, A.; Hartig, J. S. *Bioorg. Med. Chem.* **2009**, *17*, 6811-6815.; (d) Gros, J.; Webba da Silva, M.; De Cian, A.; Amrane, S.; Rosu, F.; Bourdoncle, A.; Saccà, B.; Alberti, P.; Lacroix, L.; Mergny, J.-L. *Nucleic Acids Symp. Ser.*, **2005**, 61-62.
- 97.Callis, P.R.,*Annu.Rev Phys. Chem.*,**1983**, *34*, 329-357.
- 98.(a) Mendez, M. A.; Szalai, V. A. *Biopolymers*,**2009**, *91*, 841-850, (b) Miannay, F. A.; Banyasz, A.; Gustavsson, T.; Markovitsi, D. *J. Phys. Chem.*, **2009**, *113*, 11760-11765, (c). Dao, N. T.; Haselsberger, R.; Michel-Beyerle, M.-E.; Phan, A. T. *FEBS Lett.*, **2011**, *585*, 3969-3977.
- 99.(a) Martadinata, H.; Phan, A. T. *J. Am. Chem. Soc.*, **2009**, *131*, 2470-2578.; Qi, J.; Shafer, R. H. *Biochemistry*, **2007**, *46*, 7599-7606.; (b) Collie, G. W.; Parkinson, G. N.; Neidle, S.; Rosu, F.; De Pauw, E.; Gabelica, V. *J. Am. Chem. Soc.*, **2010**, *132*, 9328-9334.
- 100.Little, D. P.; Cornish, T. J.; Odonnell, M. J.; Braun, A.; Cotter, R. J.; Koster, H., *Anal. Chem.*, **1997**, *69*, (22), 4540-4546.
- 101.Crain, P. F.; McCloskey, J. A., *Curr. Opin. Biotechnol.*, **1998**, *9*, (1), 25-34.

Chapter 2

Conformationally locked *iso*DNA

Section A

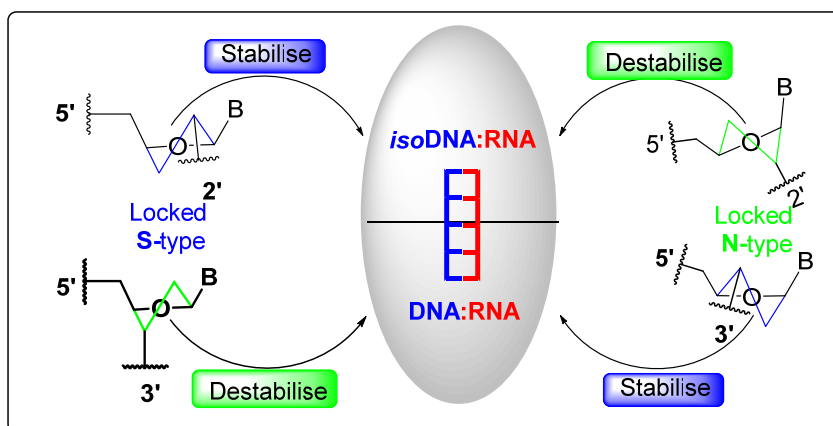
Synthesis, characterization and conformational analysis of the N-type and S-type locked monomer building blocks

Section B

Synthesis, characterization and biophysical studies of the 2'-5'- linked *iso*DNA, modified *iso*DNA and their stability towards snake venom phosphodiesterase

Chapter 2

Conformationally locked *isoDNA*



Regioisomeric nucleic acids with the 2'-5'-phosphodiester linkages compared to the 3'-5'-linkage are highly interesting biomolecules. Their study has become an area of great interest due to their possible role in the prebiotic world and their potential use in the artificial regulation of gene expression. This isomeric DNA supports Watson-Crick base pairing but with distinct properties. The 2'-5' *isoDNA* discriminates between single stranded DNA and RNA and forms duplexes exclusively with RNA. A switch in the link from 3'-5' to 2'-5' has to necessitate a concomitant switch in the preference of the sugar pucker of the repeating units of 3'-5' and 2'-5' nucleic acids. In an effort to elucidate the structural behaviour of the 2'-5' *isoDNA* when complexing with RNA, N-type and S-type conformational locks were introduced in the *isoDNA* strand so as to understand the structural preferences of sugars in the isomerically-linked strand of the chimeric duplex and thus provide for the first time an experimental evidence for their sugar pucker preference in stable duplex structures.

Section A

Synthesis, characterization and conformational analysis of N-type and S-type locked monomer building blocks

2.1 Introduction to present work

Stimulated by the potential of antisense approach to achieve specific control of gene expression, the synthesis of modified ONs has mushroomed during the past three decades.^{1,2} Among these, the 2'-5' linked ONs are specially interesting^{3,4,5} because of the interesting physical properties^{6,7,8,9,10} of these unique class of oligonucleotides such as: (1) They exhibit a remarkable preference for duplex formation with complementary 3'-5'-linked natural RNA. (2) These hetero duplexes are slightly less stable than the normal 3'-5'-linked RNA:RNA duplexes. (3) The 2'-5'-linked nucleic acids show high resistance to nuclease digestion.

2.1.1 2'-5'-linked *iso*DNA /RNA and relevant conformational restriction

In the 2'-5'-linked *iso*RNA self-complementary duplex, the NMR structure shows that the preferred furanose ring conformation is C2'-*endo* (South type)^{11,12} Whereas, NMR studies on a 2'-5'-linked single stranded *iso*RNA and the crystal structure indicates a C3'-*endo* (North type) conformation.^{13,14} This switching over of the furanose ring conformation implies that a reorganization of the structure of an ON single strand so as to match the structure of the duplex form, can lead to increased duplex stability. The concept of conformational restriction^{1,15} wherein the nucleoside analogue is conformationally locked into either the N-type or S-type can prove to be a powerful strategy for achieving duplex stability when binding with complementary DNA or RNA.

A variety of 3'-5' linked analogues have been synthesized, such as LNA/BNA,¹⁶ Hexitol nucleic acid HNA,¹⁷ tricyclic DNA (tcDNA)¹⁸ in which the sugar is locked in matching N-type geometry. These show increased affinity towards complementary RNA and compact A-type duplex formation without any base pairing properties being

compromised (Figure 1). No such studies have yet been reported in literature for the 2'-5' linked *isoDNA* analogues, which remains to be explored. Some preliminary molecular modelling studies and CD, NMR studies of unmodified *isoDNA/isoRNA* point out the reversed preferences of sugar puckers that could lead to efficient binding of *isoDNA* with RNA.

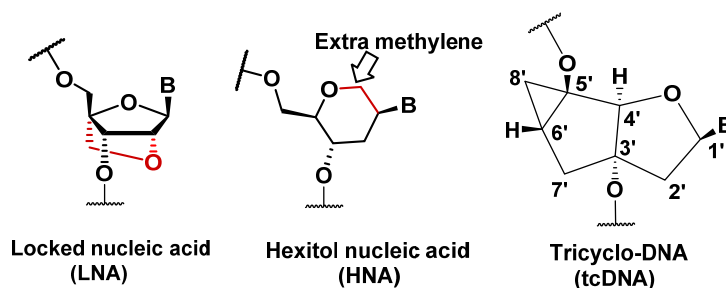


Figure 1. Examples of conformationally constrained natural nucleic acids

2.1.2 Unmodified single stranded *isoRNA/isoDNA* and *isoRNA/isoDNA:RNA* duplexes

The synthesis of unmodified 2'-5' RNA (*isoRNA*) which occurs naturally¹⁹ but does not encode the genetic information has been reported by Damha *et al.*^{6,13,20} This synthetic *isoRNA*, exhibited self pairing as well as pairing with RNA,^{6,13,20} but did not complex with complementary DNA.

The CD patterns of *isoRNA:RNA* duplexes were found to be very much similar to those of the natural 3',5'-DNA:RNA duplexes indicating comparable overall structures *i.e.*, compact A-form duplex structure.¹⁰ Solution phase NMR studies indicated that the ribose sugar pucker in the self pairing *isoRNA* duplexes¹² was C2'-*endo* (S-type). From the above described CD and NMR studies it appeared that the *isoRNA* strand in the *isoRNA:RNA* duplex may be adopting the structural features giving rise to structures similar to compact A-form in which the sugar residues of the *isoRNA* strand would be existing in the C2'-*endo* conformations. In molecular modeling studies by Yathindra *et al.*²¹ a critical examination of the stereochemistry of 2',5'- and 3',5'-linkages revealed an inverse relationship between the nucleotide geometry and nature of the phosphodiester linkage (Figure 2). A 2'-5'-linkage with a C2'-*endo* sugar produces a compact nucleotide geometry whereas the 3',5'-linkage with the same C2'-*endo* sugar gives rise to an extended nucleotide geometry. Thus

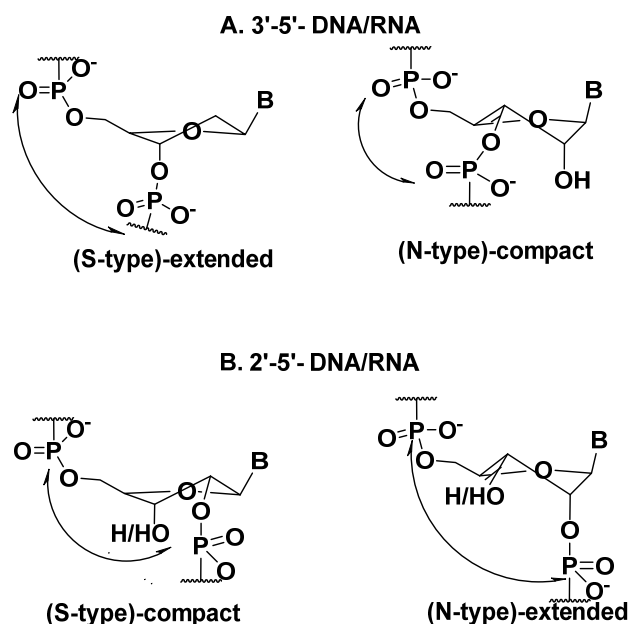


Figure 2. 3'-5'-DNA/RNA and 2'-5'-isoDNA/isoRNA in compact and extended conformations.

to have a compact A-type overall structure of *isoRNA*:RNA duplex, the S-type or C2'-*endo* sugar pucker in the repeating nucleotides is stereochemically favoured in the *isoRNA* strand of the duplex. Similar structural requirements were reported for 2',5'-linked *isoDNA*:RNA duplexes both by Breslow *et al.*⁸ and Switzer *et al.*²² CD spectroscopy^{22a} and modeling studies²³ predicted that the *isoDNA* strand in *isoDNA*:RNA duplexes would predominantly have S-type sugar conformations. On the contrary, an extended structure with N-type sugar conformations was reported on NMR studies done on single stranded *isoRNA*^{13a} and 2',5'-d(G₄C₄).^{13b} Also the crystal structure^{14a} obtained for a single strand 2',5'-RNA showed a C3'-*endo* or N-type sugar pucker. Hence the sugar conformations (N-type) observed in a single stranded *isoDNA/isoRNA* does not match with that of the sugar conformations (S-type) as seen in the *isoDNA/isoRNA* strand in *isoRNA/isoDNA*:RNA duplex. In a single stranded 2',5'-DNA oligomer, the *gauche* and anomeric effects of the 2'-hydroxyl group would dominate the preference for 3'-*endo* (N-type) sugar conformation in the absence of a 3'-hydroxyl group. Therefore in the *isoDNA*:RNA duplex it was assumed that the RNA strand would impose its structure^{14b} on the *isoDNA* strand causing the individual nucleosides in the *isoDNA* to adopt C2'-*endo* conformations so as to form a stable duplex with RNA. However, this would lead to a conformational and topological

constraint on *isoDNA* in the *isoDNA*:RNA duplex (Figure 3).²³ This constraint would lead to reduced binding strength of the duplexes of *isoDNA/isoRNA* with RNA targets, resulting in *isoDNA/isoRNA*:RNA duplexes with considerably lower stability compared to the natural DNA/RNA:RNA duplexes.

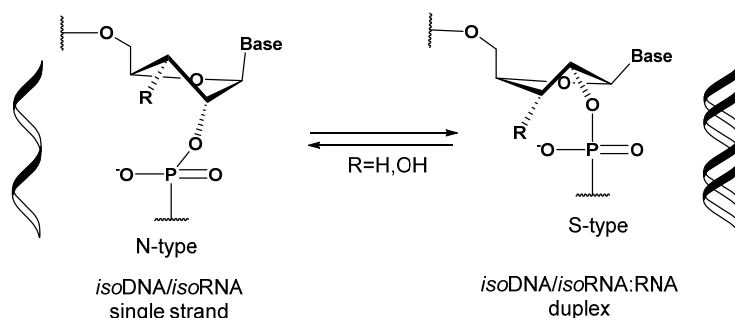


Figure 3. Sugar conformations of the 2'-5' nucleoside in single stranded *isoDNA/isoRNA* and double stranded *isoDNA/isoRNA*:RNA duplex.

2.2 Present work

Continuing the search for antisense oligonucleotides (ASOs) that bind selectively to RNA and which are more resistant to degradation by cellular enzymes, we proposed to synthesize conformationally locked nucleosides and incorporate them in 2'5'-*isoDNA* oligomers in order to improve the binding strength of these *isoDNA* ASOs. As there is no conclusive experimental evidence in literature for the preferred sugar geometries in *isoDNA* strands, we selected in this work to study both nucleoside analogues that would be N-type and S-type locked. Herein, we report for the first time, a study of the effects of incorporation of these monomers in locked N-type I and S-type II sugar conformation in *isoDNA*:RNA duplexes (Figure 4).

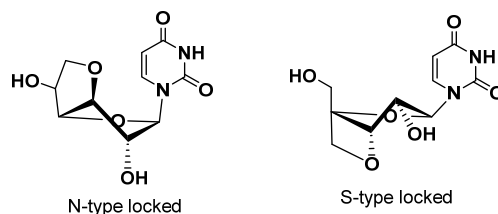
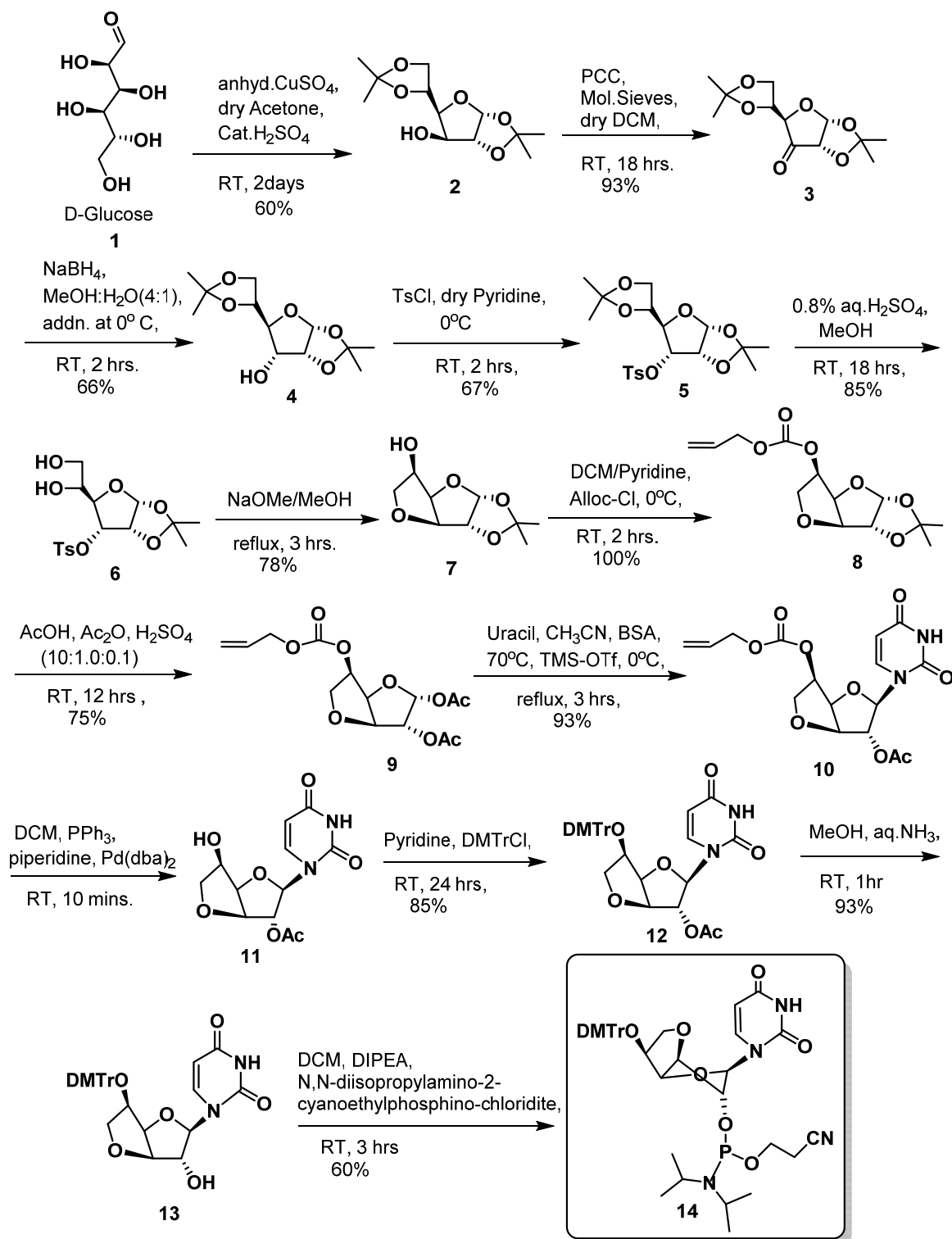


Figure 4. N-type I and S-type II locked nucleosides.

Such studies have not been reported for the *iso*DNA:RNA duplexes although there is abundant literature on locked/frozen DNA analogues in natural DNA:RNA duplexes. The locked N-type conformation of the DNA oligomers have entropic advantage while binding to RNA.^{16a,24,25} By applying such locks on the *iso*DNA strand, the structural preferences of sugars in the isomerically-linked strand of the chimeric duplex could be understood and that would provide important leads to design therapeutically useful synthetic *iso*DNA.

2.2.1 Synthesis of N-type locked monomer

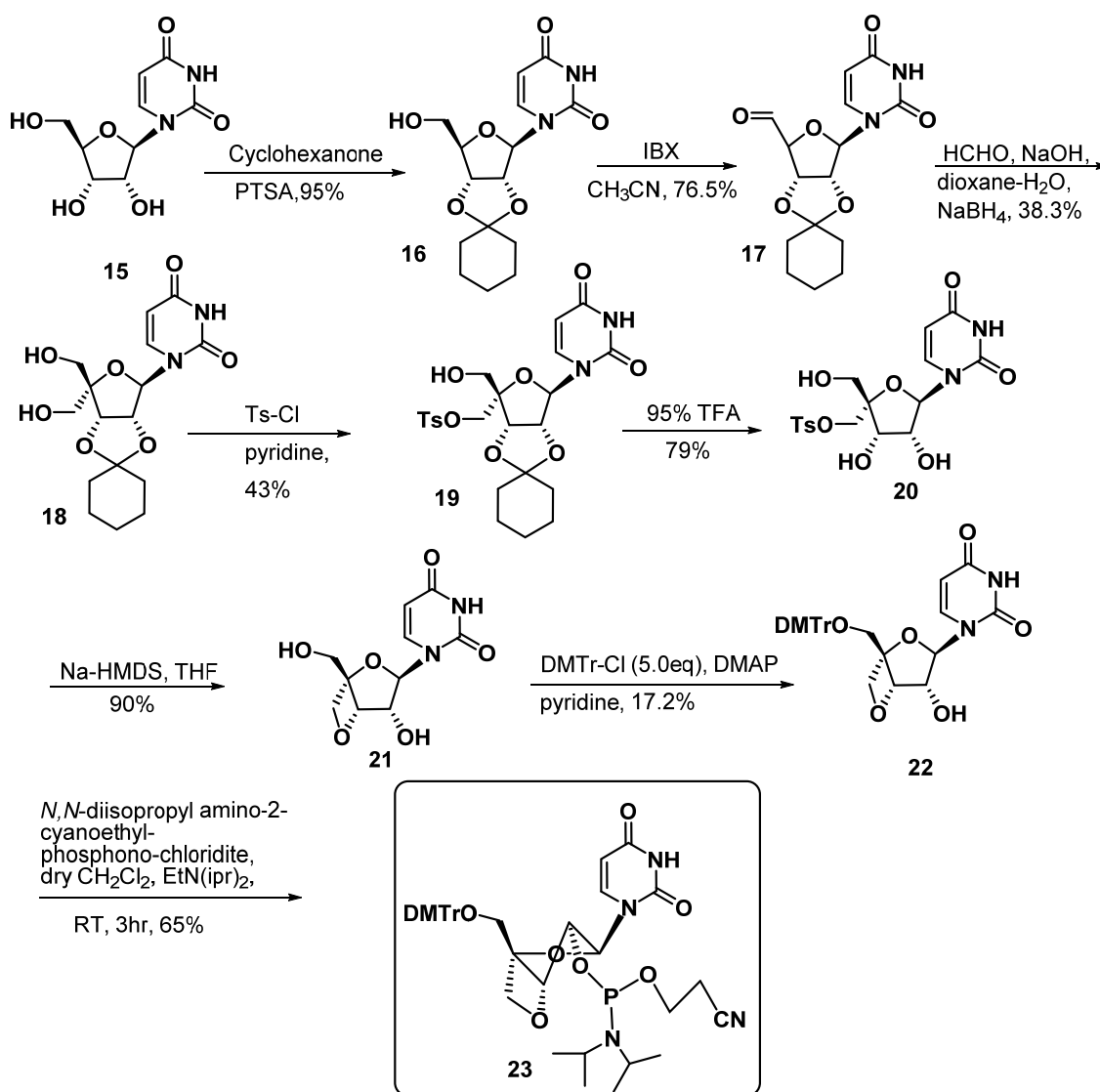
The synthesis of N-type building block is outlined in Scheme 1. D-glucose **1** was protected as 1,2,5,6-glucose diacetone (GDA) **2**. The 3'-hydroxyl was oxidized using PCC to give the keto compound **3** which was reduced using sodium borohydride to give allose diacetone (ADA) **4**. Tosylation of **4** with tosyl-Cl yielded the 3'-*O*-tosyl compound **5**. Selective hydrolysis of the 5,6-acetonide using 0.8% H₂SO₄ in methanol gave the 5,6-diol **6**. The synthesis from glucose **1** to compound **6** was done following an earlier reported multistep synthesis procedure.²⁶ Compound **6** was cyclized by treating with sodium methoxide in methanol giving the 3,6-anhydro compound **7**. The free secondary hydroxyl was protected with the allyloxycarbonyl group to give compound **8** in 99% yield (purity>90%). The acetonide group in **8** was removed and converted into its diacetate **9** by treatment with AcOH and Ac₂O in the presence of catalytic amount of H₂SO₄. Compound **9** on treatment with BSA, uracil and TMSOTf under Vorbrüggen conditions afforded exclusively the β-anomer of uridine derivative **10**, in 93% yield. The alloc group was selectively cleaved in the presence of 3'-acetate using Pd(0) to get **11** (70%). The free secondary hydroxyl group was protected as its DMT derivative using excess of DMTr-Cl in dry pyridine, to get **12** (85%). Compound **12** on ammonolysis gave the free 2'-hydroxyl compound **13** (93%). Phosphitylation of the free 2'-hydroxyl with *N,N*-diisopropylamino-2-cyanoethylphosphino-chloridite afforded the N-type locked uridine phosphoramidite monomer **14** (60%). All the compounds were purified by column chromatography. The new compounds were appropriately characterized using ¹H, ¹³C & ³¹P NMR and HRMS analysis.



Scheme 1. Synthesis of N-type locked monomer.

2.2.2 Synthesis of S-type locked monomer

Using uridine as starting material, the S-type locked amidite monomer was synthesized in 8 steps according to literature procedure (Scheme 2).²⁷ The *cis*-diol of uridine **15** was protected as a cyclohexylidene derivative **16** (95%) using cyclohexanone, *p*TSA. The 5'-hydroxyl group was oxidized using IBX to give the 5'-aldehyde **17** (76.5%) which on formylation, followed by sodium borohydride reduction gave the diastereotopic hydroxymethyl compound **18** (38.3%). Selective tosylation of **18** afforded the monotosylate



Scheme 2. Synthesis of S-type locked monomer

19 (43%) as per literature report,^{27a,27e} wherein the regioselectivity of tosylation at C4' hydroxymethyl group was determined by means of NOE measurements. Acidic hydrolysis of **19** gave triol **20** in 79% yield. Oxetane ring formation from **20** was accomplished on treatment with a large excess of sodium hexamethyldisilazide in THF at room temperature, yielding the desired product **21**(90%). The exclusive oxetane ring formation is attributed to the predominant S-conformation of the compound **20** in which only the 3'-OH is thought to be located near the 4'-methylene carbon centre. The selective protection of the primary hydroxy group in **21** with 4, 4'-dimethoxytrityl by using DMTr-Cl in five-fold excess gave the DMTr protected compound **22**(17.2%). The free 2'-hydroxyl on treatment with *N,N*-diisopropylamino-2-cyanoethylphosphino-chloridite afforded the S-type locked uridine phosphoramidite monomer **23** (65%). All the compounds were purified by column chromatography and the pure compounds were characterized using ¹H, ¹³C, ³¹P NMR and LCMS mass analysis.

2.2.3 Conformational analysis of the nucleoside analogues

The sugar conformations of 3'-deoxyuridine and the N-type/S-type locked nucleosides (Figure 4, **I** and **II**) were compared (Table 1, Figures 5 & 6) based on the ³J_{H1'-H2'} coupling constants. The homonuclear ³J_{H1'-H2'} coupling constants are very sensitive to the dihedral angle and therefore directly reflect on the sugar pucker in five-membered ribonucleosides. The %S conformation for each unit was calculated from the H1'-H2' NMR coupling constants as earlier reported.²⁷ A simple equation for the calculation of percentage of S conformation is shown in equation (1).

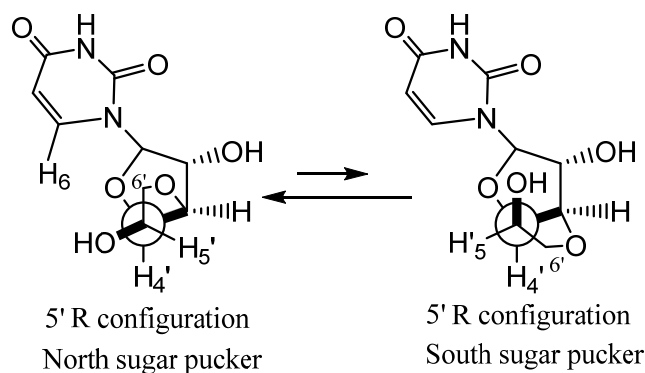
$$S (\%) = 100 \times (J_{1,2'} - 1)/6.9 \quad (1)$$

A smaller *J* value of 0-3 Hz is typical of N-type whereas the *J* value between 6-9 Hz is indicative of S-type sugar pucker.²³

Thus 3'-deoxyuridine is 97% N-type, *i.e.* C3'-*endo* sugar pucker, which is consistent with the O4'-C1'-C2'-O2' *gauche* effect as well as the anomeric effect which brings the nucleobase in pseudoaxial orientation.^{14b} The xylo-3'-O-5'-C-methylene-linked uridine (U^N, **I** Figure 6a) and the 3'-O-4'-C-methylene-linked uridine (U^S, **II** Figure 6b) would lock the monomer in N-type and S-type conformations respectively.

Table1. Conformational analysis of the nucleosides using H1'-H2' coupling constants from 1H NMR spectra.

Nucleoside derivative	H1'-H2' coupling	% S	Reference
	<i>J</i> in Hz		
3'-deoxyuridine	1.2	3	29
N-locked uridine (U ^N , I)	3.5	36	29c
S-locked uridine (U ^S , II)	7.5	94	29

**Figure 5.** Two possible conformers for N-type locked due to flexible 5-membered locked ring in I.

The 2-D NOE NMR experiments were performed to further show cross peaks between H2'-H6 protons in compounds I and II suggesting *anti* conformation of the uracil nucleobase.²⁸ Also, no additional NOE peaks were observed between H6-H1' proton, indicating *anti* conformation of the nucleobase.

In compound I, the flexible 5-membered ring allowed ~36% S-type character to the sugar ring (conformational analysis based on the $^3J_{H1'-H2'}$). Two forms of sugar conformations for I could be possible, in which the C5'-carbon is fixed in *R* configuration (as in starting material) as depicted in Figure 5. The O4'-C4'-C3'-O3' *gauche* effect in the N-type xylo-sugar would stabilize the N-type sugar ring conformation shifting the equilibrium to N-type. An additional proof for the sugar conformation in I being predominantly N-type comes from a relatively less strong NOE cross peak (5%, Figure 6a) between H2' and H6.²⁹ An additional positive NOE cross peak (1.8%) between H6 and H6' is observed. The preferred O5'-C5'-C4'-C3' geometry suggests the orientation of the 5'-OH group to be γ^t due to the fixed *R* configuration at C5' in the preferred N-type conformer of I.

The two-dimensional NOE NMR experiments revealed a strong NOE cross peak (**II**, 9.7%, Figure 6b) between H2' and nucleobase H6 thus confirming the 2'-endo sugar pucker and *anti* nucleobase conformation for compound **II**.

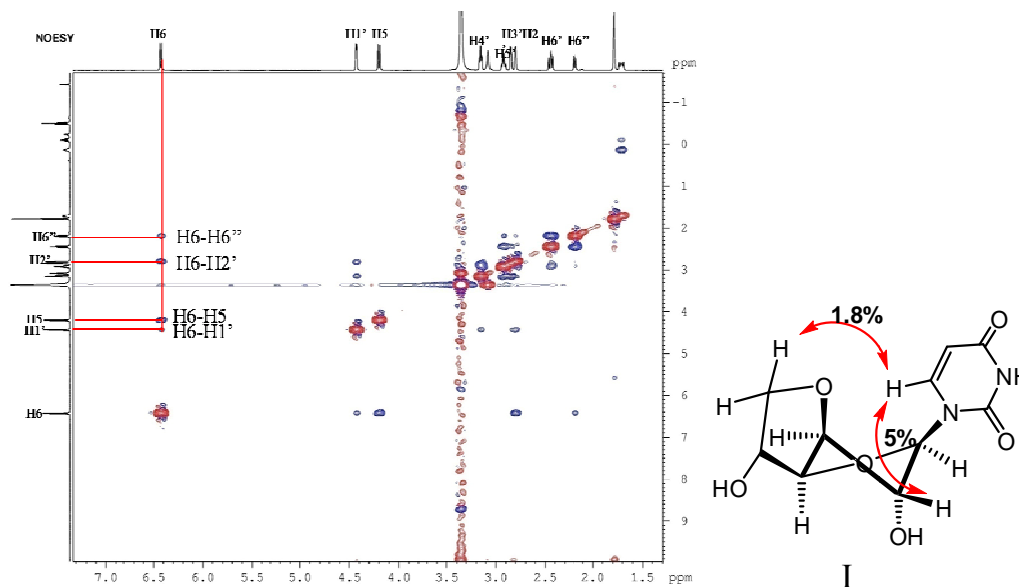


Figure 6(a). NOESY NMR (CD₃OD, 400MHz) *U^N* **I**

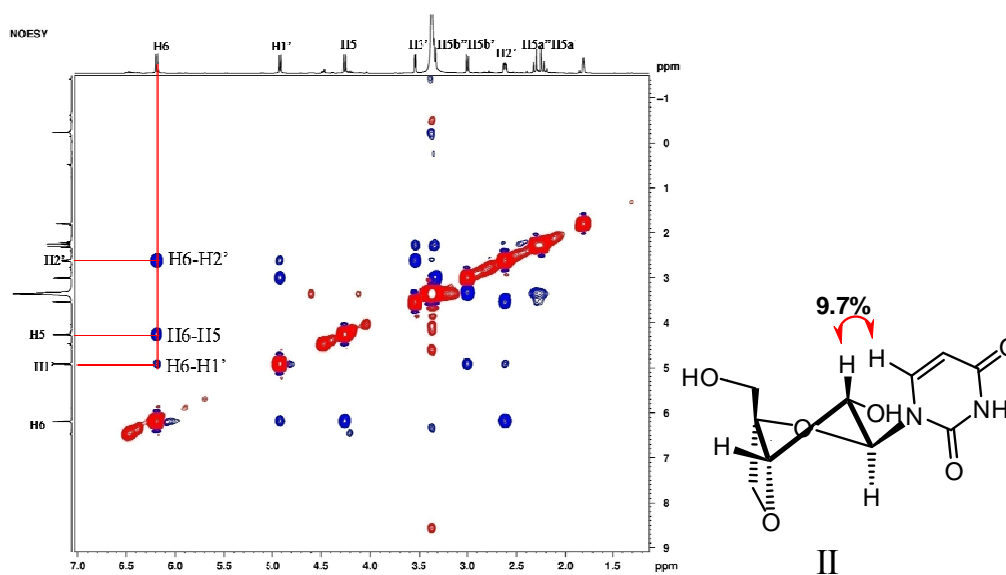


Figure 6(b). NOESY NMR (CD₃OD, 400MHz) *U^S* **II**

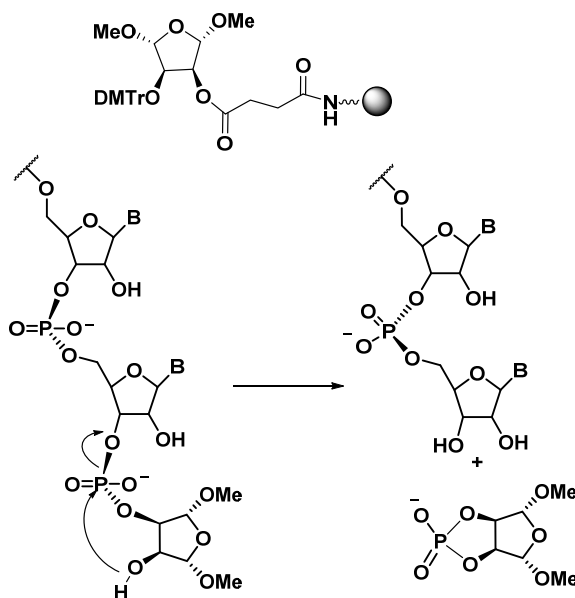
Section B

Synthesis, characterization and biophysical studies of the 2'-5'-linked *isoDNA* and modified *isoDNA* and their stability towards snake venom phosphodiesterase

2.3 Solid Phase oligonucleotide synthesis using the phosphoramidite chemistry

Standard oligonucleotide synthesis uses a solid support that contains the first nucleoside covalently linked to the support *via* a linker which gets hydrolyzed during the post synthesis cleavage step. Since this forms the 3'-terminal residue of the oligomer, four solid supports are required for DNA synthesis and another four for RNA synthesis.

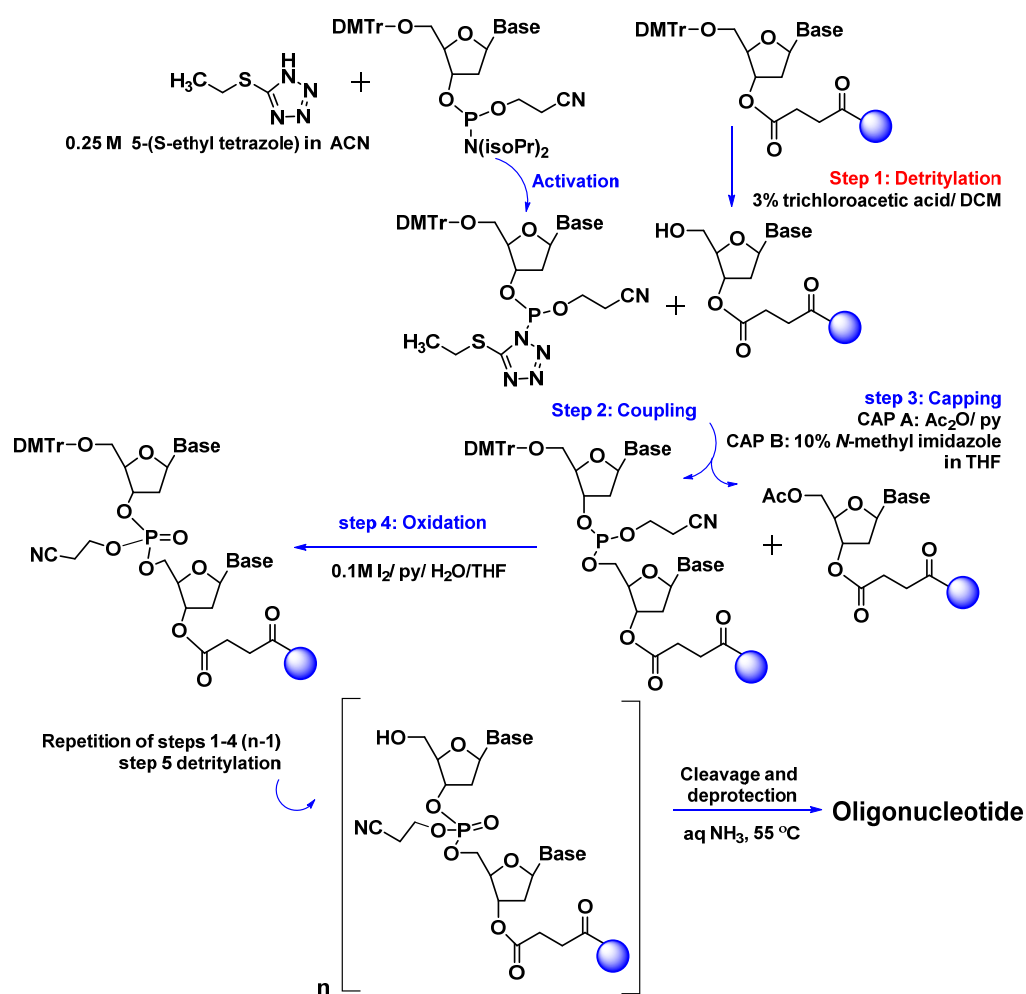
A universal support does not have the limitation of 3'-nucleoside attached. Rather, the 3'-end nucleoside is added in the first cycle, giving an undesired phosphate linkage which gets removed during the cleavage/deprotection steps. (Scheme 3) Following are the



Scheme 3. Universal support structure and dephosphorylation cleavage mechanism (Commercial product from Glen Research, 22825 Davis Drive, Sterling, Virginia 20164 USA).

advantages of using universal supports in DNA/RNA oligomer synthesis. (a) It eliminates the need for four supports for DNA synthesis and four additional supports for RNA synthesis. (b) It simplifies the synthesis of oligomers with a modified or unusual nucleoside at the 3'-terminus.³⁰ This support was conveniently used for the synthesis of 2'-5' oligonucleotides in the present work without the need of synthesizing individual solid support for each 3'-deoxy-2'-nucleoside.

The principle of phosphoramidite chemistry was developed by McBride and Caruthers in 1983 (Scheme 4).³¹ The phosphitylated nucleoside or the phosphoramidite could be made in advance, isolated as a stable solid and stored under anhydrous conditions.



Scheme 4. The oligonucleotide synthetic cycle.

The solid phase synthesis is done in the 3'-5' direction, on a solid support (CPG or polystyrene based) with the required 3'-end nucleoside attached to it *via* a linker. The A,G,C,T monomers are protected at the 5'-end with a lipophilic, acid labile 4, 4'-dimethoxytrityl group and the exocyclic amines of nucleobases are protected with base labile protecting groups. The coupling of each monomer takes place *via* an elegant synthetic cycle (Scheme 4). Repetitions of the four steps in the cycle gives rise to the 3'-5' linked requisite oligonucleotide. In the post synthetic treatment the synthesized oligonucleotide is cleaved from the support by aqueous ammonia treatment which also removes inter-nucleoside β -cyanoethyl phosphate protection, the exocyclic amino protection of the bases and the 2'-end sugar residue to get a completely modified 3'-5' DNA. The crude oligomer is then desalted and purified by RP-HPLC and characterized by MALDI-TOF mass spectrometry.

2.4. Synthesis, purification and characterization of modified *iso*DNA sequences

We used the same synthetic strategy for the SPS synthesis of 2'-5' *iso*DNA oligomers using universal support. The synthetic cycle is given in Scheme 5. The first base was attached to the universal support giving an undesired phosphate linkage which gets removed during the cleavage/deprotection steps as depicted in Scheme 3. Commercially available protected 3'-deoxy phosphoramidite building blocks (Figure 7) were used when the sites were unmodified.

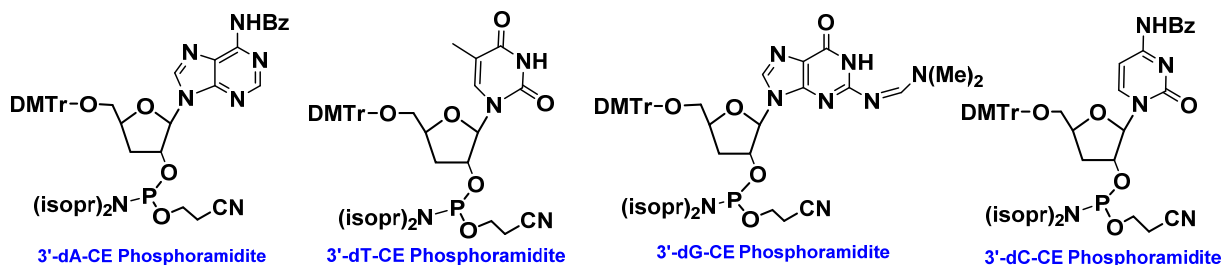


Figure 7. 3'-deoxy phosphoramidite monomers

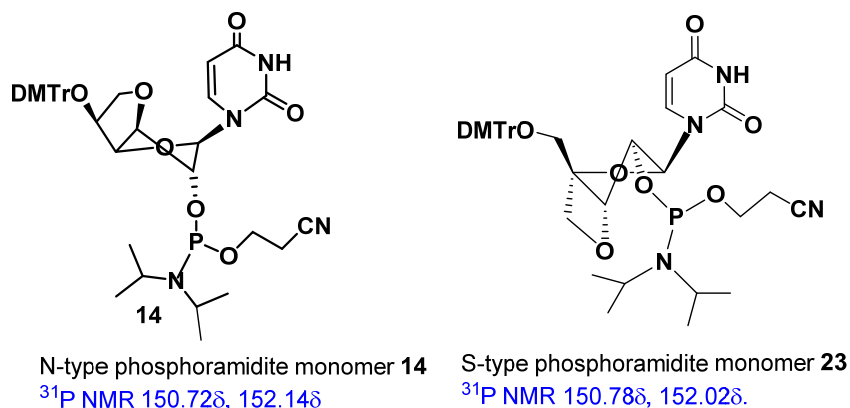


Figure 8. Modified phosphoramidite building blocks.

The solid phase synthesis of control sequences 2'-5'-linked 2'DNA-1 and 2'DNA-2 was successfully completed on a Bioautomation, Mermade -4 DNA synthesizer with commercially available 5'-DMT- 3'-deoxy-2'-phosphoramidite building blocks using the universal support columns so as to get a 2' terminus for the synthesized sequence (Scheme 5). The modified units were coupled at pre-determined positions by double coupling and an extended coupling time to achieve maximum yields of the synthesized oligomers. The synthesized oligonucleotides were treated with aqueous ammonia solution at 55°C for six hours for cleavage from solid support and removal of all protecting groups. The crude oligomers were desalted on G-25 Sephadex NAP columns followed by purification using RP-HPLC. Their purity was also re-checked by analytical HPLC prior to their use in experiments. The synthesized sequences were characterized by MALDI-TOF mass spectrometric analysis (Table 2). The control and complementary DNA oligonucleotides were synthesized as shown in Scheme 4. After the post synthetic treatment they were purified by RP-HPLC, characterised by MALDI-TOF mass and used for the UV T_m experiments. These are listed in Table 3. The two complementary RNA oligonucleotides for the DNA-1, DNA-2, 2'DNA-1 and 2'DNA-2 sequences were obtained from Sigma Aldrich.

Table 2. N-type (U^N) and S-type (U^S) modified sequences, HPLC and MALDI-TOF mass.

Code No	Sequence	HPLC (t_R) mins.	Mass (calcd.)	Mass (obsd.)
2'DNA-N-1s	5' CACCATTGTCACAC U^N CCA ^{2'}	6.70	5377	5376
2'DNA-N-1d	5' CACCATTG U^N CACAC U^N CCA ^{2'}	7.05	5391	5391
2'DNA-N-1t	5' CACCA U^N TG U^N CACAC U^N CCA ^{2'}	8.25	5405	5405
2'DNA-N-2s	5' CCTCTTACCTCAGT U^N ACA ^{2'}	11.52	5383	5386
2'DNA-N-2d	5' CCTCTTACC U^N CAGT U^N ACA ^{2'}	11.63	5397	5401
2'DNA-N-2t	5' CCTCT U^N ACC U^N CAGT U^N ACA ^{2'}	10.64	5411	5409
2'DNA-S-1s	5' CACCATTGTCACAC U^S CCA ^{2'}	5.80	5377	5380
2'DNA-S-1d	5' CACCATTG U^S CACAC U^S CCA ^{2'}	6.60	5391	5395
2'DNA-S-1t	5' CACCA U^S TG U^S CACAC U^S CCA ^{2'}	7.30	5405	5404
2'DNA-S-2s	5' CCTCTTACCTCAGT U^S ACA ^{2'}	13.00	5383	5389
2'DNA-S-2d	5' CCTCTTACC U^S CAGT U^S ACA ^{2'}	13.20	5397	5395
2'DNA-S-2t	5' CCTCT U^S ACC U^S CAGT U^S ACA ^{2'}	11.75	5411	5408

Table 3. Control and complementary DNA and isoDNA sequences, HPLC t_R and MALDI-TOF mass.

Code No	Sequence	HPLC(t_R) (min)	Mass (calcd.)	Mass (obsd.)
DNA-1	5' CACCATTGTCACACTCCA ^{3'}	10.58	5363	5364
DNA-2	5' CCTCTTACCTCAGTTACA ^{3'}	12.70	5369	5368
cDNA-1	5' TGGAGTGTGACAATGGTG ^{3'}	10.04	5634	5645
cDNA-2	5' TGTAAGTGGAGGTAAGAGG ^{3'}	10.56	5627	5633
2'DNA-1	5' CACCATTGTCACACTCCA ^{2'}	8.91	5363	5363
2'DNA-2	5' CCTCTTACCTCAGTTACA ^{2'}	8.82	5369	5366
RNA-1	5'UGGAGUGUGACAAUGGUG 3'	Purchased from		
RNA-2	5'UGUAACUGAGGUAAGAGG 3'	Sigma Aldrich.		

2.5. UV melting studies of the modified isoDNA sequences

The thermal stability of the isoDNA complexes with the complementary DNA/RNA was evaluated by conducting UV T_m experiments. HPLC purified sequences were annealed with the complementary DNA /RNA oligonucleotide. The strand concentration taken was 1 μ M in sodium phosphate buffer 10mM containing 150mM NaCl. The UV melting (T_m determination) was carried out by monitoring the absorbance at 260nm wavelength by heating the annealed samples from 10°C to 85°C. The UV chamber was gently purged with a stream of N₂ gas to remove traces of moisture from condensing on the cuvettes. The melting temperatures of the modified N-type and S-type locked isoDNA oligonucleotide duplexes with complementary RNA were determined. The melting temperatures were obtained from the maxima of the first derivatives of the melting curves ($A_{260\text{ nm}}$ versus temperature) these were compared with the unmodified control 2'DNA-1 and 2'DNA-2 duplexes respectively. The results obtained for the isoDNA:RNA complexes are summarised in Table 4.

Table 4. Comparative UV T_m values of the N-type (U^N) and S-type (U^S) modified sequences (ΔT_m gives the difference in T_m between the control and modified sequence).

Sr. No.	Code No.	Sequence	RNA UV T_m (°C)	ΔT_m
1.	2'DNA-1	5' CACCATTGTCACACTCCA ^{2'}	50.5	0.0
2.	2'DNA-N-1s	5' CACCATTGTCACACU ^N CCA ^{2'}	49.4	-1.1
3.	2'DNA-N-1d	5' CACCATTGU ^N CACACU ^N CCA ^{2'}	42.8	-7.7
4.	2'DNA-N-1t	5' CACCAU ^N TGU ^N CACACU ^N CCA ^{2'}	42.3	-8.3
5.	2'DNA-S-1s	5' CACCATTGTCACACU ^S CCA ^{2'}	51.0	+0.5
6.	2'DNA-S-1d	5' CACCATTGU ^S CACACU ^S CCA ^{2'}	52.8	+2.3
7.	2'DNA-S-1t	5' CACCAU ^S TGU ^S CACACU ^S CCA ^{2'}	50.3	-0.2
8.	2'DNA-2	5' CCTCTTACCTCAGTTACA ^{2'}	46.0	0.0
9.	2'DNA-N-2s	5' CCTCTTACCTCAGTU ^N ACA ^{2'}	46.4	+0.4
10.	2'DNA-N-2d	5' CCTCTTACCU ^N CAGTU ^N ACA ^{2'}	41.9	-4.1
11.	2'DNA-N-2t	5' CCTCTU ^N ACCU ^N CAGTU ^N ACA ^{2'}	41.9	-4.1
12.	2'DNA-S-2s	5' CCTCTTACCTCAGTU ^S ACA ^{2'}	47.0	+1.0
13.	2'DNA-S-2d	5' CCTCTTACCU ^S CAGTU ^S ACA ^{2'}	46.7	+0.7
14.	2'DNA-S-2t	5' CCTCTU ^S ACCU ^S CAGTU ^S ACA ^{2'}	47.2	+1.2

The *isoDNA* sequences in this study did not bind to complementary DNA, thus showed specific binding to RNA as earlier reported by Damha *et al.*^{6,20} for the *isoRNA* sequences (Figure 10).

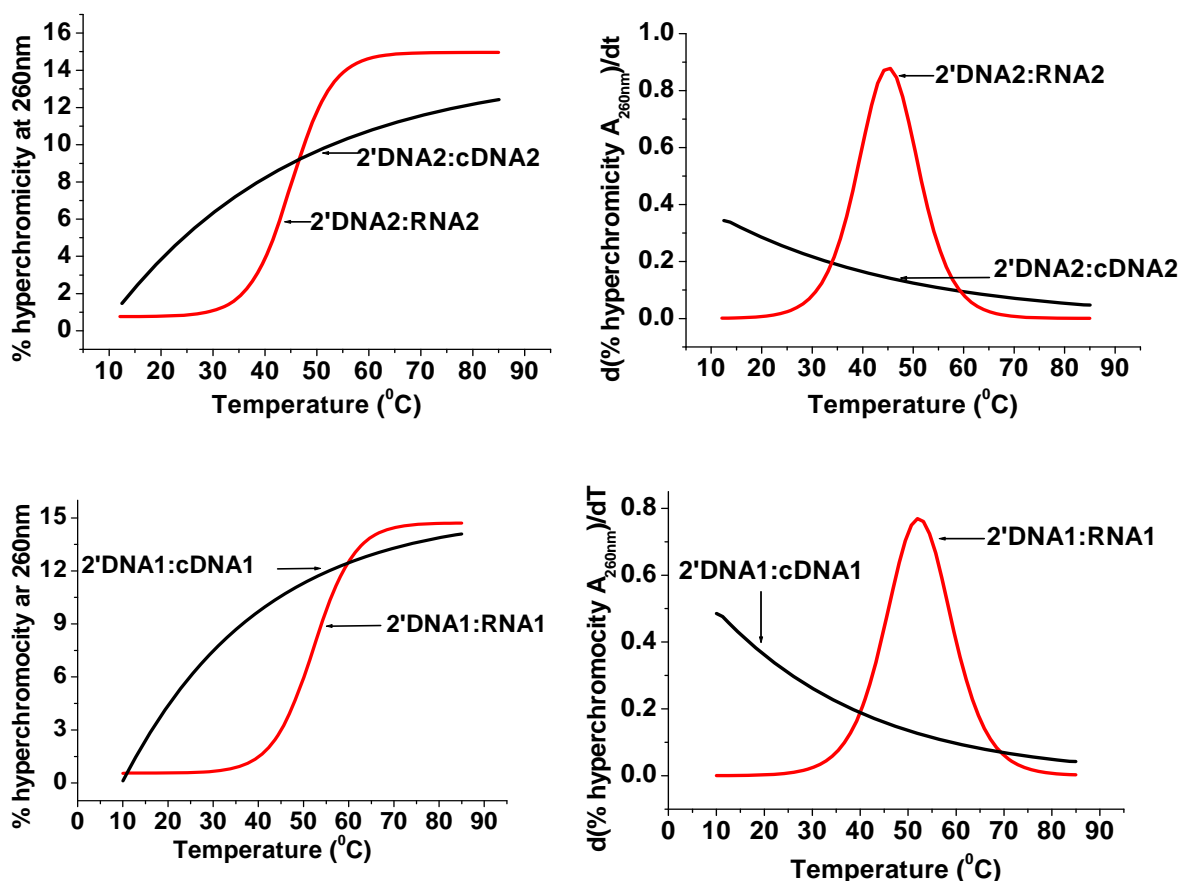


Figure 10. UV-melting plots and corresponding first derivative curves of complexes of DNA1 and DNA2 with complementary RNA1, RNA2 and complementary cDNA1 cDNA2 respectively.

Sharp, well-defined sigmoidal melting curves were observed for the complexes with complementary RNA with a 10-20% hyperchromicity at 260 nm, while complexes with complementary DNA gave no sigmoidal transition, indicating no complex formation. As seen from the entries in Table 4 and the UV T_m plots for the complexes containing modified 2'DNA-1 and 2'DNA-2, the S-type locked units were found to favour stable duplex formation with the complementary RNA (Figure 11). The N-type locked units, on the other hand, caused destabilization of the complexes with RNA (Figure 12).

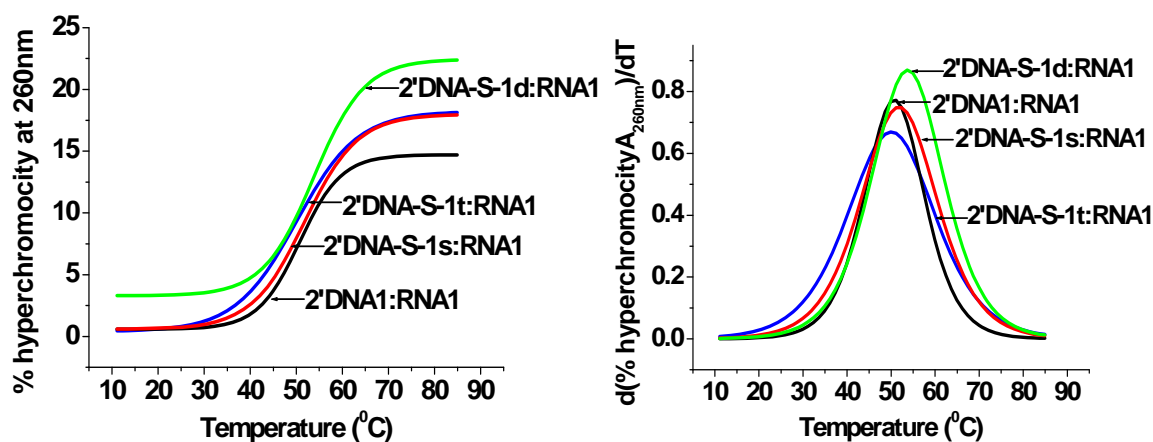


Figure 11. UV-melting plots and the respective first derivative curves of modified 2'DNA-1 of the S-type locked duplexes.

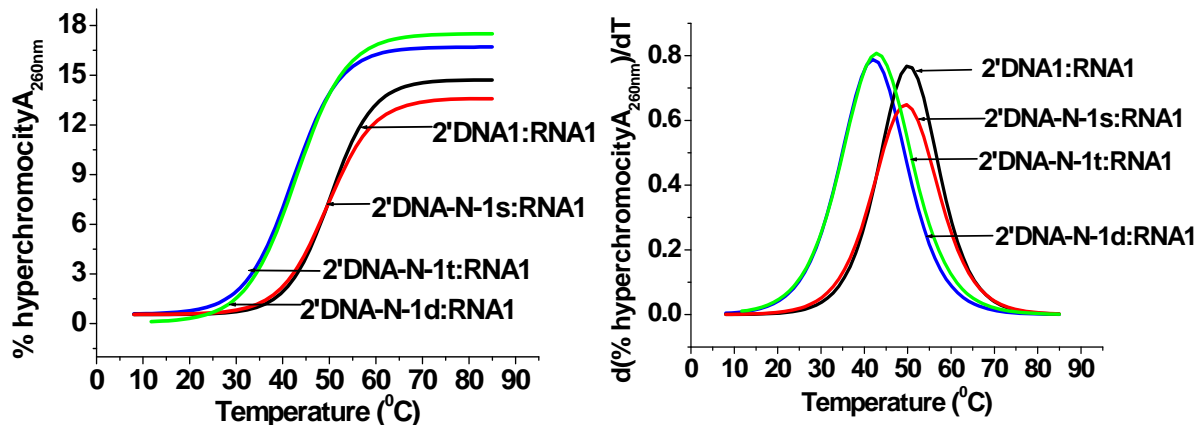


Figure 12. UV-melting plots and the respective first derivative curves of modified 2'DNA-1 of the N-type locked duplexes.

The stabilization increased with the increasing number of S-type modified units Table 4 entries **5** and **6** ($\Delta T_m = +0.5, +2.3^\circ\text{C}$). Likewise, destabilization was also more with increasing number of N-type units as seen from entries **2** and **3** ($\Delta T_m = -1.1, -7.7^\circ\text{C}$). The triple S-type modified 2'DNA-1 sequence **7** was almost as stable as the control, whereas the triple N-type modified 2'DNA-1 sequence **11** was destabilised even more ($\Delta T_m = -0.2, -8.3^\circ\text{C}$; entries **7** and **4** respectively). A similar increasing stabilization and destabilization pattern was seen for the S-type and N-type modified 2'DNA-2 sequence. A single N-type unit showed a slight stability however, double and triple N-type units considerably destabilized the sequences ($\Delta T_m = +0.4, -4.1, -4.1^\circ\text{C}$; entries **9**, **10** and **11**, Table 4, Figure 13). The S-type 2'DNA-2 sequences gave stable duplexes for single, double and triple

modifications ($\Delta T_m = +1.0, +0.7, +1.2^\circ\text{C}$, entry nos. **12**, **13** and **14**, Table 4, Figure 14). The stabilization caused by the S-type locked monomer (U^{S}) and the destabilization caused by the N-type locked monomer (U^{N}) were in accordance with the prediction of S-type conformation for the *iso*DNA strand in an *iso*DNA:RNA duplex.²³ However the pseudoequatorial orientation of the nucleobase in the U^{S} unit results in weaker stacking and hydrogen bonding interactions^{14a} in comparison with the nucleobase being in the pseudoaxial orientation (as in U^{N} unit and LNA modification). Hence the stability shown by the U^{S} unit was not as large as that by LNA. ($\Delta T_m \sim +4^\circ\text{C}/\text{modification}$)¹⁶ in 3'-5'-LNA:RNA duplexes. Thus the results obtained from this study confirm that in *iso*DNA:RNA duplexes, the DNA strand would prefer to assume S-type geometry that is

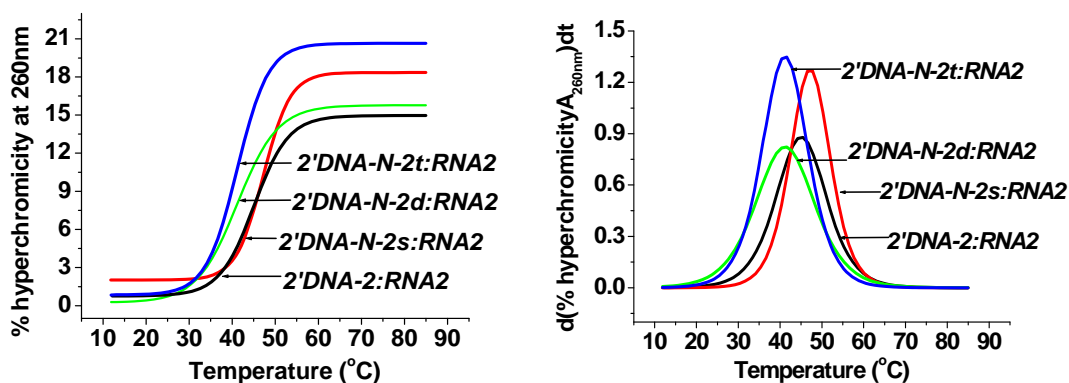


Figure 13. UV-melting plots and the respective first derivative curves of modified 2'DNA-2, of the N-type locked duplexes.

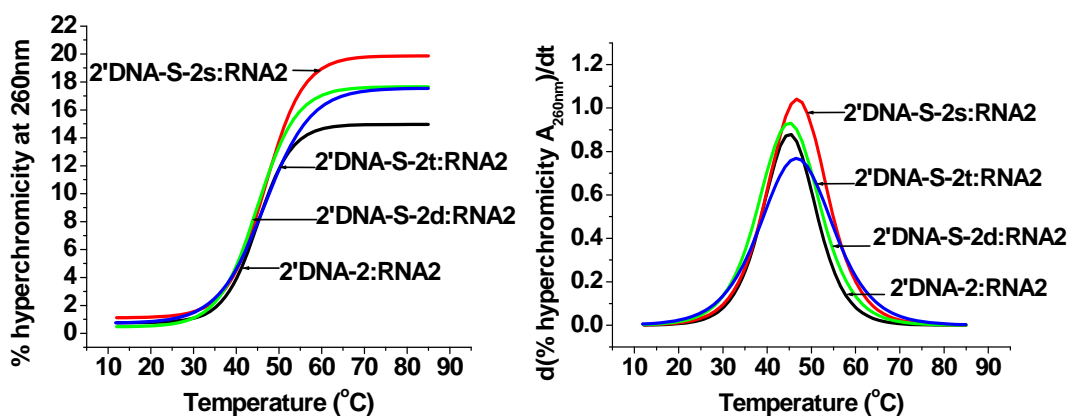


Figure 14. UV-melting plots and the respective first derivative curves of modified 2'DNA-2, of the S-type locked duplexes.

complemented by S-type locked units and the stability could be enhanced further, depending on the flanking base in the sequence.

2.6. CD spectroscopy of the duplexes

The duplex formation was further confirmed, for the sequences in the present studies, by CD spectroscopy of the 2'DNA-1 modified oligomers containing both S-type and N-type units, and the unmodified 2'DNA1 complexes with the complementary RNA sequence (Figure 15). CD spectra of the duplexes were similar for all complexes and resembled the A-type DNA:RNA duplex spectra,³⁴ when compared to the CD spectrum of 3'-5'-linked DNA1:cDNA-1 duplex- B-type. The structural features adopted due to the incorporation of modified units were not found to alter the overall structural features of the complexes formed, although the thermal stability was affected.

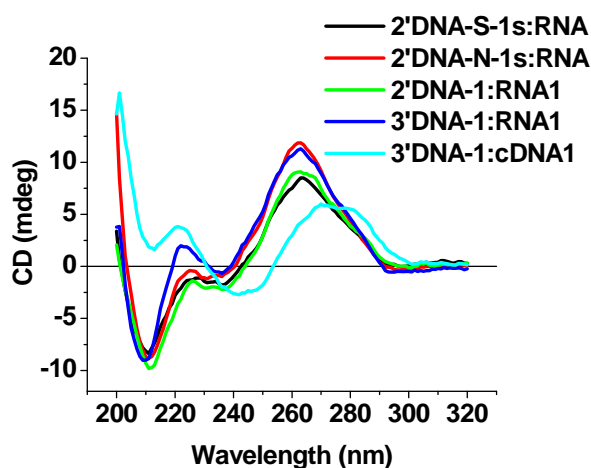


Figure 15. CD spectra of duplexes

2.7. Stability of the modified and unmodified 2'-5'-linked oligonucleotides towards snake venom phosphodiesterase (SVPD)

The stability of unmodified and modified 2'-5'-linked oligonucleotides towards the 3'-exonuclease, snake venom phosphodiesterase (SVPD) was examined and compared with the natural DNA. The oligonucleotides in this study were incubated at 37°C in the presence

of SVPD, and the reaction was monitored by RP-HPLC to determine the percentage of intact oligonucleotides at several time intervals (Figure 16).

The natural 3'-5'-ssDNA was completely digested within thirty minutes. The 2'-5'-linked 3'-deoxy-oligonucleotides were found to be stable under these conditions, however

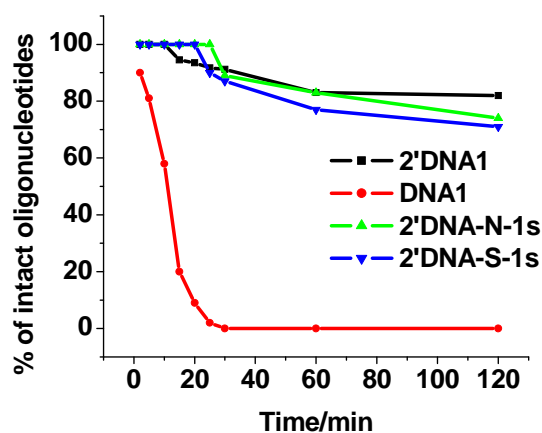


Figure 16. Stability assay of the 2'-5' oligonucleotides towards degradation by SVPD.

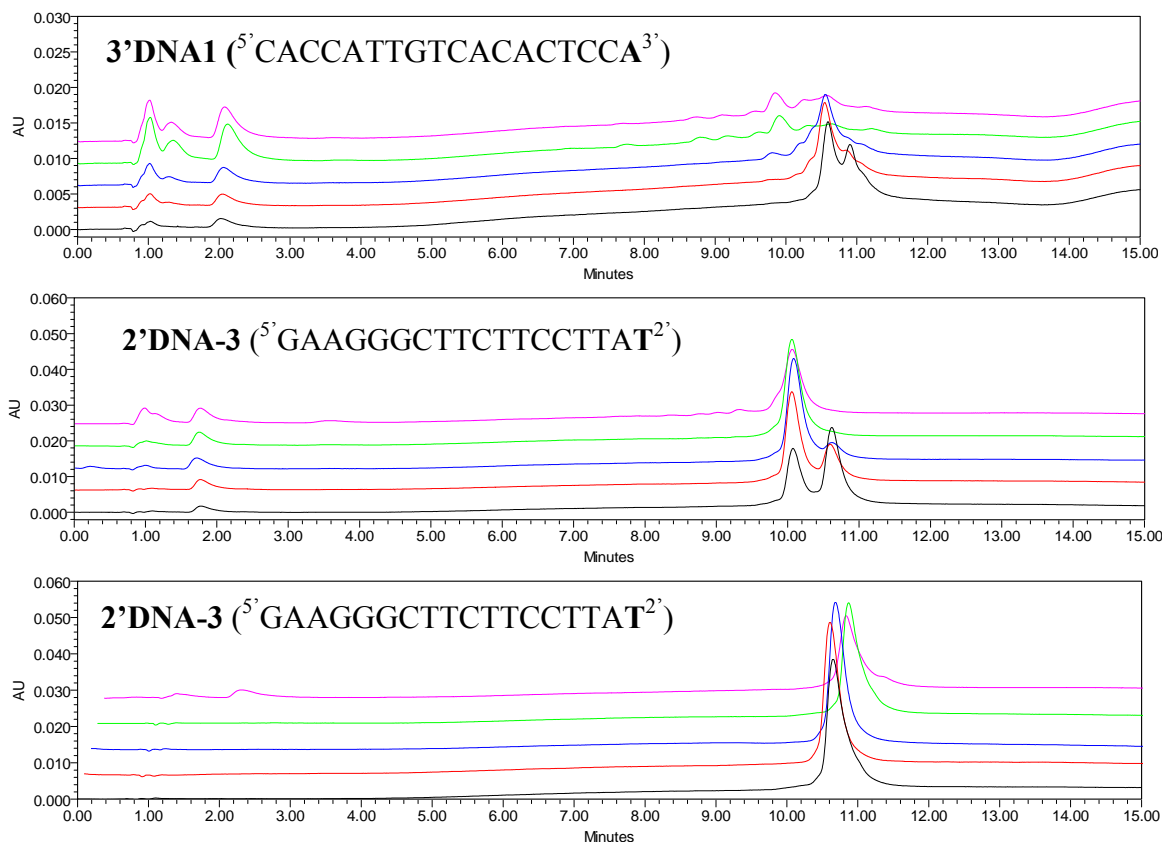


Figure 17: RP-HPLC runs overlay (Black-2min, red-5min, blue-10min, green-30min, magenta-120min.)

the 2'-terminal of the sequence, when a 3'-deoxy-riboadenosine -5'-phosphate, was cleaved. SVPD is known to cleave the tetrameric 2'-5'-adenine sequences,³⁵ and the sequences used in this study contain an adenine base at the 2'-end. This was investigated by collecting the HPLC peak seen as a one base deletion. The peak was identified by MALDI-TOF mass taken and was confirmed to be as the oligomer with one adenosine-5'-phosphate unit deleted. As an additional confirmation, an unmodified 2'-5'linked oligonucleotide 2'DNA-3 (^{5'}GAAGGGCTTCTTCCTTAT^{2'}) was synthesized. This sequence had a thymine base at the 2'end which when treated with SVPD remained stable towards the 3'-exonuclease cleavage (Figure 17).

In conclusion, the 2'-5'linked oligonucleotides were found to be resistant to digestion by the 3'-exonuclease SVPD, except for the hydrolytic cleavage of the 2'-end adenosine-5'-phosphate.

2.8. Summary

1. Synthesis and characterization of the N-type and S-type locked monomer building blocks was achieved.
2. Conformations of the N-type and S-type nucleoside analogues was determined using the H1'-H2'NMR coupling constants and NOE experiments.
3. 2'-5'-linked unmodified oligonucleotides and modified oligonucleotides containing N-type locked and S-type locked units were synthesized and characterised by MALDI-TOF.
4. UV melting studies confirmed the stabilization of oligonucleotides with S-type locked units and destabilization of the oligonucleotides containing N-type locked units.
5. CD analysis supported the A type duplex formation of the isoDNA:RNA duplexes.
6. The 2'-5'-linked unmodified oligonucleotides and modified oligonucleotides were found to be resistant to 3'-exonuclease SVPD digestion.

2.9. Conclusion

The introduction of locked N-type and S-type nucleoside analogues in 2'-5' oligonucleotides was thoroughly investigated. The results indicate that in the 2'-5'-linked

oligonucleotides preferred geometry of the furanose ring is S-type. Thus the present findings confirm that in *isoDNA*:RNA complexes, the DNA strand would prefer to assume S-type geometry that is complemented by furanose ring locked in S-type geometry resulting in A-type duplexes. The stability of these oligonucleotides towards SVPD is definitely better than the natural 3'-5'-phosphodiester linked oligomers, with the exception of a 2'-terminal adenosine-5'-phosphate.

2.10 Experimental

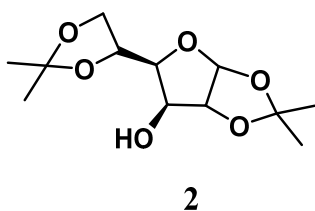
General remarks: All the reagents were purchased from Sigma-Aldrich and used without further purification. DMF, ACN, were dried over P₂O₅ and CaH₂ respectively and stored by adding 4 Å molecular sieves. Pyridine, TEA were dried over KOH and stored on KOH. THF was passed over basic alumina and dried by distillation over sodium metal. Reactions were monitored by TLC. TLCs were run in either Petroleum ether with appropriate quantity of EtOAc or DCM with an appropriate quantity of MeOH for most of the compounds. TLC plates were visualized with UV light and iodine spray and/or by spraying perchloric acid solution and heating. Usual reaction work up involved sequential washing of the organic extract with water and brine followed by drying over anhydrous Na₂SO₄ and evaporation of the solvent under vacuum. Column chromatographic separations were performed using silica gel 60-120 mesh (Merck) or 200- 400 mesh (Merck) and using the solvent systems EtOAc/Petroleum ether or MeOH/DCM. TLC was run using pre-coated silica gel GF254 sheets (Merck 5554).

¹H and ¹³C NMR spectra were obtained using Bruker AC-200, AC-400 and AC-500 NMR spectrometers. The chemical shifts (δ/ppm) are referred to internal TMS/DMSO-d₆ for ¹H and chloroform-*d*/DMSO-d₆ for ¹³C NMR. ¹H NMR data are reported in the order of chemical shift, multiplicity (s, singlet; d, doublet; t, triplet; br, broad; br s, broad singlet; m, multiplet and/ or multiple resonance), number of protons. Mass spectra were recorded on APQSTAR spectrometer, LC-MS on a Finnigan-Matt instrument. DNA oligomers were synthesized on CPG solid support using Bioautomation MerMade 4 synthesizer. The RNA oligonucleotides were obtained commercially (Sigma-Aldrich). RP-HPLC was carried out

on a C18 column using either a Varian system (Analytical semi-preparative system consisting of Varian Prostar 210 binary solvent delivery system, a Dynamax UV-D2 variable wavelength detector and Star chromatography software) or a Waters system (Waters Delta 600e quaternary solvent delivery system with 2998 photodiode array detector and Empower2 chromatography software). MALDI-TOF spectra were recorded on a Voyager-De-STR (Applied Biosystems) MALDI-TOF instrument or AB Sciex TOF/TOF™ Series Explorer™ 72085 instrument and the matrix used for analysis was THAP (2', 4', 6'-trihydroxyacetophenone). UV experiments were performed on a Varian Cary 300 UV-VIS spectrophotometer fitted with a Peltier-controlled temperature programmer. CD spectra were recorded on a Jasco J-715 Spectropolarimeter, with a ThermoHaake K20 programmable water circulator for temperature control of the sample.

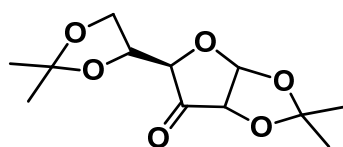
2.10.1 Synthesis of compounds/monomers

1,2:5,6-diisopropylidene D-Glucofuranose (**2**)



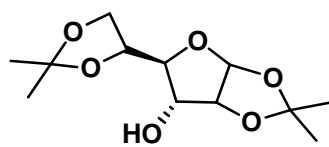
D-Glucose **1**, (10.0 g, 55.5 mmol) and anhydrous CuSO₄ (17.5 g, 1.1 mmol) were mixed together and 100 mL dry acetone was added. After vigorous stirring for few minute at ice cold temperature, catalytic amount of conc. H₂SO₄ (0.6 mL) was added dropwise. Reaction mixture was stirred at room temperature for 48 hrs. TLC showed complete product formation. The reaction mixture was neutralized with saturated aqueous solution of K₂CO₃. The reaction mixture was filtered and the filtrate along with acetone washings was concentrated to thick syrup. Co-evaporation with dichloromethane and petroleum ether gave a white solid. The crude product was recrystallized from petroleum ether to obtain compound **2** as a white solid. Yield: 8.1 g, 56%.

¹H NMR (200MHz, CDCl₃): δ 1.32 (s, 3H, CH₃), 1.37 (s, 3H, CH₃), 1.45 (s, 3H, CH₃), 1.50 (s, 3H, CH₃), 2.57 (d, 1H, *J*=3.66 Hz, exchanges with D₂O, 3-OH), 3.95-4.21 (m, 3H, H₄, H₆), 4.29-4.39 (m, 2H, H₃, H₅), 4.53 (d, 1H, *J* = 3.66Hz, H₂), 5.95 (d, 1H, *J* = 3.67 Hz, H₁). **¹³C NMR** (50MHz, CDCl₃): δ 25.1, 26.1, 26.7, 26.8, 67.6, 73.4, 75.1, 81.0, 85.0, 105.2, 109.6, 111.8. **Mass** (ESI): *m/z* 260.1260, found 283.2372 (M+Na⁺).

1, 2:5, 6-Di-*O*-isopropylidene- α -D-ribohexofuranose-3-ulose (3)**3**

Pyridinium chlorochromate (5.3 g, 24.5 mmol) and powdered molecular sieve (30 g) were added to compound **2** (1.3 g, 5.0 mmol) in dry CH₂Cl₂ (100 mL) and the mixture was stirred at room temperature for 18 hrs. The resulting suspension was diluted with diethylether (50 mL) and filtered through a silica gel bed. Several washings were added till collected fractions showed no product spot on TLC. The solvent was removed from filtrate to give the crude compound **3** as pinkish white solid which is unstable in nature, therefore was used for next reaction immediately. Yield: 1.2 g, 93 %.

IR (CHCl₃): ν_{\max} 3457, 2938, 2990, 1772, 1375, 1217, 1073.78, 846, 757.28 667.73.

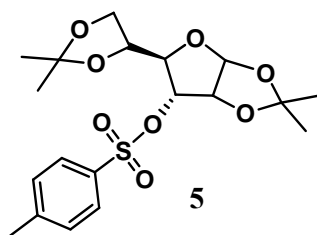
1, 2:5, 6-Di-*O*-isopropylidene- α -D-allofuranose (4)**4**

The compound **3** (1.3 g, 5.03 mmol) dissolved in mixture of MeOH (40 mL) and H₂O (10 mL) and cooled to 0°C. NaBH₄ (0.476 g, 12.5 mmol) was added in portions over half hour and reaction mixture stirred for 2 hrs. Reaction mixture was concentrated to remove methanol. Reaction mixture was then neutralized with sat. aqueous solution of NH₄Cl, extracted with CH₂Cl₂, followed by water wash and drying over Na₂SO₄. Removal of solvent yielded a sticky liquid which on coevaporation with petroleum ether gave a white solid. Yield: 0.860 g, 65.6%.

¹H NMR (200MHz, CDCl₃) : δ 1.38 (s, 3H, CH₃), 1.39 (s, 3H, CH₃), 1.47 (s, 3H, CH₃), 1.59 (s, 3H, CH₃), 2.63 (d, 1H, exchanges with D₂O, 3-OH), 3.79-3.86 (dd, $J=4.26$ and 8.4 , 1H, H3), 3.98-4.13 (m, 3H, H6, H4), 4.36-4.27 (m, 1H, H5), 4.60-4.65 (dd, 1H, $J=5.06$, 3.92Hz , H2), 5.83 (d, 1H, $J=3.8\text{Hz}$, H1). **¹³C NMR** (50MHz, CDCl₃): δ 25.2, 26.2, 26.4, 26.5, 65.7, 72.4, 75.5, 78.9, 79.6, 103.8, 109.8, 112.8. **Mass** (ESI): m/z 260.1260, found 283.2372 (M+Na⁺).

1, 2:5, 6-di-*O*-isopropylidene-3-*O*-p-toluenesulphonyl- α -D-allofuranose (5)

The substrate **4**, well dessicated (0.860 g, 3.307 mmol) was dissolved in 14 mL dry pyridine and cooled to 0°C. *p*-Toluenesulphonyl chloride (0.94 g, 4.95 mmol) was added in

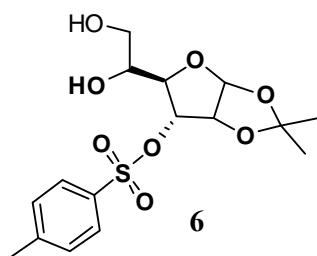


small portions and the reaction mixture was stirred for 2 hrs at room temperature. Pyridine was removed under reduced pressure. Crude product was extracted with CH₂Cl₂, washed with aqueous sodium bicarbonate and water. The extract was dried over Na₂SO₄, concentrated and coevaporated with petroleum ether to give a white solid. The crude product was

purified by silica gel (60-120 mesh) column chromatography using EtOAc / Petroleum ether (3:7) to offer the compound **5** as white solid. Yield: 0.920 g, 67% yield.

¹H NMR (200 MHz, CDCl₃): δ 1.29 (s, 3H, CH₃), 1.30 (s, 3H, CH₃), 1.33 (s, 3H, CH₃), 1.53 (s, 3H, CH₃), 2.45 (s, 3H, Tos-CH₃), 3.74-3.82 (m, 1H, H₆), 3.90-3.97 (m, 1H, H₆), 4.10-4.24 (m, 2H, H₄, H₅), 4.62-4.69 (m, 2H, H₃, H₂), 5.77 (d, 1H, *J* = 3.42Hz, H₁), 7.37 (d, 2H, Ar), 7.89 (d, 2H, Ar). **¹³C NMR** (50MHz, CDCl₃): δ 21.6, 25.0, 26.0, 26.5, 26.6, 65.1, 74.5, 76.4, 76.9, 77.9, 103.7, 109.8, 113.5, 128.3, 129.6, 133.0, 145.1. **Mass** (ESI): *m/z* 414.1348, found 437.3269 (M+Na⁺)

1, 2-*O*-isopropylidene-3-*O*-*p*-toluenesulphonyl- α -D-allofuranose (**6**)

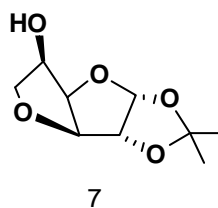


Compound **5** (1.3 g, 3.14 mmol) was dissolved in 20 mL methanol and 0.8% aqueous H₂SO₄ added to it. Overnight stirring at room temperature gave the required selectively hydrolysed product. After neutralizing the reaction mixture with aqueous K₂CO₃, solvent was removed to get a white solid which

was extracted with 15% methanol in ethyl acetate. The organic phase was dried over anhydrous Na₂SO₄. The crude white solid obtained on solvent removal was used without any further purification. Yield: 1.0 g, 84 %.

¹H NMR (200 MHz, DMSO-*d*₆): δ 1.20 (s, 3H, CH₃), 1.41 (s, 3H, CH₃), 2.42 (s, 3H, CH₃-Tos), 3.12-3.17 (m, 2H, H₆), 3.56 (m, 1H, H₅), 4.05-4.10 (m, 1H, H₄), 4.49-4.53 (m, 1H, H₂), 4.57-4.62 (m, 1H, OH, exchanges with D₂O), 4.75-4.81 (m, 1H, H₃), 4.97-4.99 (bd, 1H, OH, exchanges with D₂O), 5.7 (d, 1H, H₁, *J* = 3.58Hz), 7.46-7.50 (d, 2H, Ar, *J* = 8.02Hz), 7.80-7.84 (d, 2H, Ar, *J* = 8.58Hz). **Mass** (ESI) 374.1035, found 397.04 (M+Na⁺)

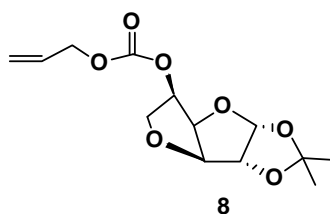
3, 6-anhydro-1,2-isopropylidene- α -D-glucofuranose (7)



Compound **6** (1.0 g, 0.267 mmol) was treated with 40 mL of sodium methoxide in methanol (0.125M) and the reaction heated at 60°C for 3h. Reaction mixture was moistened with 1mL water and neutralized with H⁺ resin. Reaction mixture was filtered quickly and the resin washed with methanol. The filtrate was concentrated to give sticky solid which was column purified on a silica gel column using and EtOAc/ petroleum ether as an eluant. The compound eluted in 35% ethyl acetate in petroleum ether. Yield: 0.422g, 78.18%.

¹H NMR (200MHz, DMSO-d₆): δ 1.26 (s, 3H, CH₃), 1.39 (s, 3H, CH₃), 3.30-3.38 (m, 1H, H₆), 3.71-3.78 (m, 1H, H₆), 4.05-4.18 (m, 1H, H₅), 4.37-4.39 (m, 1H, H₃), 4.51-4.52 (m, 1H, H₂), 4.56-4.60 (dd, 1H, H₄, J = 3.92Hz), 5.03-5.07 (d, 1H, OH, J =6.7 Hz, exchanges with D₂O) 5.92 (d, 1H, H₁, J = 3.68 Hz). **Mass** (ESI) 202.0841, found 225.2823 (M+Na⁺), 241.2968 (M+K⁺)

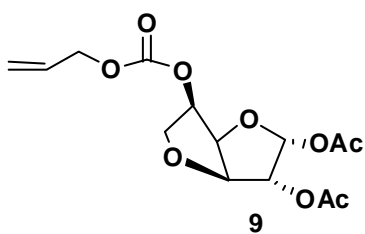
5-*O*-allyloxy-3, 6-anhydro-1,2-isopropylidene-glucofuranose (8)



Compound **7** (0.46 g, 2.28 mmol) was dissolved in dry dichloromethane (9 mL). Anhydrous pyridine (0.38 mL) was added and the reaction mixture was cooled to 0°C in an ice-bath. Allyloxycarbonyl chloride (0.3 mL, 2.91 mmol) was added dropwise and then the reaction was stirred at room temperature for 2 hrs. TLC showed absence of starting compound. The reaction mixture was extracted with CH₂Cl₂, followed by water wash and drying over sodium sulphate. Removal of solvent yielded a sticky gum having compound **8**, which was used without any further purification.

¹H NMR (200 MHz, CDCl₃): δ 1.34 (s, 3H, CH₃), 1.49 (s, 3H, CH₃), 3.78-3.86 (m, 1H, H₆), 4.00-4.08 (m, 1H, H₆), 4.54-4.56 (d, 1H, J = 3.66, H₃), 4.61-4.67 (m, 3H, H₂, H₄, H₅), 4.99-5.09 (m, 2H, allyl-H), 5.25-5.43 (m, 2H, allyl-H), 5.84-6.03 (bm, 1H, allyl-H) 6.00 (d, 1H, J = 3.55 Hz, H₁). **¹³C NMR** (50MHz, CDCl₃): δ 26.7, 27.3, 68.7, 68.8, 76.0, 80.7, 84.8, 85.2, 107.1, 112.7, 119.1, 131.1, 154.1. **HRMS** (ESI) calcd. for C₁₃H₁₉O₇ (M+H⁺) 287.1125, found: 287.1123.

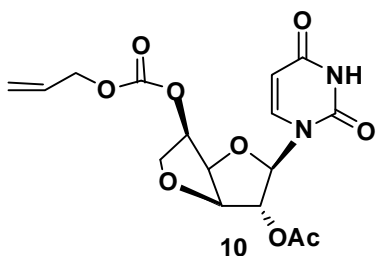
1,2-di-*O*-acetyl-3,6-anhydro-5-*O*-allyloxy- α,β -glucofuranose (**9**)



Compound **8** was desiccated (1.50 g, 0.52 mmol) and dissolved in acetic acid (16 mL). Acetic anhydride (1.6 mL) was added, after cooling the reaction flask to 10°C, followed by dropwise and slow addition of concentrated sulfuric acid (0.16 mL). The reaction mixture was stirred overnight at room temperature. TLC indicated complete product formation. The reaction was quenched with ice and 5% aqueous NaHCO₃, then extracted with CH₂Cl₂, followed by water wash and drying over sodium sulphate. After solvent removal the crude product was purified by silica gel column chromatography using petroleum ether and ethyl acetate as eluants. The compound **9** was eluted in 30% ethyl acetate in petroleum ether. Yield: 1.32 g, 76.3%.

IR (CHCl₃): ν_{\max} (cm⁻¹) 3024, 1749, 1650, 1428.16, 1371.84, 1266.85, 1114.45, 1061.37, 1024.79, 957.51, 879.82, 755.49, 667.5, 599.59. **¹H NMR** (200 MHz, CDCl₃): δ 2.07 (s, 3H, CH₃), 2.09 (s, 3H, CH₃), 3.84-3.92 (m, 1H, H6), 4.05-4.11 (m, 1H, H6), 4.64-4.67 (m, 2H, allyl-H), 4.78 (dd, 1H, $J=5.56, 3.66$ Hz, H3), 4.98 (m, 1H, H4), 5.15 (m, 1H, H5), 5.26-5.31 (m, 2H, allyl-H), 5.41 (m, 1H, H2), 5.84-6.23 (m, 1H, allyl-H), 6.52 (d, 1H, H1, $J=4.2$ Hz). **¹³C NMR** (50MHz, CDCl₃): δ 20.3, 20.75, 68.4, 68.5, 74.9, 80.3, 83.0, 85.2, 100.2, 118.7, 131.0, 153.8, 169.0. **HRMS** (ESI) calcd. for C₁₄H₁₈O₉Na (M+Na⁺) 353.0843, found: 353.080

2'-*O*-acetyl-3',6'-anhydro-5'-*O*-allyloxy-uridine (**10**)

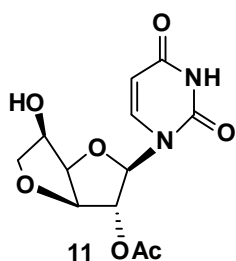


Compound **9** (1.11 g, 3.36mmol), obtained from the previous step was dissolved in anhydrous acetonitrile (35 mL). Reaction flask was flushed with nitrogen and uracil (0.45 g, 4.03 mmol) was added. N,O-Bis(trimethylsilyl)acetamide (BSA) (0.27 mL, 1.1 mmol) was added to the reaction flask under nitrogen atmosphere. Then the reaction mixture was refluxed at 70°C for one hour, followed by cooling in an ice bath. TMSOTf (0.23 mL, 1.27 mmol) was added slowly with a syringe and the reaction mixture was refluxed for three

hours. TLC showed disappearance of starting material and appearance of a lower moving UV-positive spot which charred on acid spraying and heating. The reaction mixture was cooled to room temperature, diluted with dichloromethane, washed with NaHCO_3 and water, dried over sodium sulphate followed by solvent removal. The crude product was purified by silica gel column chromatography using dichloromethane and methanol as eluants. Compound **10** eluted in 2.5% methanol in dichloromethane. Yield: 1.19g, 92.96%.

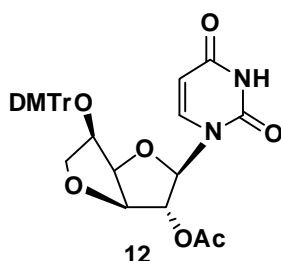
IR (CHCl_3): ν_{max} (cm^{-1}) 3391.85, 3020.46, 2924.68, 2853.76, 1751.23, 1694.89, 1458.89, 1381.57, 1265.47, 1216.15, 1090.08, 1060.10, 758.86, 668.59. **^1H NMR** (200 MHz, CDCl_3): δ 2.13 (s, 3H, CH_3), 4.09-4.12 (m, 2H, $\text{H6}'$, $\text{H6}''$), 4.54-4.57 (dd, $J=4.55$ Hz, 1H, $\text{H3}'$), 4.62-4.66 (m, 2H, allyl-H), 4.96 (m, 1H, $\text{H5}'$), 5.15-5.32(m, 3H, $\text{H4}'$ and allyl-2H), 5.41 (m, 1H, $\text{H2}'$), 5.79-6.01 (m, 2H, allyl-H, H5), 6.24 (d, 1H, $\text{H1}'$, $J=3.88\text{Hz}$), 7.62 (d, 1H, $J=8.21$ Hz, H6), 8.84 (bs, 1H, NH). **^{13}C NMR** (50MHz, CDCl_3): δ 20.4, 69.0, 70.9, 76.0, 79.2, 81.2, 85.5, 90.5, 103.4, 119.4, 130.8, 139.7, 150.3, 153.9, 163.1, 169.4. **HRMS** (ESI) calcd. for $\text{C}_{16}\text{H}_{19}\text{O}_9\text{N}_2$ ($\text{M}+\text{H}^+$) 383.1085, found: 383.1086.

5'-hydroxy-2'-*O*-acetyl-3',6'-anhydro-uridine (**11**)



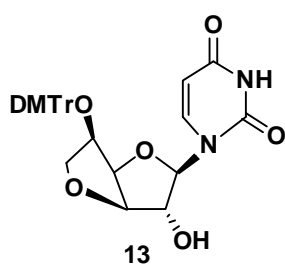
Compound **10** (1.19 g, 3.14 mmol) obtained in the previous step, was dissolved in dichloromethane (45 mL). PPh_3 (0.54 g, 2.06 mmol) was added, followed by piperidine (2.0 mL, 0.02 mmol) and tris(dibenzylidene acetone) dipalladium [$\text{Pd}_2(\text{dba})_3$] (0.15 g, 0.16 mmol). The reaction mixture was stirred for 10 minutes. TLC showed absence of starting compound. Solvent was removed and the crude product was given a wash with solvent ether. Column purification done on a silica gel column yielded the pure compound **5**, which eluted in methanol (3.5%) in dichloromethane. Yield: 0.65g, 70%.

^1H NMR (200 MHz, CD_3OD) : δ 2.13 (s, 3H, CH_3), 2.95 (d, 1H, $J=7.98\text{Hz}$, OH), 3.85-3.88 (m, 1H, $\text{H6}''$), 4.04-4.08 (m, 1H, $\text{H6}'$), 4.51-4.52 (m, 2H, $\text{H4}'$, $\text{H5}'$), 4.71-4.72 (m, 1H, $\text{H3}'$), 5.28-5.29 (m, 1H, $\text{H2}'$) 5.82 (d, 1H, H5 , $J=8.19\text{Hz}$), 6.23 (d, 1H, $\text{H1}'$, $J=3.6\text{Hz}$), 7.59 (d, 1H, H6 , $J=8.32\text{Hz}$), 8.45 (s, 1H, NH). **^{13}C NMR** (50MHz, CD_3OD): δ 20.5, 72.3, 73.8, 79.8, 82.7, 85.5, 91.3, 103.8, 140.4, 150.0, 162.4, 169.5. **HRMS** (ESI) calcd. for $\text{C}_{12}\text{H}_{15}\text{O}_7\text{N}_2$ ($\text{M}+\text{H}^+$) 299.0874, found: 299.0873.

5'-O-dimethoxytrityl-2'-O-acetyl-3',6'-anhydro-uridine (12)

The substrate **11** (0.43 g, 1.44 mmol) was co-evaporated with anhydrous pyridine twice, and then dissolved in anhydrous pyridine (10 mL). 4, 4'-Dimethoxytritylchloride (1.46 g, 4.32 mmol) was added in one lot. The reaction mixture was stirred overnight at room temperature, when TLC showed a faster moving trityl-positive spot which charred on acid spraying and heating. The reaction was quenched with methanol, extracted with dichloromethane, washed with NaHCO₃ and water, dried over sodium sulphate, followed by solvent removal. The crude product was purified by silica gel column chromatography using dichloromethane, methanol and pyridine (0.5%) as eluants. Compound **12** is eluted in methanol (1.5%) in dichloromethane. Yield: 0.73g, 84.3%.

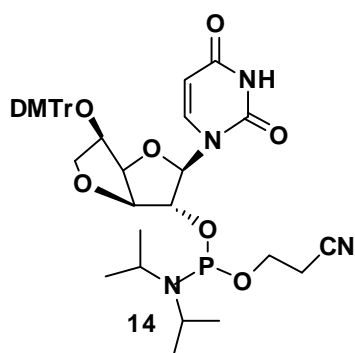
¹H NMR (200 MHz, CDCl₃): δ 2.09 (s, 3H, CH₃), 3.22-3.44 (m, 2H, H6', H6''), 3.80 (s, 6H, OCH₃), 4.13-4.30 (m, 3H, H4', H3', H5'), 5.14-5.16 (m, 1H, H2'), 5.79 (d, 1H, H5, *J*= 8.10Hz), 6.05 (d, 1H, H1', *J*= 3.4Hz), 6.82-6.87 (m, 4H, DMTr), 7.31-7.5 (m, 9H, DMTr), 7.81 (d, 1H, H6, *J*= 8.17Hz), 8.65 (s, 1H, NH). ¹³C NMR (50MHz, CDCl₃) δ 20.5, 55.2, 70.8, 74.2, 80.4, 82.4, 84.6, 87.5, 90.4, 102.9, 113.3, 172.1, 172.8, 127.8, 129.9, 135.7, 135.9, 139.9, 144.8, 149.7, 150.3, 158.8, 163.1, 169.4. HRMS (ESI) calcd. for C₃₃H₃₂O₉N₂Na (M+Na⁺) 623.2000, found: 623.2000.

5'-O-dimethoxytrityl-2'-hydroxy-3',6'-anhydro-uridine (13)

The substrate **12** (0.70 g, 1.16 mmol) was dissolved in AR grade methanol (50 mL). Aqueous ammonia (15 mL) was added and the pinkish slightly turbid reaction mixture was stirred for one hour at room temperature. TLC showed the absence of starting compound. The solvents were removed to get a yellowish solid. The solid was redissolved in dichloromethane and given a water wash. The organic layer was dried over sodium sulfate and concentrated to get a pale yellow solid foam. Purification was done by silica gel column chromatography using dichloromethane, methanol and pyridine (0.5%) as eluants. Compound **13** eluted in methanol (2.5%) in dichloromethane. Yield: 0.62g, 93.2%.

¹H NMR (200 MHz, CDCl₃): δ 3.21-3.31 (m, 2H, H6', H6''), 3.79 (s, 6H, OCH₃), 4.17-4.18 (d, 1H, *J*= 3.52 Hz, H3'), 4.34-4.38 (m, 1H, H4'), 4.44-4.47 (m, 2H, H2', H5'), 5.71 (d, 1H, *J*= 8.1Hz, H5) 5.79 (s, 1H, H1'), 6.83-6.86 (m, 4H, DMTr), 7.21-7.41 (m, 7H, DMTr), 7.48 (m, 2H), 8.30 (d, 1H, *J*= 8.1Hz, H6), 10.41 (bs, 1H). Note- Trace amount of pyridine showed peaks at 7.29 (m, 2H) 7.69 (m, 1H), 8.62 (m, 2H) **¹³C NMR** (50MHz, CDCl₃): δ 55.2, 72.2, 75.0, 80.1, 85.3, 86.7, 88.0, 95.9, 101.2, 113.3-113.4, 123.8, 127.1, 127.8, 128.1, 129.9, 135.8, 136.0, 136.0, 140.6, 144.9, 149.6, 150.8 158.8, 164.2. MS (ESI) 558.2002, **HRMS** (ESI) calcd. for C₃₁H₃₀O₈N₂Na (M+Na⁺) 581.1894, found: 581.1896.

5'-*O*-Dimethoxytrityl-3'-*O*,5'-*C*-methylene (uridine) xylonucleoside-2'-*O*-phosphoramidite (14)

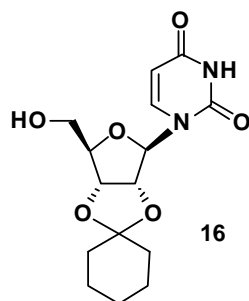


Compound **13** (0.20 g, 0.36 mmol) was co-evaporated with dry CH₂Cl₂, and then dissolved in dry dichloromethane (3.0 mL). Diisopropylethylamine (DIPEA) (0.19 mL, 1.07 mmol) was added, followed by chloro (2-cyanoethoxy)-*N*, *N*-diisopropyl amino)-phosphine (0.16 mL, 0.72 mmol) at 0°C. The reaction mixture was stirred under argon atmosphere at room temperature for 3 hours, when TLC indicated the absence of starting material. The reaction mass was diluted with dichloromethane, washed with NaHCO₃ and water, dried over sodium sulphate, followed by solvent removal. The crude product was purified by silica gel column chromatography using a 1:1 mixture of dichloromethane:ethylacetate and 1% triethylamine. Yield: 0.16g, 58.9%.

³¹P NMR (50 MHz, CDCl₃) : 150.7, 152.0. **HRMS** (ESI) calcd. for C₄₀H₄₉O₉N₄(M+H⁺) 759.3153 found: 759.3155, C₄₀H₄₈O₉N₄Na (M+Na⁺) 781.2973 found: 781.2974, and C₄₀H₄₉O₉N₄ K(M+K⁺) 797.2712 found: 797.2712.

2',3'-*O*-cyclohexylidene-uridine (16)

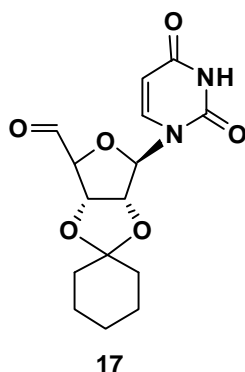
To a mixture of uridine (5.0 g, 20.49 mmol) and *p*TSA (0.352 g, 2.0492 mmol), was added cyclohexanone (30 mL). The reaction was stirred at room temperature for overnight. It was warmed at 40-50°C, 3h, when a clear solution was obtained and TLC indicated



consumption of starting material and appearance of a faster-moving spot. Addition of petroleum ether resulted in the precipitation of a white solid, which was filtered off and washed thoroughly with petroleum ether. It was then dried by desiccation to afford the desired product **16** in pure form. Yield 6.30 g, 95 %.

$^1\text{H NMR}$ (CDCl_3 , 200MHz) : δ 1.75, 1.58, 1.40 (m, 10H, cyclohexyl $\text{CH}_2 \times 5$), 3.48 (br, 1H, OH), 3.86 (m, 2H, $\text{H}5'$, $\text{H}5''$), 4.29 (m, 1H, $\text{H}4'$), 4.93 (dd, $J=3.29$, 6.32Hz, 1H, $\text{H}3'$), 5.01 (dd, $J=2.78, 6.31$ Hz, 1H, $\text{H}2'$), 5.65 (d, $J_{1'2'}=2.65$ Hz, 1H, $\text{H}1'$), 5.74 (d, $J=8.09$ Hz, 1H, $\text{H}5$), 7.46 (d, $J=8.09$ Hz, 1H, $\text{H}6$), 9.88 (s, 1H, $\text{N}3\text{H}$), $^{13}\text{C NMR}$ (CDCl_3 , 50.32MHz): δ 37.0, 34.6, 24.8, 23.9 and 23.5, 62.4, 79.9, 83.3, 87.1, 95.3, 102.5, 115.1, 143.1, 150.5, 163.9. **Mass** (ESI) 324.1321, found 325.7817 ($\text{M}+\text{H}^+$).

5'-aldehyde- 2',3'-*O*-cyclohexylidene-uridine (**17**)

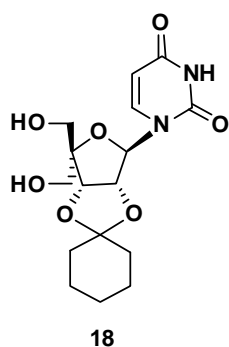


2',3'-*O*-cyclohexylidene-uridine **16** (0.2 g, 0.62 mmol) was dissolved in acetonitrile (20.0ml). To this, IBX (0.519 g, 1.85 mmol) was added and the mixture was heated at 80°C, 2.5h, when TLC examination revealed absence of starting material. The reaction was allowed to cool to r.t. and then, cooled on ice, before filtering off the IBX through a pad of Celite. The filtrate was concentrated, adsorbed on silica gel and immediately purified by short column chromatography on silica gel (60-120 mesh). Elution was carried out from 10 to 50% acetone/petroleum ether. The pure fractions were concentrated to give a solid white foam which was used for next reaction. Yield 160 mg, 76.5%.

Mass (ESI) 322.1165, found 323.2378 ($\text{M}+\text{H}^+$)

2',3'-*O*-cyclohexylidene-4'-hydroxymethyl uridine (**18**)

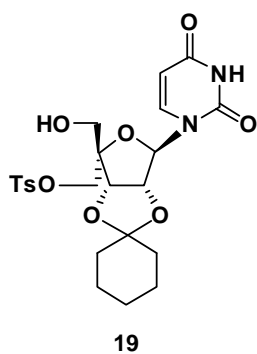
To a solution of 5'-aldehyde-2',3'-*O*-cyclohexylidene-uridine **17** (150 mg, 0.466 mmol) in dioxane (1.0 mL), was added aqueous formaldehyde (37%, 0.088 mL, 0.88 mmol), while cooling in a water bath. This was followed by addition of aqueous NaOH (2N, 0.44 mL,



0.88mmol). After 5min, the reaction was cooled in an ice-bath and NaBH₄ (32 mg, 0.839 mmol) was added. The clear yellow solution developed turbidity, but stayed yellow. Stirring was continued in an ice-bath, 15min and then, at ~20°C (solution turned clear), 2h. TLC examination revealed the consumption of starting material and appearance of a lower-moving spot. The reaction was neutralized using Tulsion H⁺ resin. A small amount of white solid was formed, which did not dissolve in dioxane, water or ethanol. The resin and white solid were filtered off and washed with dioxane and ethanol. The filtrate was concentrated, silica gel was added to adsorb, and the mixture was immediately purified by column chromatography on silica gel (60-120mesh). Elution was carried out from 5 to 10% MeOH in CHCl₃. The fractions of pure product were concentrated under vacuum to get a white solid. Yield 60 mg, 38.3%.

¹H NMR (DMSO-*d*₆, 200MHz): δ 1.67, 1.51, 1.36 (m, 10H, CH₂x5), 3.55, 3.63 (m, 4H, CH₂OHx2), 4.66 (t, *J*_{5,6}=5.56, 5.81Hz, 1H, 3'-OH), 4.76 (d, *J*_{2',3'}=6.07Hz, 1H, H3'), 4.87 (t, *J*_{1',2'}=4.17, *J*_{2',3'}=6.06Hz, 1H, H2'), 4.87 (t, *J*_{1',2'}=4.17, *J*_{2',3'}=6.06Hz, 1H, H2'), 5.19 (t, *J*_{4,5}=4.93, 4.80Hz, 1H, 2'-OH), 5.66 (d, *J*_{5,6}=8.08Hz, 1H, H5), 5.90 (d, *J*_{6,1'}=4.04Hz, 1H, H1'), 7.92 (d, *J*_{6,1'}=8.08Hz, 1H, H6), 11.37 (br s, 1H, NH). **¹³C NMR** (DMSO-*d*₆, 50MHz): δ 23.2, 23.7, 24.5, 34.1, 36.3, 60.8, 62.9, 81.2, 83.6, 89.1, 89.7, 102.0, 113.4, 141.4, 150.6, 163.2. **Mass** (ESI) 354.1427, found 377.3726 (M+Na⁺).

2',3'-*O*-cyclohexylidene-4'-(*p*-toluenesulfonyloxymethyl)uridine (**19**)

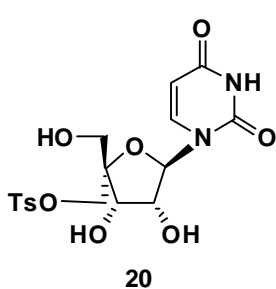


p-Toluenesulphonyl chloride (0.458 g, 2.40 mmol) was dissolved in anhydrous pyridine (3.0 mL) and added drop-wise to a stirred, ice-cooled solution of 2',3'-*O*-cyclohexylidene-4'-hydroxymethyl uridine **18** (0.5 g, 1.41 mmol) in anhydrous pyridine (10.0 mL). After 10min, the reaction was heated at 110°C, 4.5h. The reaction was then cooled to r.t., and satd. NaHCO₃ was added. The product was extracted in CH₂Cl₂ (x4). The organic layer was washed with brine, dried (Na₂SO₄) and concentrated to get a brown gum that was purified by silica gel column chromatography (100-200mesh). Elution was carried out with 20 to 80% EtOAc in

petroleum ether to get the pure product. Yield 310 mg, 43%. The un-reacted starting material could be recovered by elution with 1-3% MeOH in EtOAc.

¹H NMR (Acetone-*d*₆, 200MHz): δ 1.39-1.63 (m, 10H, CH₂x5), 2.46 (s, 3H, CH₃), 3.72 (ABq, *J*=11.25Hz, 2H, CH₂OH), 4.21 (ABq, *J*=10.36Hz, 2H, CH₂OTs), 4.94 (d, *J*=6.32Hz, 1H, H3'), 5.06 (dd, *J*=3.67Hz, 1H, H2'), 5.64 (d, *J*=8.08Hz, 1H, H5), 5.77 (d, *J*=3.66Hz, 1H, H1'), 7.51 (d, *J*=7.09Hz, 2H, Ar), 7.80 (dd, *J*=7.46, 7.07Hz, 2H, Ar, H6). **¹³C NMR** (Acetone-*d*₆, 50MHz): δ 21.6, 24.2, 24.6, 25.5, 34.8, 36.9, 63.5, 69.8, 82.5, 84.8, 87.8, 92.8, 102.9, 115.4, 128.9, 130.8, 133.7, 142.9, 146.0, 151.3, 164.0. **Mass** (ESI) 508.1516, found 509.1921 (M+H⁺).

4'-(*p*-toluenesulfonyloxymethyl)uridine (**20**)

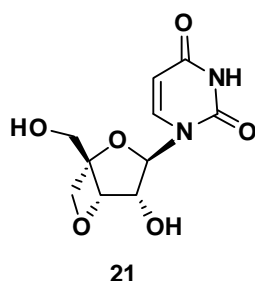


To 2',3'-*O*-cyclohexylidene-4'-(*p*-toluenesulfonyloxymethyl)uridine **19** (120 mg) was added de-ionized water (0.020 mL) and trifluoroacetic acid (0.98 mL). The reaction was stirred at r.t., 45 min. The TFA was evaporated under vacuum and co-evaporated with ethanol (x3). It was adsorbed on silica gel and purified by column chromatography (60-120mesh). Elution was carried out from 0 to 20% MeOH in CHCl₃ to afford the product **20**. Yield 80 mg, 79%. Unreacted starting material (20mg) was recovered.

¹H NMR (Acetone-*d*₆) δ: 2.44 (s, 3H, Ar-CH₃), 3.71 (s, 2H, CH₂OTs), 4.29 (ABq, *J*=10.74Hz, 2H, CH₂OH), 4.38 (m, 2H, H2', H3'), 5.62 (dd, *J*=1.8, 8.21Hz, 1H, H5), 5.85 (d, *J*=6.69Hz, 1H, H1'), 7.47 (d, *J*=7.96Hz, 2H, Ar), 7.83 (overlapping d, *J*=8.33, 8.21Hz, 3H, H6, Arx2), 10.11 (br s, 1H, NH). **Mass** (ESI) 428.0890, found 429.1259 (M+H⁺), 251.1037 (M+Na⁺).

3'-*O*, 4'-*C*-methyleneuridine (**21**)

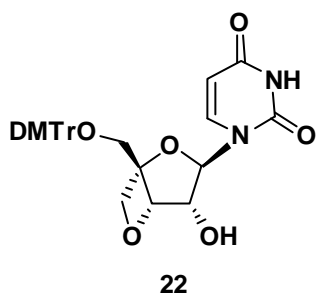
To a solution of 4'-(*p*-toluenesulfonyloxymethyl)uridine **20** (150 mg, 0.350 mmol) in anhydrous toluene, was added sodium hexamethyldisilazane (1.0 M in THF, 3.51 mL, 3.50 mmol), while cooling in a water-bath (~20°C), under nitrogen atmosphere. The reaction



was stirred 3.5 h. A satd. solution of NaHCO_3 was added and the solvents were evaporated under vacuum. The residue was adsorbed on silica gel (60-120mesh) and purified by column chromatography. Elution was carried out from 10 to 40% MeOH in dichloromethane. The pure product was obtained as a solid. Yield 80 mg, 90%.

$^1\text{H NMR}$ ($\text{DMSO}-d_6$) δ : 11.48 (br s, 1H, NH), 7.69 (d, $J=8.08\text{Hz}$, 1H, H6), 6.25 (d, $J=7.83\text{Hz}$, 1H, H1'), 5.72 (d, $J=8.08\text{ Hz}$, 1H, H5), 5.16 (t, $J=5.93\text{ Hz}$), 4.92 (d, $J=4.30\text{Hz}$, 1H), 4.75 (d, $J=7.58\text{Hz}$, 1H), 4.32 (d, $J=7.71\text{Hz}$, 1H), 4.01 (m, 1H), 3.60 (m, 2H).

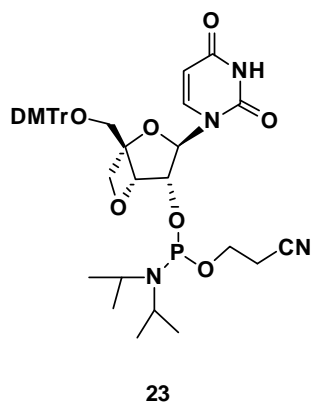
5'-*O*-(4,4'-dimethoxytrityl)-3'-*O*,4'-*C*-methyleneuridine (22)



3'-*O*, 4'-*C*-methyleneuridine **21** (80 mg, 0.313 mmol) was co-evaporated with anhydrous pyridine (x3) and re-dissolved in anhydrous pyridine (0.5 mL). Dimethoxytrityl chloride (0.529 g, 1.563 mmol) and DMAP (0.191 g, 1.563mmol) were added and the reaction was stirred at room temperature overnight. TLC examination showed appearance of a faster-moving spot, but starting material left largely unconsumed. However, the reaction was worked up. Methanol (1.0ml) was added and the solvents were removed in vacuo. The residue was dried by co-evaporation with dichloromethane (x3), adsorbed on silica gel (60-120mesh, pre-inactivated with 1% Et_3N) and purified by column chromatography. Elution was carried out on pre-inactivated silica gel using 50 to 100% EtOAc in petroleum ether, when the upper impurities were eluted. Subsequent elution with 2-3% MeOH in EtOAc yielded the pure product in 17.2% yield (30 mg). The unreacted starting material was recovered by elution with 20-30% MeOH in EtOAc.

$^1\text{H NMR}$ (CDCl_3) δ : 2.84 (s, 1H, OH), 3.48 (m, 2H, H5', H5''), 3.79 (s, 6H, $\text{OCH}_3 \times 2$), 4.15 (m, 1H, H3'), 4.52, 4.73 (ABq, $J=8.09\text{Hz}$, 2H, 4'- $\text{CH}_2\text{-O-3}'$), 5.08 (d, $J=8.21\text{Hz}$, 1H, H2'), 5.56 (d, $J=8.21\text{Hz}$, 1H, H5), 6.46 (d, $J=6.57\text{Hz}$, 1H, H1'), 6.84 (d, $J=8.84\text{Hz}$, 4H, Ar), 7.27 (m, 7H, Ar), 7.32 (m, 2H, Ar), 7.49 (d, $J=8.21\text{Hz}$, 1H, H6).

2'-O-[2-cyanoethoxy (diisopropylamino)phosphino]-5'-O-(4,4'-dimethoxytrityl)-3'-O,4'-C-methyleneuridine (23)



Compound **22** (0.15 g, 0.27 mmol) was co-evaporated with dry CH₃CN, and then dissolved in dry dichloromethane (3.0 mL). Diisopropylethylamine (DIPEA) (0.19 mL, 1.07 mmol) was added, followed by chloro (2-cyanoethoxy)-N, N-diisopropyl amino)-phosphine (0.09 mL, 0.40 mmol) at 0°C. The reaction mixture was stirred under argon atmosphere at room temperature for 3 hours, when TLC indicated the absence of starting material.

The reaction mixture was diluted with dichloromethane, washed with NaHCO₃ and brine, dried over sodium sulphate, followed by solvent removal. The crude product was purified by silica gel column chromatography using a 1:1 mixture of dichloromethane:ethylacetate and 1% triethylamine. Yield: 0.13g, 65%.

³¹P NMR (50 MHz, CDCl₃): 150.03, 150.62.

2.10.2 Synthesis of buffers

Phosphate buffer (pH = 7.2, 150 mM NaCl)

Na₂HPO₄ (110 mg), NaH₂PO₄·H₂O (35.3 mg), NaCl (877.5 mg) was dissolved in minimum quantity of water and the total volume was made 100 mL. The pH of the solution was adjusted 7.2 with aq. NaOH solution in DI water, and stored at 4°C.

Triethyl ammonium acetate (TEAA) buffer

TEA (101.19 g ≈ 139.38 mL, 1 M) was diluted up to 500 mL DI water and kept aside, then in another container AcOH (60.05 g ≈ 57.24 mL, 1 M) was diluted up to again with 500 mL DI water. Then slowly the AcOH solution was added to the TEA in ice bath with vigorous stirring to make total volume 1 L, the pH of the solution was adjusted to 7.0 using either AcOH or TEA, this 1M stock buffer was stored at room temperature.

2.10.3 Synthesis of oligonucleotides

DNA oligonucleotides were synthesized on a CPG solid support using Bioautomation MerMade- 4 synthesizer using standard β -cyanoethyl phosphoramidite chemistry. The 2'-5'-linked DNA oligomers were synthesized in 2'-5' direction using universal columns as solid support. All the monomer (0.06M) solutions in anhydrous acetonitrile were prepared freshly and stored over 3Å molecular sieves. The modified amidite monomer solution concentration was (0.1M) in acetonitrile. For the modified monomers double coupling and longer coupling time(300 s x 2) were employed. Post synthesis, the sequences were subjected to ammonia treatment for 6 h at 55°C, cleavage of the oligomer from the support, deprotection of the β -cyanoethyl protecting group and the exocyclic amino protecting groups used during the synthesis takes place. The crude oligonucleotides were desalted by passing them over G-25 sephadex columns, followed by purification using RP-HPLC (C18 column). The pure oligomers were characterized by MALDI-TOF before using for the biophysical studies.

2.10.4 Purification and characterization

High performance liquid chromatography

The purity of synthesized oligonucleotides were ascertained using by RP-HPLC on a C18 column with either a Varian system (Analytical semi-preparative system consisting of Varian Prostar 210 binary solvent delivery system and Dynamax UV-D2 variable wavelength detector and Star chromatography software) or a Waters system (Waters Delta 600e quaternary solvent delivery system and 2998 photodiode array detector and Empower 2 chromatography software). A gradient elution method 0% A to 100%B in 15 min was used with flow rate 1.5 mL/min and the eluent was monitored at 260nm. [A = 5% ACN in TEAA (0.1 M, pH 7); B = 30% ACN in TEAA (0.1 M, pH 7)].

MALDI-TOF characterization

The MALDI-TOF spectra were recorded on both Voyager-De-STR (Applied Biosystems) MALDI-TOF instrument or a AB Sciex TOF/TOFTM Series ExplorerTM 72085

instrument. A nitrogen laser (337 nm) was used for desorption and ionization. The matrix used for analysis was THAP (2', 4', 6'-trihydroxyacetophenone), and diammonium citrate used as additive. The sample was prepared by mixing 1 μ L oligomer (10-50 μ M in DI H₂O) with 10 μ L of THAP (0.55 M in EtOH) mixed well followed by 5 μ L diammonium citrate (0.1 M in DI H₂O) again mixed well and then 1 μ L of the mixture was spotted on metal plate. The metal plate was loaded to the instrument and the analyte ion were then accelerated by an applied high voltage (15-25 kv) in linear mode and detected as an electrical signal.

HPLC purified oligonucleotides were characterized through this method and were observed to give good signal to noise ratio, mostly producing higher molecular ion signals. The purity was re-checked and found to be >95%.

2.10.5 Biophysical techniques

UV- T_m experiments

UV experiments were performed on a Varian Cary 300 Bio UV-Visible spectrophotometer fitted with a Peltier-controlled temperature programmer. The concentration of DNA ONs were calculated on the basis of absorbance from molar extinction coefficients of the corresponding nucleobases (A = 15400, T = 8800, C = 7300 and G = 11700, U = 9900 L/(M.cm) of DNA/RNA. The complexes were prepared by mixing 1 μ M strand concentrations of ONs and complementary strand together (1:1) in 1 mL of 10 mM sodium phosphate buffer, pH 7.2 containing NaCl (150 mM) and were annealed by keeping the samples at 90°C for 2 min followed by slow cooling to room temperature and refrigeration for at least 5 hours prior to running the experiments. The sample was held at the starting temperature 10°C for at least 15 min, N₂-gas was purged through the cuvette chamber below 20°C to prevent condensation of moisture on cuvette walls. Absorbance *versus* temperature profiles were obtained by monitoring the absorbance at 260nm from 10–85°C at a ramp rate of 0.5°C per minute. The data were processed using Microcal Origin 6.1 and T_m (°C) values were derived from the maxima of the first

derivative plots. All values are an average of at least 3 independent experiments and accurate to within $\pm 0.5^\circ\text{C}$.

CD experiments

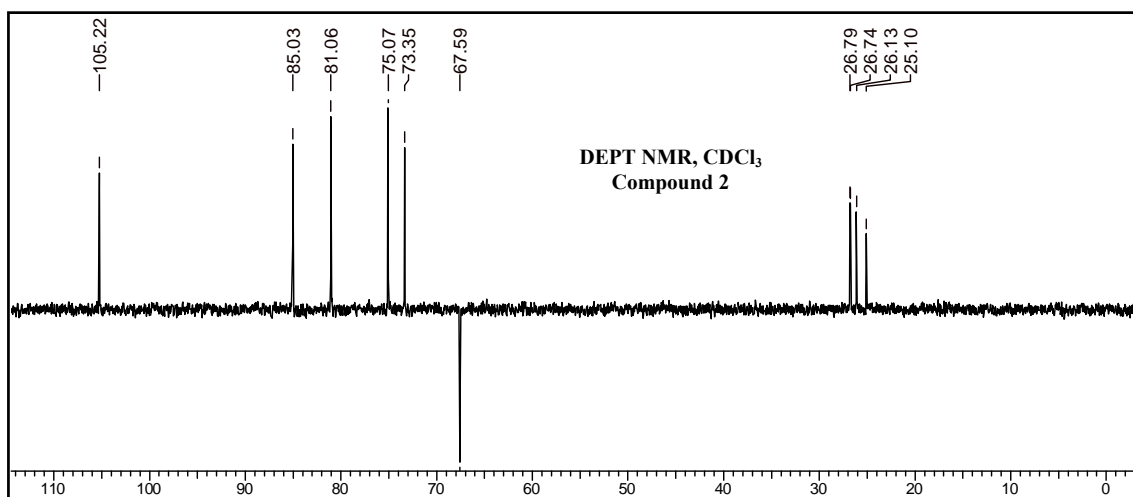
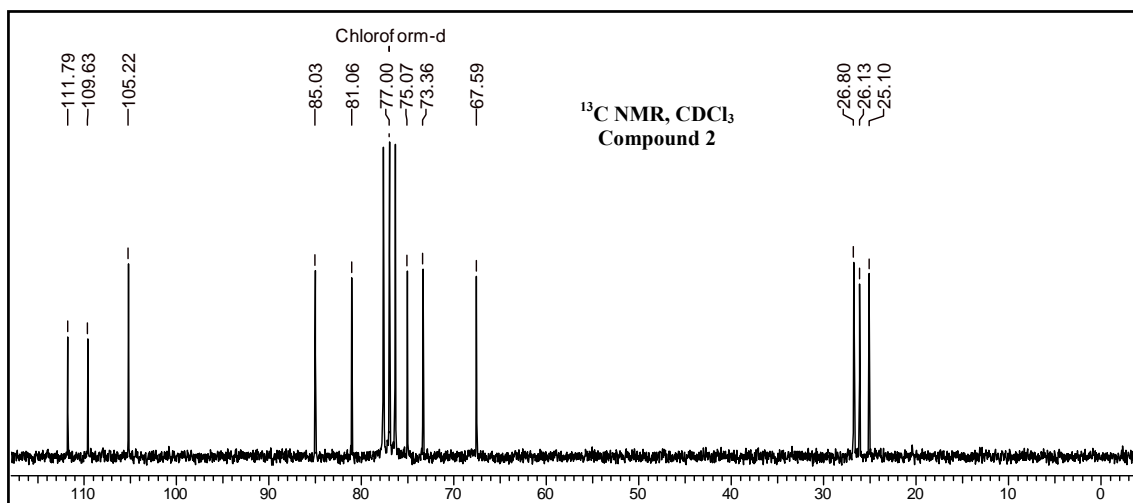
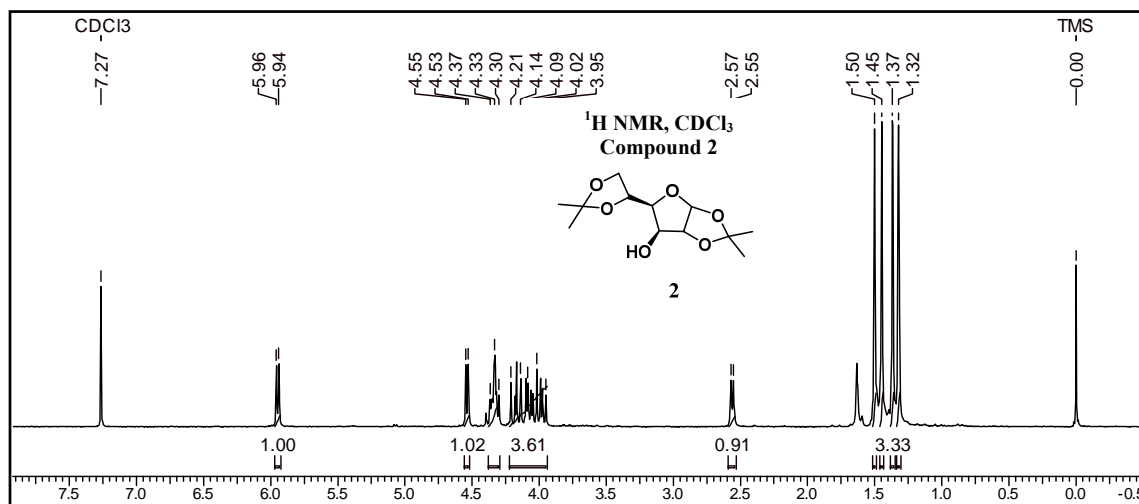
The samples for CD experiments were prepared as for the UV-T_m experiments. Thus, 1 μM concentration of each strand was used. The complexes were prepared in 10 mM sodium phosphate buffer, pH 7.4 containing NaCl (150 mM) and were annealed by keeping the samples at 90°C for 2 min followed by slow cooling to room temperature then refrigerated for at least 5 hours prior to running the experiments. CD spectra were recorded in a 1 cm path length cuvette at 10°C, as an accumulation of 3 scans, and using a resolution of 1 nm, bandwidth of 1 nm, sensitivity of 20mdeg, response of 1 s and a scan speed of 200 nm/min.

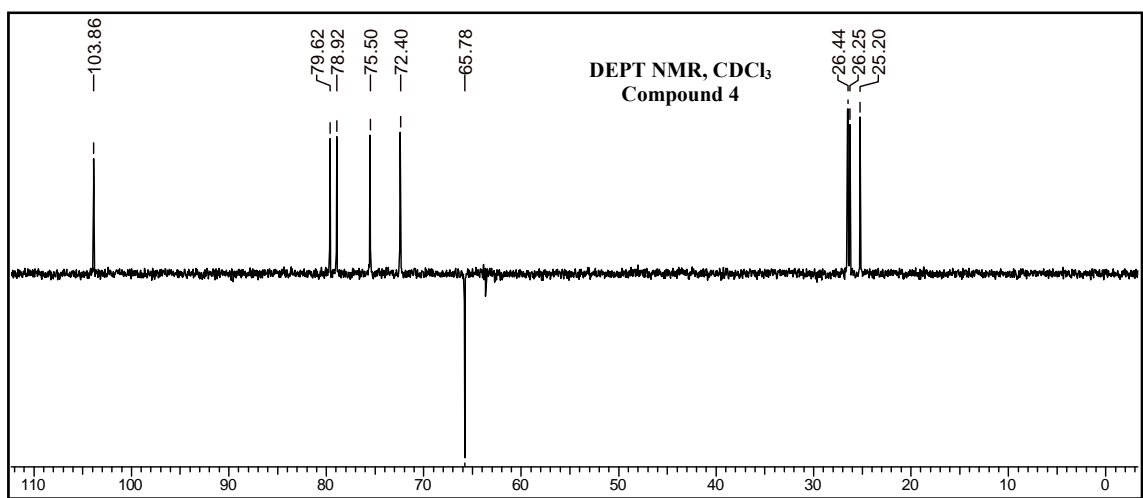
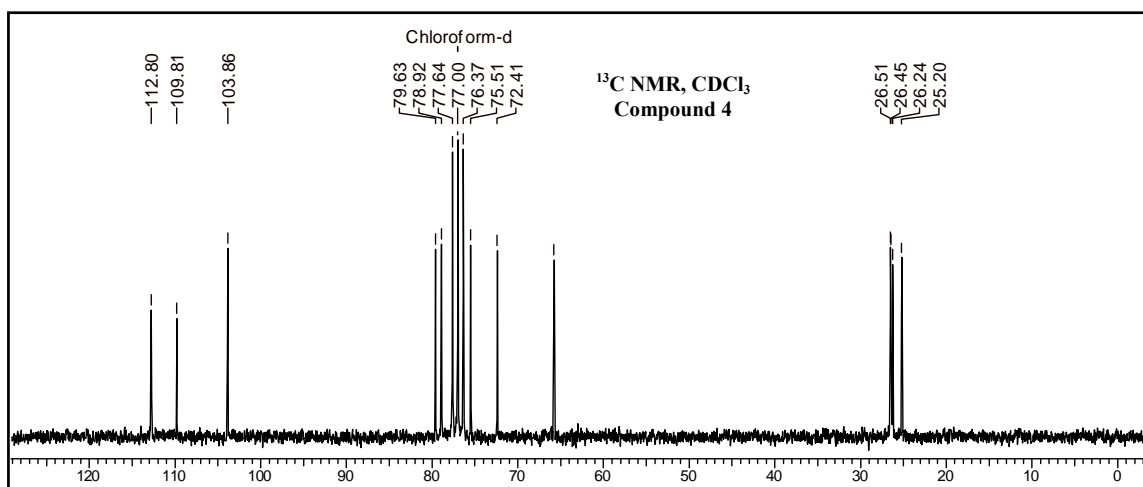
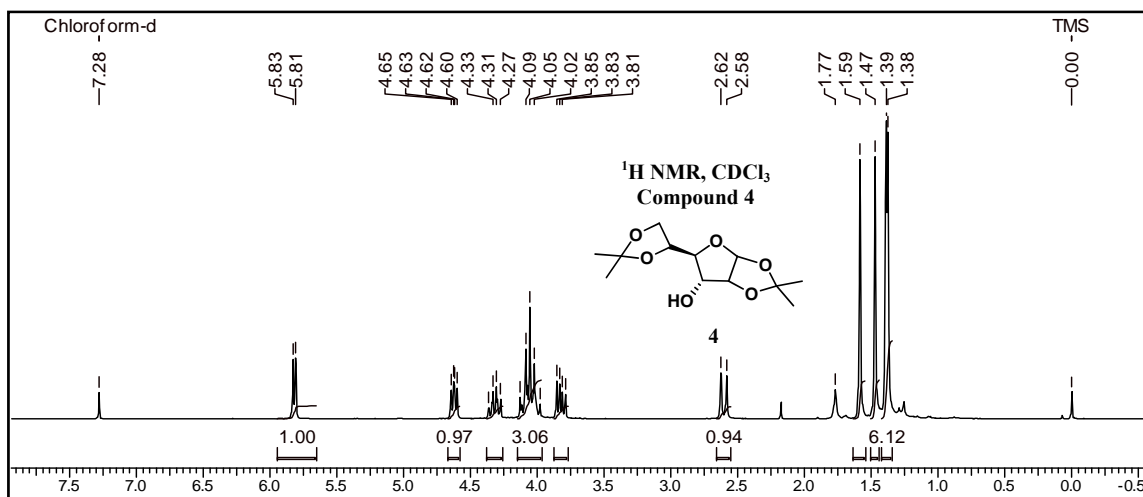
Snake venom phosphodiesterase stability experiments

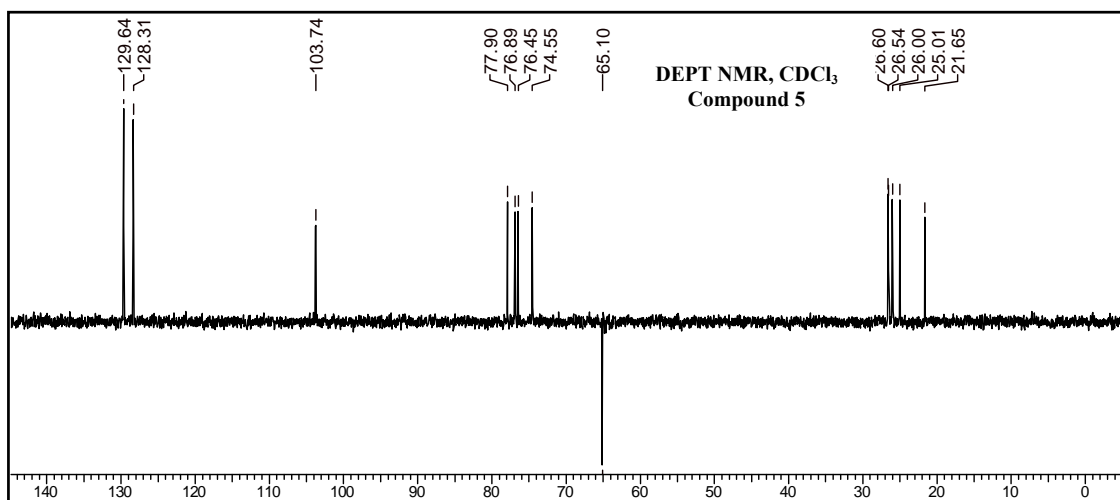
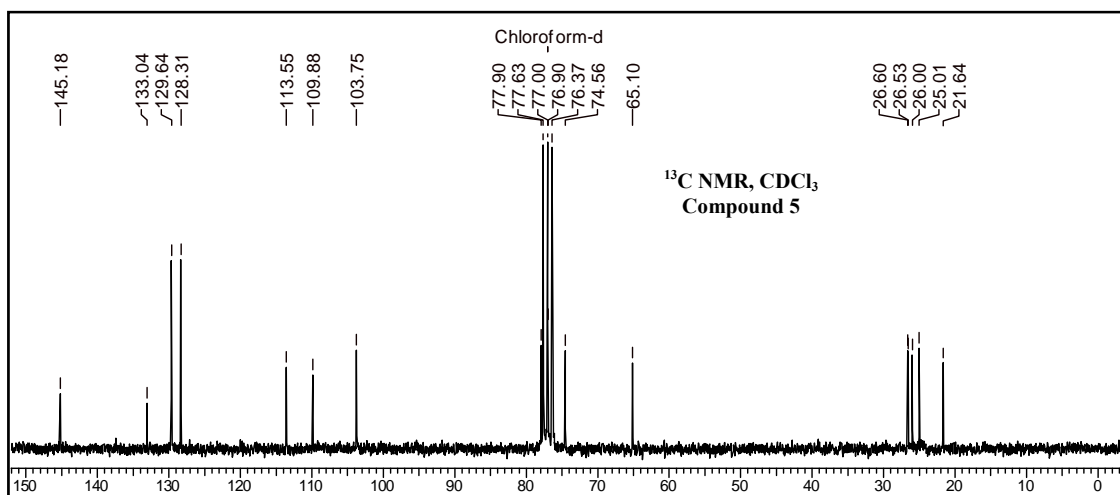
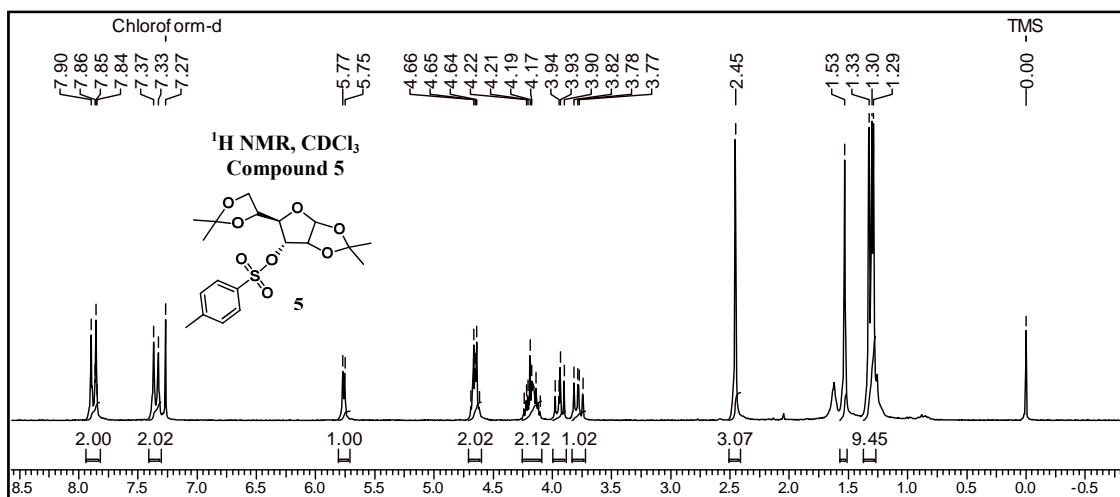
Enzymatic hydrolysis of the DNA and isoDNA oligomers (7.5 μM) was carried out at 37°C in 100 μl buffer (100mM Tris-HCl (pH 8.5), 15mM MgCl₂, 100mM NaCl) and SVPD (2 μg , 1.2 x 10⁻⁴ U). Aliquots were taken at several time intervals. Each aliquot was heated at 90°C for 2 min to inactivate the nuclease enzyme. The intact oligomer at each time interval was monitored by RP-HPLC. Percentage of intact oligomer was plotted against time to show the degradation of oligomers with respect to time.

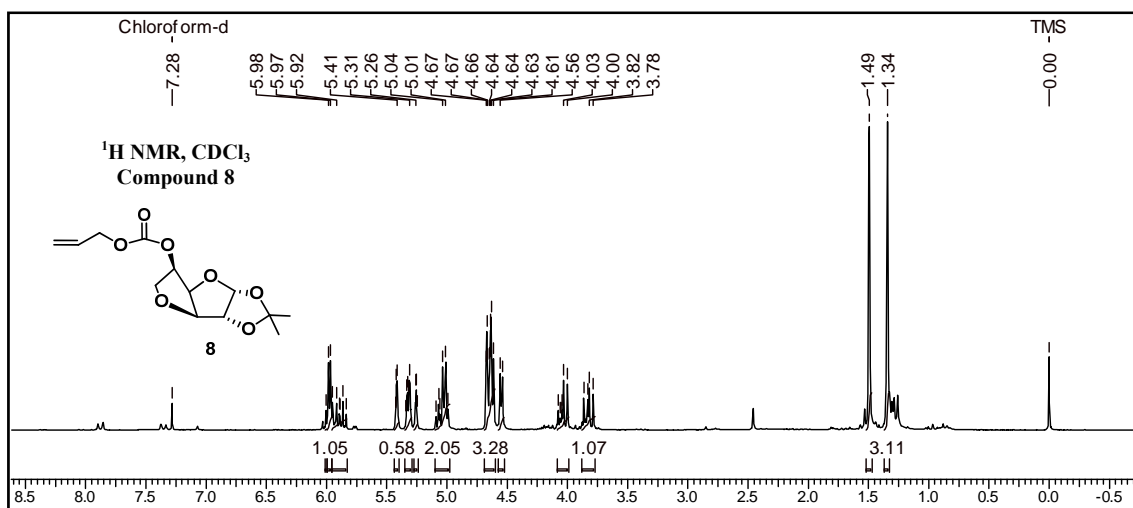
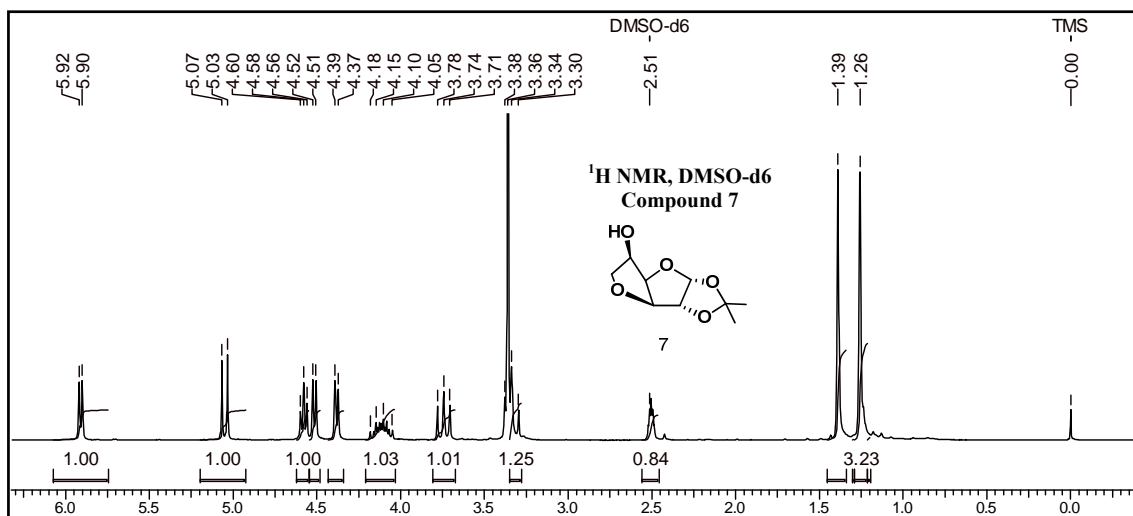
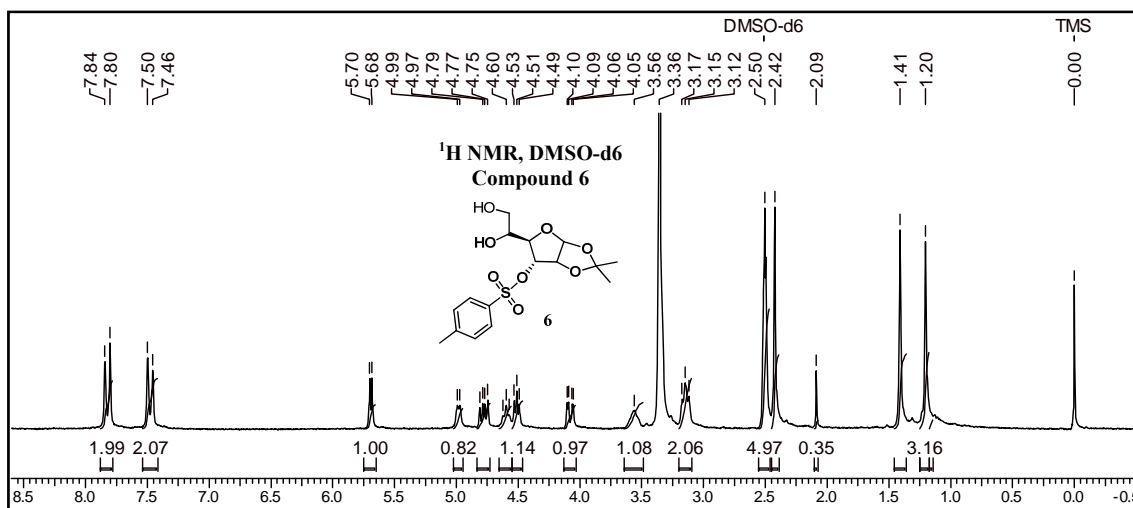
2.11 Appendix

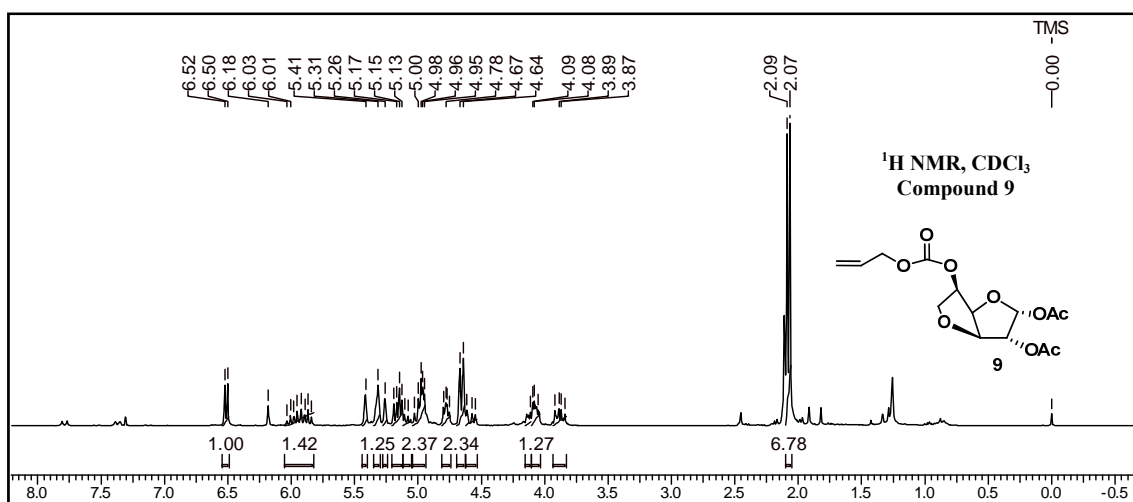
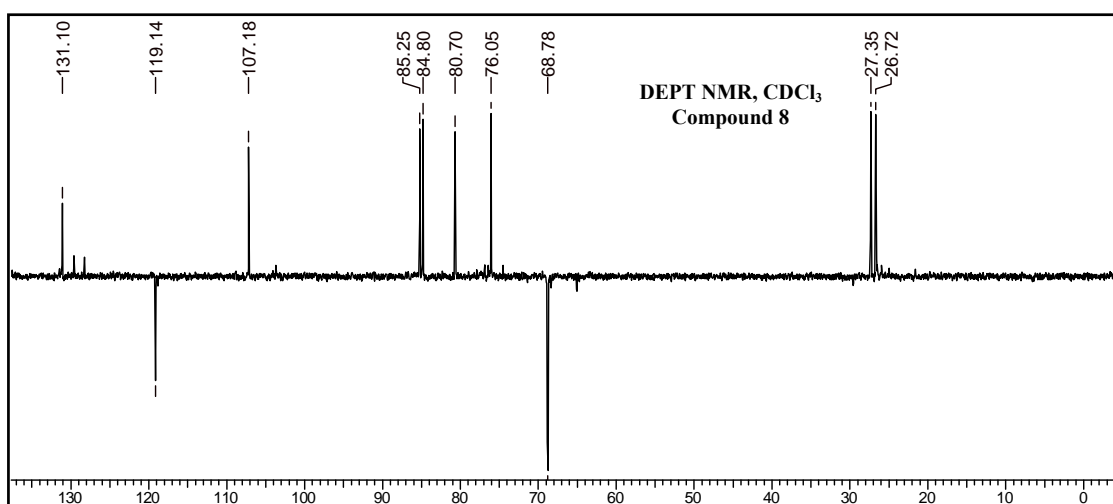
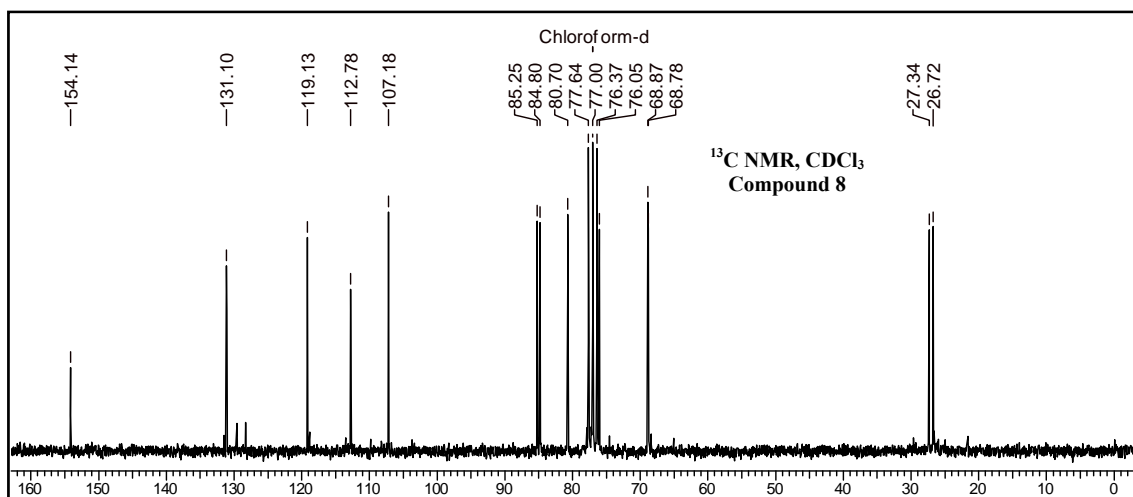
Compounds	Page No.
compound 2: ^1H , ^{13}C NMR and DEPT	82
compound 4: ^1H , ^{13}C NMR and DEPT	83
compound 5: ^1H , ^{13}C NMR and DEPT	84
compound 6: ^1H NMR	86
compound 7: ^1H NMR	86
compound 8: ^1H , ^{13}C NMR and DEPT	85-86
compound 9: ^1H , ^{13}C NMR and DEPT	86-87
compound 10: ^1H , ^{13}C NMR and DEPT	87-88
compound 11: ^1H , ^{13}C NMR and DEPT	88-89
compound 12: ^1H , ^{13}C NMR and DEPT	89-90
compound 13: ^1H , ^{13}C NMR and DEPT	90-91
compound 14: ^{31}P NMR and HRMS	91-92
compound 16: ^1H , ^{13}C NMR and DEPT	92-93
compound 18: ^1H , ^{13}C NMR and DEPT	93-94
compound 19: ^1H , ^{13}C NMR and DEPT	94-95
Compound 20: ^1H NMR	95
compound 21: ^1H NMR	95
compound 22: ^1H NMR	96
compound 23: ^{31}P NMR	96
HPLC spectra of Oligomers	96-97
MALDI spectra of Oligomers	98-103

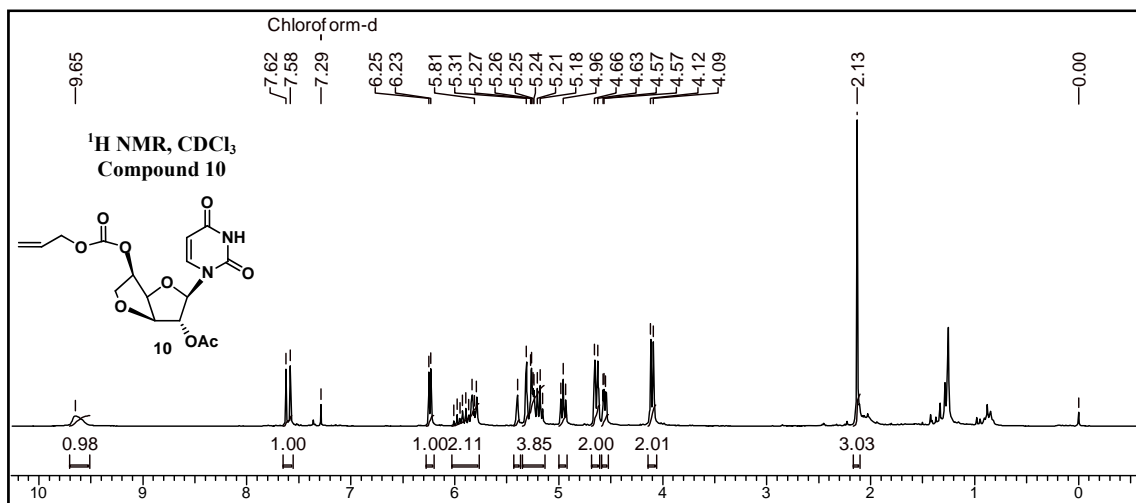
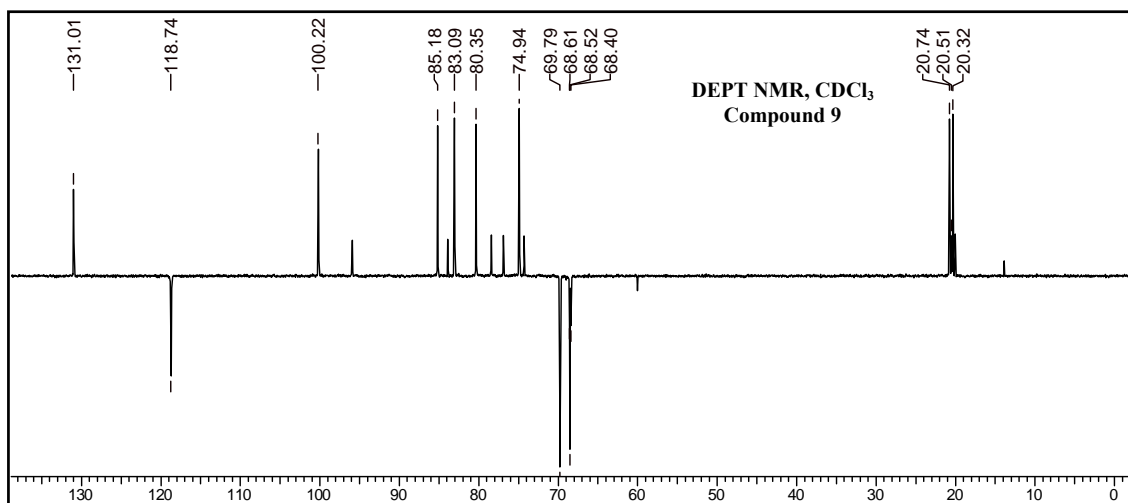
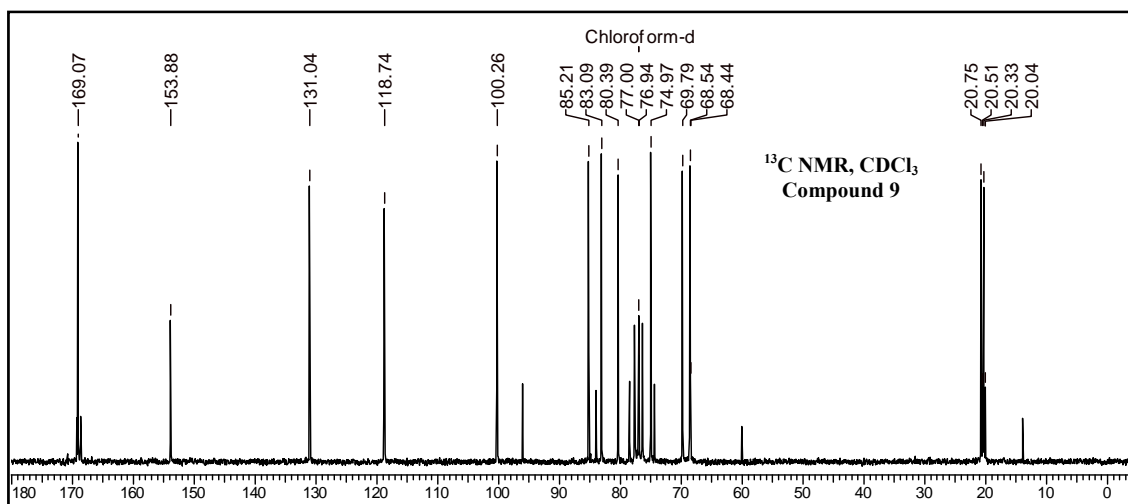


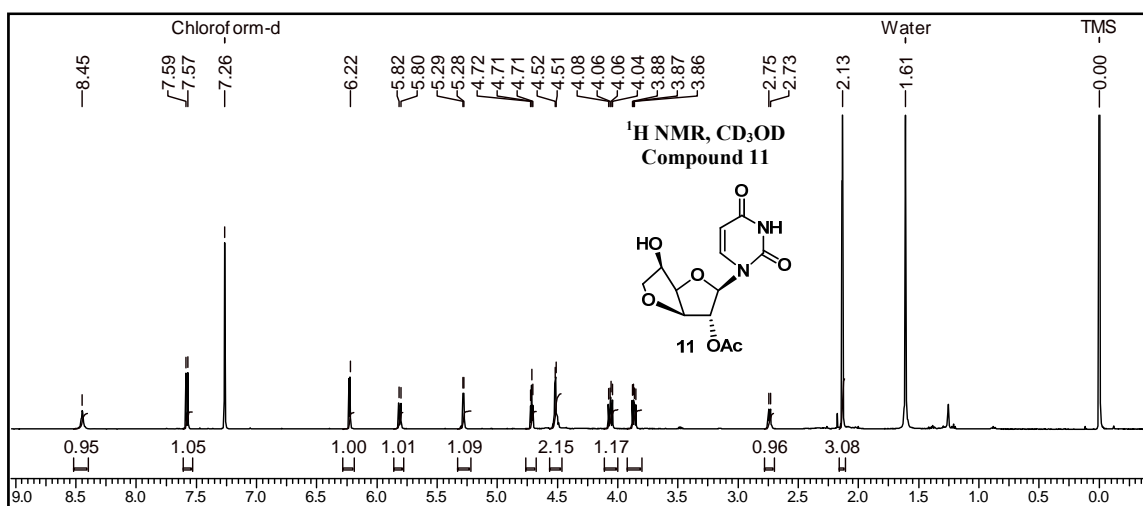
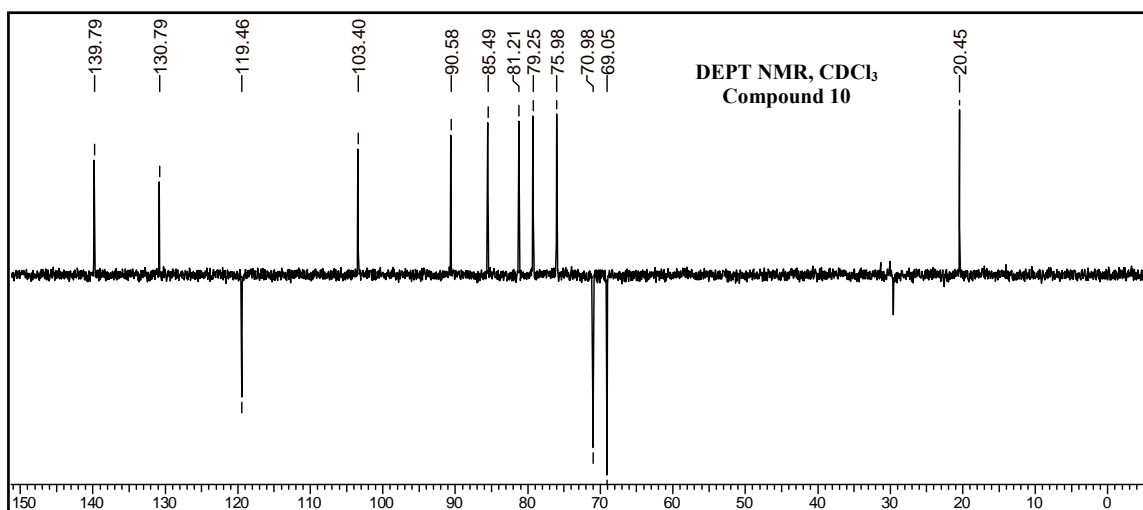
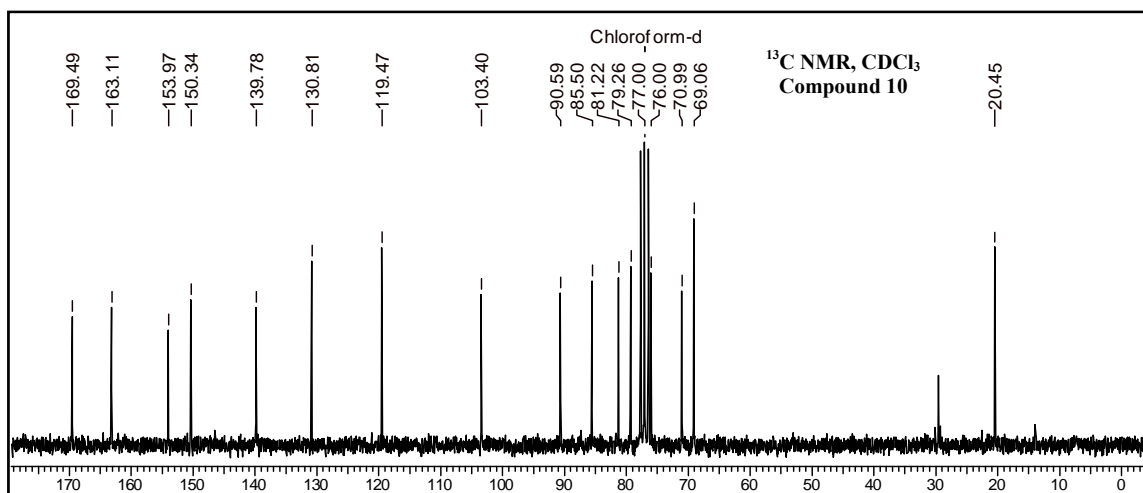


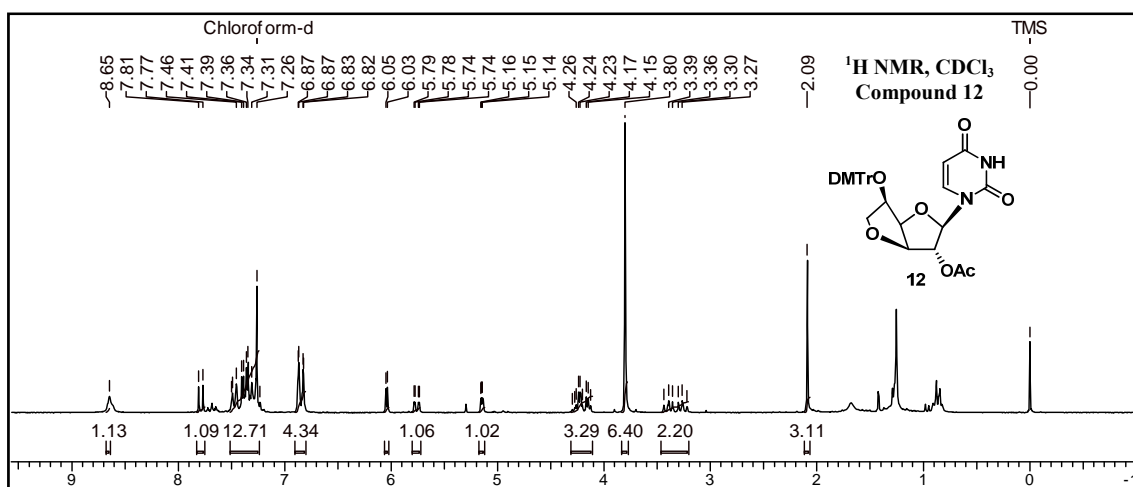
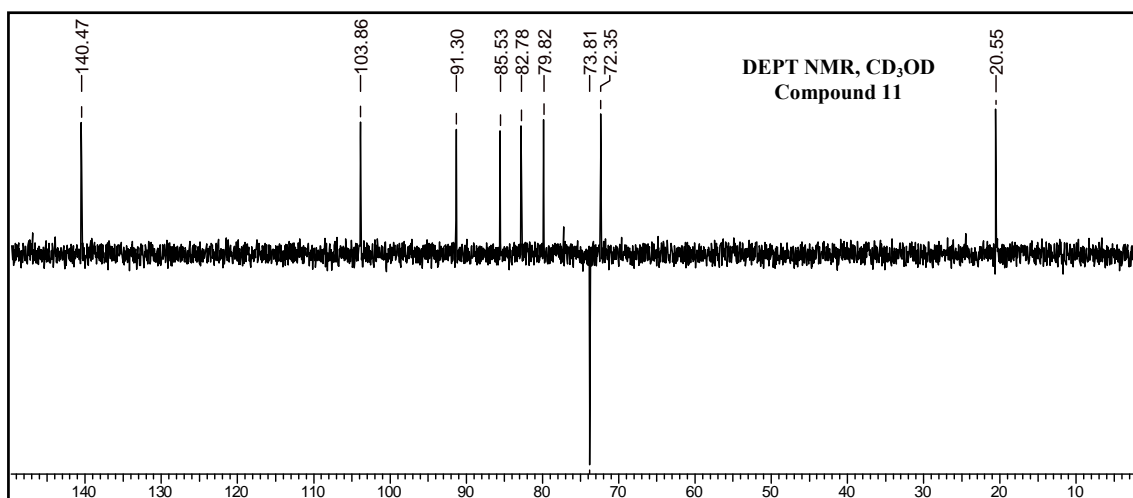
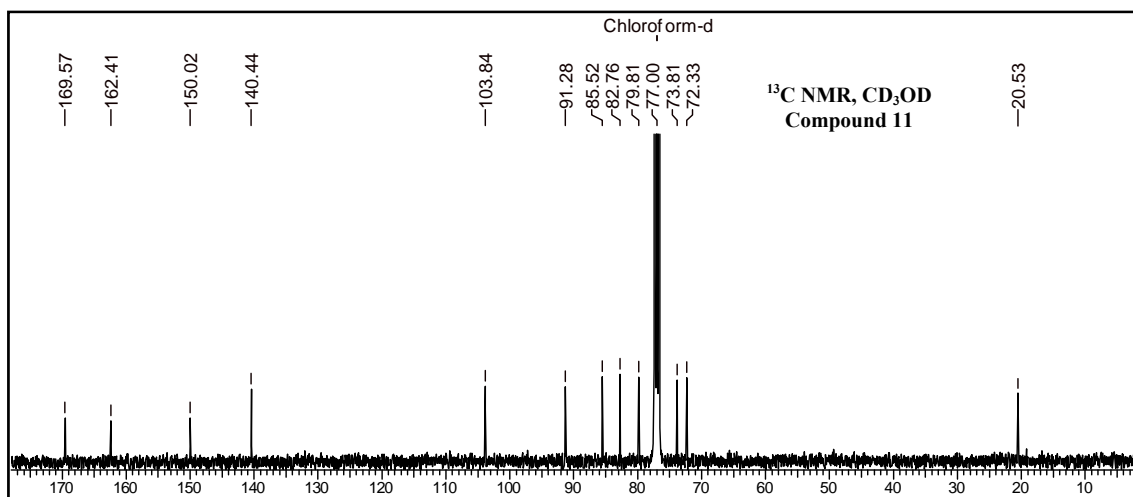


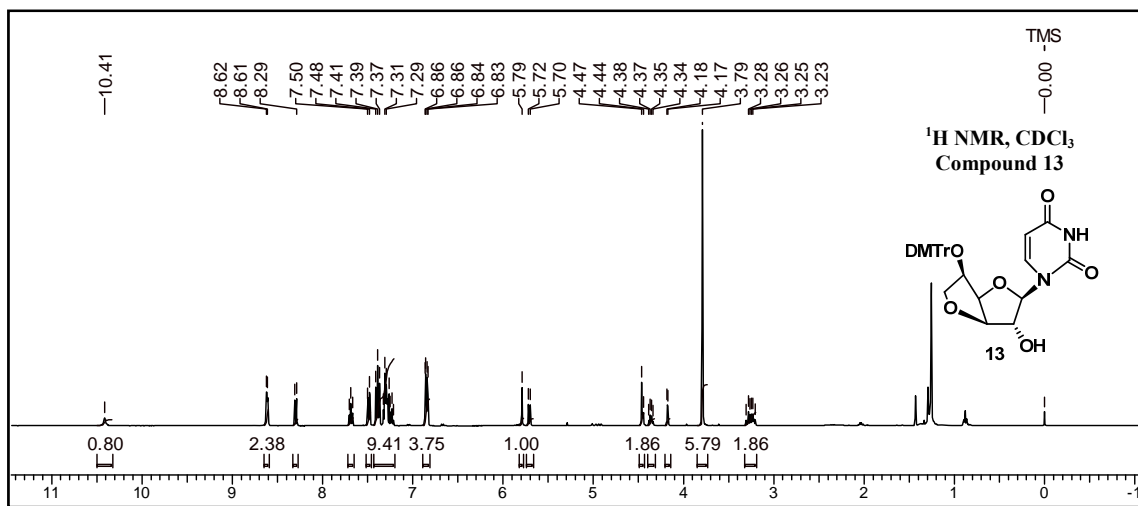
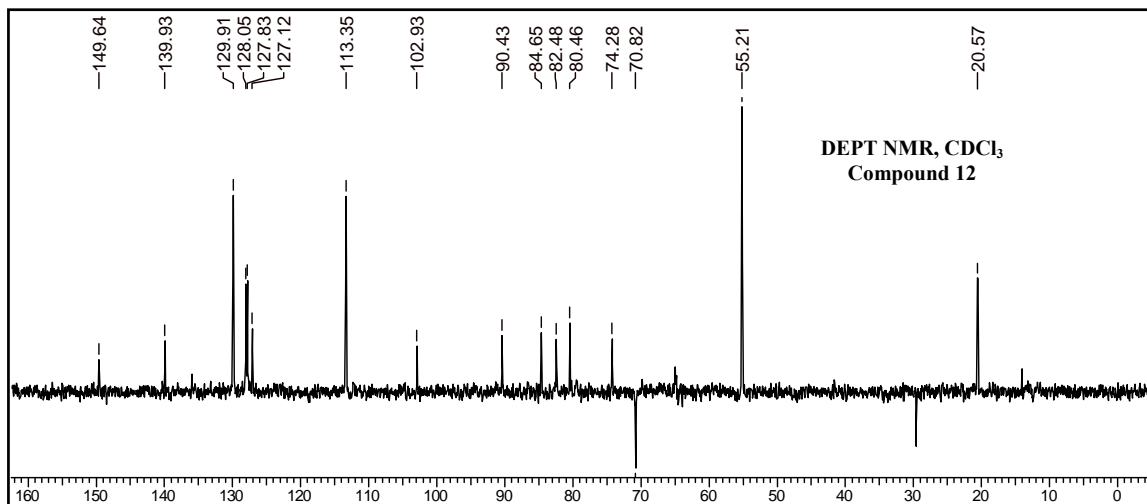
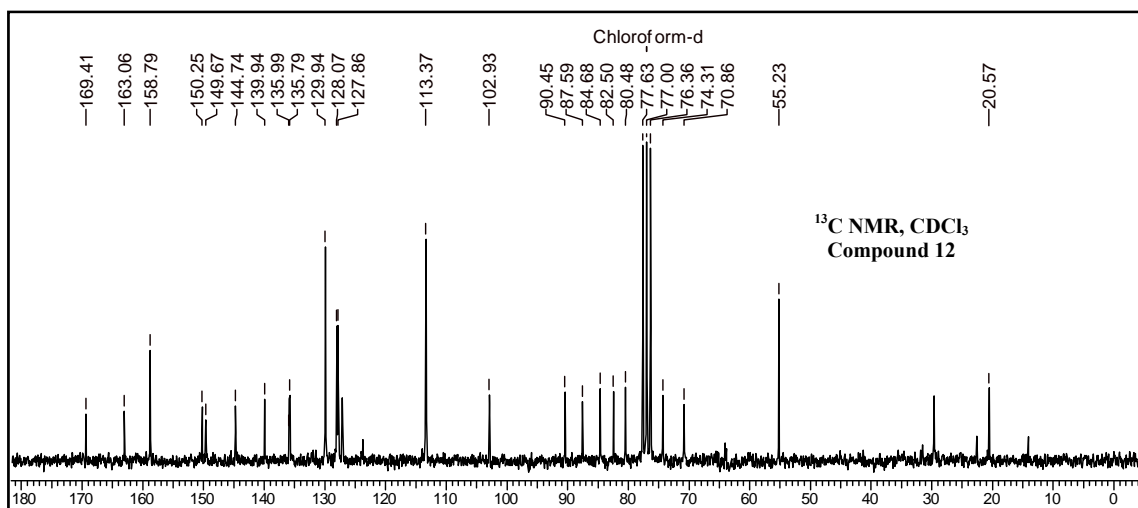


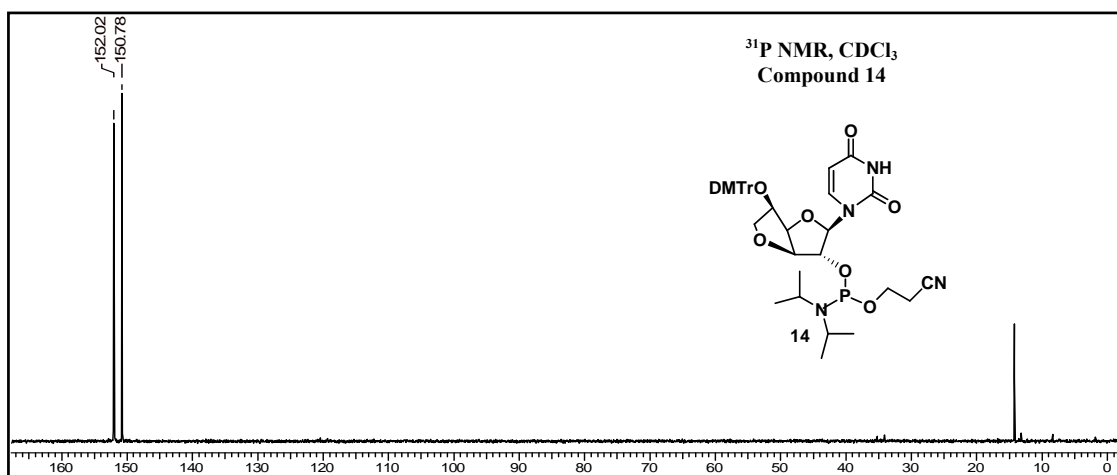
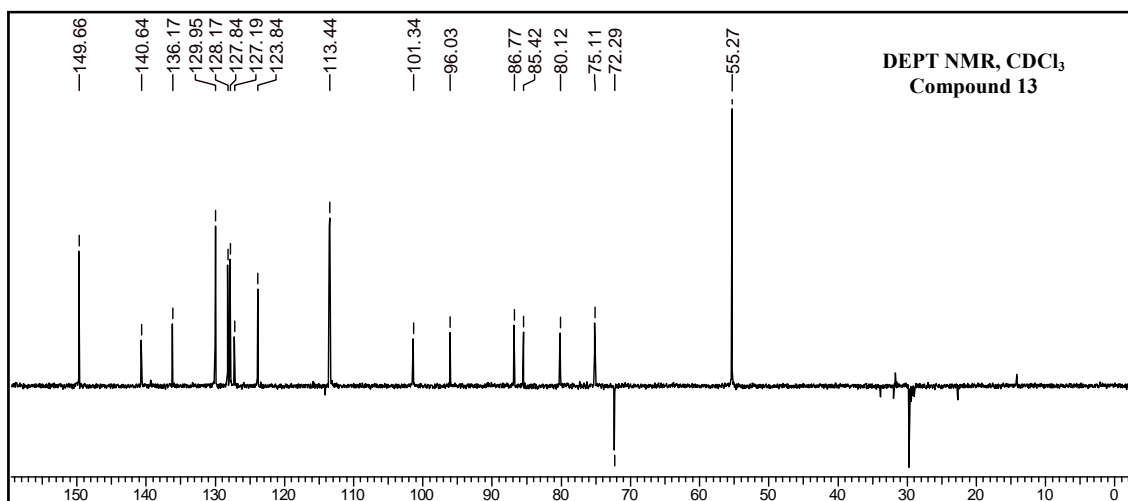
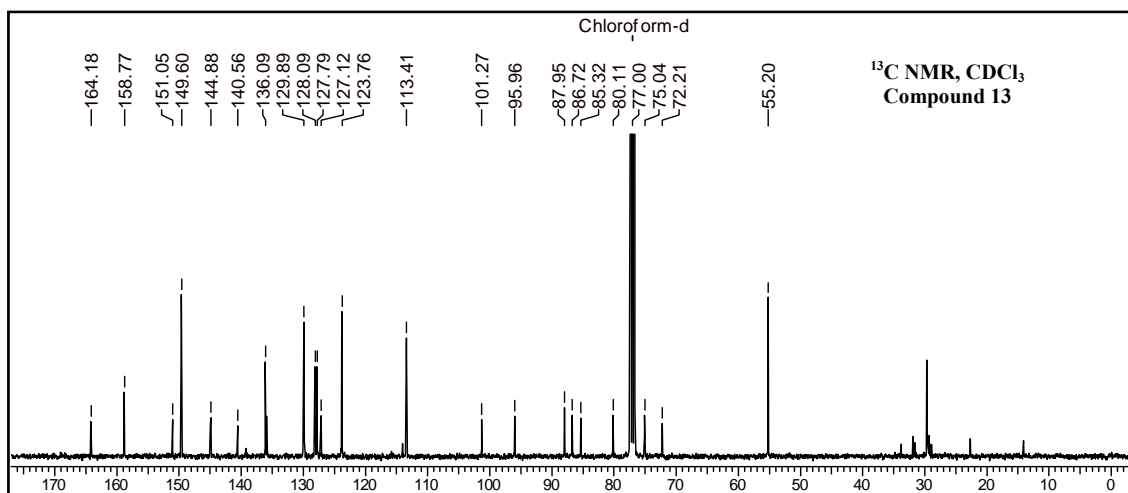


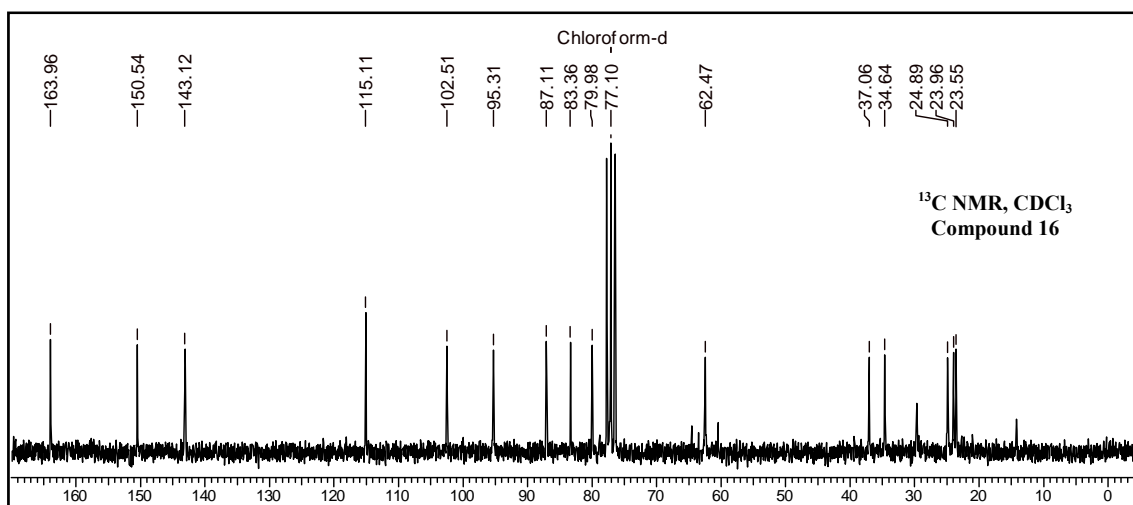
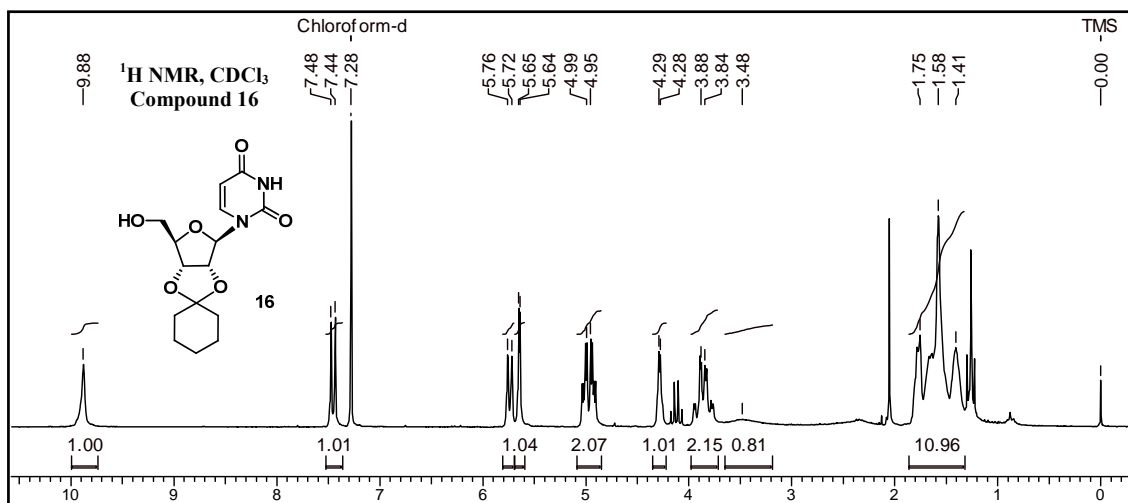
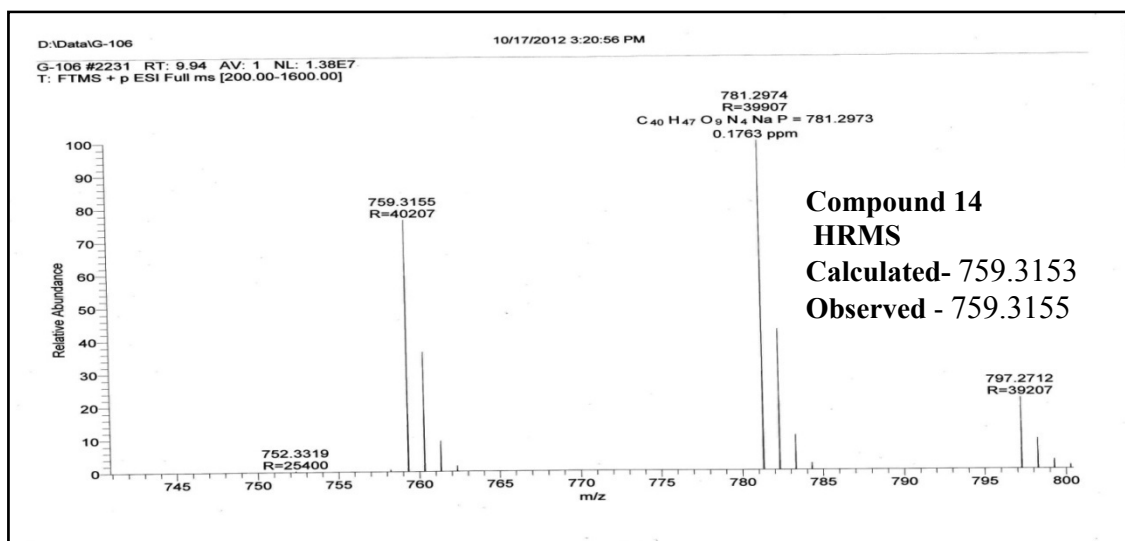


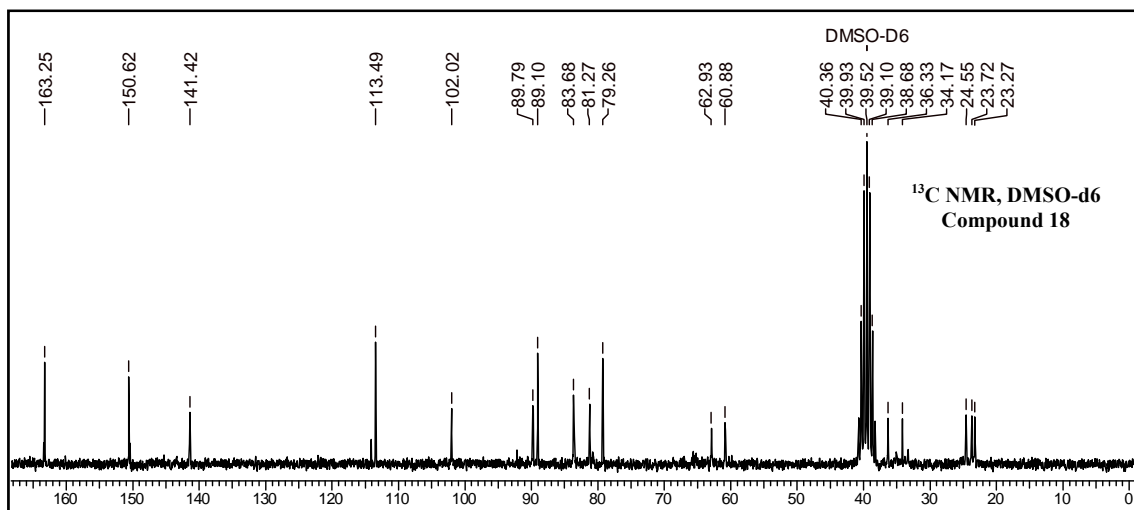
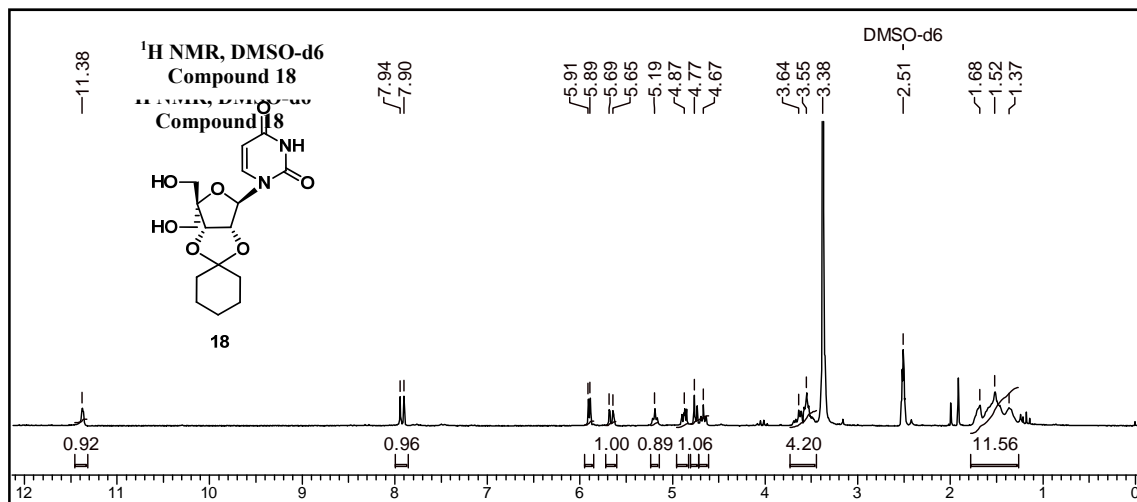
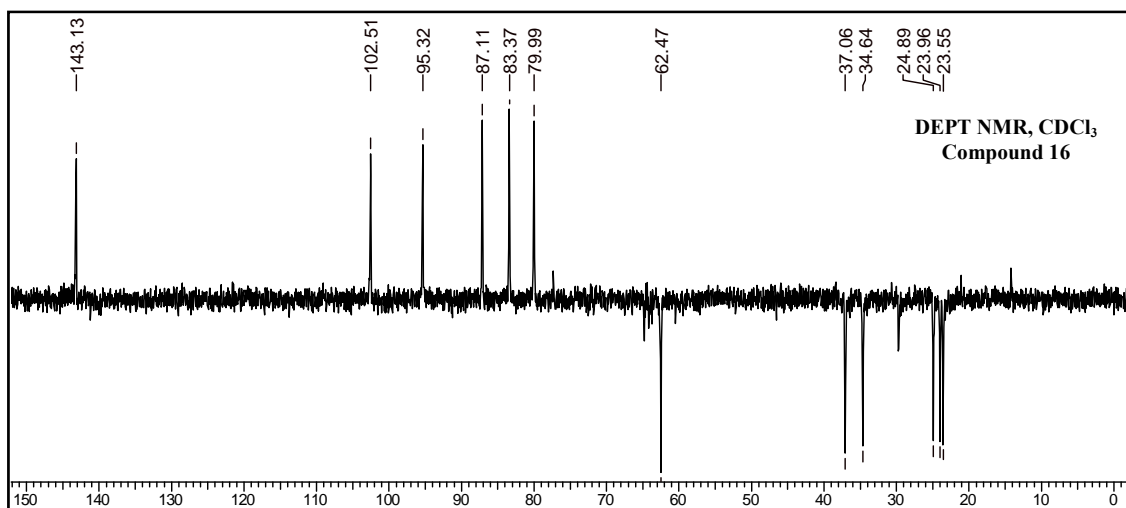


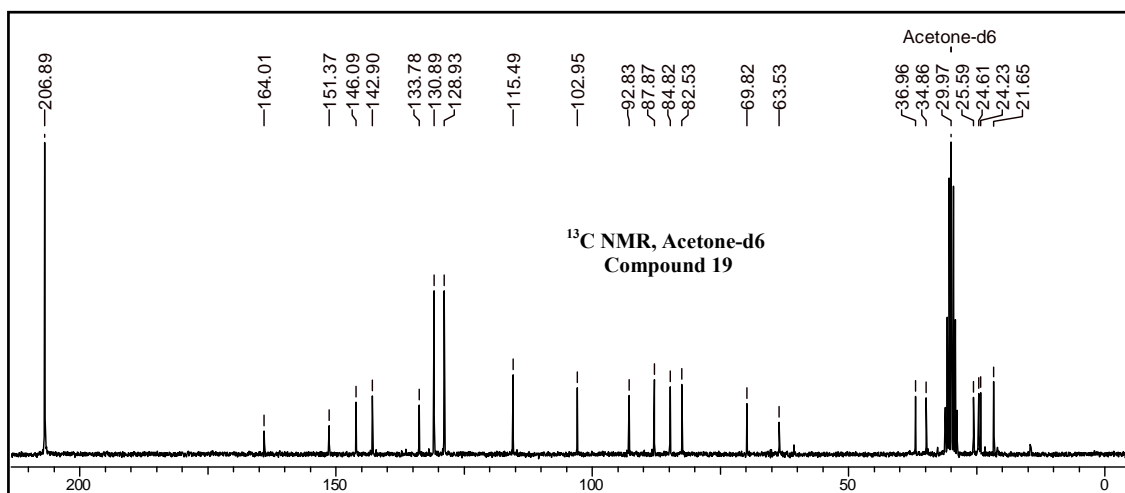
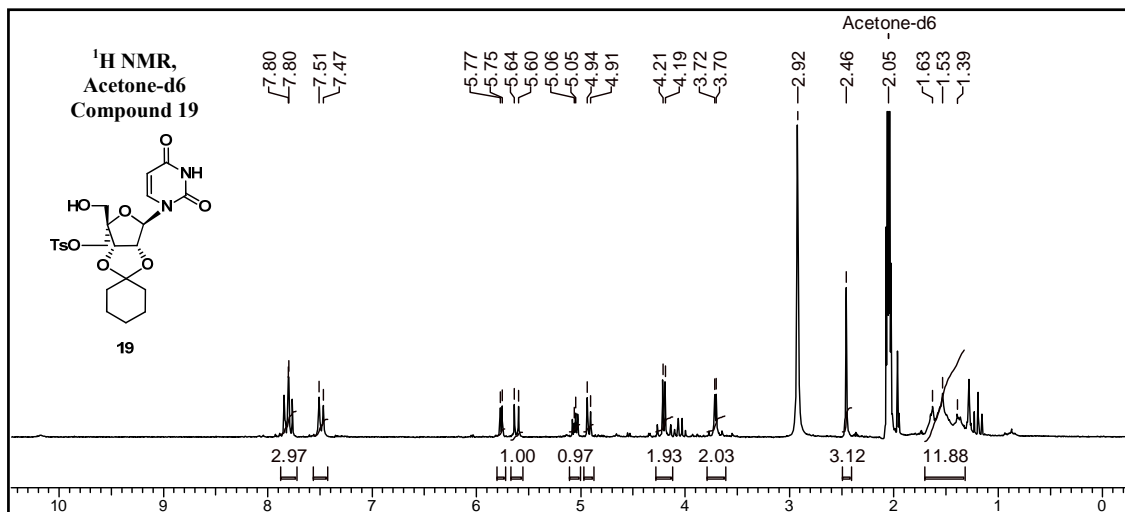
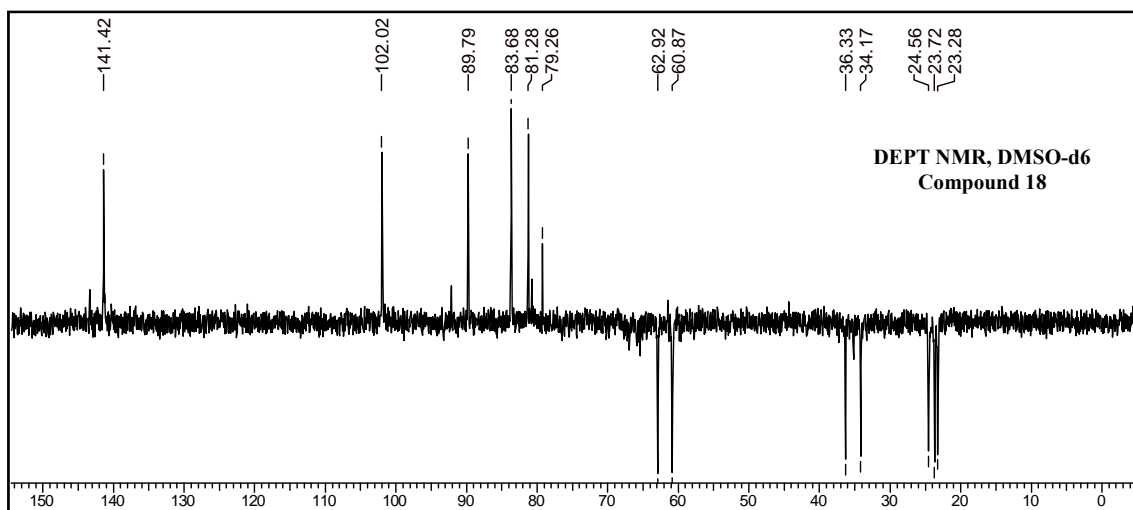


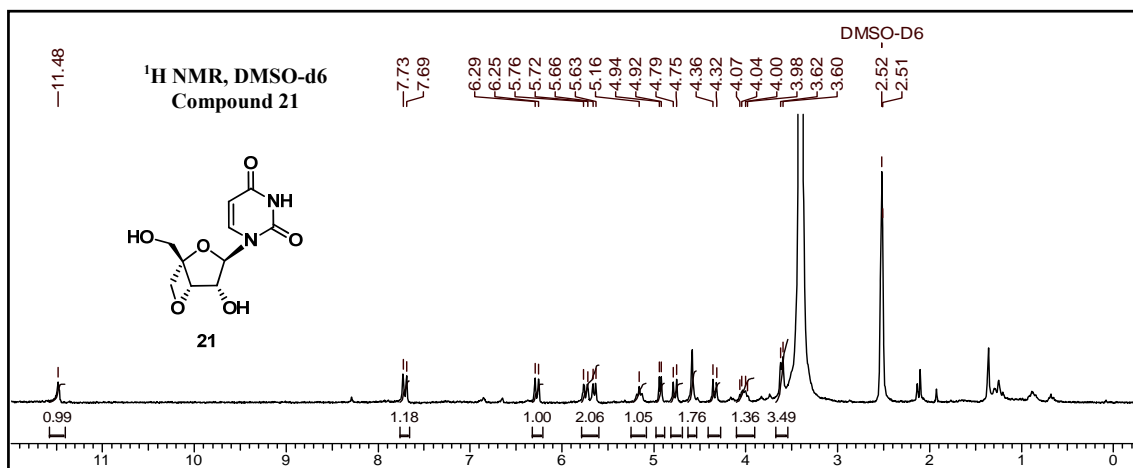
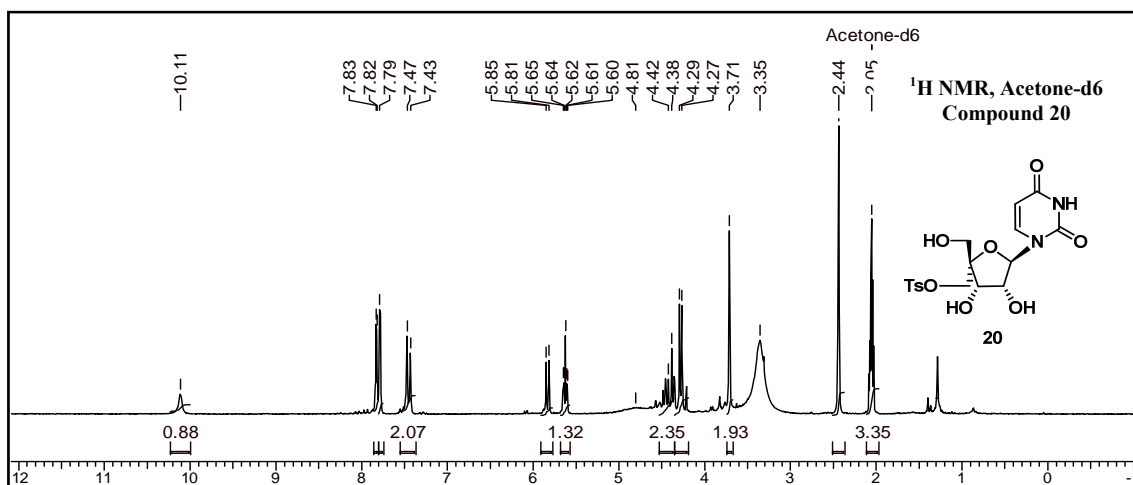
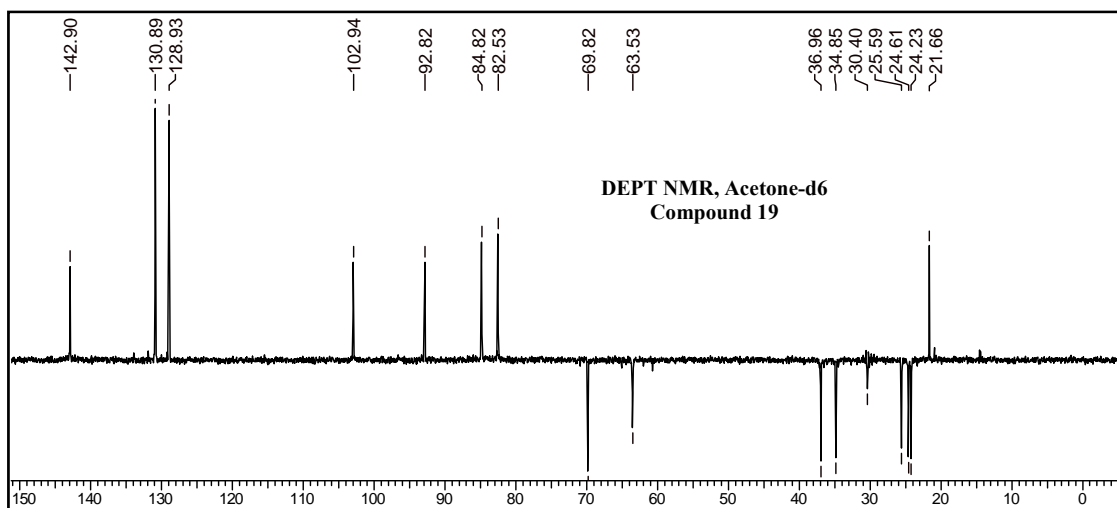


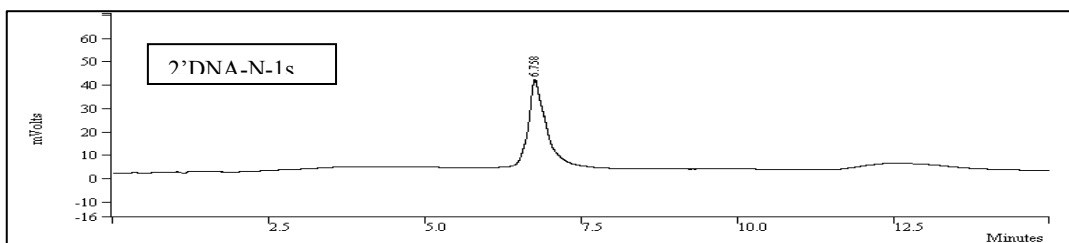
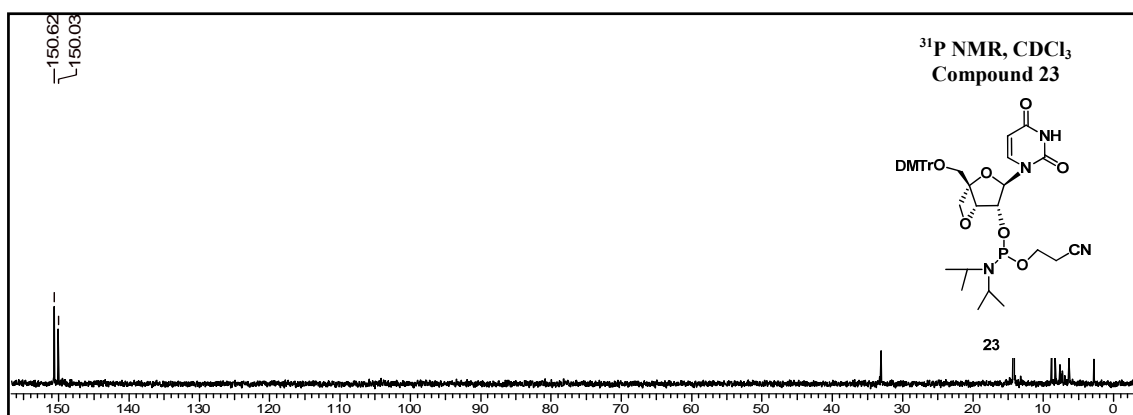
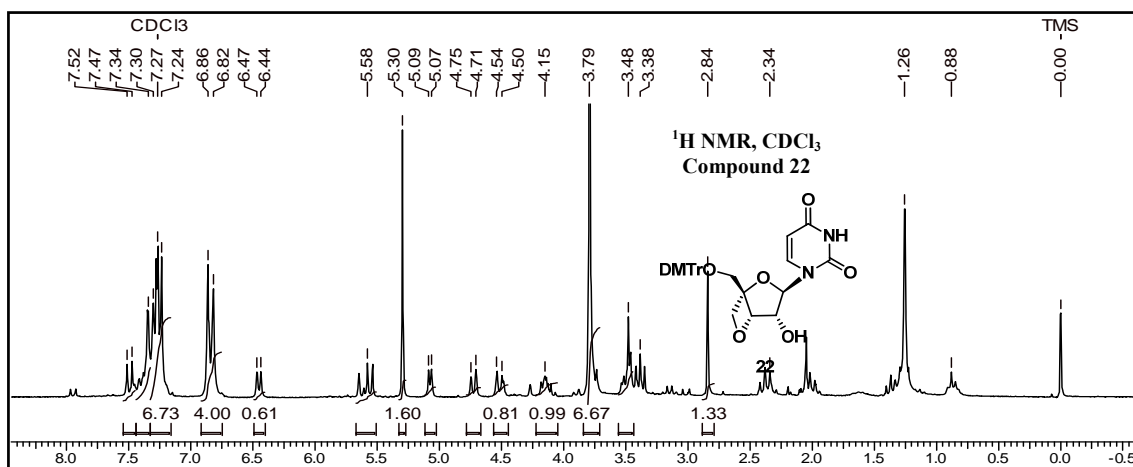




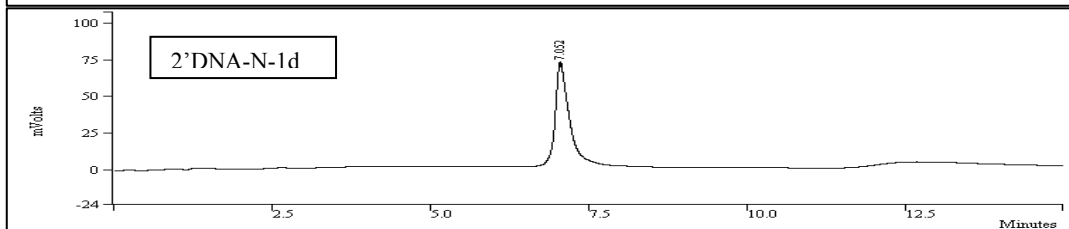




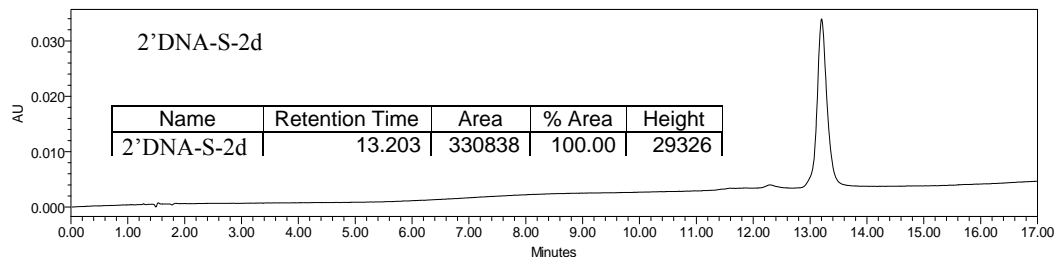
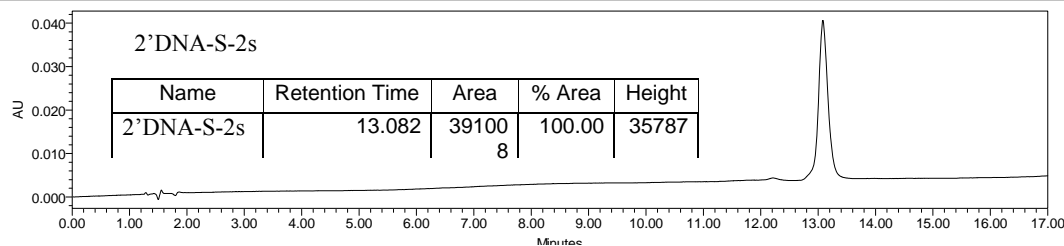
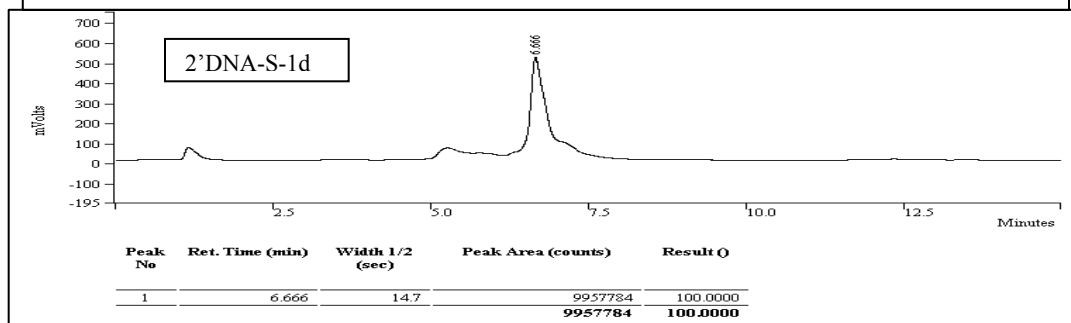
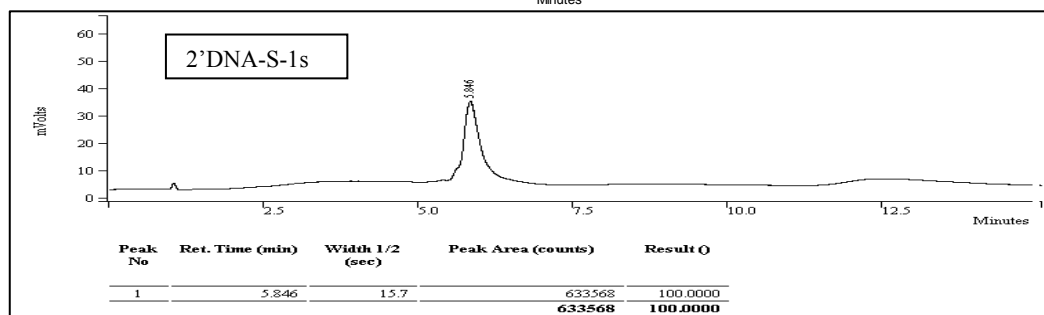
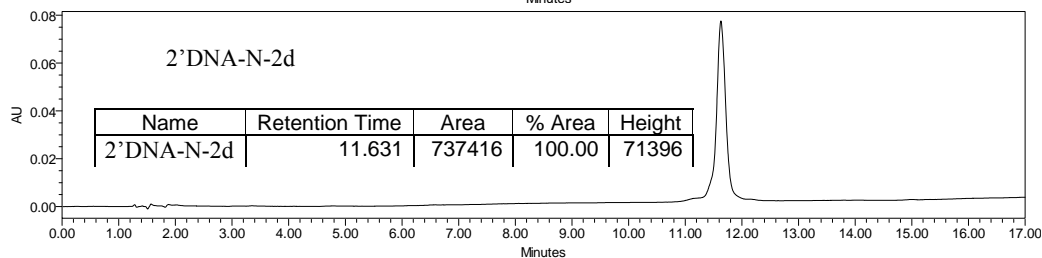
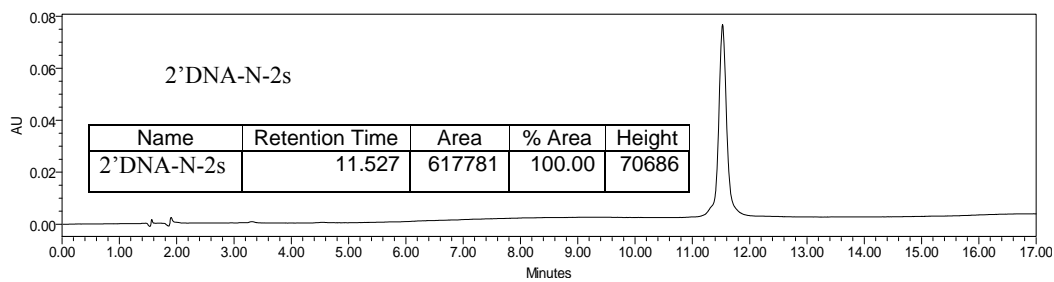




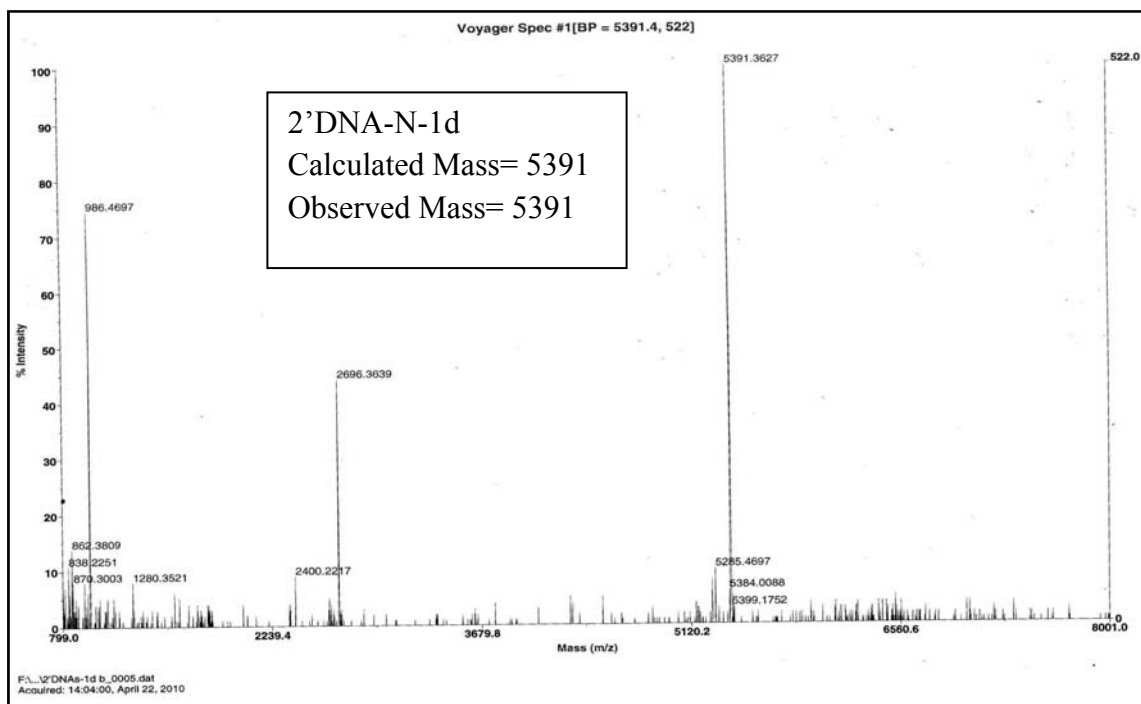
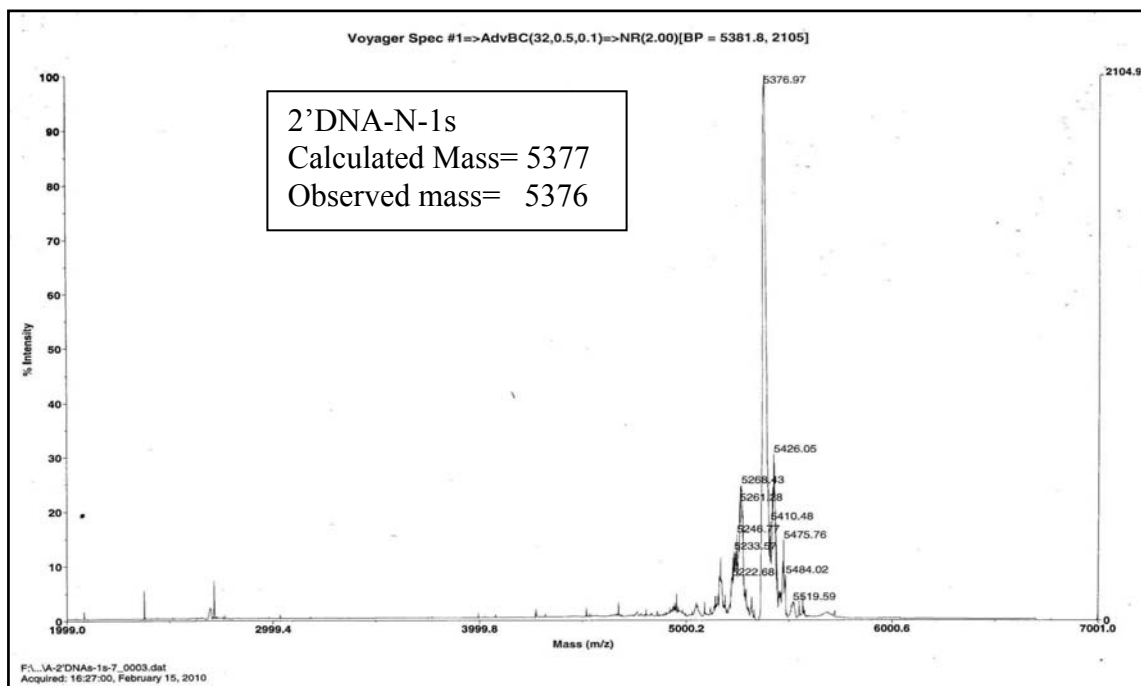
Peak No	Ret. Time (min)	Width 1/2 (sec)	Peak Area (counts)	Result Q
1	6.758	16.8	796753	100.0000
			796753	100.0000

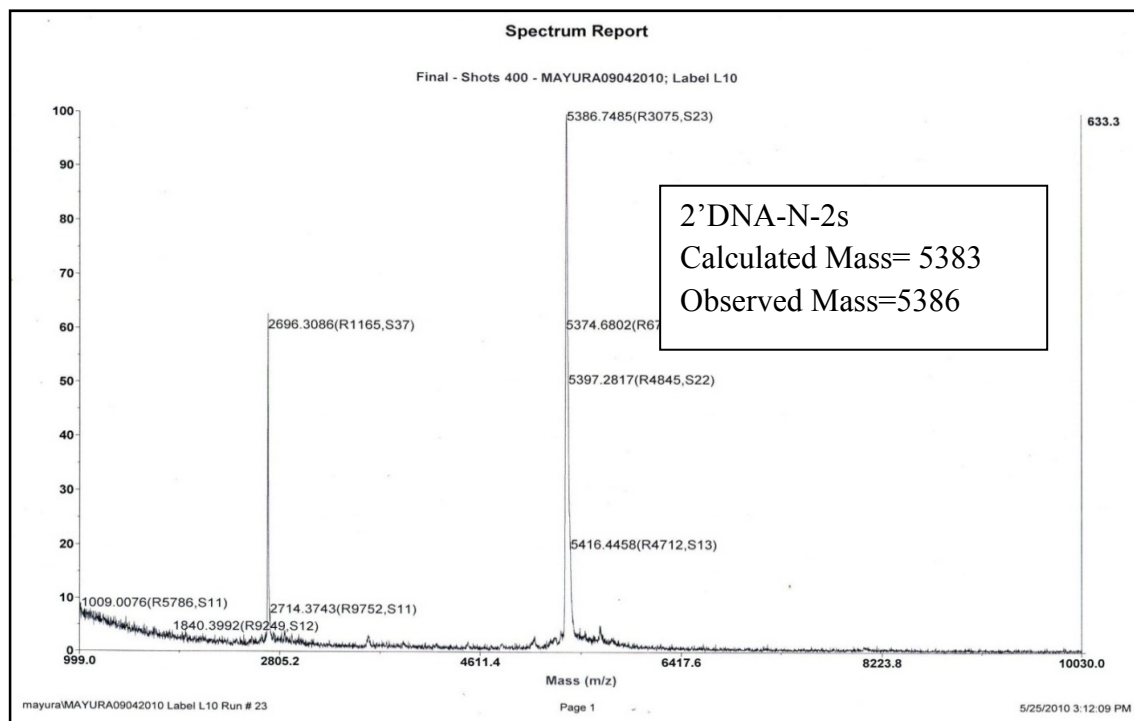
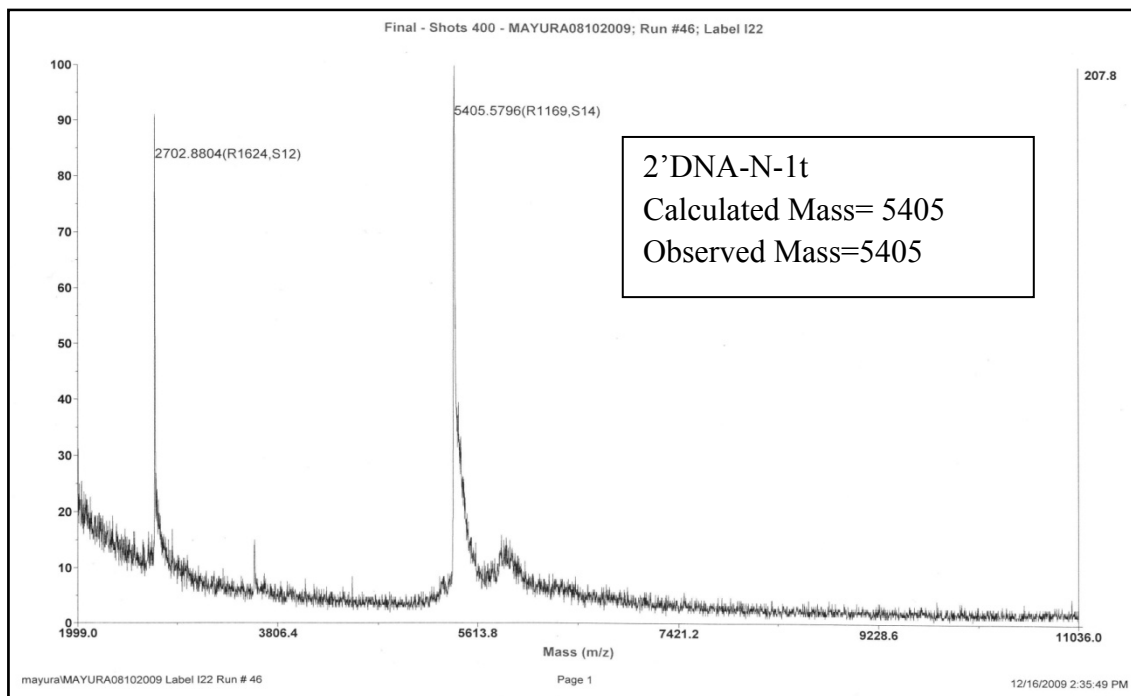


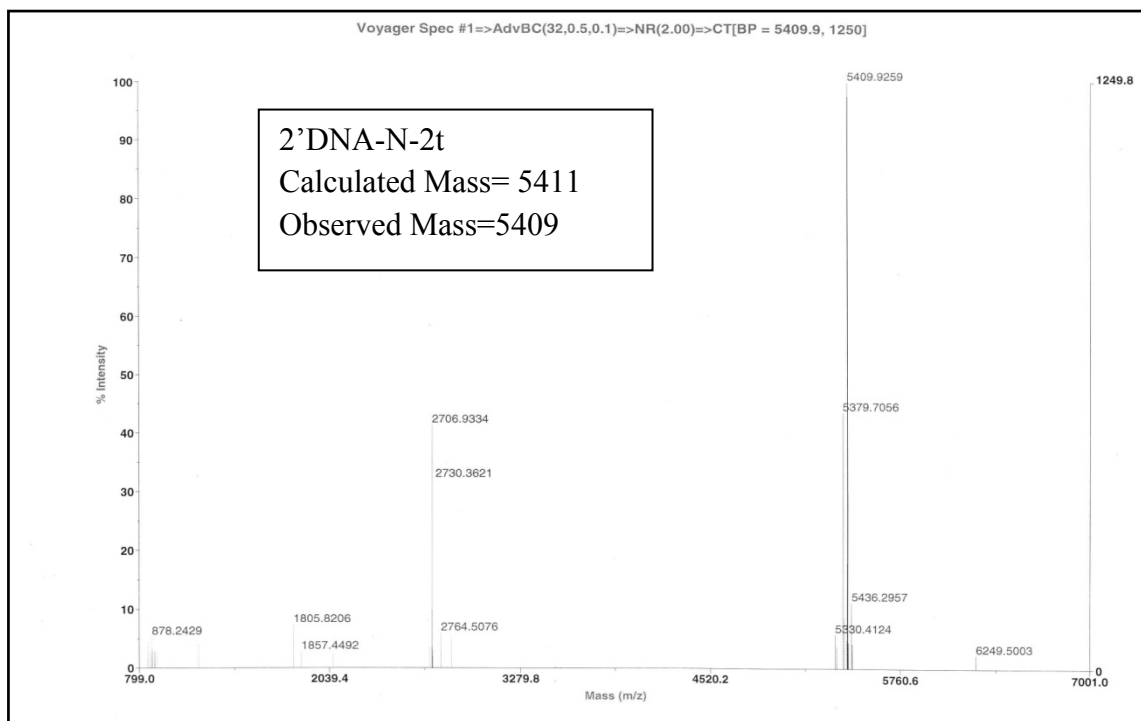
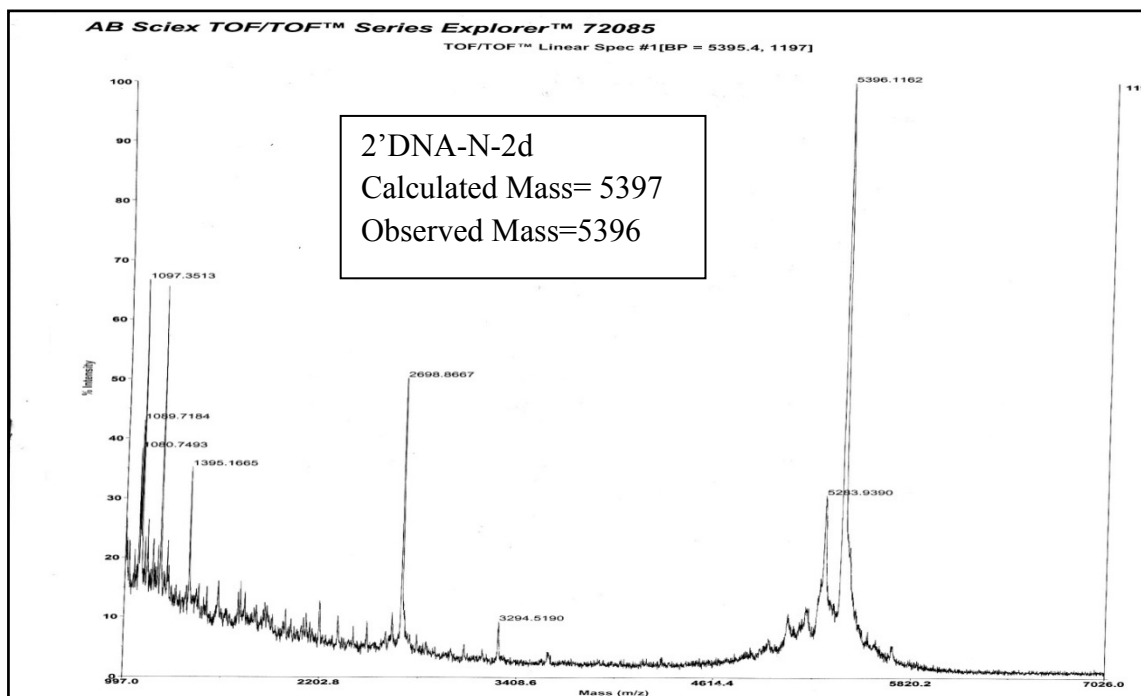
Peak No	Ret. Time (min)	Width 1/2 (sec)	Peak Area (counts)	Result Q
1	7.052	13.1	1183090	100.0000
			1183090	100.0000

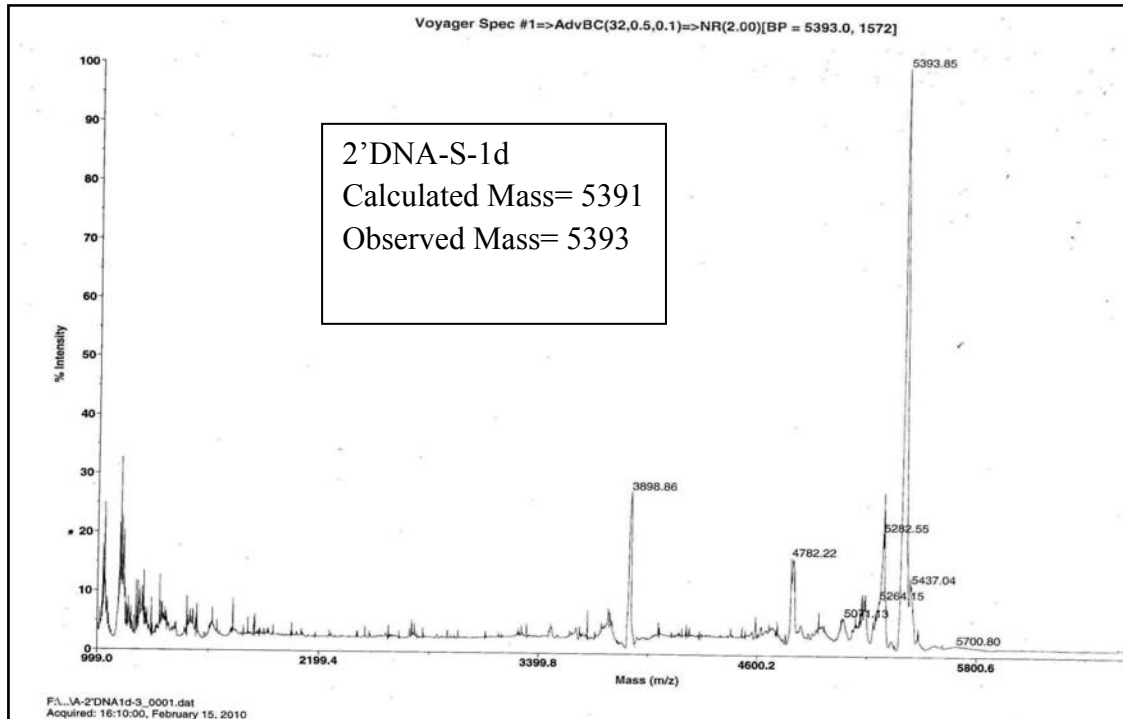
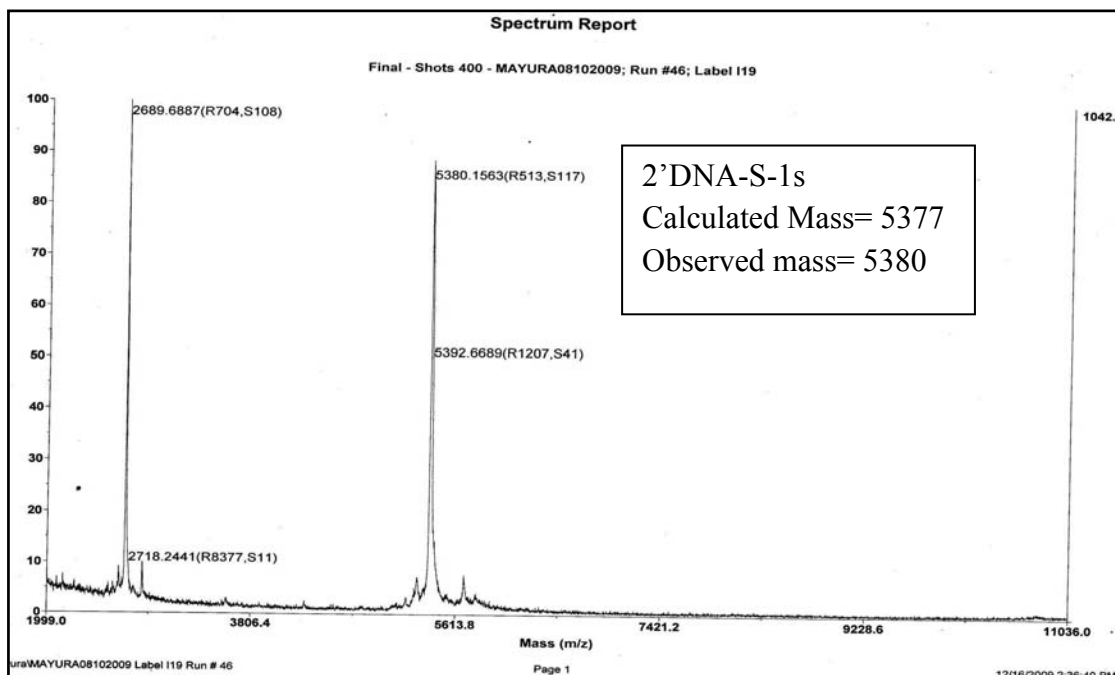


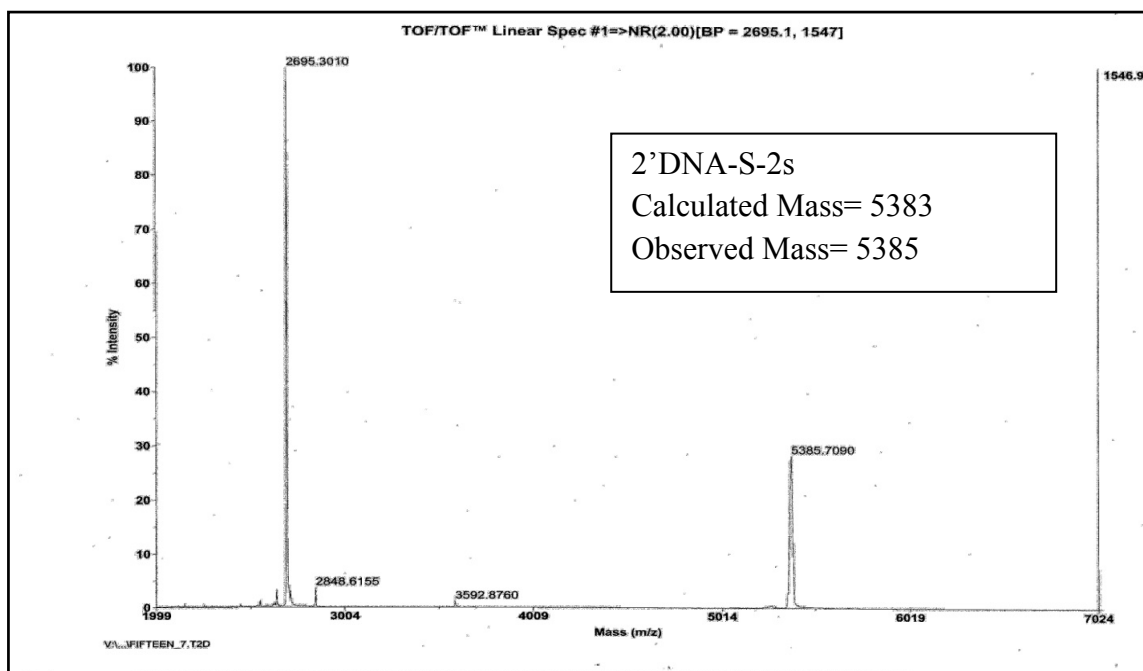
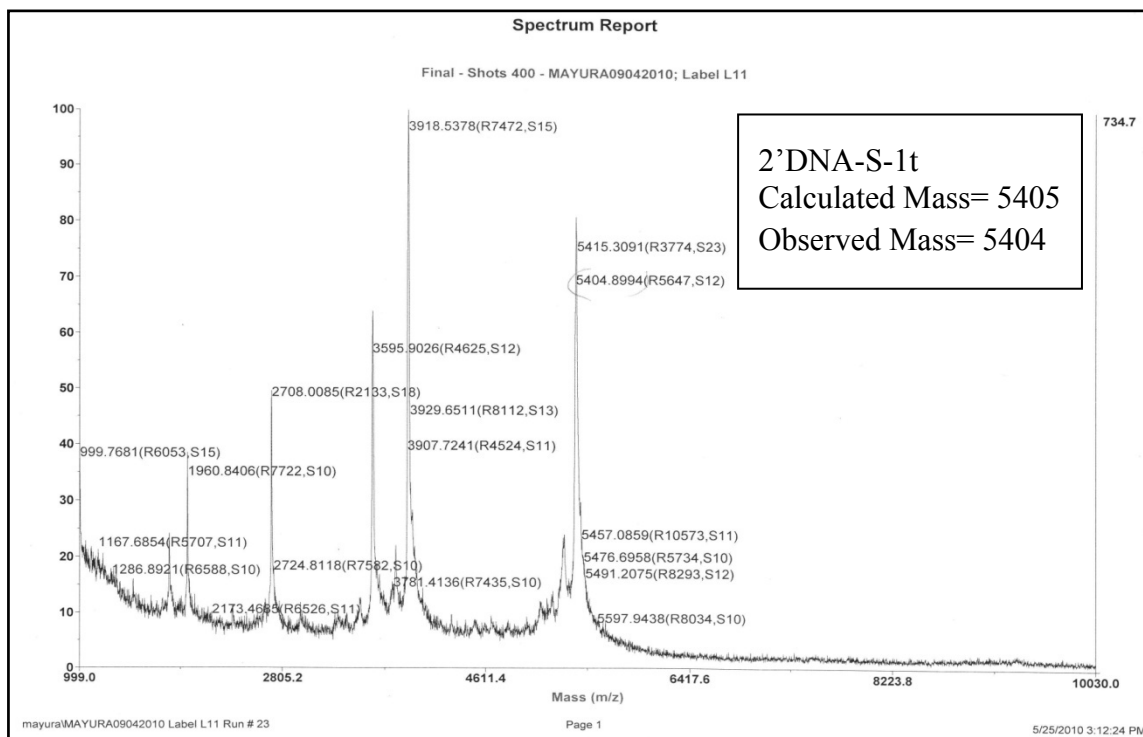
MALDI-TOF spectra of oligomers

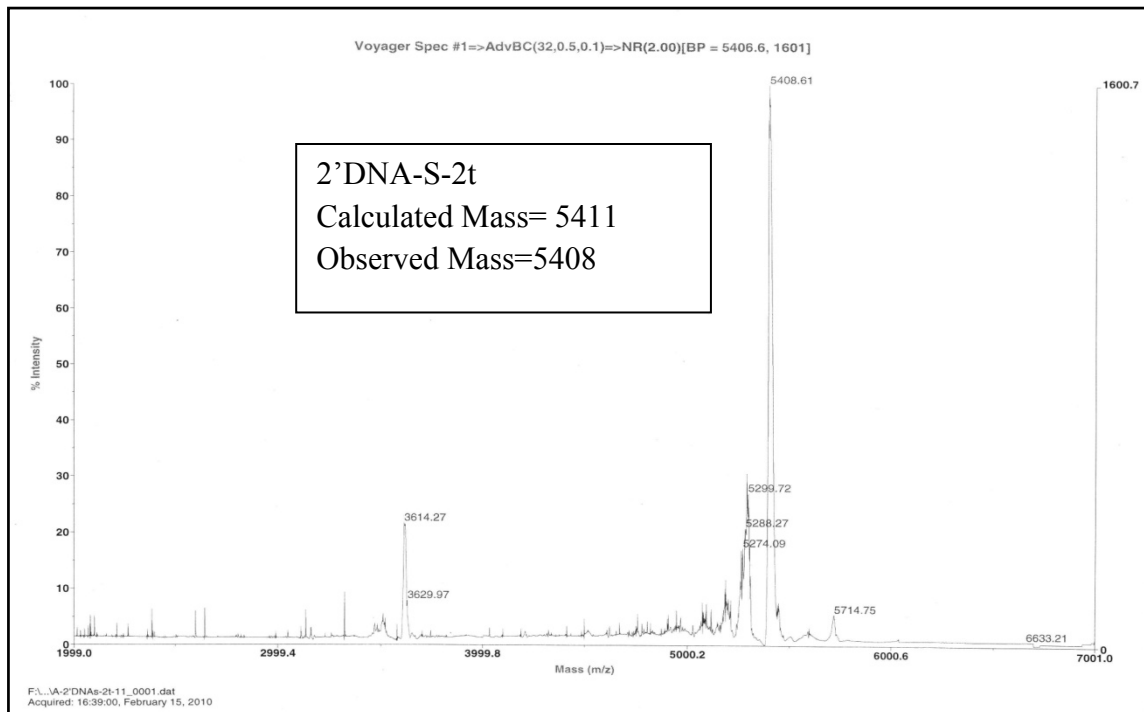
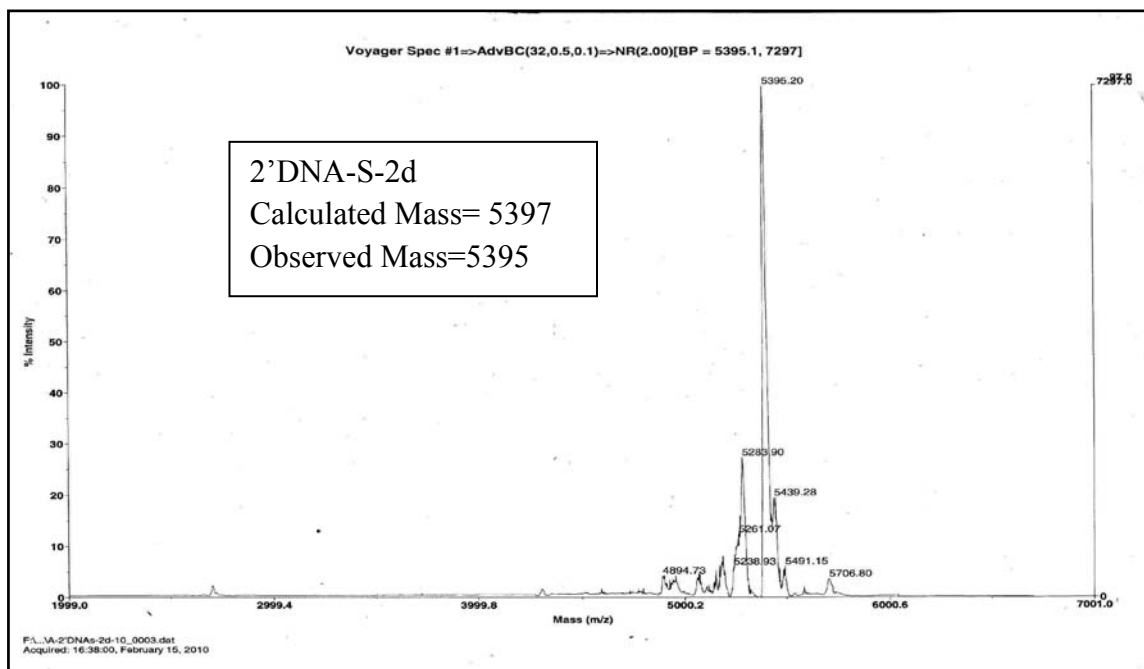












2.12 References

1. Leumann, C.J. *Bioorg.Med.Chem.*, **2002**, *10*, 841-854.
2. Meldgaard, M., Wengel, J., *J.Chem.Soc.,Perkin TransI*, **2000**, 3539-3554.
3. Kierzek, R., He, L., Turner, D.H., *Nucleic Acids Res.*, **1992**, *20*, 1685-1690.
4. Dougharty, J.P., Rizzo, R., Breslow, J., *J. Am.Chem.Soc.*, **1992**, *114*, 6254-6255.
5. Hashimoto, H., Switzer, C.J., *J. Am.Chem.Soc.*, **1992**, *114*, 6255-6256.
6. Giannaris, P.A., Damha, M.J., *Nucleic Acids Res.*, **1993**, *21*, 4742-4749
7. Alul, R., Hoke, G., *Antisense Res. Develop.*, **1995**, *5*, 3-11.
8. Sheppard, T.L., Breslow, R.C., *J. Am.Chem.Soc.*, **1996**, *118*, 9810-9811.
9. Kandimalla, E.R., Manning, A., Zhao, Q., Shaw, D.R., Byrn, R.A., Sasisekharan, V., Agarwal, S., *Nucleic Acids Res.*, **1997**, *25*, 370-378.
10. Wasner, M., Arion, D., Borkow, G., Noronha, A.Uddin, A.H., Parniak, M.A., Damha, M.J., *Biochemistry*, **1998**, *37*, 7478-7486.
11. Premraj, B.J., Yathindra, N., *J.Biomol.Struc.Dyn.*, **1998**, *16*, 313-328.
12. Premraj, B.J., Patel, P.K., Kandimalla, E.R., Agarwal, S., Hosur, R.V., Yathindra, N., *Biochem. Biophys. Res. Commun.*, **2001**, *283*, 537-543.
13. (a) Polak, M., Manoharan, M., Inamati, G.B., Plavec, J., *Nucleic Acids Res.*, **2003**, *31*, 2066. (b) Premraj, B.J., Raja, S., Bhavesh, N.S., Shi, K.; Hosur, R.V., Sundaralingam, M., Yathindra, N.; *Eur. J. Biochem.*, **2004**, *271*, 2956.
14. (a) Wodak, S.Y., Liu, M.Y., Wyckoff, H.W., *J.Mol. Chem.*, **1977**, *116*, 6059. (b) Saenger, W., *Principles of Nucleic Acid Structure*, Springer-Verlag: Berlin, 1984
15. (a) Imanishi, T., Obika, S., *Chem. Commun.*, **2002**, 1653. (b) Herdewijn, P., *Biochim. Biophys. Acta, Gene Struct. Expression*, **1999**, *1489*, 167. (c) Mathé, C., Périgaud, C., *Eur. J. Org. Chem.*, **2008**, 1489.
16. (a) Koshkin, A., Singh, S.K., Nielsen, P., Rajwanshi, V.K., Kumar, R., Meldgaard, M., Olsen, C.E., Wengel, J., *Tetrahedron*, **1998**, *54*, 3607, (b) Obika, S., Nanbu, D., Hari, Y., Andoh, J., Morio, K., Doi, T., Imanishi, T., *Tetrahedron. Lett.*, **1998**, *39*, 5401. (c) Braasch, D.A., Corey, D.R., *Chem. Biol.*, **2001**, *8*, 1. (d) Vester, B., Wengel, J., *Biochemistry*, **2004**, *43*, 13233. (e) Koizumi, M., *Biol. Pharm. Bull.*, **2004**, *27*, 453.

17. (a) Hendrix, C., Rosemeyer, H., Verheggen, I., Seela, F. Aerschot, A. Van., Herdewijn, P., *Chem. Eur. J.*, **1997**, *3*, 110, (b) Aerschot, A. Van., Verheggen, I., Hendrix, C., Herdewijn, P., *Angew. Chem., Int. Ed. Engl.*, **1995**, *34*, 1338.
18. (a) Steffens, R., Leumann, C.J., *J. Am. Chem. Soc.*, **1997**, *119*, 11548, (b) Steffens, R., Leumann, C.J., *J. Am. Chem. Soc.*, **1999**, *121*, 3249. (c) Renneberg D., Leumann, C.J., *J. Am. Chem. Soc.*, **2002**, *124*, 5993.
19. (a) Wallace, J.C., Edmons, M. *Proc. Natl. Acad. Sci. USA*, **1983**, *80*, 950-954. (b) Kerr, I.M., Brown, R.E.; *Proc. Natl. Acad. Sci. USA*; **1978**, *75*, 256
- 20.(a) Damha, M.J., Giannaris, P.A., Marfey, P., Reid, L.S., *Tetrahedron. Lett.*, **1991**, *32*, 2573.
21. V. Lalitha, Yathindra, N. *Current Science*; **1995**, Vol. 68. (1), 68-75
22. (a) Prakash, T.P., Jung, K.-E., Switzer, C., *Chem. Commun.*, **1996**, 1793-1794. (b) Jung, K.-E., Switzer, C. *J. Am. Chem. Soc.*, **1994**, *116*, 6059-6061.
23. Premraj, B.J., Raja, S., Yathindra, N.; *Biophys. Chem.*, **2002**, *95*, 253.
24. Lescrinier, E., Esnouf, R., Schraml, J., Busson, R., Heus, H.A., Hilbers, C.W., Herdewijn, P., *Chem. Biol.*, **2000**, *7*, 719-73
25. Kawasaki, A.M., Casper, M.D., Freier, S.M., Lesnik, E.A., Zounes, M.C., Cummins, L.L., Gonzalez, C., Cook, P.D., *J. Med. Chem.*, **1993**, *36*, 831-841. b) Damha, M.J., Wilds, C.J., Noronha, A., Brukner, I., Borkow, G., Arion, D., Parniak, M.A., *J. Am. Chem. Soc.*, **1998**, *120*, 12976-12977 c) Lok, C.N., Viazovkina, E., Min, K.L., Nagy, E., Wilds, C.J., Damha, M.J., Parniak, M.A., *Biochemistry*, **2002**, *41*, 3457- 3467 d) Wilds, C.J., Damha, M.J., *Nucleic Acids Res.*, **2000**, *28*, 3625-3635.
26. Zou, R., Matteucci, M.D., *Tetrahedron Lett.*, **1996**, *37*, 941-944.
27. (a) Obika, S., Morio, K., Nanbu, D., Imanishi, T., *Chem. Commun.*, **1997**, 1643-1644. (b) Obika, S., Morio, K., Nanbu, D., Hari, Y., Hiromi, I., Imanishi, T., *Tetrahedron*, **2002**, *58*, 3039. (c) Obika, S., Morio, K., Hari, Y., Imanishi, T., *Bioorg. Med. Chem. Lett.*, **1999**, *9*, 515. (d) Obika, S., Morio, K., Nanbu, D., Hari, Y., Imanishi, T., *Chem. Commun.*, **1999**, 2423-2424. (e) Imanishi, T.; Obika, S. **2004**, US Patent US6770748 B2.

28. Kumar, A., Katti, S.B., Rosemeyer, H., Seela, F., *Nucleosides Nucleotides*, **1996**, *15* (10), 1595-1601.
29. Zhang, N., Zhang, S., Szostak, J.W., *J. Am. Chem. Soc.*, **2012**, *134*, 3691-3694.
30. Scott, S., Hardy, P., Sheppard, R.C., McLean, M.J., *Innovations and Perspectives in Solid Phase Synthesis, 3rd International Symposium*, **1994**, Ed. Roger Epton, Mayflower Worldwide, 115-124.
31. McBride, L.J., Caruthers, M.H., *J. Am. Chem. Soc.*, **1981**, *103*, 3185-3191.
32. Krutzfeldt, J., Rajewsky, N., Braich, R., Rajeev, K.G., Tuschel, T., Manoharan, M., Stoffel, M., *Nature*, **2005**, *438*, 685.
33. Kang, S.H., Cho, M.J., Kole, R., *Biochemistry*, **1998**, *37*, 6235
34. Steely Jr., H.T., Gray, D.M., Ratcliff, R.L., *Nucleic Acids. Res.*, **1986**, *14*, 10071.
35. (a) Morita, K., Obika, S., Imanishi, T., Kitade, Y., Koizumi, *Nucleic Acids Symp. Ser.*, **2008**, *52*, 637. (b) Nagaoka, K., Kito, S., Kitamura, Y., Ueno, Y., Kitade Y., *Nucleic Acids Symp. Ser.*, **2009**, *53*, 123. (c) Nagaoka, K., Kitamura, Y., Ueno, Y., Kitade Y., *Bioorg. Med. Chem Lett.*, **2010**, *20*, 1186.

Chapter 3

Synthesis, characterization and biophysical studies of 2'-*O*-allyl/3'-*O*-allyl derived DNA and *iso*DNA oligonucleotides

Section A

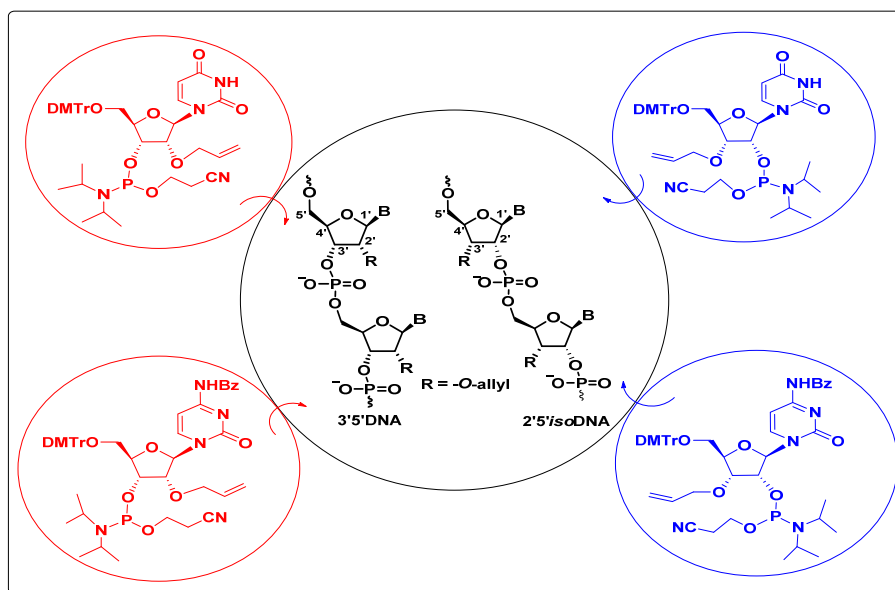
Synthesis of 2'-*O*-allyl/3'-*O*-allyluridine monomers and conversion of 2'-*O*-allyl/3'-*O*-allyluridine derivatives to the respective cytidine monomers

Section B

Synthesis of 2'-*O*-allyl/3'-*O*-allyl modified DNA and *iso*DNA sequences and their biophysical study

Chapter 3

Synthesis, characterization and biophysical studies of 2'-O-allyl/ 3'-O-allyl derived DNA and *iso*DNA oligonucleotides



Antisense oligonucleotides (ASOs) play a major role in nucleic acid therapeutics. Among the several oligonucleotide modifications, the 2'-sugar modifications particularly enhance the potency and pharmacokinetics of ASOs. The properties of 2'-O-allyl oligoribonucleotides have been reported to be superior to 2'-O-methyl and 2'-O-dimethylallyl analogues and well suited for general use as antisense reagents.¹ The regioselective 2'/3'-O-allylation of pyrimidine ribonucleosides using phase transfer catalysis provided a short route to the synthesis of isomeric 2'/3'-O-allyl uridine derivatives followed by their conversion to the isomeric 2'/3'-O-allyl cytidine derivatives. Since 2'-5'-linked *iso*DNA are better ASOs, we have introduced the 3'-O-allyl uridine and cytidine monomers into 2'-5'-linked *iso*DNA, similarly the 2'-O-allyluridine and cytidine monomers were introduced in the 3'-5'-linked DNA oligomers to compare their thermal stability when complexed with the complementary DNA as well as RNA.

Section A

Synthesis of 2'-O-allyl/3'-O-allyluridine monomers and conversion of 2'-O-allyl/3'-O-allyluridine derivatives to the respective cytidine monomers

3.1 Introduction to present work

The antisense therapeutic approach discovered more than three decades ago by Zamecnik and Stephenson² continues to attract chemists towards the design and synthesis of modified antisense oligonucleotides (ASOs). The renewed interest is especially due to potential applications in the siRNA³ and miRNA⁴ therapeutic targeting. Also an additional encouraging factor is the approval of only the second antisense drug, Mipovirsen from ISIS pharmaceuticals. There are numerous oligonucleotide modifications that enhance the properties of antisense oligonucleotides.⁵ Modifications to the base, sugar, and backbone are known to increase the binding affinity for the target RNA.⁶ Among the first generation antisense oligonucleotides are the backbone modified phosphorothioates,⁷ in which the non-bridging oxygen atoms in the phosphodiester linkage is substituted by a sulfur atom. They support the RNase H activity and exhibit acceptable pharmacokinetics for systemic and local delivery. Modifications to the sugar have been useful, particularly the 2'-sugar modifications, for enhancing the potency and pharmacokinetics of ASOs. The most advanced second generation sugar modifications 2'-O-methyl and 2'-O-methoxyethyl (MOE) (Figure 1) resulted in a 3-10 fold increase in potency in cell-based assays compared to phosphorothioate oligonucleotides, an increase in nuclease resistance and decreased cytotoxicity.⁸

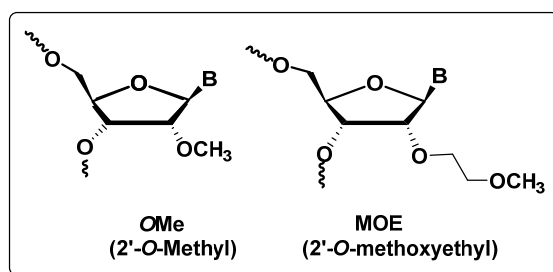


Figure 1. Second generation ASO modifications.

Chemically synthesized 2'-*O*-methyloligoribonucleotides^{9,10} and 2'-*O*-alkyloligoribonucleotides earlier reported^{1,11} are of interest as antisense probes due to their high thermal stability as a RNA:RNA duplex. The modified duplex is not a substrate for RNase H cleavage, but the 2'-*O*-alkyl oligomers are resistant to nuclease degradation and as well as exhibit better cell uptake.⁹ Since a uniform 2'-*O*-alkyl modified ASO does not support an RNase H cleavage mechanism, a new chimeric strategy has been reported in which the oligonucleotide has a central DNA region of 8-16 nucleotides, flanked on the 5' and 3' ends with 2 to 5 2'-*O*-methoxyethyl (MOE) residues.^{5a} This “gapmer” design (Figure 2) supports the RNase H cleavage mechanism due to the central DNA region. The potency of these gapmer ASOs was found to increase by reducing the ASO length, and using constrained/locked-MOE residues on the 5' and 3' ends of the ASO.¹² Sproat *et al.*¹³ have reported 2'-*O*-allylribonucleotides as superior antisense compounds for investigating inhibition of reverse transcription. Fully-modified 2'-*O*-allyl 17mers were able to specifically block reverse transcription *via* an RNase H-independent mechanism, with efficiencies comparable to those observed with phosphodiester (PO) and phosphorothioate oligonucleotides. Sandwich(gapmer) 2'-*O*-alkyl/PO/2'-*O*-alkyl oligonucleotides, supposed to combine the properties of 2'-alkyl modifications (physical blocking of the RT) to those of the PO window (RNase H-mediated cleavage of the RNA) were quasi-stoichiometric inhibitors when adjacent to the primer, but remained without any effect when non-adjacent.



GAPMER design

Figure 2. Chimeric gapmer design.

Hammerhead ribozymes can catalyze highly specific *trans* cleavage of any RNA containing a dinucleotide UH (H= C,A,U).¹⁴ This high specificity suggests the use of these ribozymes as therapeutic agents in gene regulation.¹⁵ Incorporation of 2'-*O*-allylribonucleotides at non-essential positions of the hammerhead ribozyme domain resulted in catalytically active and stable ribozymes.¹⁶ Ribozymes having 2'-NH₂ uridine 2'-*C*-allyluridine, 2'-*O*-methyl uridine modifications resulted in the best combination of

cleavage activity and nuclease stability.¹⁷ Recently, application of 3'-*O*-allyl group as a reversible capping moiety for the 3'-OH of photocleavable nucleotide analogue for sequencing by synthesis (SBS) and as probes for 3'-*O*-Mass Tag is also reported.¹⁸

3.1.1 Present work

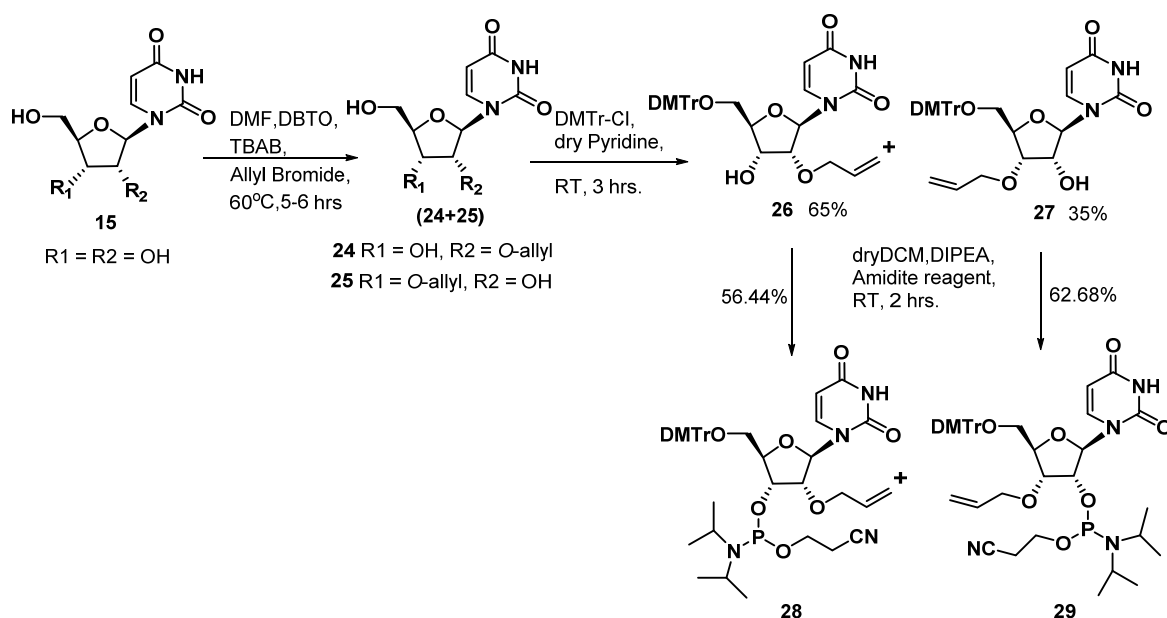
The encouraging literature reports of 2'-*O*-allyl oligoribonucleotides as effective antisense probes and in continuation of the theme of synthesis and biophysical study of 2'-5'-linked *iso*DNA analogues, as better antisense oligonucleotides, the synthesis of 2'-*O*-allyl and 3'-*O*-allyl ribonucleotides was undertaken.

Methylation and benzylation of uridine using dibutyltin oxide (DBTO) are known¹⁹ to be directed to the 2'/3' *cis*-diol system without affecting the 5'-hydroxyl or the N3 ring amide. This selectivity is attributed to the activation of the hydroxyls due to the formation of cyclic 2',3'-*O*-dibutylstannylidene intermediate resulting in monoalkylation at the 2'/3'-hydroxyls of uridine. Regiospecific allylation of polyhydroxy compounds was reported²⁰ to give high yields of *O*-monoallyl derivatives when tetrabutylammonium bromide (TBAB) was used as a phase transfer catalyst along with DBTO. The catalysis by TBAB salt probably involves the enhancement of nucleophilicity of the sugar oxygen in the stannylidene complex by co-ordination of the halide ion to tin. DMF proved to be a better solvent for the allylation reaction to proceed with an enhanced rate.

A short and convenient method for the synthesis of regiospecific 2'/3'-*O*-allylation of pyrimidine ribonucleosides using phase transfer catalysis was reported²¹ earlier by our group. Following this simple but efficient method with some modifications, the synthesis of 2'-*O*-allyluridine and 3'-*O*-allyluridine phosphoramidite monomers was accomplished (Scheme 3). The isomeric 2'-*O*-allyl and 3'-*O*-allyluridine nucleosides were converted to the respective cytidine derivatives using reported procedure for conversion of uridine to cytidine.²² The *N*-benzoyl protected cytidine isomers were then converted into their respective amidite monomers (Scheme 4).

3.1.2 Synthesis of 2'-O-allyl and 3'-O-allyl-uridine monomers

Uridine **15**, was treated with allyl bromide (1eq), DBTO (1.2eq) and TBAB (1.1eq) in DMF (Scheme 3), giving a mixture of 2'- and 3'-O-allyluridine **24+25** (60-70%) having very close R_f values on TLC. The reaction gave very poor yield of the alkylated products, in the absence of either DBTO or TBAB. The mixture **24+25** was converted into the 5'-O-DMT derivatives which could be resolved by silica gel column chromatography. This method gave 60% 5'-O-DMT-2'-O-allyluridine **26** and 40% 5'-O-DMT-3'-O-allyluridine **27**. The compounds **26** and **27** were then converted into the respective 2'-O-allyl and 3'-O-allyl uridine phosphoramidite monomers **28** and **29**. All the pure compounds were characterised by ^1H and ^{13}C NMR spectroscopy and LCMS mass analysis.

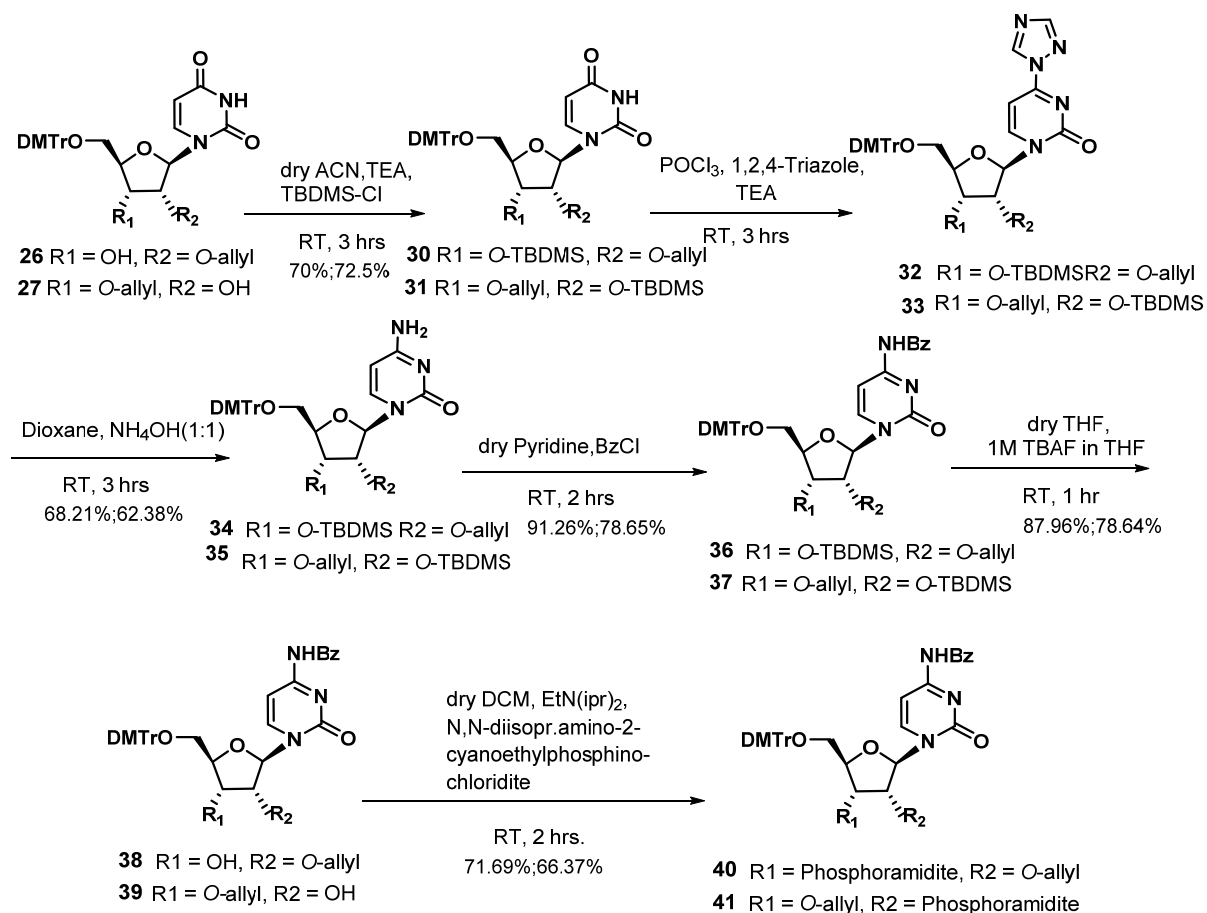


Scheme 3. Synthesis of 2'-O-allyl and 3'-O-allyluridine monomers

3.1.3 Conversion of the 2'-O-allyl and 3'-O-allyluridine to the respective cytidine monomers

The 3'-OH and 2'-OH group of compounds **26** and **27**, respectively, was protected using TBDMS-Cl giving the 2' and 3'-O-TBDMS protected derivatives **30** and **31** (Scheme 4). Using a well established reported method¹¹ compounds **30** and **31** were converted into the 1,2,4-triazolyl intermediates **32** and **33**. Treating **30** and **31** with a 2 fold excess of

tri(1H-1,2,4-triazol-1-yl) phosphine oxide (prepared *in situ* by treating phosphoryl chloride with 3 mol equiv, each of 1,2,4-triazole and triethylamine) in acetonitrile solution in the presence of additional 1,2,4-triazole and triethylamine in acetonitrile at room temperature for 3 h gave the required products **32** and **33**. Addition of aqueous ammonia to the compounds **32** and **33** in dioxane at room temperature yielded the desired cytidine derivatives **34** and **35**. The exocyclic amino group of 2'-O-allyl and 3'-O-allylcytidine derivatives was protected as N4-benzoyl, followed by TBDMS deprotection to get compounds **38** and **39**. The compounds **38** and **39** were then converted into the respective 2'-O-allyl and 3'-O-allyl cytidine phosphoramidite monomers, **40** and **41**. All the compounds were characterised by ^1H and ^{13}C NMR spectroscopy and LCMS mass.



Scheme 4. Synthesis of 2'-O-allyl, 3'-O-allylcytidine monomers

3.1.4 2'-O-allyl and the 3'-O-allyl isomers differentiation using ^{13}C NMR

The 2'-O-allyl and the 3'-O-allyl isomers could be differentiated on the basis of assignments of ^{13}C NMR shifts of the sugar carbons. It is reported in literature²³ that in free nucleosides, C3' is shifted downfield as compared to C2' by about 5ppm. C2'-O-alkylation leads to down field shifts of 10-12ppm for C2', and an upfield shift by 4-6ppm for C3'. The observed ^{13}C NMR signals for the isomers are largely in agreement with these reports. In the case of C3'-O-allylation downfield shifts are observed for both C3'(\approx 5ppm) and C2'(\approx 1.0ppm) carbons.(Table 1.)

Table 1. ^{13}C NMR shifts of the C2' and C3' sugar carbons of the 2'-O-allyl and 3'-O-allylcytidine derivatives

Nucleoside	^{13}C NMR Chemical shift (δ)	
	C2'	C3'
Uridine	73.20	70.60
5'-O-DMT-2'-O-allyluridine 26	81.39	68.51
5'-O-DMT-3'-O-allyluridine 27	74.05	76.17
Cytidine	73.20	70.60
5'-O-DMT-2'-O-allylcytidine 38	81.39	67.70
5'-O-DMT-3'-O-allylcytidine 39	74.30	75.77

Section B

Synthesis of 2'-O-allyl and 3'-O-allyl modified DNA and *iso*DNA sequences and their biophysical study

3.2 Synthesis, purification and characterization of modified DNA and *iso*DNA sequences

The four phosphoramidite monomers 2'-O-allyluridine monomer **28**, 2'-O-allylcytidine monomer **40**, and the 3'-O-allyl-uridine monomer **29**, 3'-O-allylcytidine monomer **41** were characterised by ^{31}P NMR (Figure 3) and incorporated into 3'-5'DNA (**28** and **40**) and 2'-5'*iso*DNA (**29** and **41**) oligonucleotides respectively.

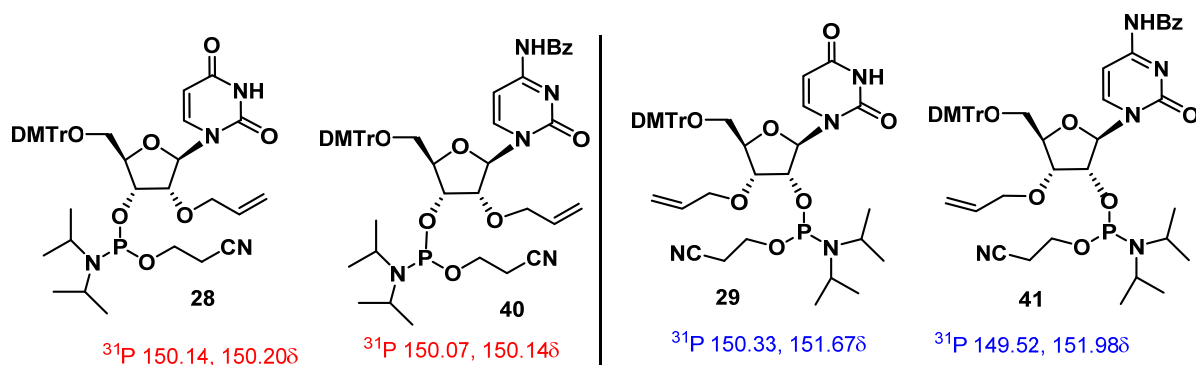


Figure 3. Modified phosphoramidite building blocks.

The 2'-O-allyl monomers of both uridine and cytosine were introduced as a single, double and triple modifications in the 3'-5'-linked oligomers to compare their thermal stability when complexed with the complementary DNA as well as RNA. The 3'-O-allyl uridine and cytosine monomers were introduced similarly as a single, double and triple modifications into 2'-5'-linked *iso*DNA oligomers, at predefined positions to determine their stability with complementary RNA only, as the *iso*DNA oligonucleotides do not bind to 3'-5'-linked DNA. The site of modifications selected in both DNA-1, 2'DNA-1 and

DNA-2, 2'DNA-2 was such that these were separated by 4-5 nucleotides. In 3'-5'-linked DNA-1 a single modification and a consecutive modification was also introduced towards the 5'-end for comparing their relative thermal stabilities. The in-house, automated four column DNA synthesizer (Bioautomation MM-4) was used for the synthesis of all the sequences used for this study. For introducing the allyl modifications two 18mer sequences were selected, which are used in biological studies. DNA-1 is used for miRNA down-regulation²⁴ and DNA-2 is used in the splice-correction assay developed by Kole *et al.*²⁵ The solid phase synthesis was done as described in the DNA synthetic cycle (Chapter 2, Section B). The activator used for coupling reaction was 5-ethylthiotetrazole. A double coupling step was used along with longer coupling time for the modified monomers. The 2'-5'-linked oligonucleotides were synthesized using 3'-deoxy-2'-phosphoramidite monomers procured from Glen Research Corporation, USA. As described in Chapter 2, Section B universal support columns were used for the synthesis, so as to get a 2'-terminus for the synthesized sequence. The synthesis of control sequences 3'-5'-linked DNA-1, DNA-2 was done using normal CPG support. Both 3'-5'DNA oligonucleotides and 2'-5'DNA oligonucleotides were deprotected by ammonia treatment at 55°C for six hours followed by removal of ammonia and concentrating the aqueous solution. The fully deprotected crude oligomers were desalted using Sephadex NAP-5 column. Purification of all the oligonucleotides was done by reverse phase-HPLC using a gradient elution. The sequences were characterized by MALDI-TOF mass spectrometry. The Table 2a, 2b gives the list of the synthesized oligonucleotides, the RP-HPLC retention time (t_R) and the MALDI-TOF mass obtained. The control and complementary DNA, *isoDNA* oligonucleotides synthesized and used for this study are listed in (Table 3). The complementary RNA oligonucleotides for the DNA, *isoDNA* oligomers were procured from Sigma Aldrich.

Table 2a. 2'-O-allyl uridine (**U**) and 2'-O-allyl cytidine (**C**) modified sequences, HPLC and MALDI-TOF mass. (1s,1d,1t indicate single,double and triple modifications in DNA-1 18mer and 2s,2d,2t indicate single,double and triple modifications in DNA-2 18mer).

Code No	Name	Sequence	HPLC (t _R) mins.	Mass (calcd.)	Mass (obsd.)
3'DNA1-1	DNA2'allU-1s	5'CACCATTGTCACAC <u>U</u> CCA ^{3'}	9.52	5405	5406
3'DNA1-2	DNA2'allU-1d	5'CACCATTG <u>U</u> CACAC <u>U</u> CCA ^{3'}	10.06	5447	5450
3'DNA1-3	DNA2'allU-1t	5'CACCA <u>U</u> TG <u>U</u> CACAC <u>U</u> CCA ^{3'}	10.42	5489	5490
3'DNA1-4	DNA2'allU-1S ^{5'}	5'CACCA <u>U</u> TGTCACACTCCA ^{3'}	9.40	5405	5408
3'DNA1-5	DNA2'allU-1D ^{5'}	5'CACCA <u>UU</u> GTCACACTCCA ^{3'}	10.12	5447	5452
3'DNA2-1	DNA2'allU-2s	5'CCTCTTACCTCAGT <u>U</u> ACA ^{3'}	9.80	5411	5413
3'DNA2-2	DNA2'allU-2d	5'CCTCTTAC <u>U</u> CAGT <u>U</u> ACA ^{3'}	10.21	5453	5460
3'DNA2-3	DNA2'allU-2t	5'CCTCT <u>U</u> AC <u>U</u> CAGT <u>U</u> ACA ^{3'}	10.63	5495	5502
3'DNA1-6	DNA2'allC-1s	5'CACCATTGTCACACT <u>C</u> CA ^{3'}	9.83	5419	5418
3'DNA1-7	DNA2'allC-1d	5'CACCATTGT <u>C</u> ACACT <u>C</u> CA ^{3'}	10.19	5475	5486
3'DNA1-8	DNA2'allC-1t	5'CA <u>C</u> CATTGT <u>C</u> ACACT <u>C</u> CA ^{3'}	10.62	5531	5536
3'DNA2-4	DNA2'allC-2s	5'CCTCTTACCTCAGTTA <u>C</u> A ^{3'}	10.21	5425	5424
3'DNA2-5	DNA2'allC-2d	5'CCTCTTAC <u>C</u> TCAGTTA <u>C</u> A ^{3'}	10.48	5481	5477
3'DNA2-6	DNA2'allC-2t	5' <u>C</u> <u>C</u> TCTTAC <u>C</u> TCAGTTA <u>C</u> A ^{3'}	10.94	5536	5533

Table 2b. 3'-O-allyl uridine (**U**) and 3'-O-allyl cytidine (**C**) modified sequences, HPLC and MALDI-TOF mass. (1s,1d,1t is single,double and triple modifications in DNA-1 18mer and 2s,2d,2t is single,double and triple modifications in DNA-2 18mer)

Code No	Name	Sequence	HPLC (t _R) mins	Mass (calc.)	Mass (obt.)
2'DNA1-1	2'DNA3'allU-1s	5' CACCATTGTCACAC U CCA ^{2'}	10.79	5405	5413
2'DNA1-2	2'DNA3'allU-1d	5' CACCATTG U CACAC U CCA ^{2'}	11.26	5447	5463
2'DNA1-3	2'DNA3'allU-1t	5' CACCA U TG U CACAC U CCA ^{2'}	11.73	5489	5502
2'DNA2-1	2'DNA3'allU-2s	5' CCTCTTACCTCAGT U ACA ^{2'}	10.69	5411	5432
2'DNA2-2	2'DNA3'allU-2d	5' CCTCTTACC U CAGT U ACA ^{2'}	11.02	5453	5465
2'DNA2-3	2'DNA3'allU-2t	5' CCTCT U ACC U CAGT U ACA ^{2'}	11.10	5495	5507
2'DNA1-4	2'DNA3'allC-1s	5' CACCATTGTCACACT C CA ^{2'}	10.73	5419	5421
2'DNA1-5	2'DNA3'allC-1d	5' CACCATTGT C ACACT C CA ^{2'}	10.94	5475	5484
2'DNA1-6	2'DNA3'allC-1t	5' CA C CATTGT C ACACT C CA ^{2'}	10.21	5531	5544
2'DNA2-4	2'DNA3'allC-2s	5' CCTCTTACCTCAGTTA C A ^{2'}	10.92	5425	5449
2'DNA2-5	2'DNA3'allC-2d	5' CCTCTTAC C TCAGTTA C A ^{2'}	10.83	5481	5500
2'DNA2-6	2'DNA3'allC-2t	5' C C TCCTTAC C TCAGTTA C A ^{2'}	9.06	5536	5547

(a) RNA-1 5'UGGAGUGUGACAAUGGUG 3' (b) RNA-2 5'UGUAACUGAGGUAAGAGG 3'

Table 3. Control and complementary DNA and isoDNA sequences ,HPLC t_R and MALDI-TOF mass

Code No	Sequence	HPLC (t _R) min	Mass (calcd.)	Mass (obsd.)
DNA-1	5' CACCATTGTCACACTCCA ^{3'}	10.58	5363	5364
DNA-2	5' CCTCTTACCTCAGTTACA ^{3'}	12.70	5369	5368
cDNA-1	5' TGGAGTGTGACAATGGTG ^{3'}	10.04	5634	5645
cDNA-2	5' TGTAAGTGGAGGTAAGAGG ^{3'}	10.56	5627	5633
2'DNA-1	5' CACCATTGTCACACTCCA ^{2'}	8.91	5363	5363
2'DNA-2	5' CCTCTTACCTCAGTTACA ^{2'}	8.82	5369	5366

3.3 A comparative study of the thermal stability of modified 2'-5' DNA:RNA duplexes and the modified 3'-5' DNA:DNA, DNA:RNA duplexes by UV melting experiments

UV melting (T_m) experiments were carried out to determine the binding efficiency of the modified ONs with complementary DNA and RNA respectively. The HPLC pure ONs were annealed with the complementary DNA /RNA oligonucleotide. The strand concentration taken was 1 μ M in sodium phosphate buffer 10 mM containing 150 mM NaCl. The UV melting (T_m) was carried out at 260nm wavelength by heating the annealed samples from 10°C to 85°C. The UV chamber was gently purged with a stream of N₂ gas to remove traces of moisture from condensing on the cuvettes.

3.3.1 Thermal stability of 2'-O-allyluridine modified sequences

The 2'-O-allyl uridine modified DNA-1 (sequences 2-6) and DNA-2 (sequences 8-10) exhibited stabilization (Table 4, Figure 5, 6b), when complexed with the complementary RNA as reported in literature,⁹ whereas, the modified DNA:DNA duplexes were destabilised (Figure 4, 6a). The DNA:RNA duplexes of Sequences 5 and 6 with a single and double modification towards the 5' end of the sequence in DNA-1, showed a stabilization for sequence 6 having a consecutive double modification ($\Delta T_m = +0.6^\circ\text{C}$), (Table 4, Figure 5) when compared to the single modification in sequence 5 which had a destabilizing effect ($\Delta T_m = -0.6^\circ\text{C}$).

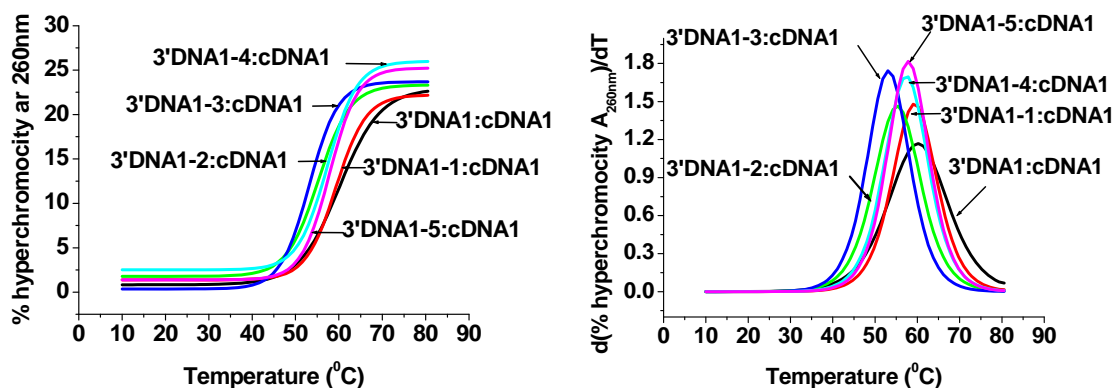


Figure 4. UV-melting plots and corresponding first derivative curves of complexes of sequences 1-6 with complementary cDNA1

Table 4. The UV T_m of the 3'-5'-linked 2'-O-allyluridine modified complexes with complementary DNA and RNA respectively. (The values in parentheses with + or - sign gives ΔT_m , the difference in T_m between the control and modified sequence).

Seq No.	Code No	Name	Sequence	UV T_m °C	
				cDNA1	RNA1
1	3'DNA1	DNA-1	5' CACCATTGTCACACTCCA 3'	60.0	59.0
2	3'DNA1-1	DNA2'allU-1s	5'CACCATTGTCACAC UCCA 3'	59.2 (-0.8)	59.4 (+0.4)
3	3'DNA1-2	DNA2'allU-1d	5'CACCATTG UCACACUCCA 3'	54.9 (-6.1)	59.2 (+0.2)
4	3'DNA1-3	DNA2'allU-1t	5'CACCA UTGUCACACUCCA 3'	53.0 (-7.0)	58.1 (-0.9)
5	3'DNA1-4	DNA2'allU-1S ^{5'}	5'CACCA UTGTCACACTCCA 3'	57.2 (-2.8)	58.4 (-0.6)
6	3'DNA1-5	DNA2'allU-1D ^{5'}	5'CACCA UUGTCACACTCCA 3'	57.6 (-2.4)	59.6 (+0.6)
7	3'DNA2	DNA-2	5' CCTCTTACCTCAGTTACA 3'	54.0	56.0
8	3'DNA2-1	DNA2'allU-2s	5'CCTCTTACCTCAGT UACA 3'	51.8 (-2.2)	57.6 (+1.6)
9	3'DNA2-2	DNA2'allU-2d	5'CCTCTTACC UCAGTUACA 3'	48.6 (-5.4)	57.6 (+1.6)
10	3'DNA2-3	DNA2'allU-2t	5'CCTCT UACCUAGTUACA 3'	46.1 (-7.9)	56.8 (+0.8)

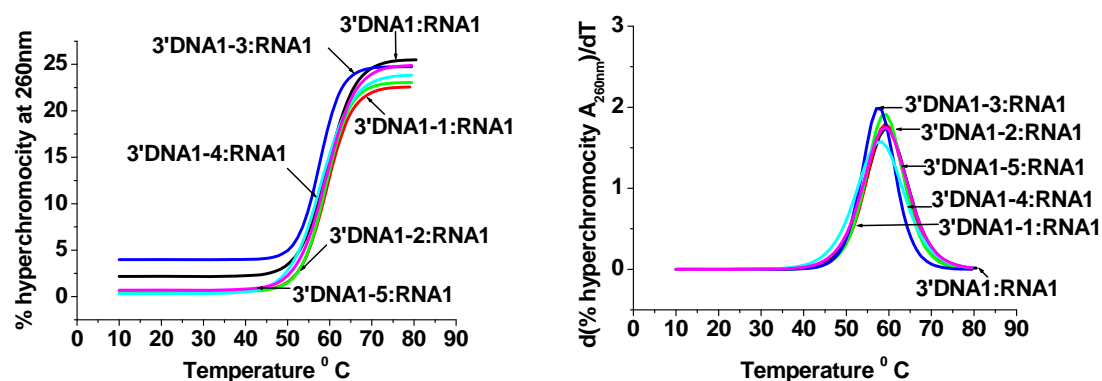


Figure 5. UV-melting plots and corresponding first derivative curves of complexes of sequences 1-6 with complementary RNA1

The consecutive double modification towards the 5' end sequence **6** (3'DNA1-5) also showed a marginally better stabilization ($\Delta T_m = +0.6^\circ\text{C}$) as compared to the double modification in the middle and towards the 3' end in sequence **3** ($\Delta T_m = +0.2$). This is in accordance with the better stabilization obtained for consecutive modifications in the 3'-5' LNA:RNA duplexes due to increased base stacking interactions²⁶ when the nucleobases are axially oriented.

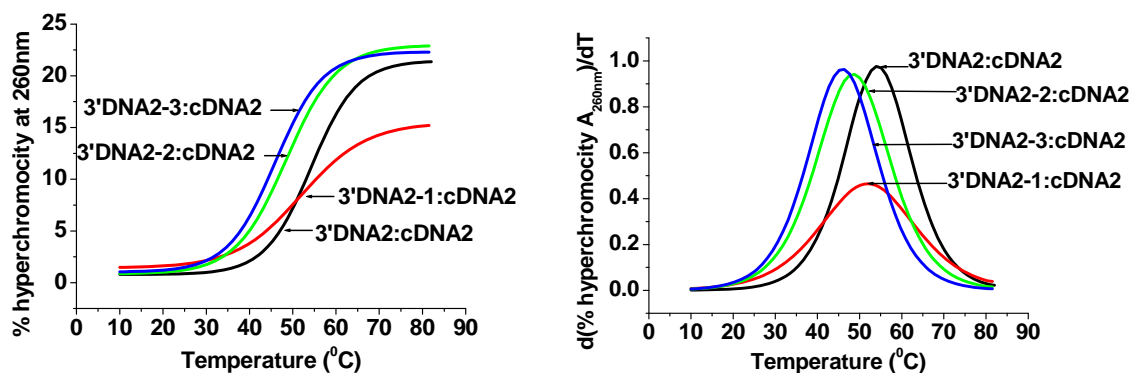


Figure 6a. UV-melting plots and corresponding first derivative curves of complexes of sequences 7-10 with complementary DNA2.

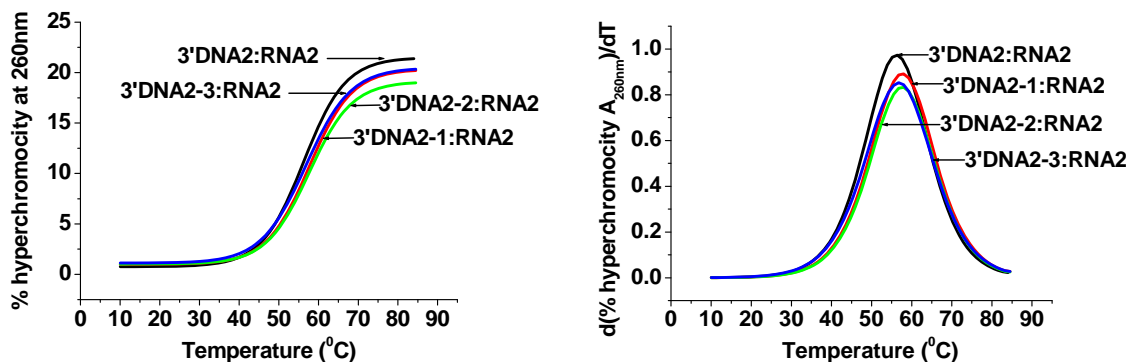


Figure 6b. UV-melting plots and corresponding first derivative curves of complexes of sequences 7-10 with complementary RNA2

3.3.2 Thermal stability of 2'-O-allylcytidine modified sequences

The 2'-O-allylcytidine-incorporated 3'-5' linked DNA-1 and DNA-2 oligomers **11-16** (Table 5) showed a trend similar to the 2'-O-allyl uridine oligomers of destabilization

when forming DNA:DNA duplexes ($\Delta T_m = -0.8$ to -4.8°C ; Figures 7a, 8a). The DNA:RNA duplexes containing 2'-O-allylcytidine resulted in a fairly good stabilization for single (Sequences **11**, **14**), double (Sequences **12**, **15**) and triple (Sequences **13**, **16**) modifications, especially the DNA-2:RNA complexes (sequences **14**, **15**, **16**; $\Delta T_m = +2.2$, $+1.4$ and $+2.3^\circ\text{C}$ respectively; Figure 8b) Thus, the 2'-O-allylcytidine modifications resulted in a better stabilization for the DNA:RNA duplexes as compared to the 2'-O-allyluridine containing DNA:RNA duplexes.

Table 5. The UV T_m of the 3'-5'-linked 2'-O-allylcytidine modified complexes with complementary DNA and RNA respectively. (The values in parentheses with + or - sign gives ΔT_m , the difference in T_m between the control and modified sequence).

Seq No	Code No	Name	Sequence	UV T_m °C	
				DNA	RNA
1	3'DNA1	DNA-1	5' CACCATTGTCACACTCCA 3'	60.0	59.0
11	3'DNA1-6	DNA 2'allC-1s	5' CACCATTGTCACACTCCA 3'	59.2 (-0.8)	60.6 (+1.6)
12	3'DNA1-7	DNA 2'allC-1d	5' CACCATTGTCACACTCCA 3'	55.9 (-4.1)	60.1 (+1.1)
13	3'DNA1-8	DNA 2'allC-1t	5' CACCATTGTCACACTCCA 3'	53.9 (-6.1)	59.9 (+0.9)
2	3'DNA2	DNA-2	5' CCTCTTACCTCAGTTACA 3'	54.0	56.0
14	3'DNA2-4	DNA 2'allC-2s	5' CCTCTTACCTCAGTTACA 3'	51.8 (-2.2)	58.2 (+2.2)
15	3'DNA2-5	DNA 2'allC-2d	5' CCTCTTACCTCAGTTACA 3'	49.2 (-4.8)	57.4 (+1.4)
16	3'DNA2-6	DNA 2'allC-2t	5' CCTCTTACCTCAGTTACA 3'	-	58.3 (+2.3)

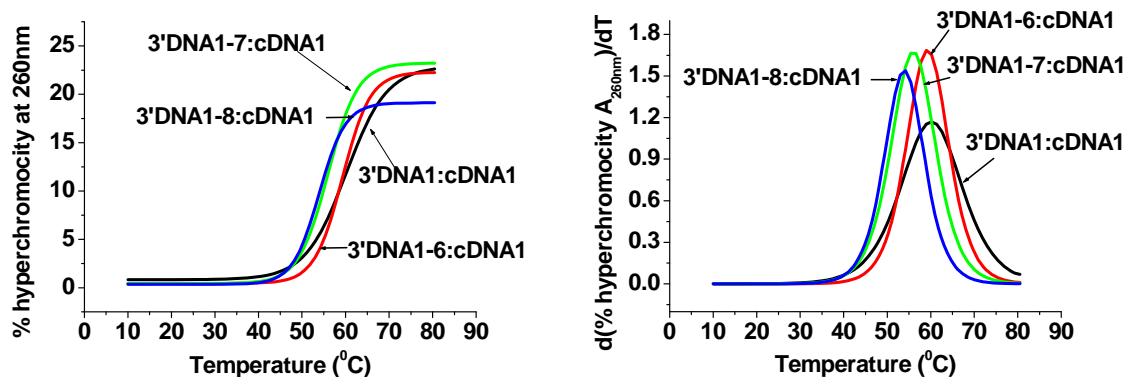


Figure 7a. UV-melting plots and corresponding first derivative curves of complexes of sequences 11-13 with complementary DNA1.

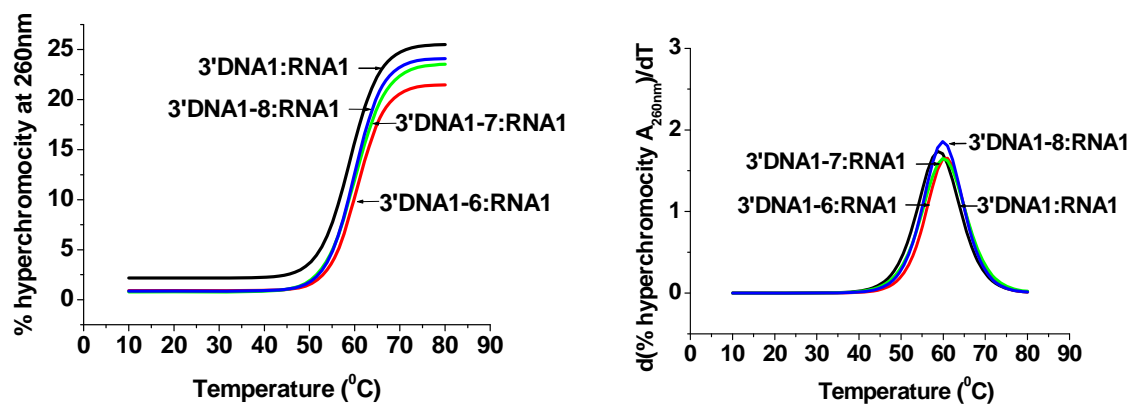


Figure 7b. UV-melting plots and corresponding first derivative curves of complexes of sequences 11-13 with complementary RNA1

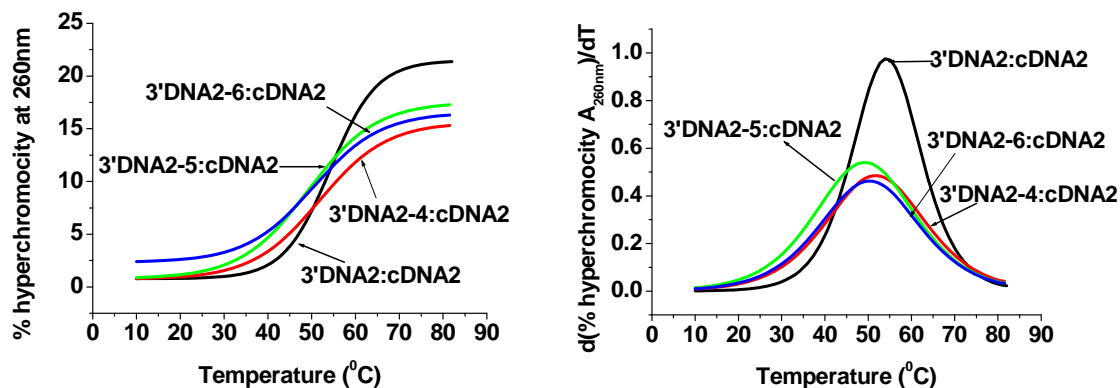


Figure 8a. UV-melting plots and corresponding first derivative curves of complexes of sequences 14-16 with complementary DNA2.

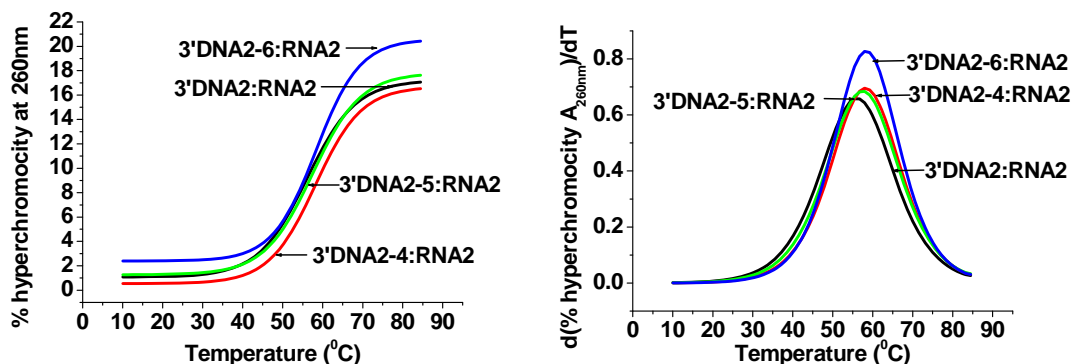


Figure 8b. UV-melting plots and corresponding first derivative curves of complexes of sequences 14-16 with complementary RNA2

3.3.3 Thermal stability of 3'-O-allyluridine modified sequences

The 2'-5' *iso*DNA oligonucleotides do not show complex formation with 3'-5' DNA as reported by Damha *et al.*²⁷ Therefore, the thermal stability of only *iso*DNA:RNA duplexes was determined (Table 6). Introduction of 3'-O-allyluridine unit in the 2'-5'-linked *iso*DNA oligonucleotides resulted in stabilization of all the 2'DNA-1 oligonucleotides **18**, **19** and **20** with increasing modifications ($\Delta T_m = +0.5$, $+1.8$ and $+1.4^\circ\text{C}$ respectively; Figure 9). Surprisingly, however, all the 2'DNA-2 modified sequences **22**, **23** and **24** resulted in destabilization ($\Delta T_m = -1.1$, -1.7 and -2.3°C respectively; Figure 10)

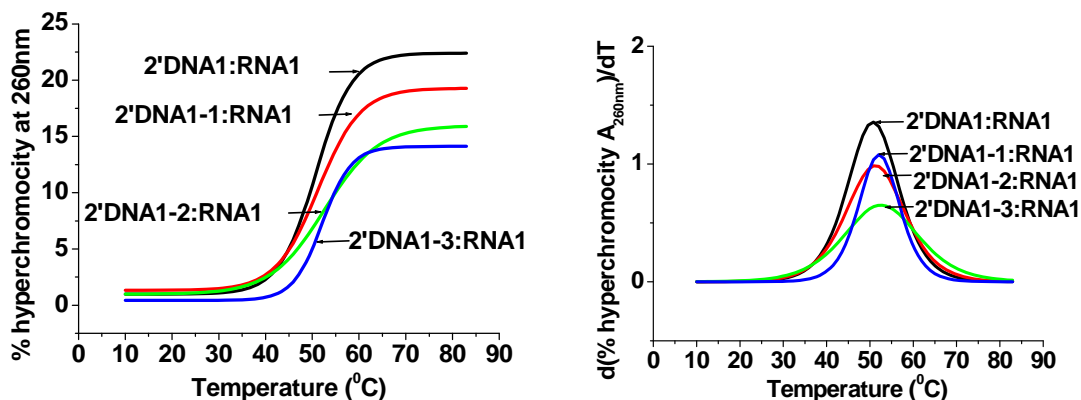


Figure 9. UV-melting plots and corresponding first derivative curves of complexes of sequences 17-20 with complementary RNA1

Table 6. The UV T_m values of the 2'-5'-linked 2'-O-allyluridine modified complexes with complementary RNA. The 2'-5'-linked *isoDNA* did not complex with DNA as reported in literature.²⁷ (The values in parentheses with + or - sign gives ΔT_m , the difference in T_m between the control and modified sequence).

Seq No	Code No	Name	Sequence	UV T_m °C	
				DNA	RNA
17	2'DNA1	2'DNA-1	5'CACCATTGTCACACTCCA ^{2'}	ND	50.5
18	2'DNA1-1	2'DNA3'allU-1s	5'CACCATTGTCACACUCCA ^{2'}	ND	51.0 (+0.5)
19	2'DNA1-2	2'DNA3'allU-1d	5'CACCATTGUCACACUCCA ^{2'}	ND	52.3 (+1.8)
20	2'DNA1-3	2'DNA3'allU-1t	5'CACCAUTGUCACACUCCA ^{2'}	ND	51.9 (+1.4)
21	2'DNA2	2'DNA-2	5'CCTCTTACCTCAGTTACA ^{2'}	ND	46.0
22	2'DNA2-1	2'DNA3'allU-2s	5'CCTCTTACCTCAGTUACA ^{2'}	ND	44.9 (-1.1)
23	2'DNA2-2	2'DNA3'allU-2d	5'CCTCTTACCUCAGTUACA ^{2'}	ND	44.3 (-1.7)
24	2'DNA2-3	2'DNA3'allU-2t	5'CCTCTUACCUCAGTUACA ^{2'}	ND	43.7 (-2.3)

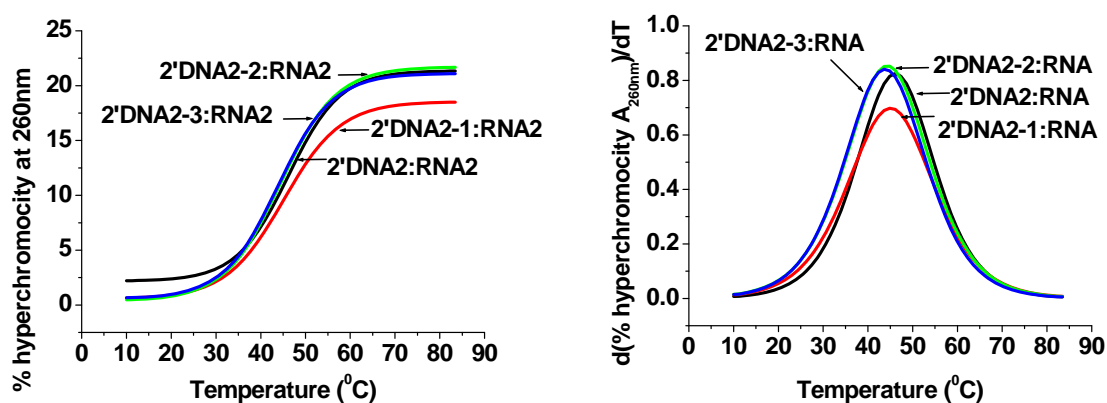


Figure 10. UV-melting plots and corresponding first derivative curves of complexes of sequences 21-24 with complementary RNA2

3.3.4 Thermal stability of 3'-O-allylcytidine modified sequences

In the case of 3'-O-allylcytidine containing 2'DNA-1 modified oligonucleotides (Table 7, Figure11), only the sequence **25** with single modification stabilized the isoDNA:RNA duplex ($\Delta T_m = +0.8^\circ\text{C}$). Sequences **26** and **27** caused considerable destabilization of the resulting complexes ($\Delta T_m = -2.4$ and -8.1°C respectively). On the other hand, the 2'DNA-2 modifications containing 3'-O-allylcytidine (Figure12) resulted in stabilization of the single and double modified sequences **28** ($\Delta T_m = +1.6^\circ\text{C}$) and **29** ($\Delta T_m = +1.3^\circ\text{C}$). Triple modification in sequence **30** again resulted in some destabilization ($\Delta T_m = -1.4^\circ\text{C}$).

Table 7. The UV T_m values of the 2'-5'-linked 2'-O-allyluridine modified complexes with complementary RNA . (The bracketed values with + or - sign gives ΔT_m , the difference in T_m between the control and modified sequence).

Seq No	Sr No	Code No	Sequence	UV T_m °C	
				DNA	RNA
17	2'DNA1	2'DNA-1	5'CACCATTGTCACACTCCA ^{2'}	ND	50.5
25	2'DNA1-4	2'DNA3'allC-1s	5'CACCATTGTCACACTCCA ^{2'}	ND	51.3 (+0.8)
26	2'DNA1-5	2'DNA3'allC-1d	5'CACCATTGTCACTCCA ^{2'}	ND	48.1 (-2.4)
27	2'DNA1-6	2'DNA3'allC-1t	5'CACTTGTCACTCCA ^{2'}	ND	42.4 (-8.1)
21	2'DNA2	2'DNA-2	5'CCTCTTACCTCAGTTACA ^{2'}	ND	46.0
28	2'DNA2-4	2'DNA3'allC-2s	5'CCTCTTACCTCAGTTACA ^{2'}	ND	47.6 (+1.6)
29	2'DNA2-5	2'DNA3'allC-2d	5'CCTCTTACCTCAGTTACA ^{2'}	ND	47.3 (+1.3)
30	2'DNA2-6	2'DNA3'allC-2t	5'CCTCTTACCTCAGTTACA ^{2'}	ND	44.6 (-1.4)

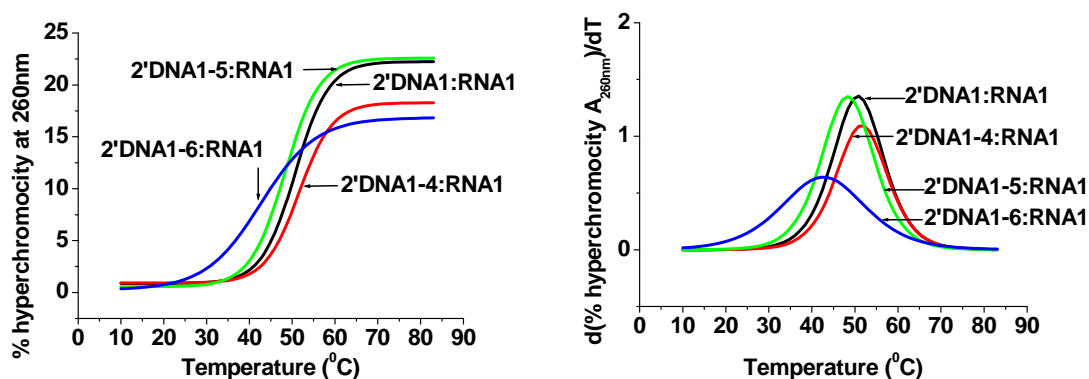


Figure 11. UV-melting plots and corresponding first derivative curves of complexes of sequences 25-27 with complementary RNA1

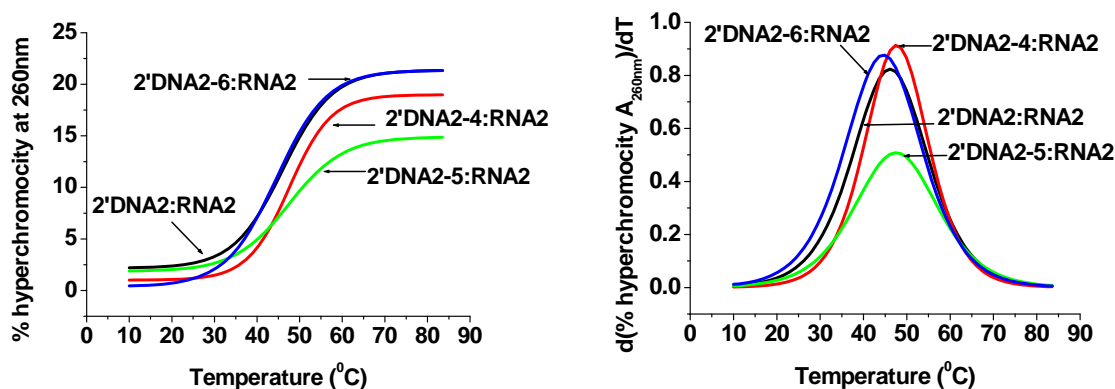


Figure 12. UV-melting plots and corresponding first derivative curves of complexes of sequences 28-30 with complementary RNA2

The pattern of stabilization and destabilization observed for the modified *iso*DNA oligonucleotides involving introduction of the 3'-*O*-allyluridine or 3'-*O*-allylcytidine modification in these sequences seems to be sequence dependent. It is unclear at this point to comment upon the nucleobase and sequence dependence of the modifications and more work would be necessary to understand the results in the context of sequence, nucleobase and site of modification.

3.3.5 Summary

- Synthesis of 2'-*O*-allyluridine and 3'-*O*-allyluridine phosphoramidite monomers was accomplished and the conversion of the 2'-*O*-allyluridine and 3'-*O*-allyluridine derivatives into the respective 2'-*O*-allyl and 3'-*O*-allyl cytidine phosphoramidite monomers was achieved.

- 2'-O-allyl monomers of both uridine and cytidine were introduced as a single, double and triple modifications in the 3'-5'-linked DNA oligomers and the 3'-O-allyluridine and cytidine monomers were introduced similarly as a single, double and triple modifications into 2'-5'-linked *isoDNA* oligomers.
- The 2'-O-allyl uridine oligomers exhibited stabilization when complexed with the complementary RNA. Better still, the 2'-O-allylcytidine modification in these sequences resulted in a higher stabilization for the DNA:RNA duplexes as compared to the 2'-O-allyluridine containing DNA:RNA duplexes.
- Stabilization and destabilization observed for the modified *isoDNA* oligonucleotides implies that the effects observed upon the introduction of 3'-O-allyluridine or 3'-O-allylcytidine modification in these sequences may be sequence-specific. The sequences with 3'-O-allyluridine modifications showed stability in 2'DNA-1, while the 3'-O-allylcytidine modifications caused destabilization and *vice versa*.

3.3.6 Conclusions

- Introduction of the 2'-O-allyluridine modifications in 3'-5'DNA, stabilize the resulting DNA:RNA complexes. 2'-O-allylcytidine modifications in 3'-5'DNA render even better stability to the resulting DNA:RNA duplexes.
- Alkylation at the 3' position of uridine did not result in a uniform stabilization in the 2'-5'-linked *isoDNA*:RNA duplexes of 3'-O-allyluridine/cytidine as was seen in the 3'-5'DNA:RNA duplexes containing 2'-O-allyluridine /cytidine modifications.
- Both 3'-O-allyluridine and 3'-O-allylcytidine modifications introduced in the 2'-5'-linked *isoDNA* showed a variation in stability in the *isoDNA*:RNA duplexes.
- However, both 3'-O-allyluridine and 3'-O-allylcytidine derivatives may be successfully used in gapmer designs of ASOs.

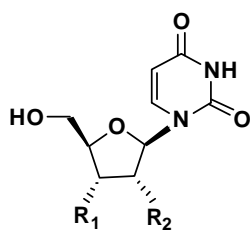
3.4 Experimental

General remarks: All the reagents were purchased from Sigma-Aldrich and used without further purification. DMF, ACN, were dried over P₂O₅ and CaH₂ respectively and stored by adding 4 Å molecular sieves. Pyridine, TEA were dried over KOH and stored on KOH. THF was passed over basic alumina and dried by distillation over sodium metal. Reactions were monitored by TLC. TLCs were run in either Petroleum ether with appropriate quantity

of EtOAc or DCM with an appropriate quantity of MeOH for most of the compounds. TLC plates were visualized with UV light and iodine spray and/or by spraying perchloric acid solution and heating. Usual reaction work up involved sequential washing of the organic extract with water and brine followed by drying over anhydrous Na₂SO₄ and evaporation of the solvent under vacuum. Column chromatographic separations were performed using silica gel 60-120 mesh (Merck) or 200- 400 mesh (Merck) and using the solvent systems EtOAc/Petroleum ether or MeOH/DCM. TLC was run using pre-coated silica gel GF254 sheets (Merck 5554).

¹H and ¹³C NMR spectra were obtained using Bruker AC-200, AC-400 and AC-500 NMR spectrometers. The chemical shifts (δ/ppm) are referred to internal TMS/DMSO-d₆ for ¹H and chloroform-d/DMSO-d₆ for ¹³C NMR. ¹H NMR data are reported in the order of chemical shift, multiplicity (s, singlet; d, doublet; t, triplet; br, broad; br s, broad singlet; m, multiplet and/ or multiple resonance), number of protons. Mass spectra were recorded on APQSTAR spectrometer, LC-MS on a Finnigan-Matt instrument. DNA oligomers were synthesized on CPG solid support using Bioautomation MerMade 4 synthesizer. The RNA oligonucleotides were obtained commercially (Sigma-Aldrich). RP-HPLC was carried out on a C18 column using either a Varian system (Analytical semi-preparative system consisting of Varian Prostar 210 binary solvent delivery system, a Dynamax UV-D2 variable wavelength detector and Star chromatography software) or a Waters system (Waters Delta 600e quaternary solvent delivery system with 2998 photodiode array detector and Empower2 chromatography software). MALDI-TOF spectra were recorded on a Voyager-De-STR (Applied Biosystems) MALDI-TOF instrument or AB Sciex TOF/TOF™ Series Explorer™ 72085 instrument and the matrix used for analysis was THAP (2', 4', 6'-trihydroxyacetophenone). UV experiments were performed on a Varian Cary 300 UV-VIS spectrophotometer fitted with a Peltier-controlled temperature programmer.

3.4.1 Synthesis of compounds/monomers

2'/3'-O-allyl uridine (24+25)

24 R1 = OH, R2 = O-allyl

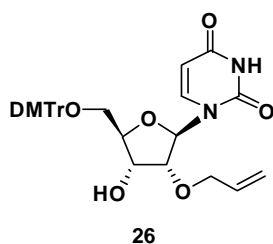
25 R1 = O-allyl, R2 = OH

Uridine, **15** (2.44 g, 10 mmol) was dissolved in DMF (20 mL) and treated with allyl bromide (2.1 mL, 25 mmol) in presence of DBTO (2.8 g, 12 mmol) and TBAB (2.4 g, 11 mmol). The reaction mixture was heated at 60°C for 5-6 hrs. The resulting clear solution was concentrated at reduced pressure to remove DMF. The crude product was purified on a silica gel column using CH₂Cl₂ with increasing amounts of MeOH to obtain a mixture of 2'/3'-O-allyl uridine **24+25** in the ratio of 60 : 40 as estimated from ¹H NMR of the mixture. Yield 1.90 g, 67%.

Mass (ESI): m/z 284.1008, found 283.05 (M-1).

2'-O-allyl- 5'-O-(4, 4'-dimethoxytrityl)-uridine (26) and**3'-O-allyl- 5'-O-(4, 4'-dimethoxytrityl)-uridine (27)**

The mixture, 2'/3'-O-allyl uridine, **24+25** (1.9 g, 6.69 mmol) was coevaporated with dry pyridine twice (2 x 5 mL), then redissolved in 20 mL dry pyridine. DMTr-Cl (2.26 g, 6.69 mmol) was added in small portions over a period of 2 hrs. Reaction completion was checked by TLC run in 5% MeOH in CH₂Cl₂. MeOH (1.0 mL) was added and the solvents were removed in vacuo. Aq. NaHCO₃ solution was added and the product was extracted with CH₂Cl₂. The organic layer was washed with water, dried over Na₂SO₄ and evaporated to get foam. This was chromatographed on a silica gel (100-200 mesh) column using CH₂Cl₂ (containing 0.5% pyridine) with increasing amounts of MeOH to obtain compound **26** (1.82 g, 65%). On increasing polarity compound **27** (0.980 g, 35%) was eluted from the column.

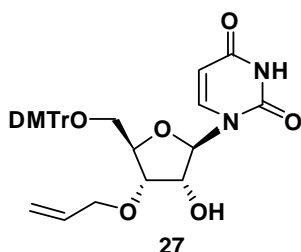
2'-O-allyl- 5'-O-(4, 4'-dimethoxytrityl)-uridine (26):

26

¹H NMR (200 MHz, CDCl₃): δ 3.55 (m, 2H, H5' & H5''), 3.80 (s, 6H, 2 X OCH₃), 3.98-4.07 (m, 2H, -OCH₂ allyl), 4.20-4.29 (ddd, *J* = 1.2, 6.2, 12.8 Hz, H4'), 4.40-4.49 (m, 2H, H3' & H2'), 5.24-5.38 (m, 3H, H5 & =CH₂), 5.88 (m, 1H, =CH), 5.97 (d, *J*

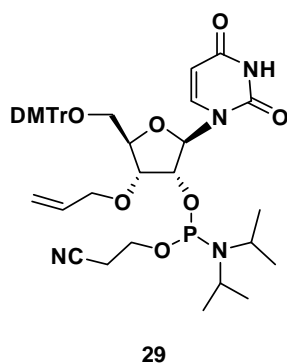
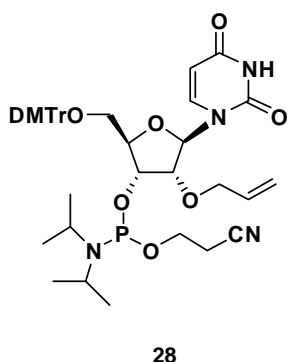
=1.7 Hz, H1'), 6.62-6.87 (m, 4H, Ar), 7.26-7.40 (m, 9H, Ar), 8.02 (d, 1H, J = 8.2 Hz, H6), 8.80 (bs, NH). ^{13}C NMR (50 MHz, CDCl_3): δ 55.2, 61.2, 68.4, 71.3, 81.3, 83.3, 86.9, 87.3, 102.0, 113.2, 118.4, 123.7, 127.0, 127.9, 128.0, 130.0, 130.1, 133.3, 134.9, 135.2, 136.0, 139.9, 144.2, 149.5, 150.2, 158.6, 163.6. **Mass** (ESI): m/z 586.2315, found 609.16 ($\text{M}+\text{Na}^+$).

3'-O-allyl- 5'-O-(4, 4'-dimethoxytrityl)-uridine (27):



^1H NMR (200 MHz, CDCl_3): δ 3.36 & 3.57 (2 dd, 1H each, J = 2.15, 11.37 Hz, H5' & H5''), 3.80 (s, 6H, 2 X OCH_3), 4.07 (d, 2H, $-\text{OCH}_2$ allyl), 4.17-4.32 (m, 3H, H4', H3', H2'), 5.20-5.32 (m, 2H, $=\text{CH}_2$ allyl), 5.38 (d, 1H, J = 8.0 Hz H5), 5.76-5.93 (m, 1H, $=\text{CH}$ allyl), 5.95 (d, J = 3.9 Hz, H1'), 6.82-6.87 (m, 4H, Ar), 7.24-7.39 (m, 9H, Ar), 7.84 (d, 1H, J = 8.0 Hz, H6). ^{13}C NMR (50 MHz, CDCl_3): δ 55.2, 62.0, 71.5, 73.9, 76.0, 81.4, 86.9, 89.7, 102.4, 113.2, 118.5, 123.7, 127.1, 127.9, 130.0, 130.1, 133.5, 135.0, 135.1, 136.0, 140.0, 144.1, 149.6, 150.7, 158.6, 163.3. **Mass** (ESI): m/z 586.2315, found 609.14 ($\text{M}+\text{Na}^+$).

2'-O-allyl- 3'-O-[2-cyanoethoxy(diisopropylamino)phosphino]-5'-O-(4, 4'-dimethoxytrityl)-uridine (28) and 3'-O-allyl- 2'-O-[2-cyanoethoxy (diisopropylamino) phosphino]-5'-O-(4, 4'-dimethoxytrityl)-uridine (29)



Compound **26/27** (0.200 g, 0.340 mmol) was coevaporated with dry CH_2Cl_2 , then dissolved in 2.5 mL of dry CH_2Cl_2 . Diisopropylethylamine (DIPEA) (0.320 mL, 1.70 mmol) was added followed by *N,N*-diisopropylamino-2-cyanoethylphosphinochloridite (0.245 mL, 1.02 mmol) at 0°C . The reaction mixture was stirred under argon atmosphere at room temperature for 3 hrs. TLC showed product formed and absence of starting material. The reaction was diluted with CH_2Cl_2 , washed with NaHCO_3 and water, dried over Na_2SO_4 followed by solvent removal.

The crude product was purified on a silica gel column using 1:1 mixture of CH₂Cl₂: EtOAc and 1% triethylamine to afford compound **28** (0.162 g, 56.44%) / **29** (0.179 g, 62.68%).

2'-O-allyl-3'-O-[2-cyanoethoxy(diisopropylamino)phosphino]-5'-O-(4,4'-dimethoxytrityl)-uridine (28) :

³¹P NMR (50 MHz, CDCl₃): δ 150.14, 150.20.

Mass (ESI): m/z 786.3394, found 809.47 (M+Na⁺).

3'-O-allyl-2'-O-[2-cyanoethoxy(diisopropylamino)phosphino]-5'-O-(4,4'-dimethoxytrityl)-uridine (29):

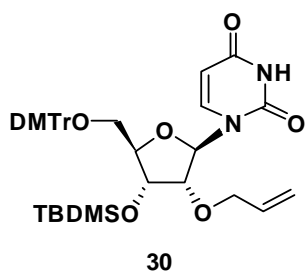
³¹P NMR (50 MHz, CDCl₃): δ 150.33, 151.67.

Mass (ESI): m/z 786.3394, found 809.29 (M+Na⁺).

2'-O-allyl-5'-O-(4, 4'-dimethoxytrityl)-3'-O-(tert-butyldimethyl silyl)-uridine (30) and 3'-O-allyl-5'-O-(4, 4'-dimethoxytrityl)-2'-O-(tert-butyldimethyl silyl)-uridine (31)

Compound 26/27 (0.2 g, 0.341 mmol) was dissolved in dry DMF (2.0 mL). To this suspension imidazole (0.058 g, 0.853 mmol) was added followed by TBDMS-Cl (0.154 g, 1.02 mmol). The reaction was stirred at RT for 2 hr. TLC showed completion of reaction. DMF was removed under reduced pressure. The crude compound was taken in CH₂Cl₂, washed with NaHCO₃ and water, dried over Na₂SO₄ followed by solvent removal. The gummy solid was purified on a 60-120 mesh silica gel column using gradient system of CH₂Cl₂, MeOH containing 0.5% pyridine to get pure compound **30** (0.167 g, 70%)/ **31** (0.172 g, 72.5 %).

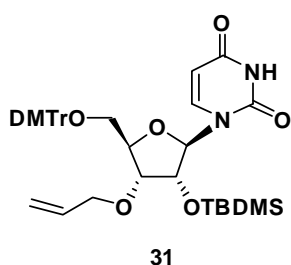
2'-O-allyl-5'-O-(4, 4'-dimethoxytrityl)-3'-O-(tert-butyldimethyl silyl)-uridine (30):



¹H NMR (200 MHz, CDCl₃): δ -0.01 and 0.10 (2 x s, 3H each, CH₃), 0.85 (s, 9H, CH₃), 3.38-3.44 & 3.72-3.78 (2 dd, 1H each, *J* = 1.52, 10.9 Hz, H5' & H5''), 3.84-3.86 (singlet merged with multiplet, 7H), 4.17-4.26 (m, 2H), 4.37-4.46 (m, 2H), 5.21-5.42 (m, 3H, H5 & =CH₂ allyl), 5.92 (m, 1H, =CH allyl), 6.03 (d, *J* = 1.3 Hz, H1'), 6.87-6.91 (m, 4H, Ar), 7.27-7.43 (m, 9H, Ar), 8.20 (d, 1H, *J* = 8.2 Hz, H6), 10.1 (bs, 1H, NH). ¹³C NMR (50 MHz, CDCl₃): δ -5.1, -4.6,

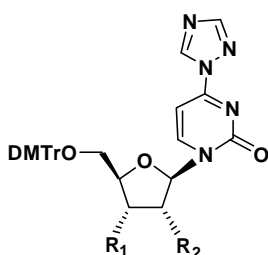
17.9, 25.4, 55.1, 60.5, 69.1, 71.0, 81.6, 82.6, 86.8, 88.0, 101.9, 113.1, 117.5, 127.1, 127.8, 128.2, 130.1, 133.9, 134.8, 134.9, 140.1, 143.9, 150.2, 158.6, 163.9. **Mass** (ESI): m/z 700.3180, found 723.41 ($M+Na^+$).

3'-O-allyl-5'-O-(4, 4'-dimethoxytrityl)-2'-O-(tert-butyldimethyl silyl)-uridine (31):



¹H NMR (200 MHz, $CDCl_3$): δ 0.14, 0.20 (2 x s, 3H each, CH_3), 0.91 (s, 9H, CH_3), 3.42, 3.60 (2 dd, 1H each, $J = 1.6, 11.24$ Hz, $H5'$ & $H5''$), 3.80 (s, 6H, 2 X OCH_3), 3.89 (m, 1H), 4.07-4.18 (m, 2H), 4.24-4.35 (m, 2H), 5.17-5.32 (m, 3H, $H5$ & $=CH_2$ allyl), 5.80 (d, $J = 1.5$ Hz, $H1'$) merged with 5.75-5.94 (m, 1H, $=CH$ allyl), 6.82-6.86 (m, 4H, Ar), 7.30-7.40 (m, 9H, Ar), 8.14 (d, 1H, $J = 8.2$ Hz, H6), 9.51 (bs, 1H, NH). **¹³C NMR** (50 MHz, $CDCl_3$): δ -5.2, -4.6, 18.0, 25.5, 55.2, 61.0, 71.4, 74.4, 75.4, 80.8, 86.9, 90.4, 101.7, 113.2, 117.7, 127.1, 127.9, 128.0, 130.0, 133.9, 134.9, 135.1, 140.2, 144.2, 150.1, 158.6, 163.6. **Mass** (ESI): m/z 700.3180, found 723.42 ($M+Na^+$).

2'-O-allyl-5'-O-(4, 4'-dimethoxytrityl)-3'-O-(tert-butyldimethyl silyl)- 4-(1,2,4-triazol-1-yl)uridine (32)/ 3'-O-allyl-5'-O-(4, 4'-dimethoxytrityl)-2'-O-(tert-butyldimethyl silyl)- 4-(1,2,4-triazol-1-yl) uridine (33)



32 $R_1 = TBDMS, R_2 = O\text{-allyl}$
33 $R_1 = O\text{-allyl}, R_2 = TBDMS$

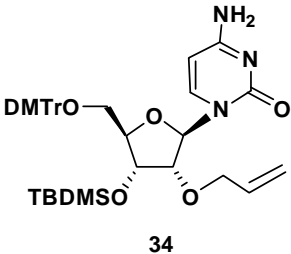
In a RB flask (having a side arm with a sinter, a stopper and B19 joint for vacuum filtration), 1,2,4-triazole (0.288 g, 4.17 mmol) was suspended in dry CH_3CN (2.5 mL). After stirring for 10 mins under argon atmosphere, the flask was cooled to $0^\circ C$, $POCl_3$ (0.110 mL, 1.18 mmol) was added dropwise. The reaction mixture was stirred at $0^\circ C$ for 20mins. Triethylamine (TEA) (1.2 mL, 8.6 mmol) was added dropwise and stirring at $0^\circ C$ was continued for half an hour. The triazolide complex formed was filtered into a flask containing the substrate **30**, (0.167gm, 0.238mmol) solution in dry CH_3CN 1.0 mL, TEA 0.5 mL. The reaction mixture was stirred for 3 hrs at RT. TLC showed product spot and no starting present. TEA 0.5ml was added followed by 1.0 ml of ice water. The reaction mixture was concentrated to give a brown solid. The crude compound was taken in CH_2Cl_2 , washed with $NaHCO_3$ and water, dried

over Na₂SO₄ followed by solvent removal to give brown foam. This crude compound **32/33** was used for the next reaction without further purification.

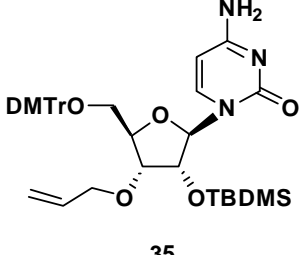
2'-O-allyl-5'-O-(4, 4'-dimethoxytrityl)-3'-O-(tert-butyldimethyl silyl)-cytidine (34)/ and 3'-O-allyl-5'-O-(4, 4'-dimethoxytrityl)-2'-O-(tert-butyldimethyl silyl)-cytidine (35)

The crude compound **32/33** was dissolved in 2 mL dioxane to which 2.0 mL aq. Ammonia solution was added and stirred for 2 hrs at RT. TLC done showed product spot and no starting present. The reaction mixture was concentrated to remove ammonia and dioxane. The crude product was purified on a silica gel column to yield the pure product **34** (0.106 g, 68.21%) / **35** (0.090 g, 62.38%).

2'-O-allyl-5'-O-(4, 4'-dimethoxytrityl)-3'-O-(tert-butyldimethyl silyl)-cytidine (34):

 **34** ¹H NMR (200 MHz, CDCl₃): δ -0.09 and 0.02 (2 x s, 3H each, CH₃), 0.77 (s, 9H, CH₃), 3.29 (dd, 1H, *J* = 1.6, 10.7 Hz, H5'), 3.70-3.83 (8H, singlet for 2 x OCH₃ & multiplet for 2H), 4.15-4.31 (m, 2H), 4.38 (dd, 1H, *J* = 4.4, 9.10 Hz), 4.45 (dd, *J* = 5.17, 12.8 Hz), 5.12-5.39 (m, 3H, H5 & =CH₂ allyl), 5.83 (m, 2H, =CH allyl & H1'), 6.82-6.86 (m, 4H, Ar), 7.24-7.37 (m, 9H, Ar), 8.30 (d, 1H, *J* = 7.5 Hz, H6). ¹³C NMR (50 MHz, CDCl₃): δ -5.1, -4.6, 17.9, 25.5, 55.2, 60.4, 68.7, 70.9, 81.9, 86.7, 88.9, 94.0, 113.0, 117.1, 127.0, 127.8, 128.3, 130.2, 134.3, 135.1, 135.2, 141.4, 144.1, 155.6, 158.6, 165.8. **Mass** (ESI): *m/z* 699.3340, found 722.49 (M+Na⁺).

3'-O-allyl-5'-O-(4, 4'-dimethoxytrityl)-2'-O-(tert-butyldimethyl silyl)-cytidine (35):

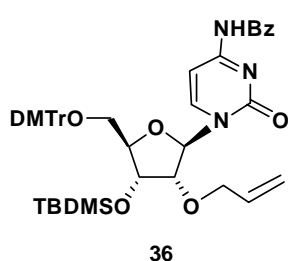
 **35** ¹H NMR (200 MHz, CDCl₃): δ 0.13 and 0.23 (2 x s, 3H each, CH₃), 0.90 (s, 9H, CH₃), 3.38, 3.61 (2 x dd, 1H each, *J* = 1.7, 10.9 Hz, 5' & H5''), 3.78 (s, 6H, 2 X OCH₃), 3.89 (m, 1H), 4.03-4.10 (m, 2H), 4.20-4.36 (m, 2H), 5.13-5.26 (m, 2H, =CH₂ allyl), 5.30 (d, 1H, *J* = 7.45 Hz, H5), 5.71-5.91 (m, 2H, =CH allyl & H1'), 6.82-6.86 (m, 4H, Ar), 7.22-7.43 (m, 9H, Ar), 8.22 (d, 1H, *J* = 7.46 Hz, H6). ¹³C NMR (50MHz, CDCl₃): δ -5.3, -4.4, 18.0, 25.6, 55.1, 60.8, 71.1, 73.8, 75.0, 80.1, 86.6, 91.5, 93.6,

113.1, 117.5, 126.9, 127.8, 128.1, 130.1, 134.0, 135.3, 135.4, 141.4, 144.4, 155.6, 158.5, 165.8. **Mass** (ESI): m/z 699.3340, found 722.28 ($M+Na^+$).

N⁴-Benzoyl-2'-O-allyl-5'-O-(4, 4'-dimethoxytrityl)-3'-O-(tert-butyldimethyl silyl)-cytidine (36) and N⁴-Benzoyl-3'-O-allyl-5'-O-(4, 4'-dimethoxytrityl)-2'-O-(tert-butyldimethyl silyl)-cytidine (37)

Compound **34/35** (0.200 g, 0.286 mmol) was dissolved in 2.0 mL dry pyridine. Benzoyl chloride (0.100 mL, 0.858 mmol) was added and the reaction was stirred for 1hr. TLC showed completion of reaction. Reaction mixture was quenched with ice, extracted with CH_2Cl_2 , washed with $NaHCO_3$ and water, dried over Na_2SO_4 followed by solvent removal to give crude product which was column purified to give pure compound **36** (0.209 g, 91.26%)/ **37** (0.180 g, 78.65%).

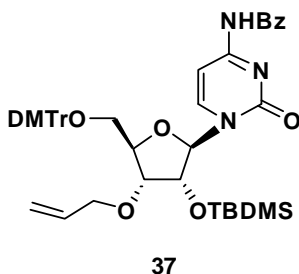
N⁴-Benzoyl-2'-O-allyl-5'-O-(4, 4'-dimethoxytrityl)-3'-O-(tert-butyldimethyl silyl)-cytidine (36):



¹H NMR (200 MHz, $CDCl_3$): δ -0.07 and 0.04 (2 x s, 3H each, CH_3), 0.79 (s, 9H, CH_3), 3.39-3.46 (dd, 1H, $J = 1.5, 10.9$ Hz, $H5'$), 3.79 (m, 1H, merged with 3.84, $H5''$), 3.84 (6H, singlet for 2 x OCH_3), 3.92 (d, 1H, $J = 4.42$ Hz), 4.25-4.44 (m, 3H), 4.60 (m, 1H), 5.16-5.33 (dd, 1H, $J = 1.5$ and 10.36 Hz), 5.34-5.44 (dd, 1H, $J = 1.6, 17.06$ Hz), 5.87-6.04 (m, 1H, =CH) 6.06 (s, 1H, $H1'$), 6.87 (m, 4H, Ar), 7.30-7.58 (m, 1H, Ar and $H5$), 8.71 (m, 2H, Ar), 8.87 (d, 1H, $J = 7.8$ Hz, $H6$). **¹³C NMR** (50 MHz, $CDCl_3$): δ -5.1, -4.6, 17.9, 25.5, 55.1, 60.0, 68.4, 71.1, 81.7, 82.2, 87.0, 89.3, 97.0, 113.2, 117.2, 127.2, 127.9, 128.2, 128.5, 130.0, 130.1, 132.8, 133.0, 133.2, 134.1, 143.5, 145.5, 154.4, 158.7, 163.4, 167.1. **Mass** (ESI): m/z 803.3602, found 826.40 ($M+Na^+$).

N⁴-Benzoyl-3'-O-allyl-5'-O-(4, 4'-dimethoxytrityl)-2'-O-(tert-butyldimethyl silyl)-cytidine (37):

¹H NMR (200 MHz, $CDCl_3$): δ 0.18 and 0.30 (2 x s, 3H each, CH_3), 0.92 (s, 9H, CH_3), 3.47 and 3.66 (2 x dd, 1H each, $J = 2.02, 11.37$ Hz, $H5'$ & $H5''$), 3.83 (s, 6H, 2 x OCH_3), 3.89 (m, 1H), 4.04-4.14 (m, 2H), 4.33-4.43 (m, 2H), 5.20 (m, 2H), 5.73-5.92 (m, 1H, allyl

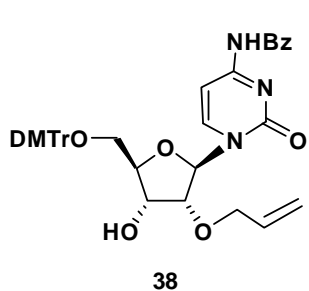


=CH), 5.84 (s, 1H, H1'), 6.86-6.90 (m, 4H, Ar), 7.26-7.62 (m, 13H, Ar and H5), 8.0 (m, 2H, Ar), 8.77 (d, 1H, $J=7.6$ Hz, H6). ^{13}C NMR (50 MHz, CDCl_3): δ -5.3, -4.3, 18.0, 25.6, 55.2, 60.5, 71.3, 73.7, 74.7, 80.5, 87.0, 92.1, 96.5, 113.3, 117.7, 127.2, 127.9, 128.2, 128.8, 130.0, 130.1, 133.1, 133.8, 135.3, 135.5, 143.9, 145.4, 154.5, 158.7, 162.7, 170.8. **Mass** (ESI): m/z 803.3602, found 826.36 ($\text{M}+\text{Na}^+$).

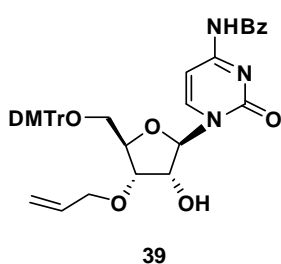
N^4 -Benzoyl-2'-O-allyl-5'-O-(4, 4'-dimethoxytrityl)-cytidine (38) and N^4 -Benzoyl-3'-O-allyl-5'-O-(4, 4'-dimethoxytrityl)-cytidine (39)

Substrate **36/37** (0.120 g, 0.149 mmol) is dissolved in AR grade THF (1 mL). To this 1M TBAF solution in THF (0.4 mL, 0.388 mmol) was added and reaction stirred for 1.5 hr, till TLC showed no starting present. Reaction mixture was concentrated under reduced pressure to remove THF. The crude product was extracted with CH_2Cl_2 , given a water wash followed by drying over Na_2SO_4 . Then the CH_2Cl_2 phase was concentrated followed by column purification to give pure compound **38** (90 mg, 87.96%) / **39** (80 mg, 78.64%).

N^4 -Benzoyl-2'-O-allyl-5'-O-(4, 4'-dimethoxytrityl)-cytidine (38):



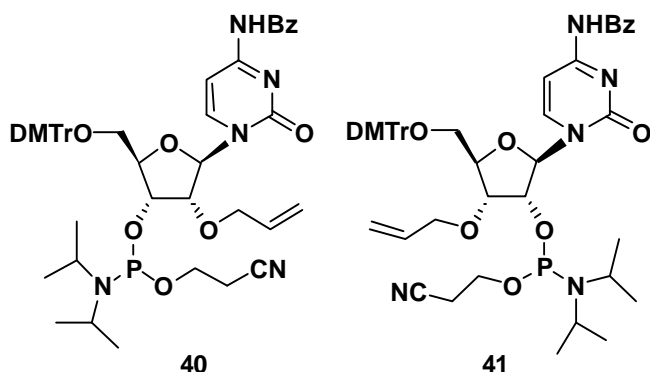
^1H NMR (200 MHz, CDCl_3): δ 3.53- 3.67 (m, 2H, H5' & H5''), 3.83 (s, 6H, 2 X OCH_3), 4.00 (d, 1H, $J=5.18$ Hz), 4.12 (dt, 1H, $J=2.20, 9.09$ Hz), 4.34-4.51 (m, 2H), 4.59-4.68 (m, 1H), 5.21 (dd, 1H, $J=1.5, 10.3$ Hz, allyl), 5.34 (dd, 1H, $J=1.5, 17.1$ Hz, allyl), 5.92 (m, 1H, =CH allyl), 6.02 (s, 1H, H1'), 6.86 (m, 4H, Ar), 7.20-7.48 (m, 12H, Ar), 7.51(d, $J=7.45$ Hz, 1H, H5), 7.90 (m, 2H, Ar), 8.60 (d, 1H, $J=7.45$ Hz, H6). ^{13}C NMR (50 MHz, CDCl_3): δ 55.1, 60.6, 67.6, 71.2, 81.2, 83.2, 87.0, 88.7, 96.8, 113.2, 118.1, 127.1, 127.9, 128.2, 128.7, 129.9, 130.0, 133.0, 133.5, 135.5, 143.9, 145.1, 149.1, 154.5, 158.6, 162.9, 168.8. **Mass** (ESI): m/z 689.2737, found 712.36 ($\text{M}+\text{Na}^+$).

N⁴-Benzoyl-3'-O-allyl-5'-O-(4, 4'-dimethoxytrityl)- cytidine (39):

¹H NMR (200 MHz, CDCl₃): δ 3.45 and 3.59 (2 x dd, 1H each, *J* = 1.7, 10.9 Hz, H5' & H5''), 3.81 (s, 6H, 2 X OCH₃), 4.00 (m, 1H), 4.13-4.25 (m, 2H), 4.33 (m, 1H), 4.46 (m, 1H), 5.22 (m, 2H, =CH₂ allyl), 5.77-5.96 (m, 1H, =CH allyl), 6.01 (d, *J*=2.02 Hz, 1H, H1') 6.85 (m, 4H, Ar), 7.24-7.46 (m, 12H, Ar), 7.53 (d, *J* = 7.46 Hz, 1H, H5), 7.90 (m, 2H, Ar), 8.49 (d, 1H, *J* = 7.46 Hz, H6). ¹³C NMR (50 MHz, CDCl₃): δ 55.1, 61.3, 71.4, 74.1, 75.6, 81.6, 86.8, 92.0, 96.7, 113.2, 118.0, 127.0, 127.5, 128.0, 128.8, 129.9, 132.9, 133.7, 135.1, 135.3, 135.9, 143.9, 144.7, 149.6, 155.1, 158.6, 162.3, 166.5. **Mass** (ESI): *m/z* 689.2737, found 712.31 (M+Na⁺).

N⁴-Benzoyl -2'-O-allyl- 3'-O-[2-cyanoethoxy(diisopropylamino)phosphino]-5'-O-(4, 4'-dimethoxytrityl)-cytidine (40) and 3'-O-allyl-2'-O-[2-cyanoethoxy(diisopropylamino) phosphino]-5'-O-(4, 4'-dimethoxytrityl)-uridine (41)

Compound **38/39**, (0.206 g, 0.3 mmol) was coevaporated with dry dichloromethane then dissolved in 3.0 mL of dry CH₂Cl₂. DIPEA (0.200 mL, 1.2 mmol) was added followed by



chloro(2-cyanoethoxy)-N,N-diisopropyl amino)-phosphine (0.190 mL, 0.837 mmol) at 0°C. The reaction mixture was stirred under argon atmosphere at room temperature for 3 hours. TLC done showed product formed and absence of starting material. The

reaction was diluted with CH₂Cl₂, washed with NaHCO₃ and water, dried over Na₂SO₄ followed by solvent removal. The crude product **40/41** was purified on a silica gel column using 1:1 mixture of CH₂Cl₂ : EtOAc and 1% TEA. Compound **40** (0.190 g, 71.69%)/ **41** (0.176 g, 66.37%).

N⁴-Benzoyl -2'-O-allyl- 3'-O-[2-cyanoethoxy(diisopropylamino)phosphino]-5'-O-(4, 4'-dimethoxytrityl)-cytidine (40):

³¹P NMR (50 MHz, CDCl₃): δ 150.07, 150.14. Mass (ESI): m/z 889.3816, found 912.49 (M+Na⁺).

3'-O-allyl- 2'-O-[2-cyanoethoxy(diisopropylamino)phosphino]-5'-O-(4, 4'-dimethoxytrityl)-uridine (41):

³¹P NMR (50 MHz, CDCl₃): δ 149.52, 151.98. Mass (ESI): m/z 889.3816, found 912.43 (M+Na⁺).

3.4.2 Synthesis of buffers

Phosphate buffer (pH = 7.2, 150 mM NaCl)

Na₂HPO₄ (110 mg), NaH₂PO₄·H₂O (35.3 mg), NaCl (877.5 mg) was dissolved in minimum quantity of water and the total volume was made 100 mL. The pH of the solution was adjusted 7.2 with aq. NaOH solution in DI water, and stored at 4°C.

Triethyl ammonium acetate (TEAA) buffer

TEA (101.19 g ≈ 139.38 mL, 1 M) was diluted up to 500 mL DI water and kept aside, then in another container AcOH (60.05 g ≈ 57.24 mL, 1 M) was diluted up to again with 500 mL DI water. Then slowly the AcOH solution was added to the TEA in ice bath with vigorous stirring to make total volume 1 L, the pH of the solution was adjusted to 7.0 using either AcOH or TEA, this 1M stock buffer was stored at room temperature.

3.4.3 Synthesis of oligonucleotides

DNA oligonucleotides were synthesized on a CPG solid support using Bioautomation MerMade- 4 synthesizer using standard β-cyanoethyl phosphoramidite chemistry. The 2'-5'-linked DNA oligomers were synthesized in 2'-5' direction using universal columns as solid support. All the monomer (0.06M) solutions in anhydrous acetonitrile were prepared freshly and stored over 3Å molecular sieves. The modified amidite monomer solution concentration was (0.1M) in acetonitrile. For the modified monomers double coupling and

longer coupling time (300 s x 2) were employed. Post synthesis, the sequences were subjected to ammonia treatment for 6 h at 55°C, cleavage of the oligomer from the support, deprotection of the β -cyanoethyl protecting group and the exocyclic amino protecting groups used during the synthesis takes place. The crude oligonucleotides were desalted by passing them over G-25 sephadex columns, followed by purification using RP-HPLC (C18 column). The pure oligomers were characterized by MALDI-TOF before using for the biophysical studies.

3.4.4 Purification and characterization

High performance liquid chromatography

The purity of synthesized oligonucleotides were ascertained using by RP-HPLC on a C18 column with either a Varian system (Analytical semi-preparative system consisting of Varian Prostar 210 binary solvent delivery system and Dynamax UV-D2 variable wavelength detector and Star chromatography software) or a Waters system (Waters Delta 600e quaternary solvent delivery system and 2998 photodiode array detector and Empower 2 chromatography software). A gradient elution method 0% A to 100%B in 15 min was used with flow rate 1.5 mL/min and the eluent was monitored at 260nm. [A = 5% ACN in TEAA (0.1 M, pH 7); B = 30% ACN in TEAA (0.1 M, pH 7)].

MALDI-TOF characterization

The MALDI-TOF spectra were recorded on both Voyager-De-STR (Applied Biosystems) MALDI-TOF instrument or a AB Sciex TOF/TOFTM Series ExplorerTM 72085 instrument. A nitrogen laser (337 nm) was used for desorption and ionization. The matrix used for analysis was THAP (2', 4', 6'-trihydroxyacetophenone), and diammonium citrate used as additive. The sample was prepared by mixing 1 μ L oligomer (10-50 μ M in DI H₂O) with 10 μ L of THAP (0.55 M in EtOH) mixed well followed by 5 μ L diammonium citrate (0.1 M in DI H₂O) again mixed well and then 1 μ L of the mixture was spotted on metal plate. The metal plate was loaded to the instrument and the analyte ion were then accelerated by an applied high voltage (15-25 kv) in linear mode and detected as an electrical signal.

HPLC purified oligonucleotides were characterized through this method and were observed to give good signal to noise ratio, mostly producing higher molecular ion signals. The purity was re-checked and found to be >95%.

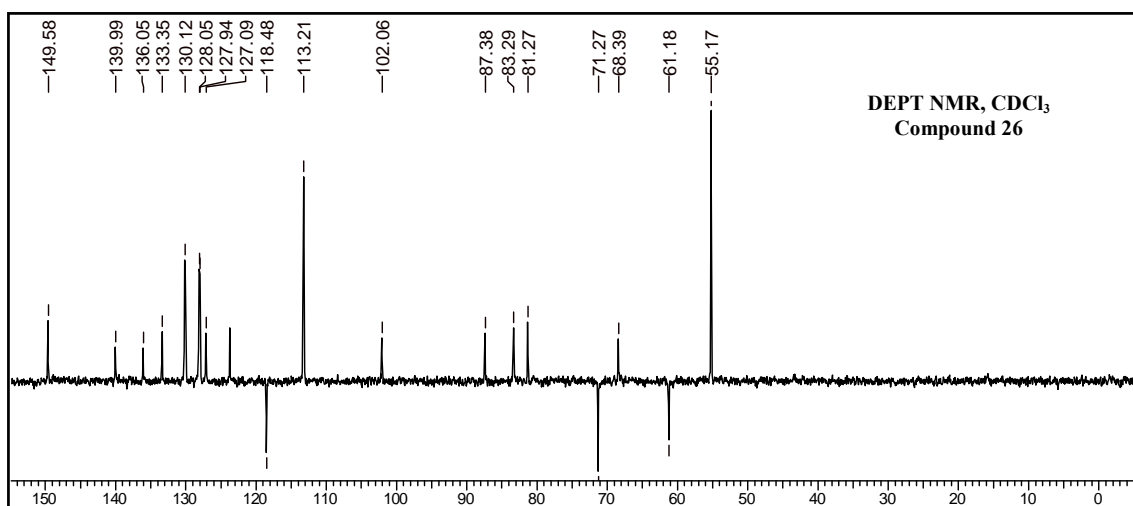
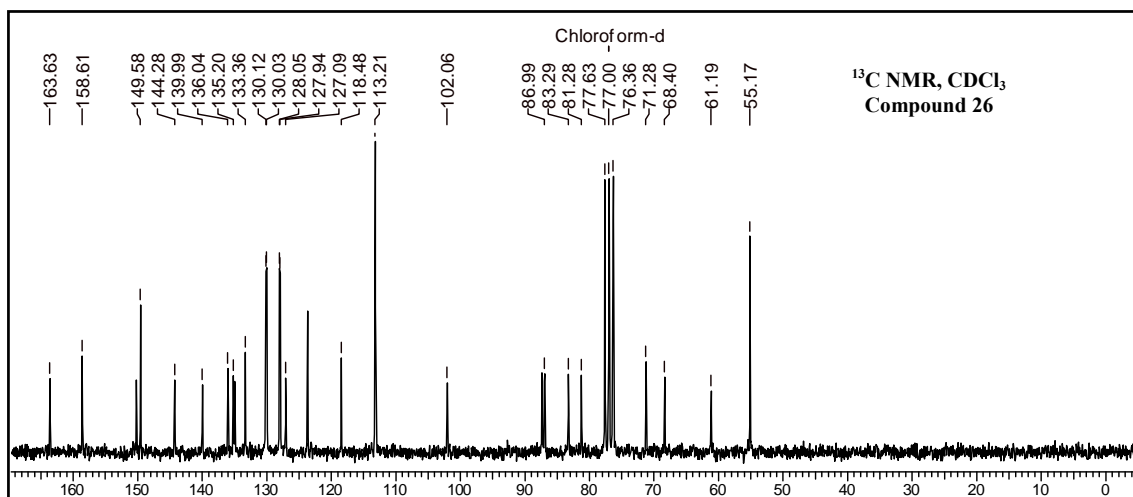
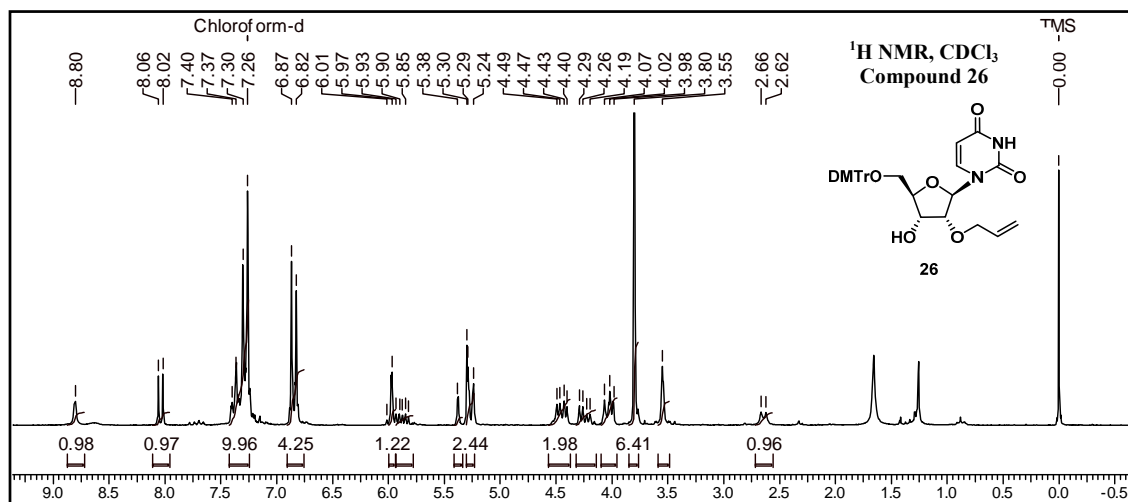
3.4.5 Biophysical techniques

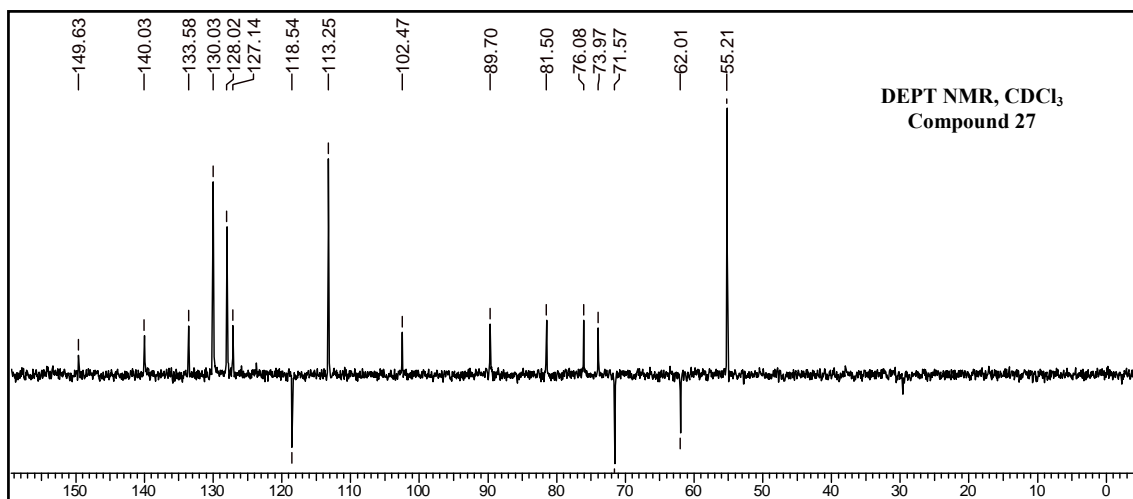
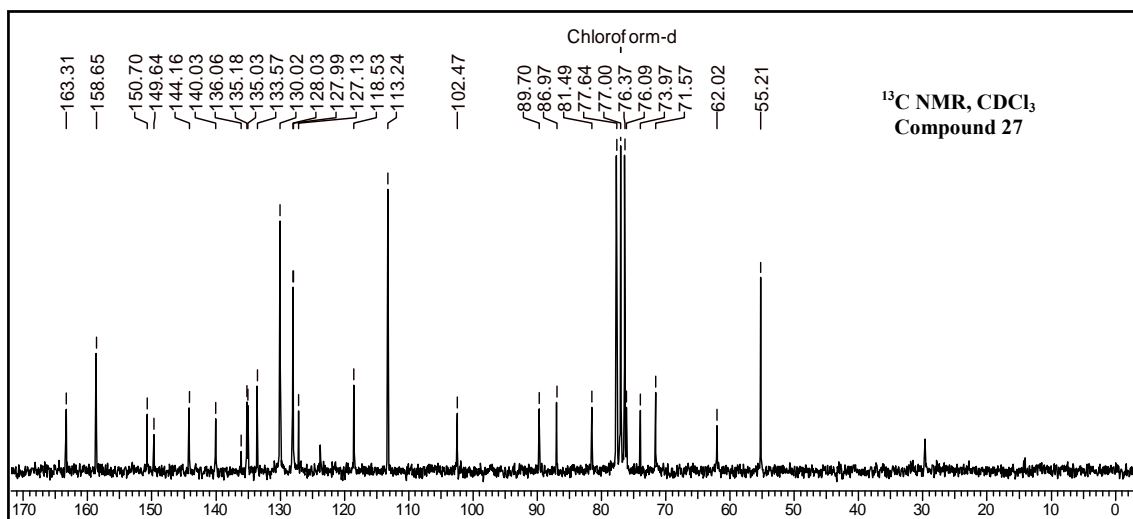
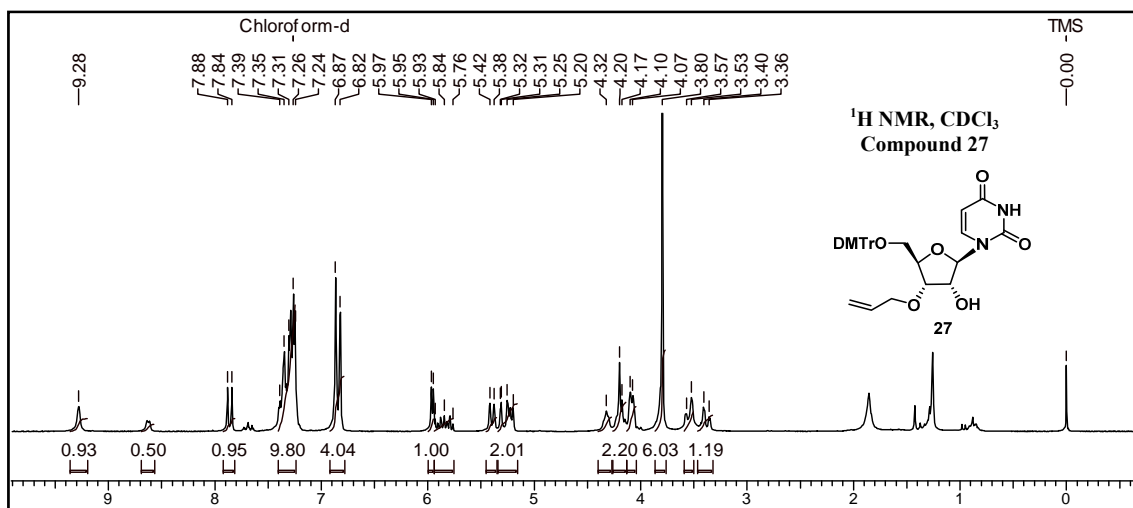
UV- T_m Experiments

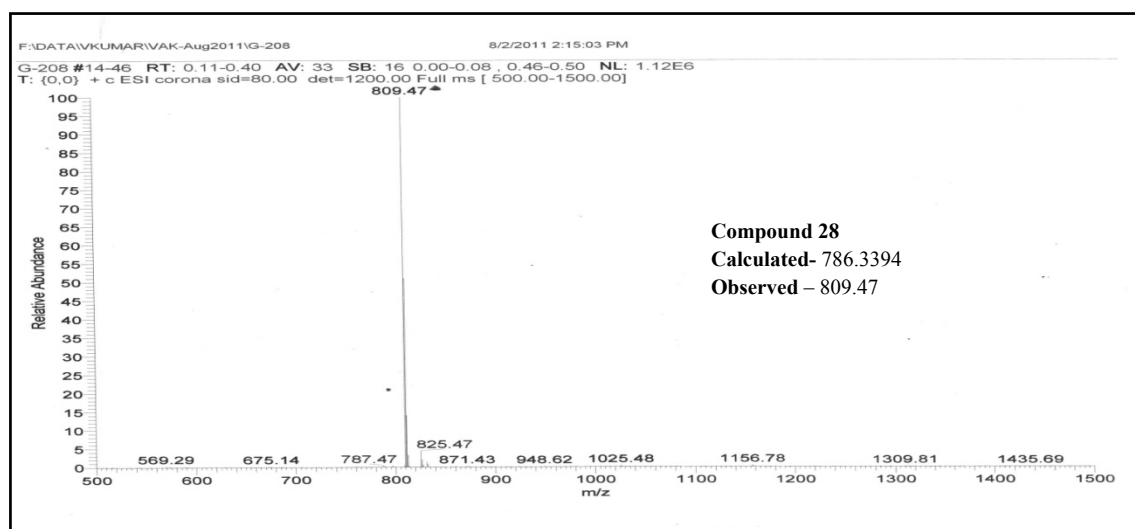
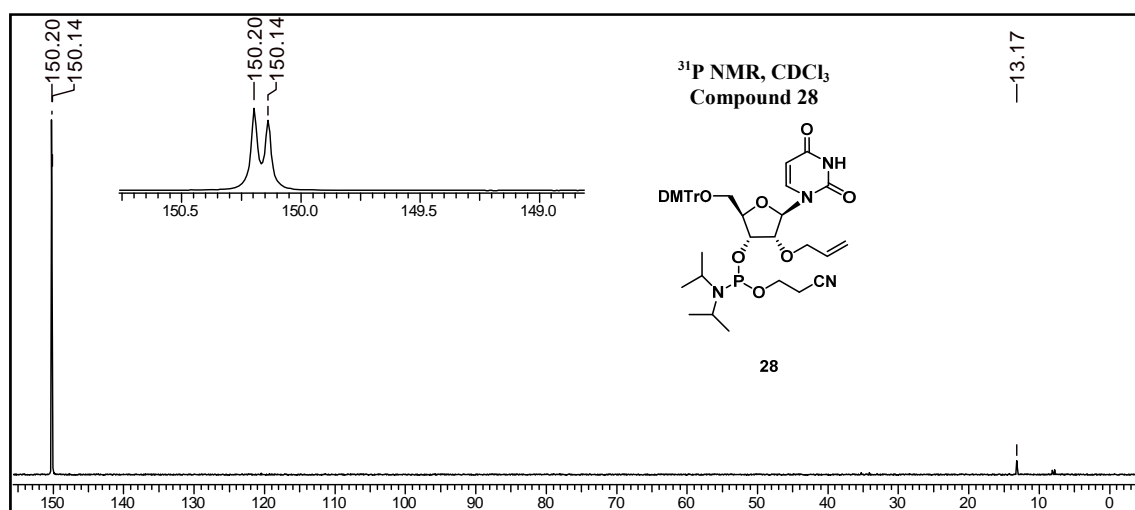
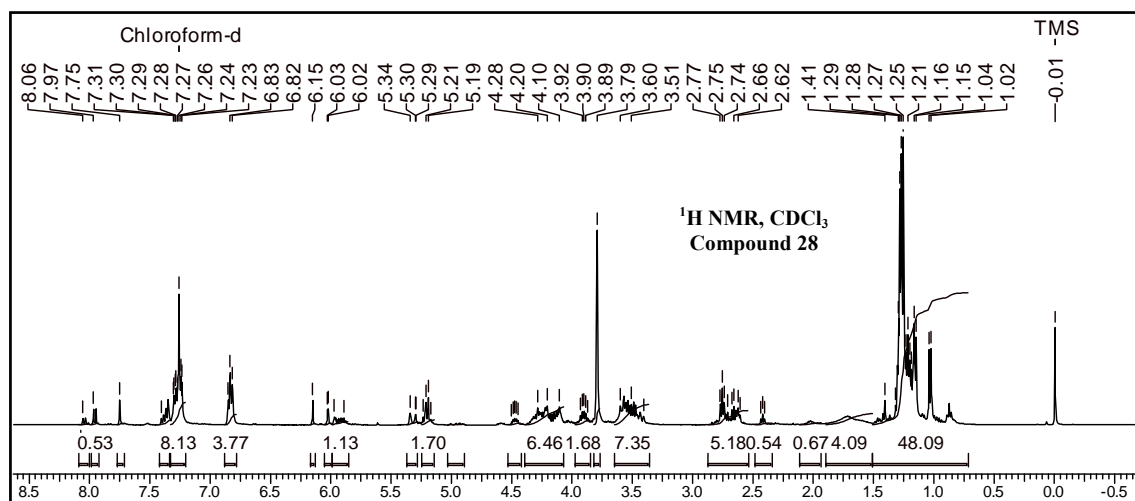
UV experiments were performed on a Varian Cary 300 Bio UV-Visible spectrophotometer fitted with a Peltier-controlled temperature programmer. The concentration of DNA ONs were calculated on the basis of absorbance from molar extinction coefficients of the corresponding nucleobases (A = 15400, T = 8800, C = 7300 and G = 11700, U = 9900 L/(M.cm) of DNA/RNA. The complexes were prepared by mixing 1 μ M strand concentrations of ONs and complementary strand together (1:1) in 1 mL of 10 mM sodium phosphate buffer, pH 7.2 containing NaCl (150 mM) and were annealed by keeping the samples at 90°C for 2 min followed by slow cooling to room temperature and refrigeration for at least 5 hours prior to running the experiments. The sample was held at the starting temperature 10°C for at least 15 min, N₂-gas was purged through the cuvette chamber below 20°C to prevent condensation of moisture on cuvette walls. Absorbance *versus* temperature profiles were obtained by monitoring the absorbance at 260nm from 10–85°C at a ramp rate of 0.5°C per minute. The data were processed using Microcal Origin 6.1 and T_m (°C) values were derived from the maxima of the first derivative plots. All values are an average of at least 3 independent experiments and accurate to within $\pm 0.5^\circ\text{C}$.

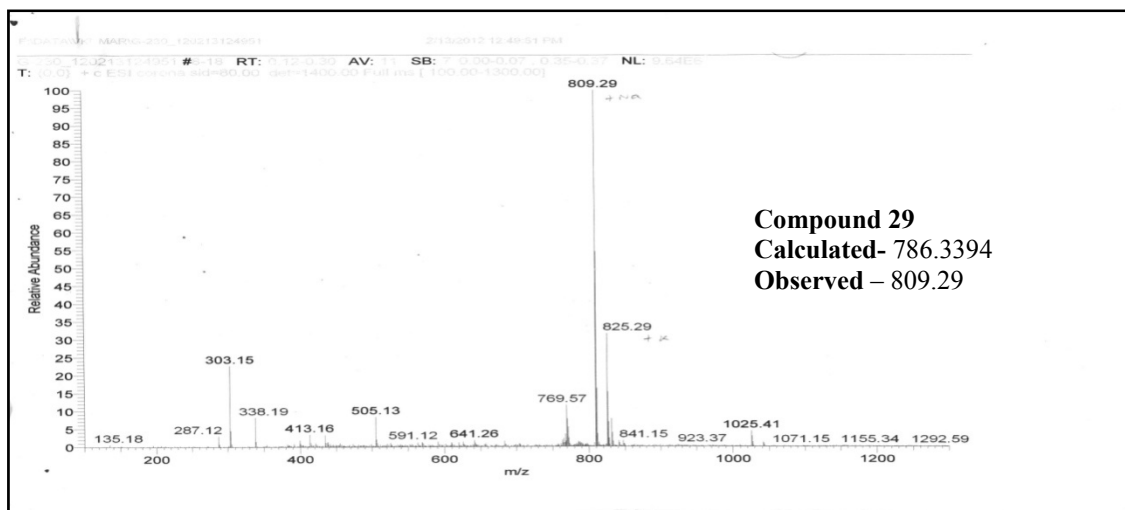
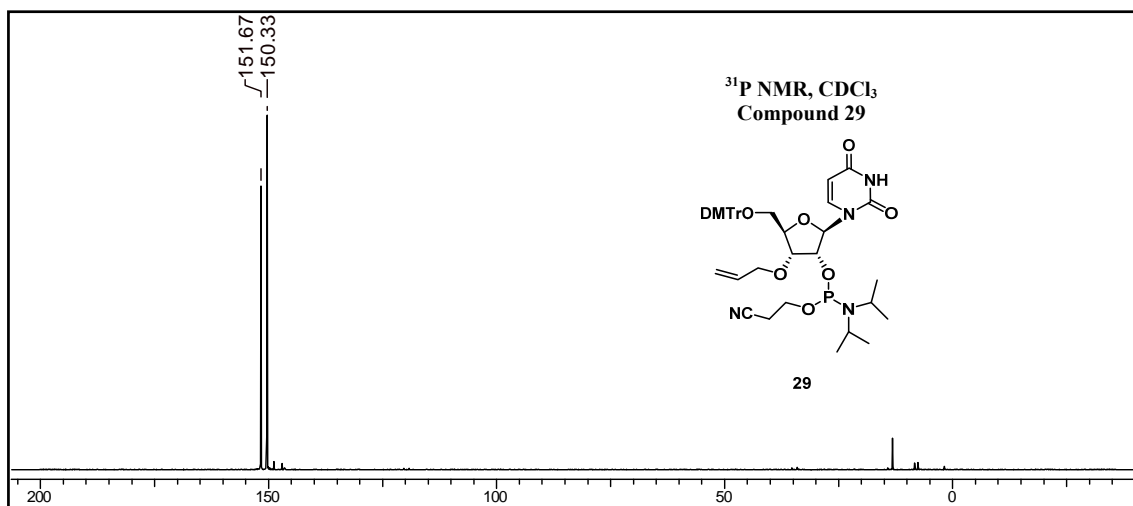
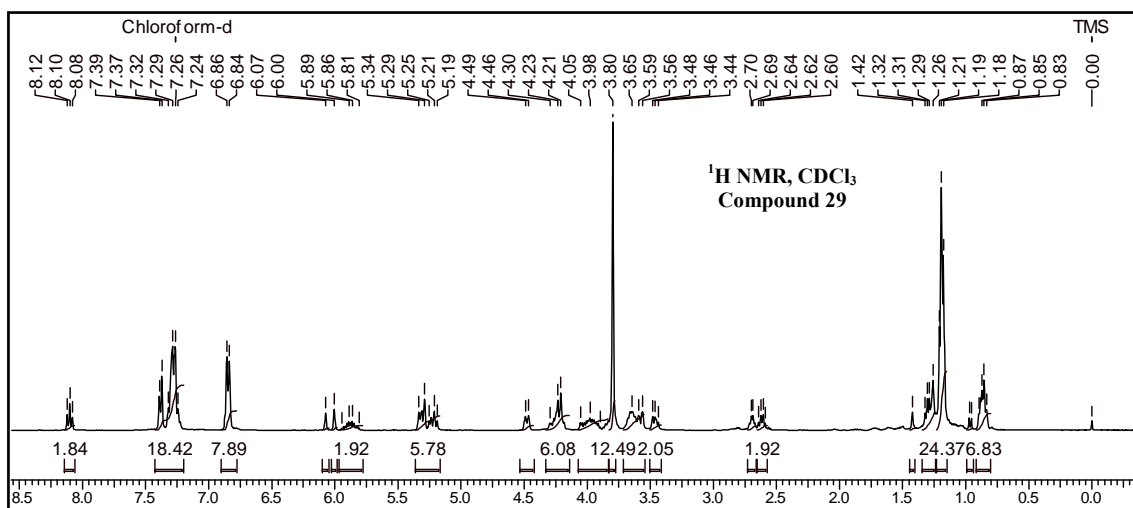
3.5 Appendix

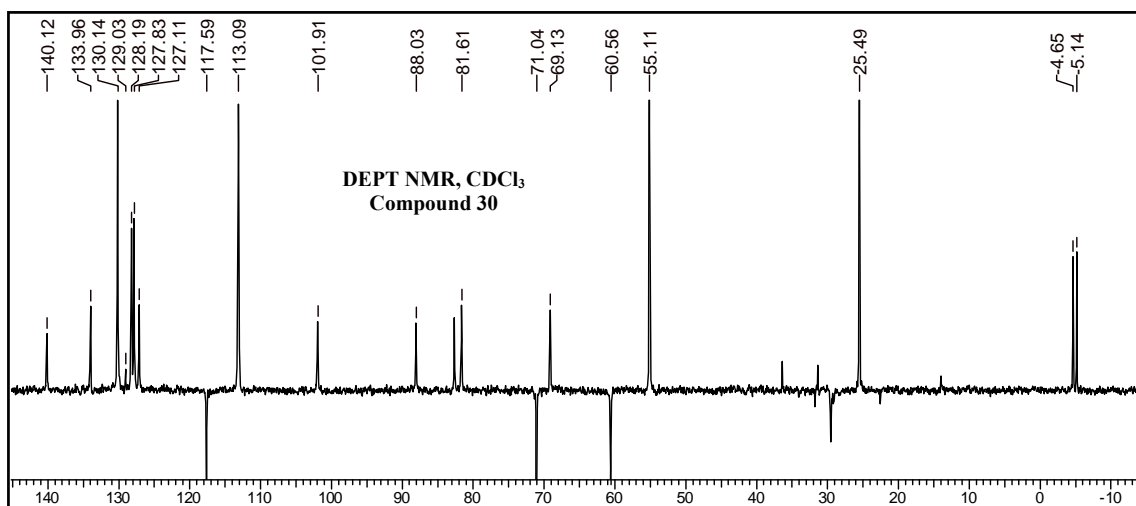
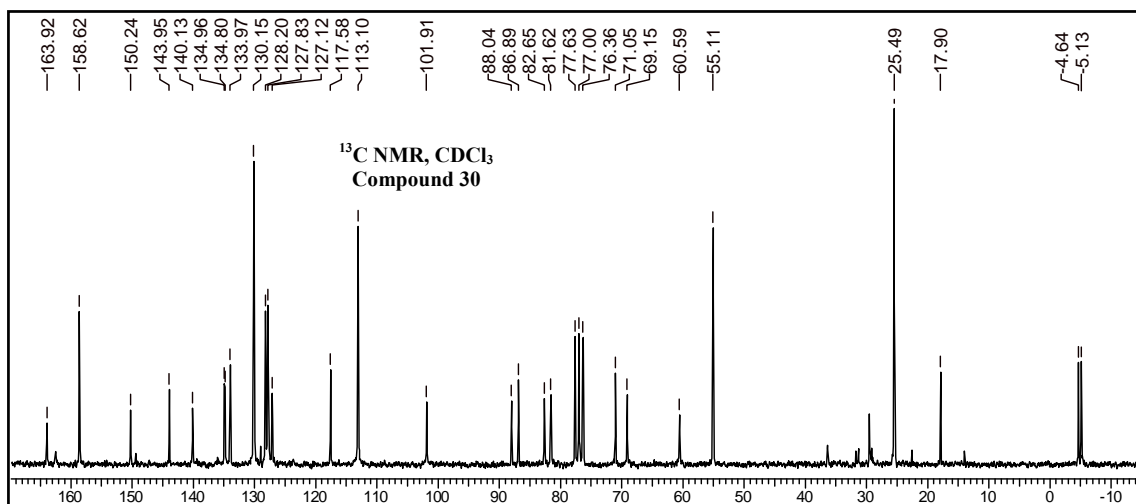
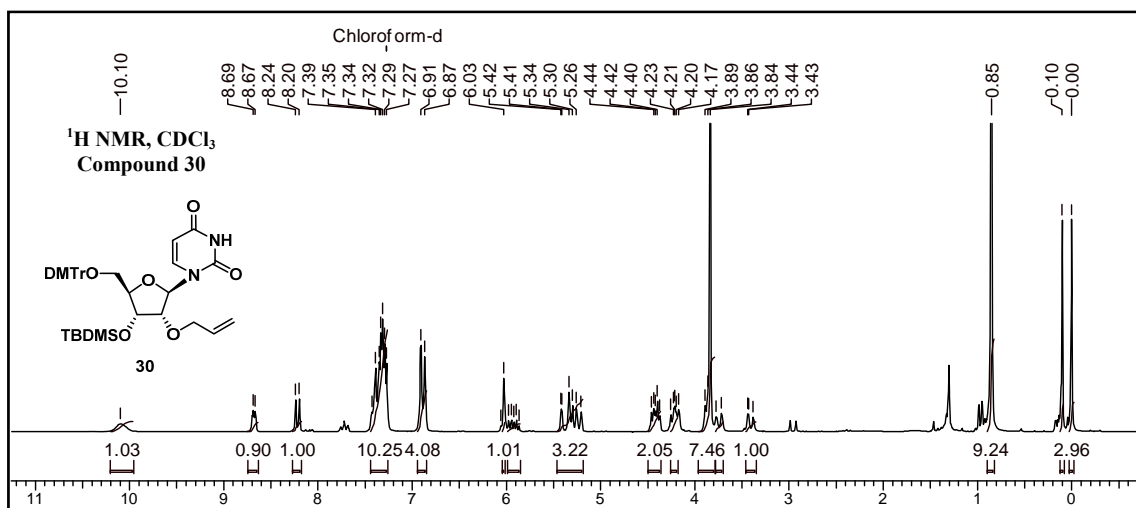
Compound No.	Page No.
compound 26: ^1H , ^{13}C NMR and DEPT	141
compound 27: ^1H , ^{13}C NMR and DEPT	142
compound 28: ^1H , ^{31}P NMR and Mass	143
compound 29: ^1H , ^{31}P NMR and Mass	144
compound 30: ^1H , ^{13}C NMR and DEPT	145
compound 31: ^1H , ^{13}C NMR and DEPT	146
compound 34: ^1H , ^{13}C NMR and DEPT	147
compound 35: ^1H , ^{13}C NMR and DEPT	148
compound 36: ^1H , ^{13}C NMR and DEPT	149
compound 37: ^1H , ^{13}C NMR and DEPT	150
compound 38: ^1H , ^{13}C NMR and DEPT	151
compound 39: ^1H , ^{13}C NMR and DEPT	152
compound 40: ^1H , ^{31}P NMR and Mass	153
compound 41: ^1H , ^{31}P NMR and Mass	154
HPLC chromatogram of oligomers	155-157
MALDI spectra of oligomers	157-166

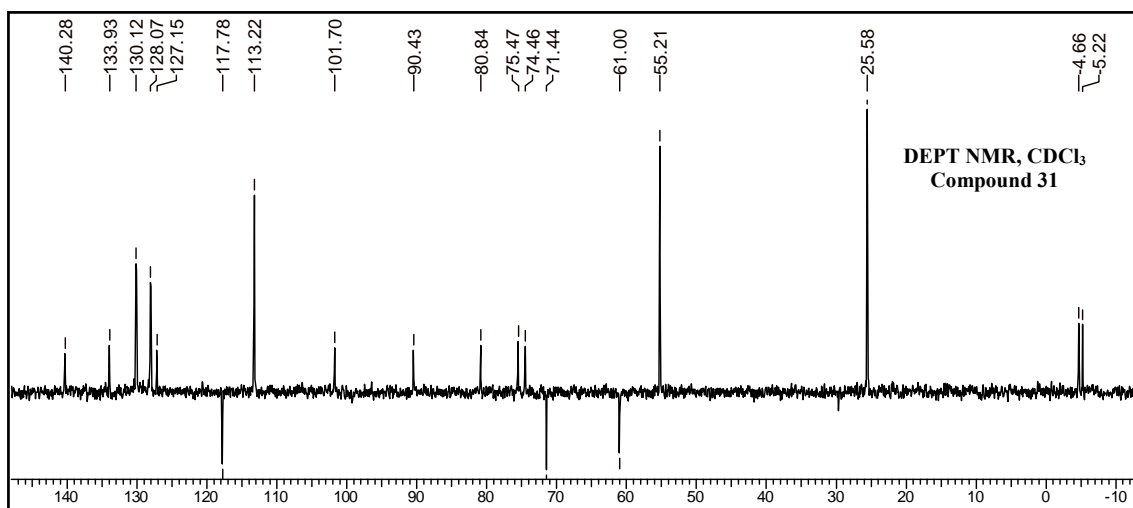
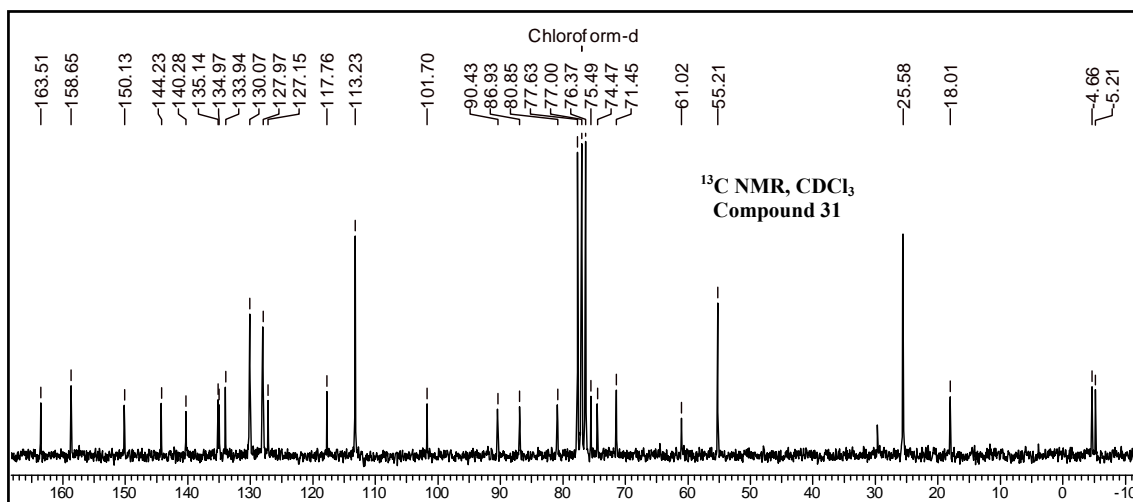
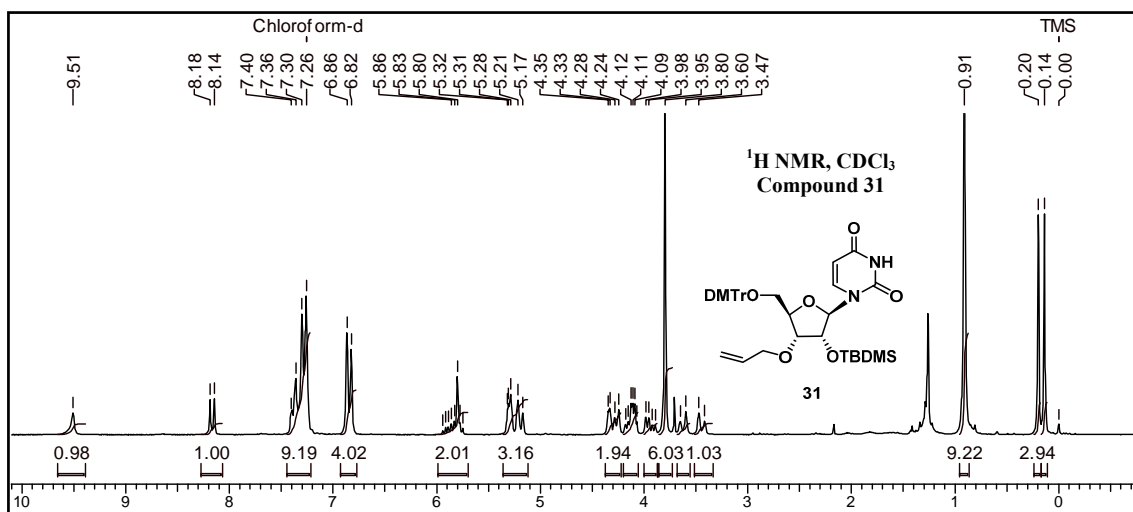


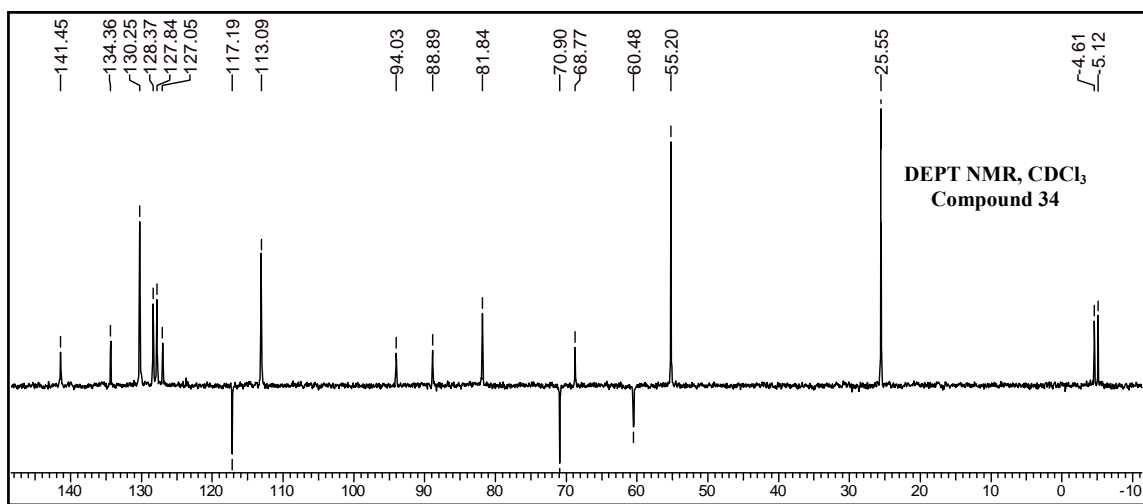
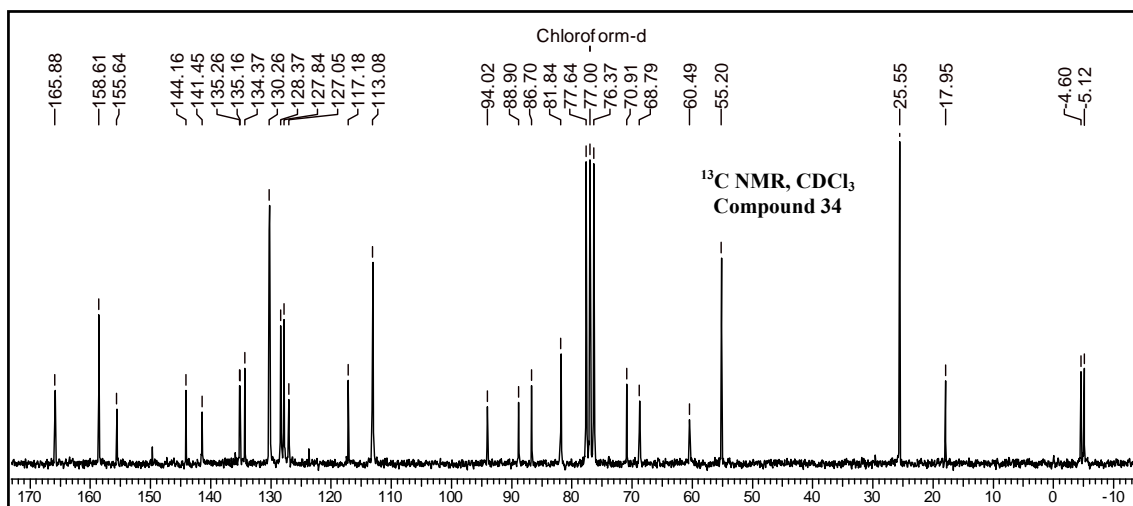
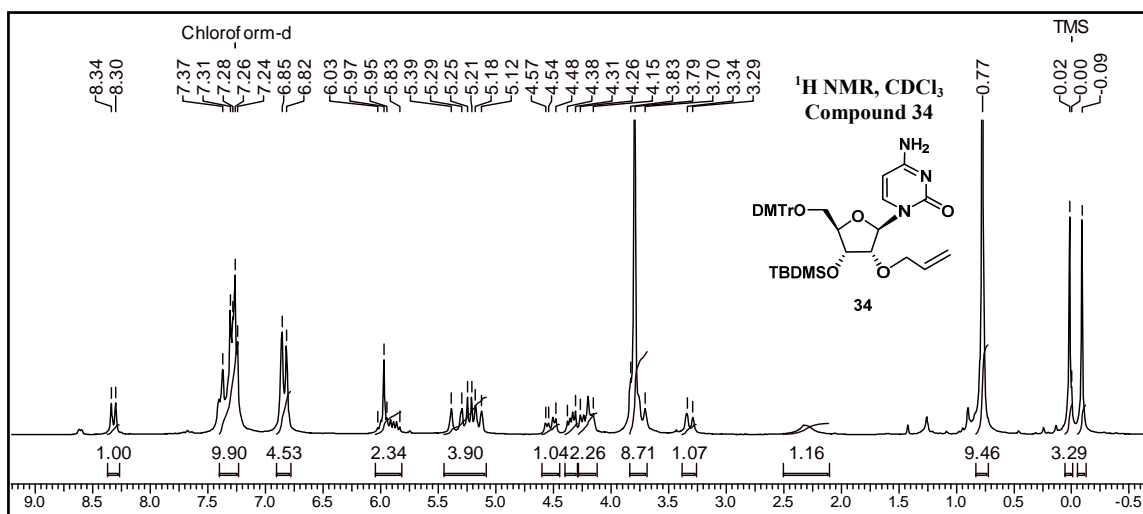


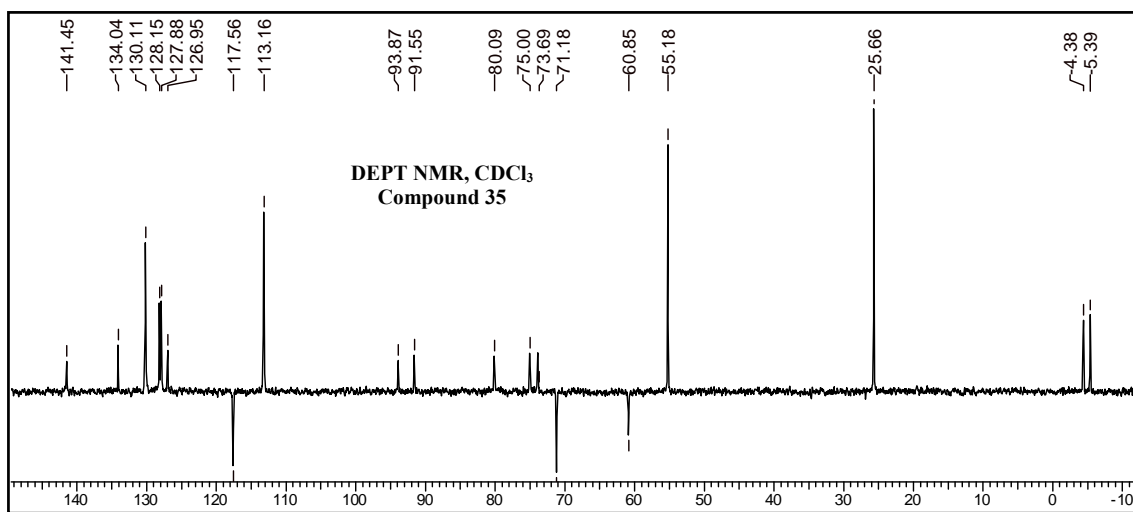
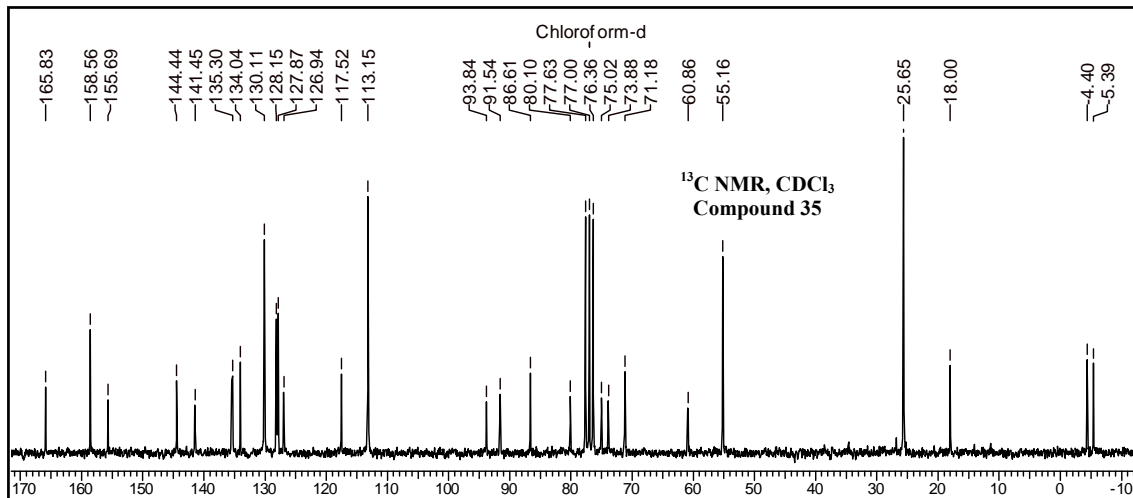
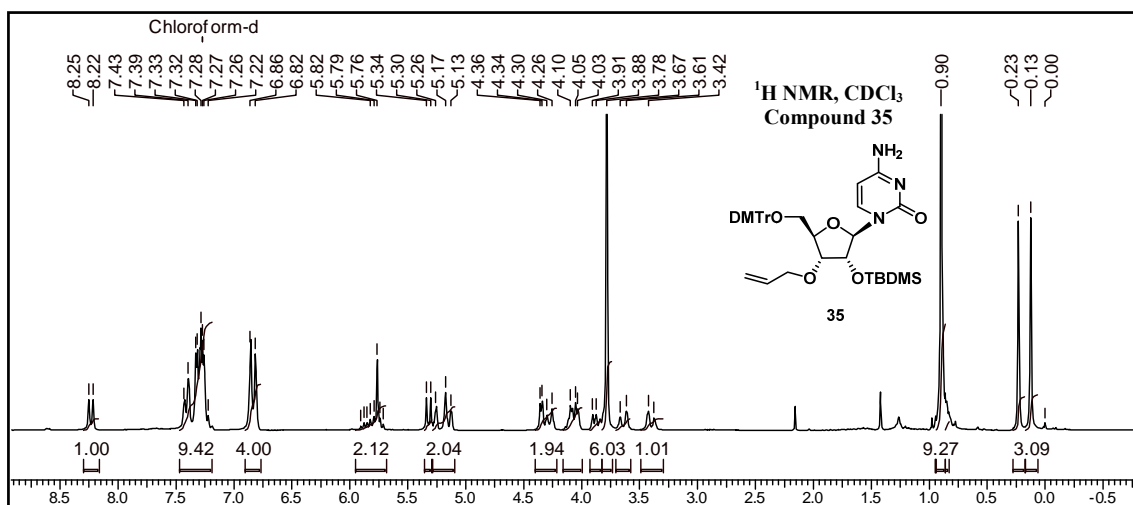


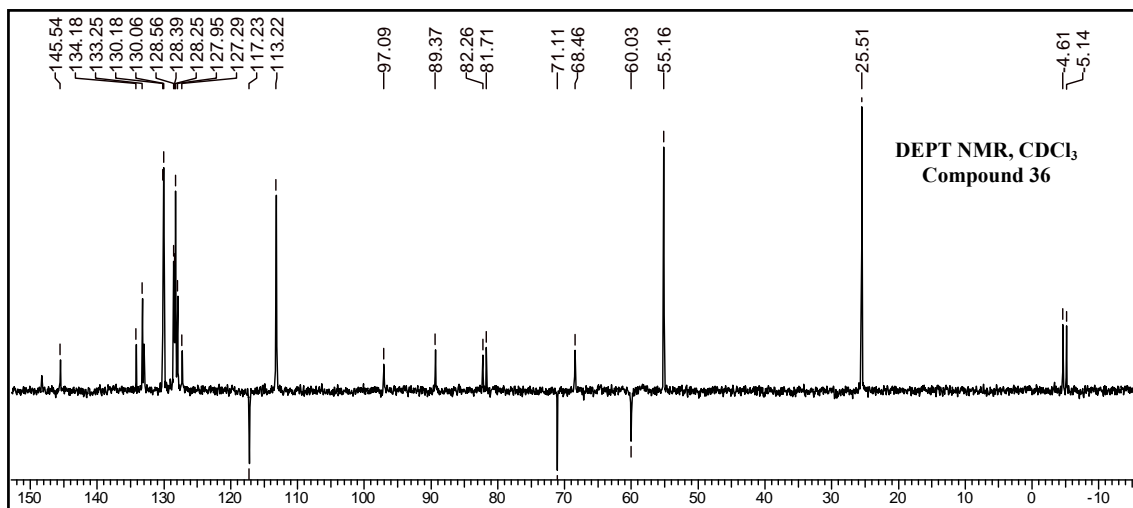
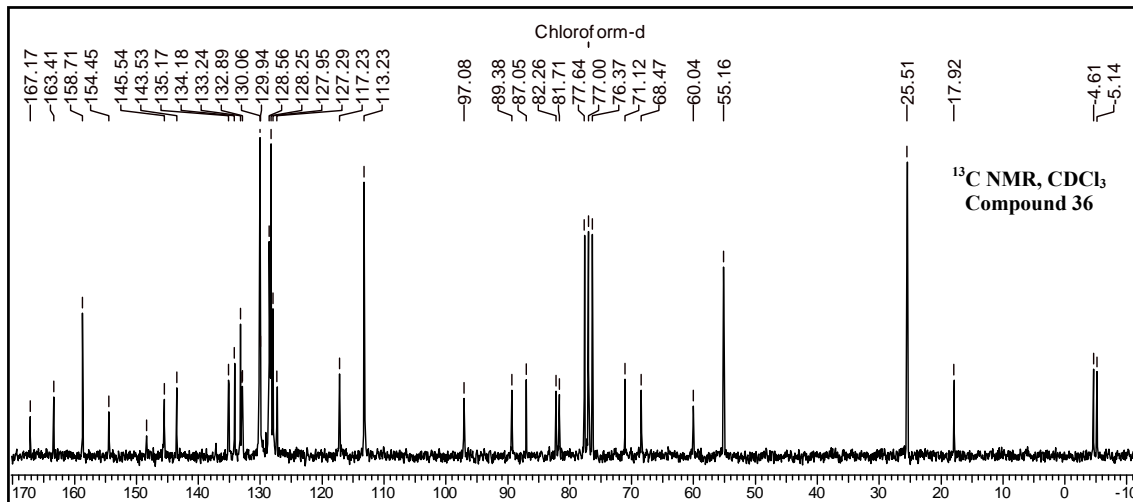
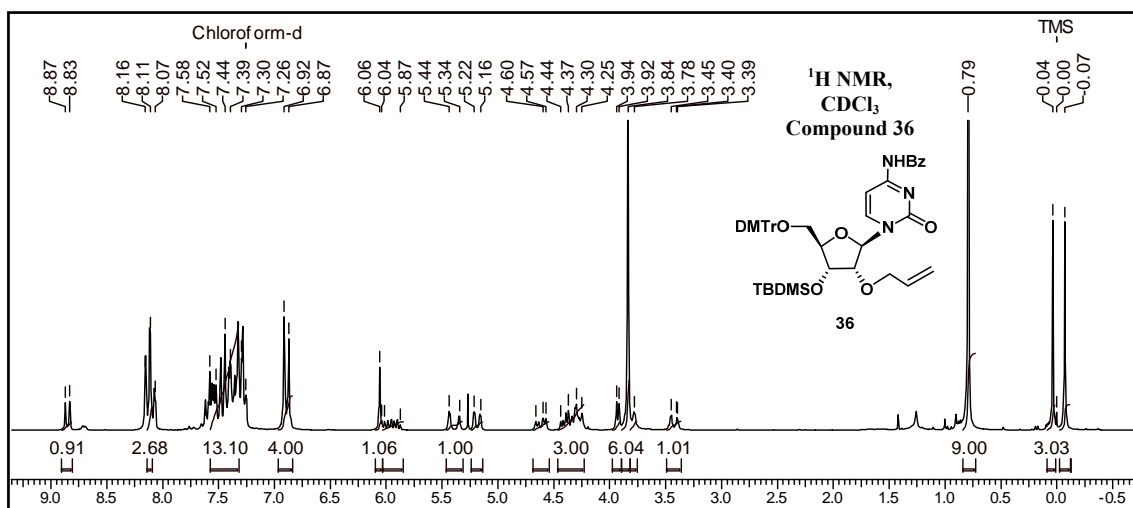


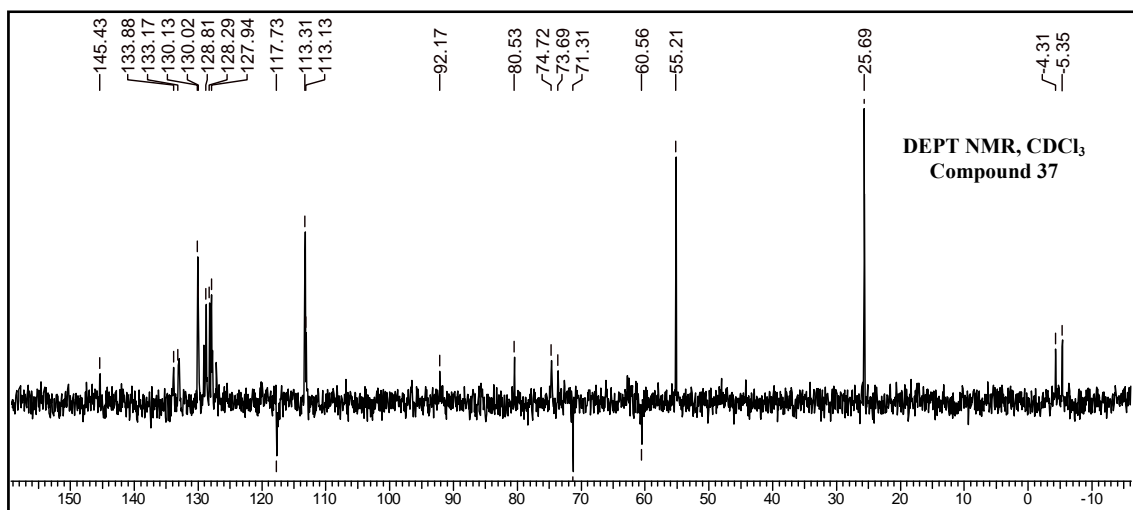
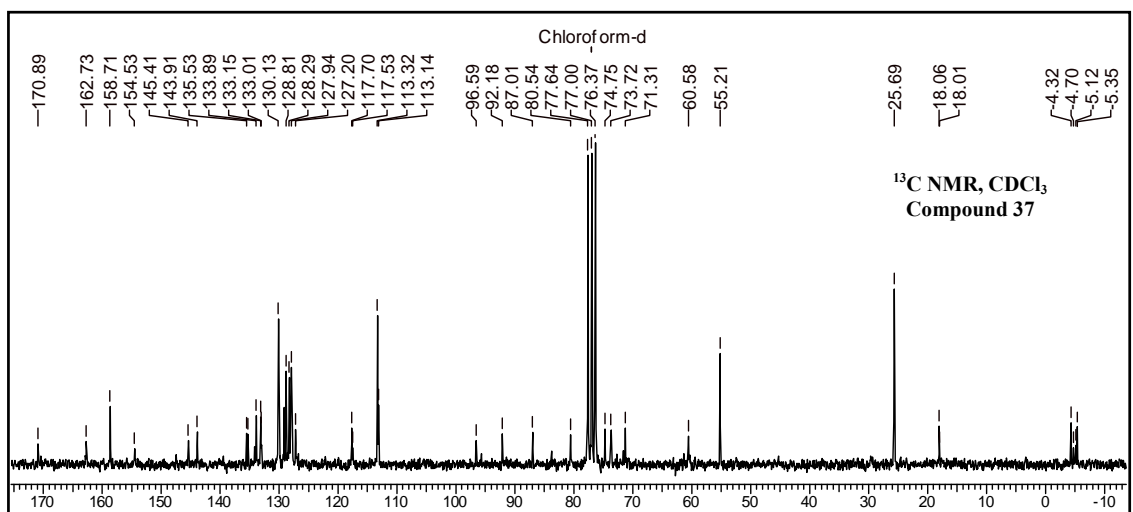
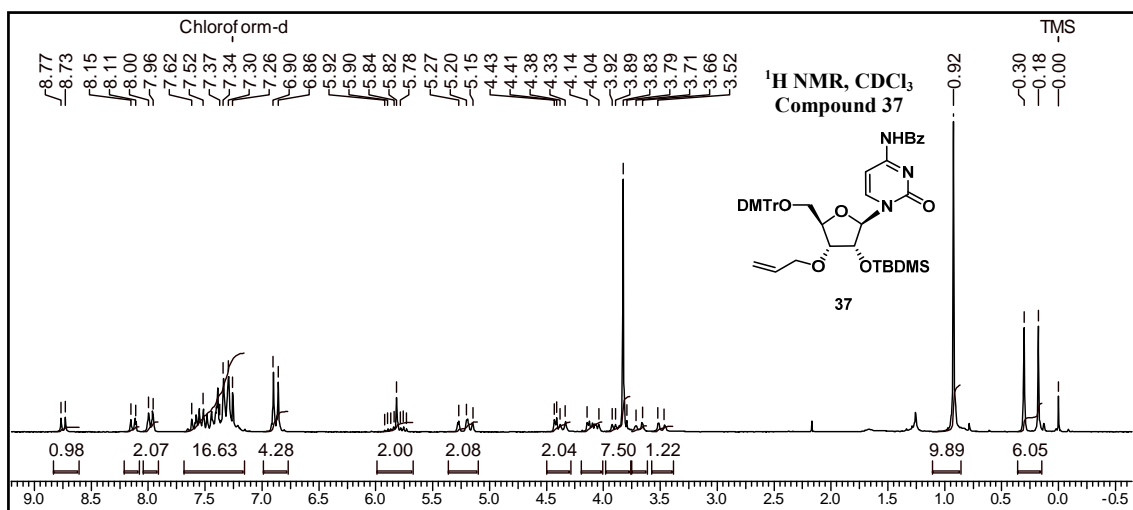


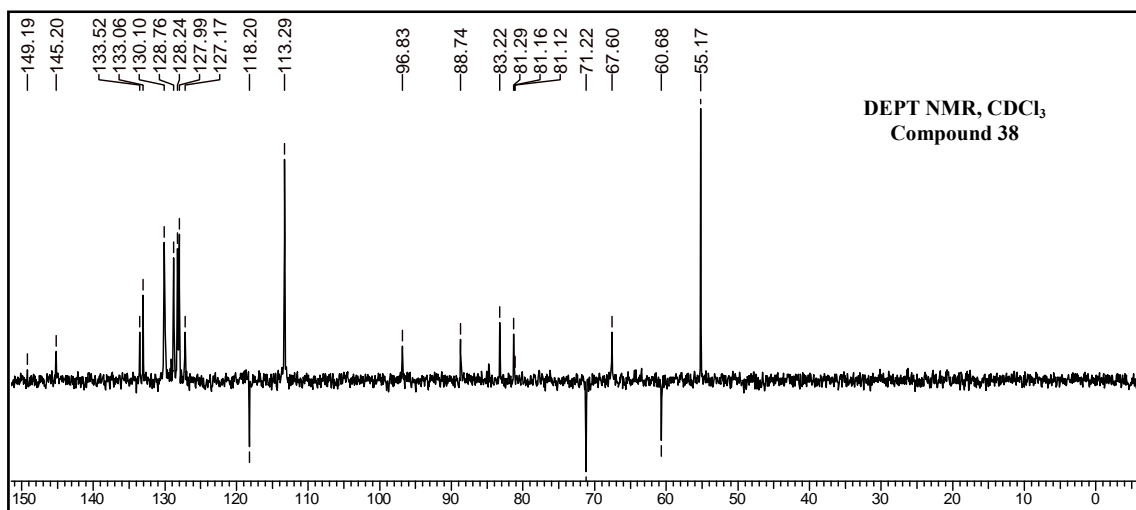
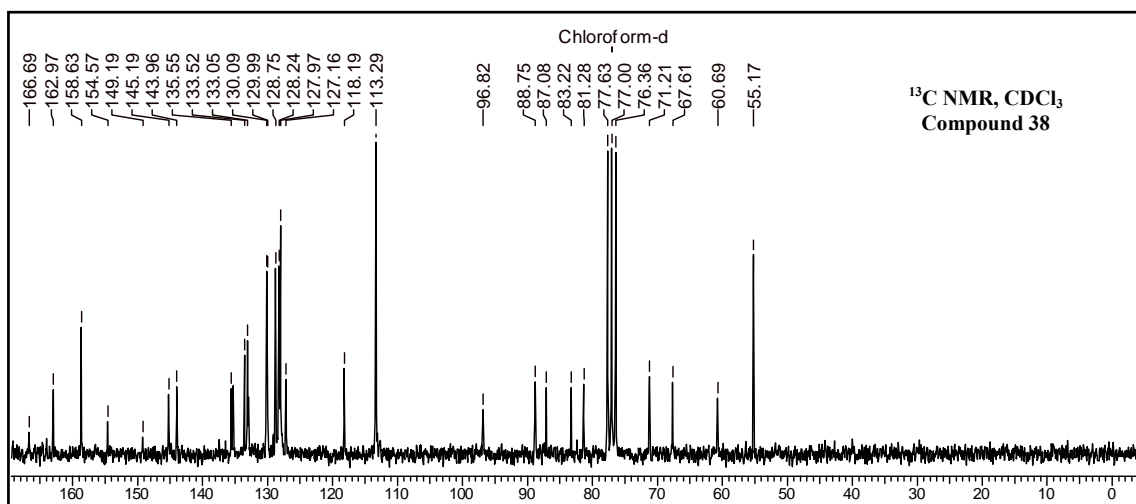
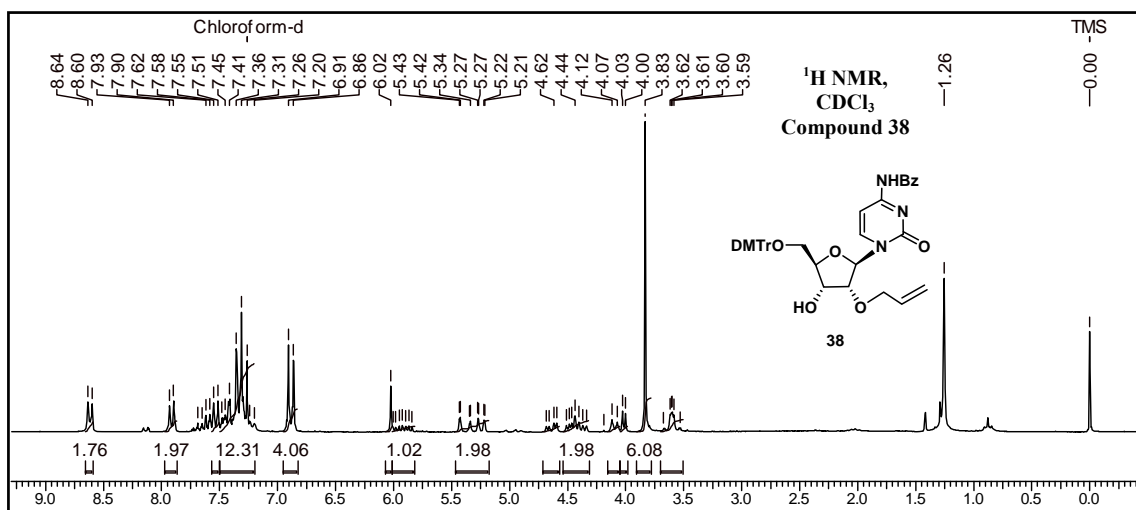


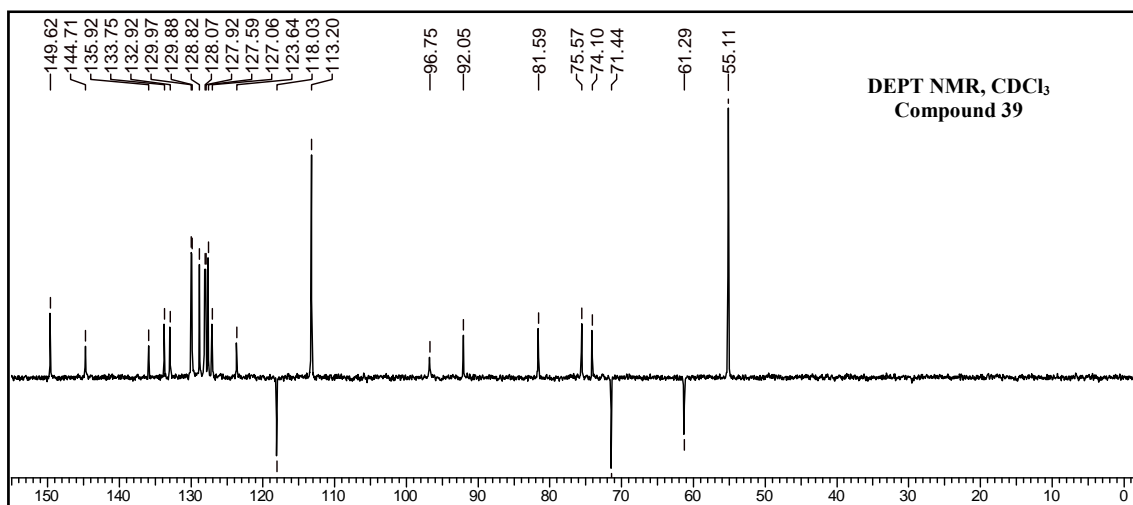
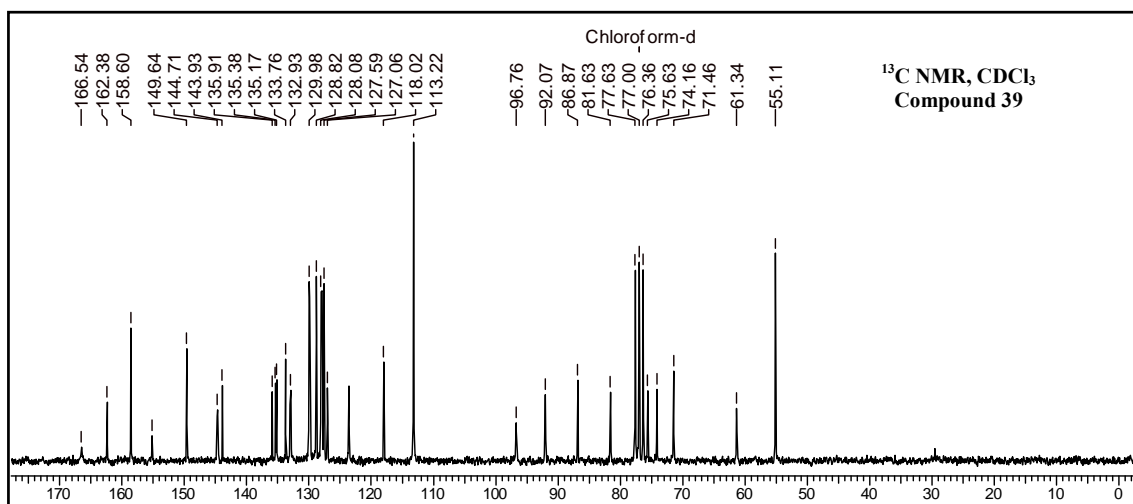
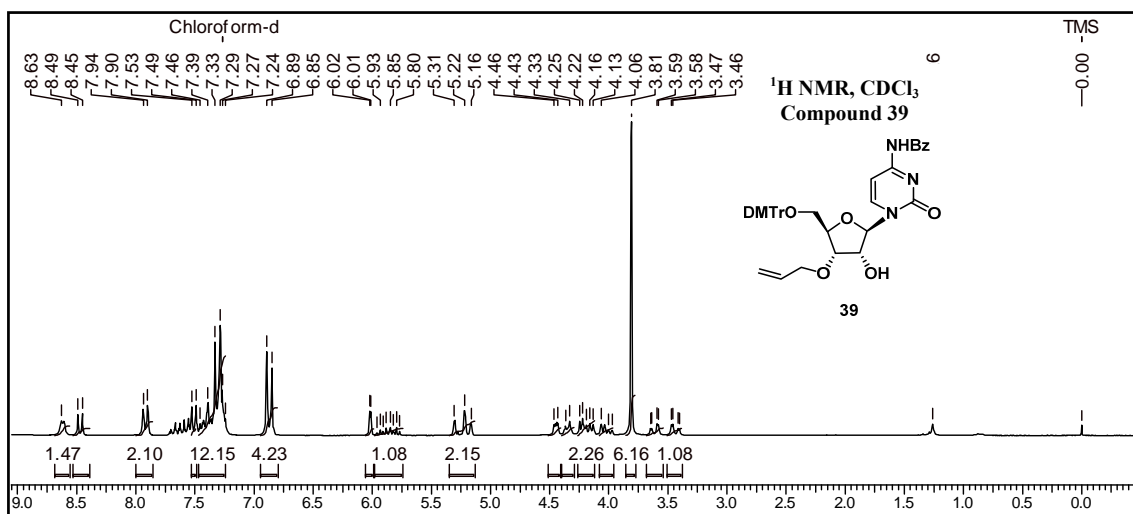


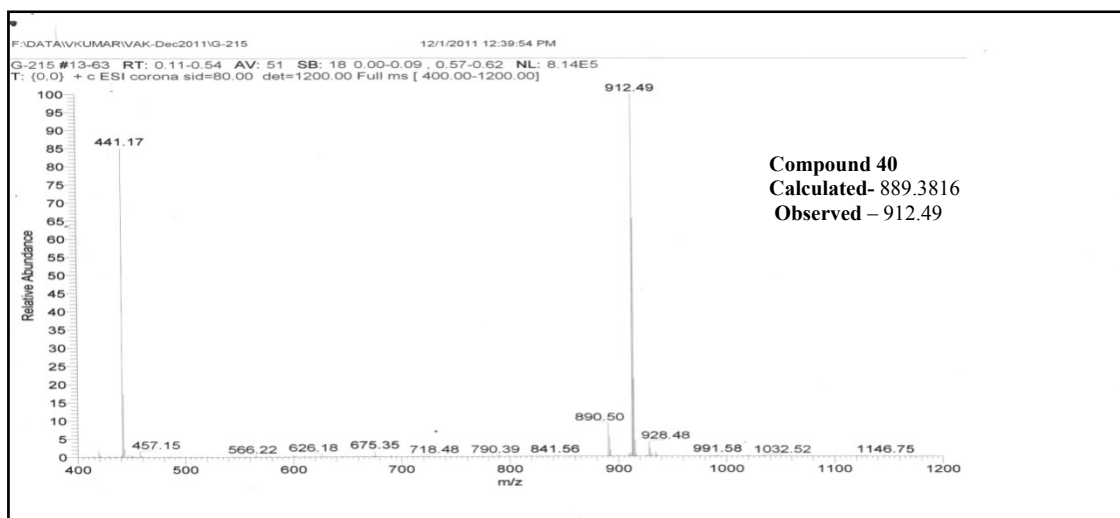
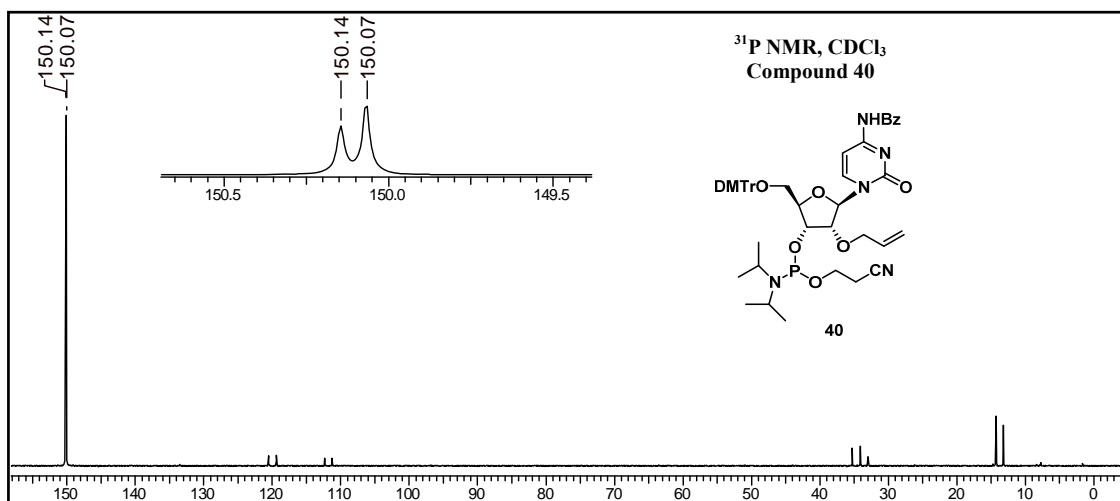
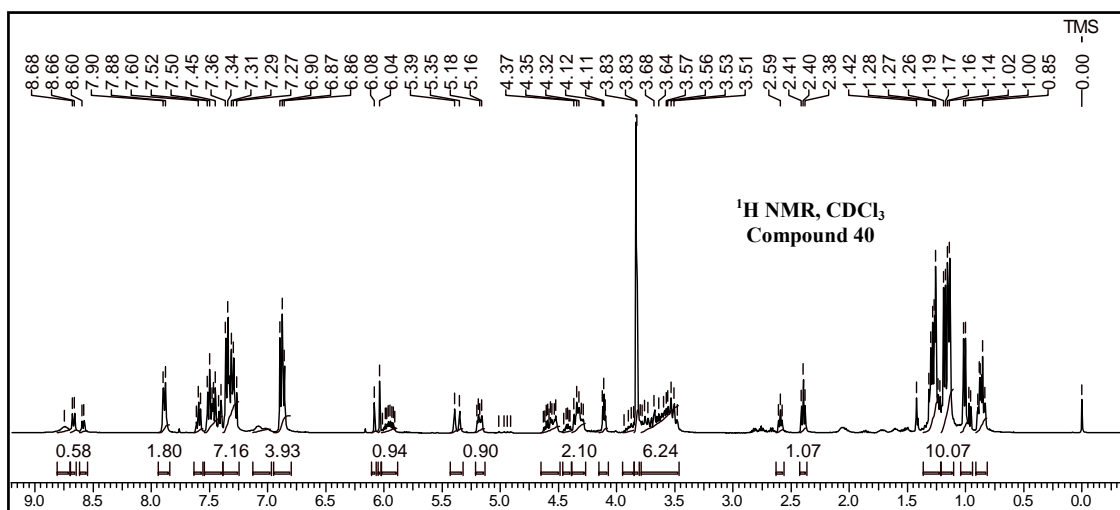


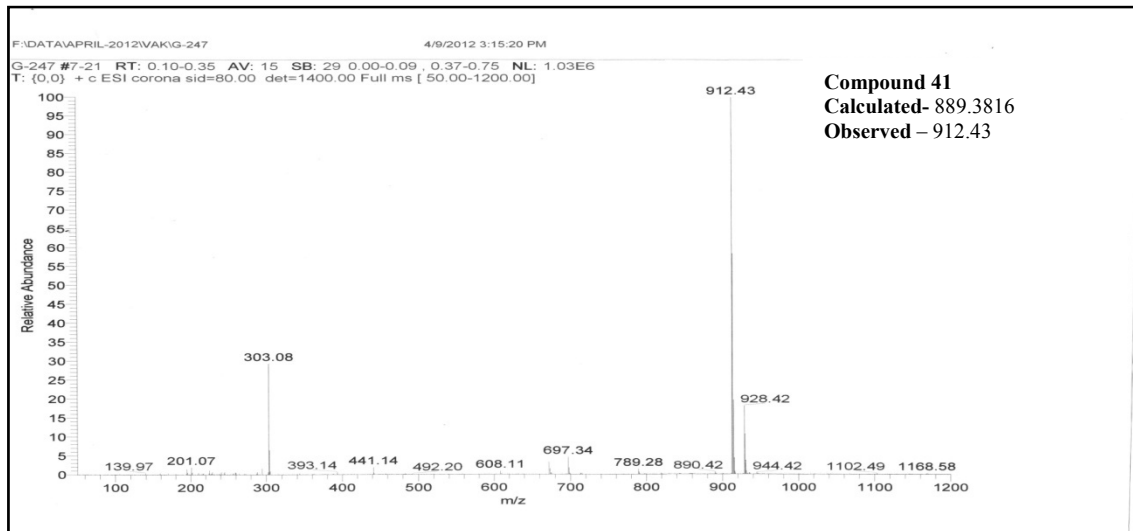
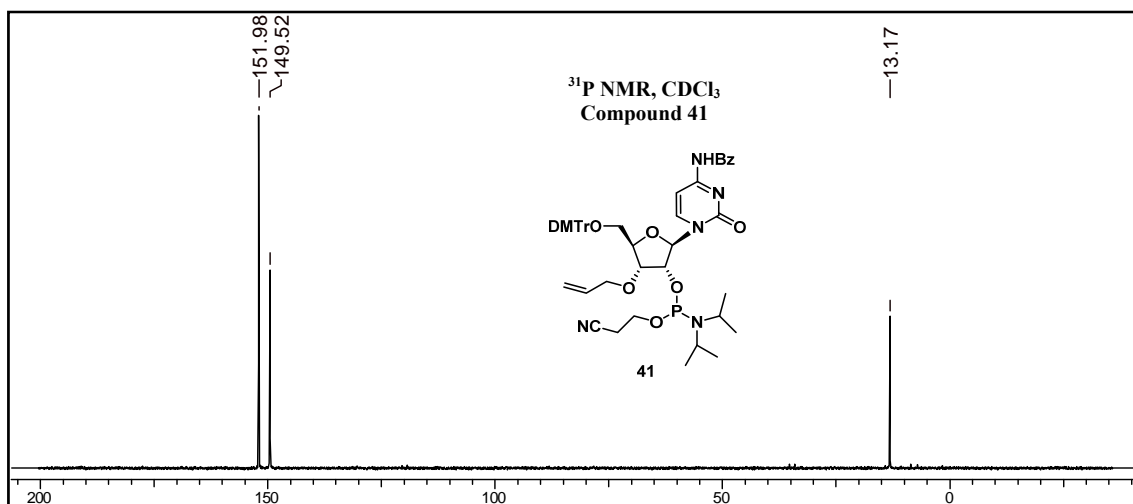
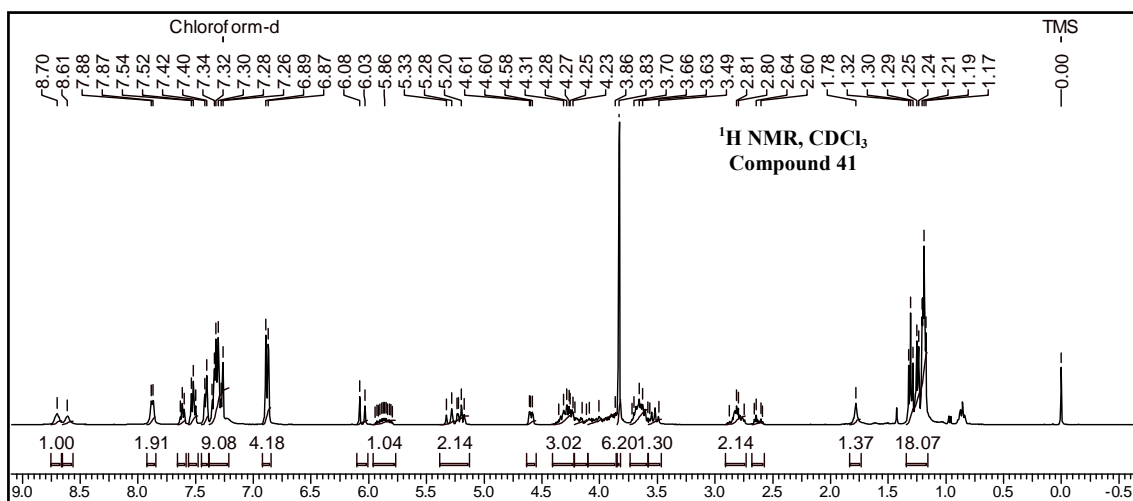


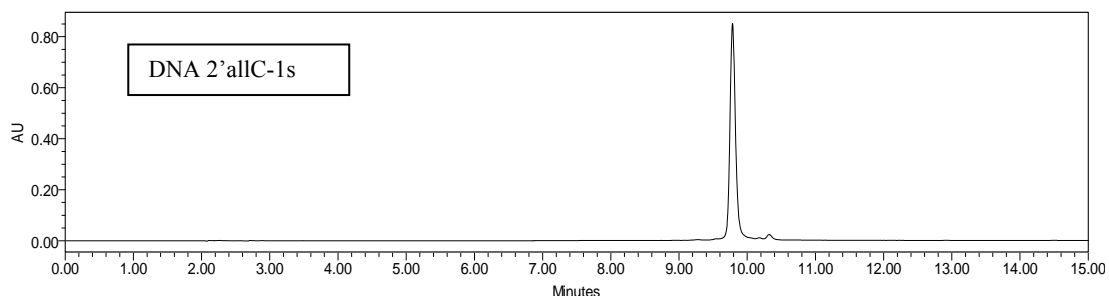
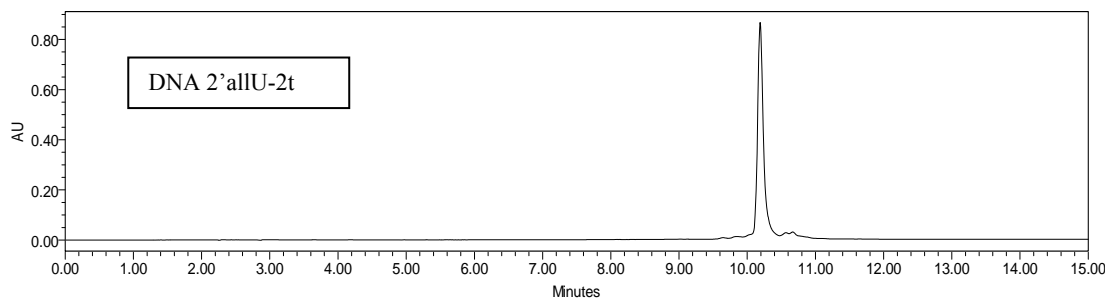
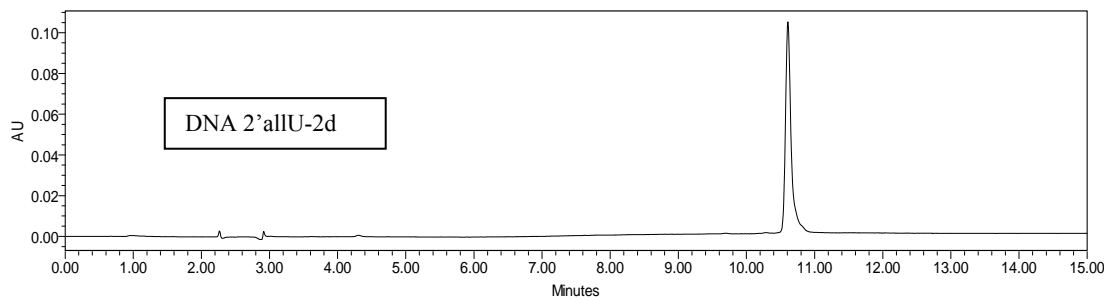
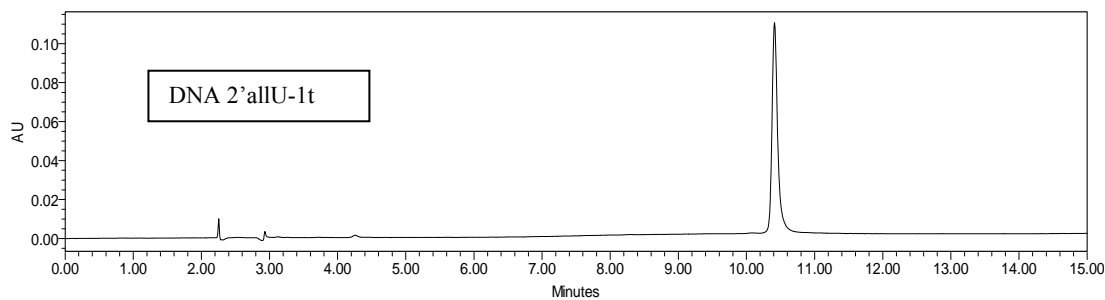
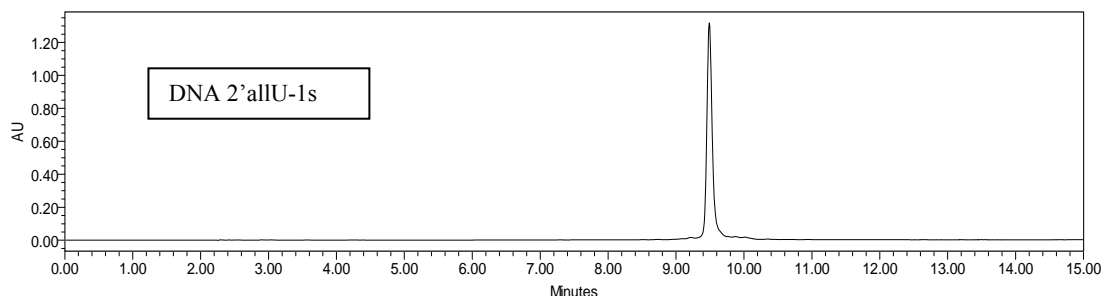


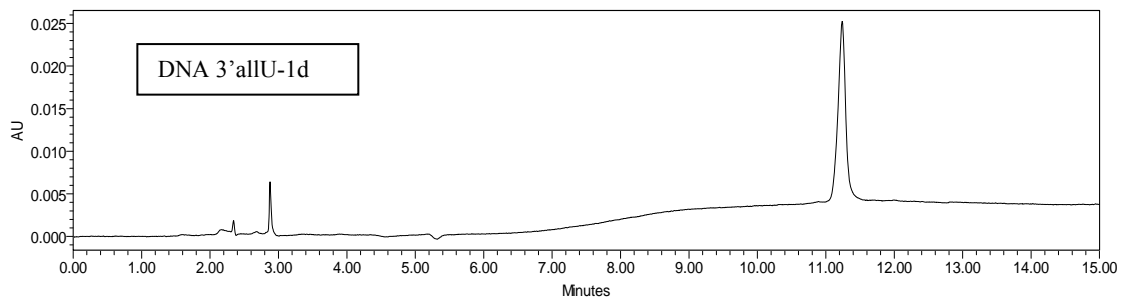
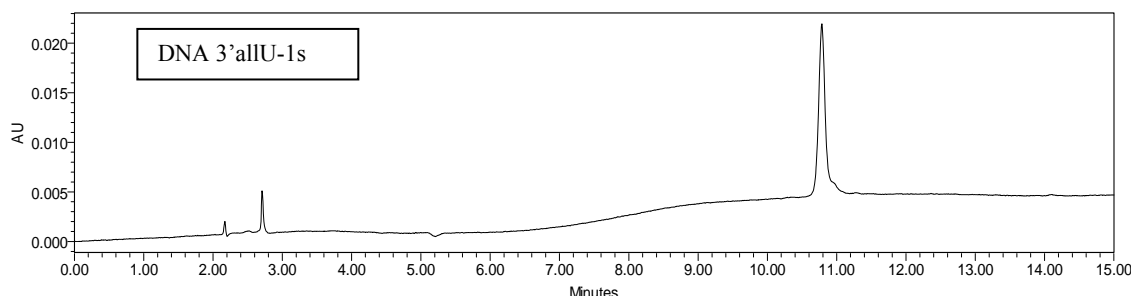
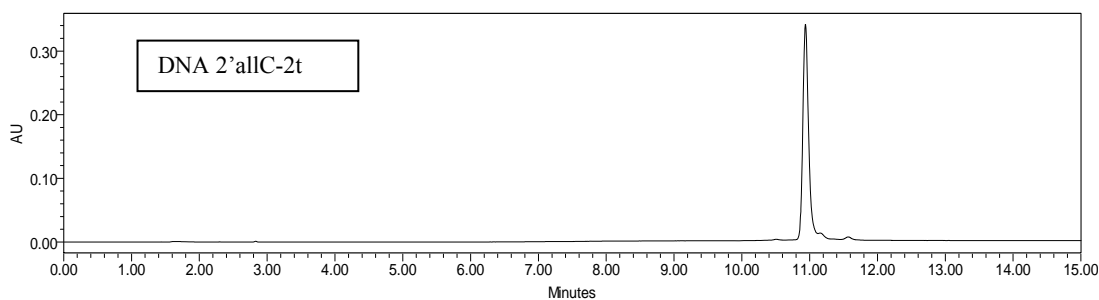
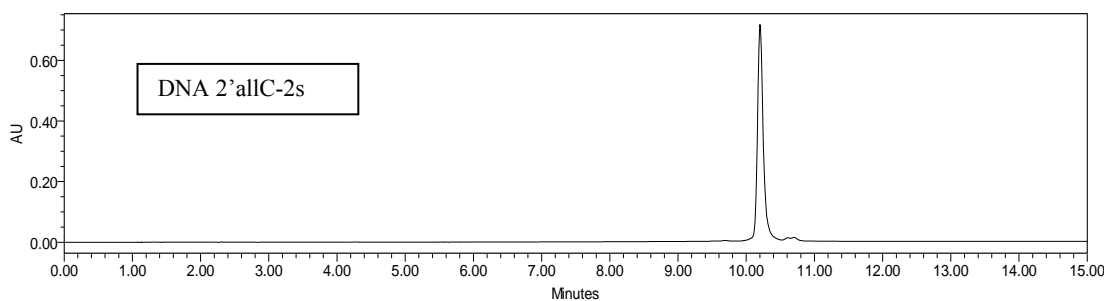
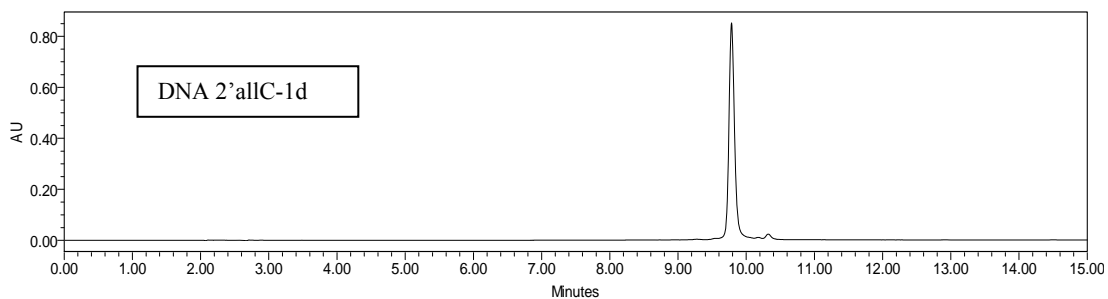


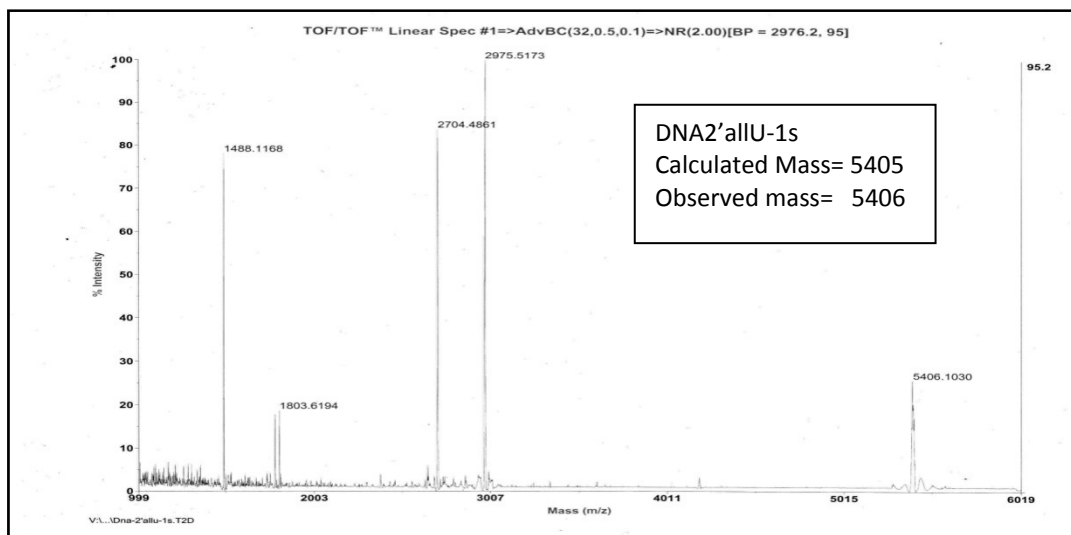
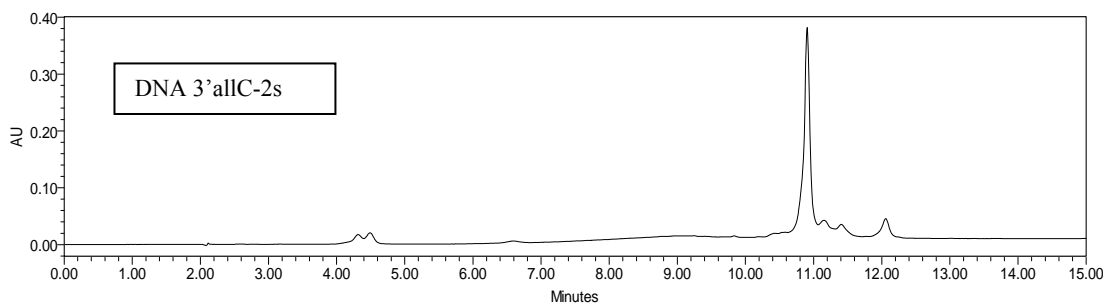
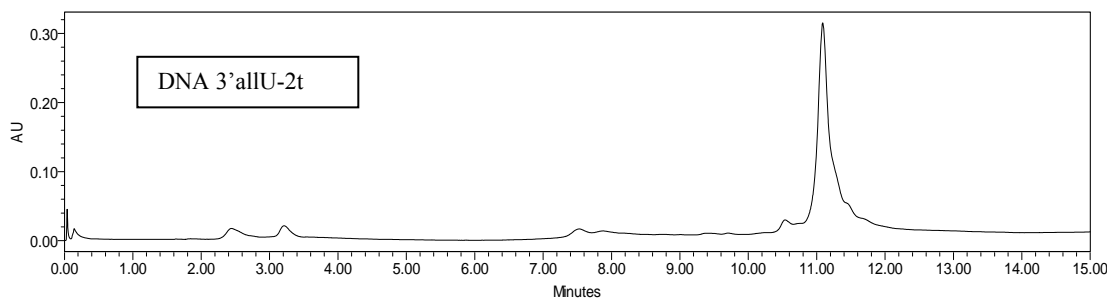


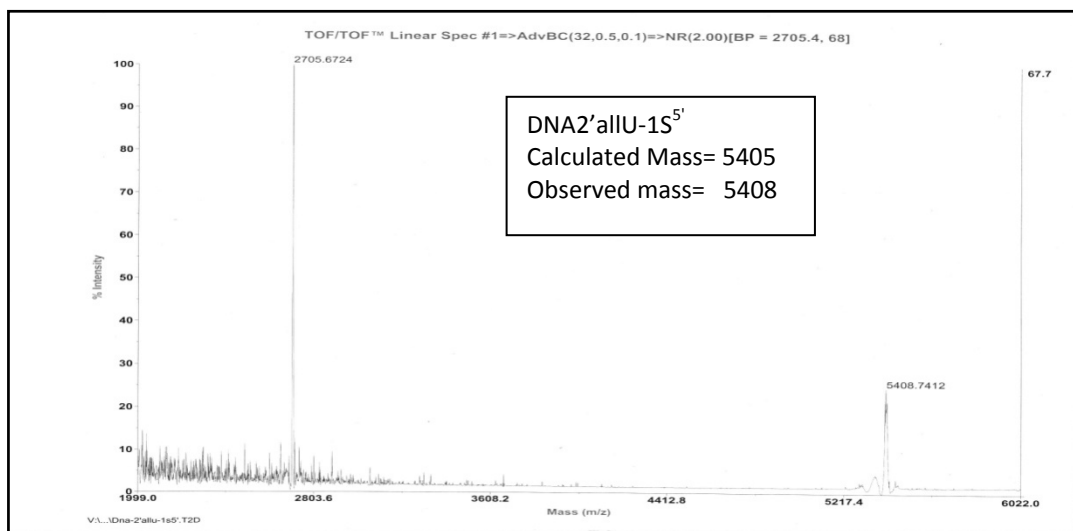
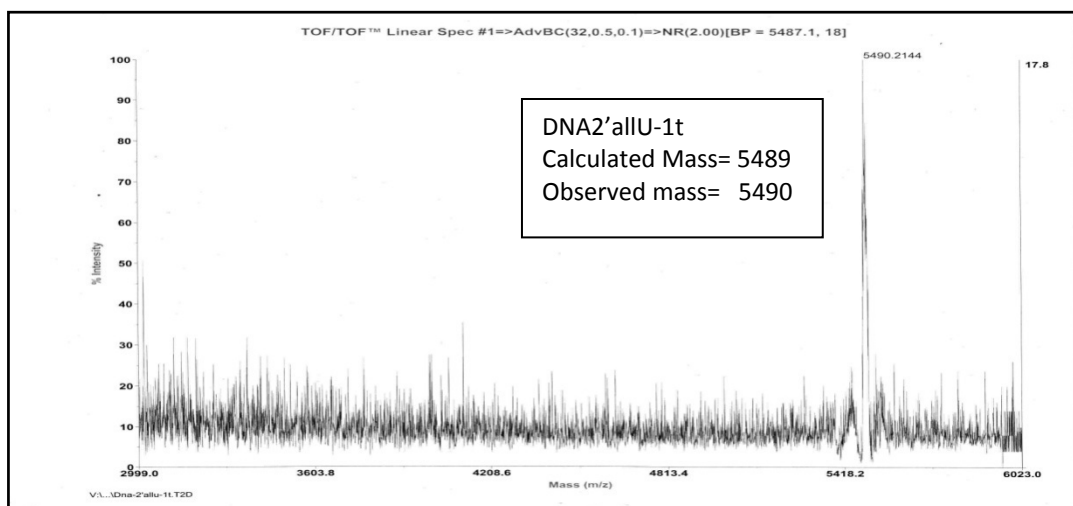
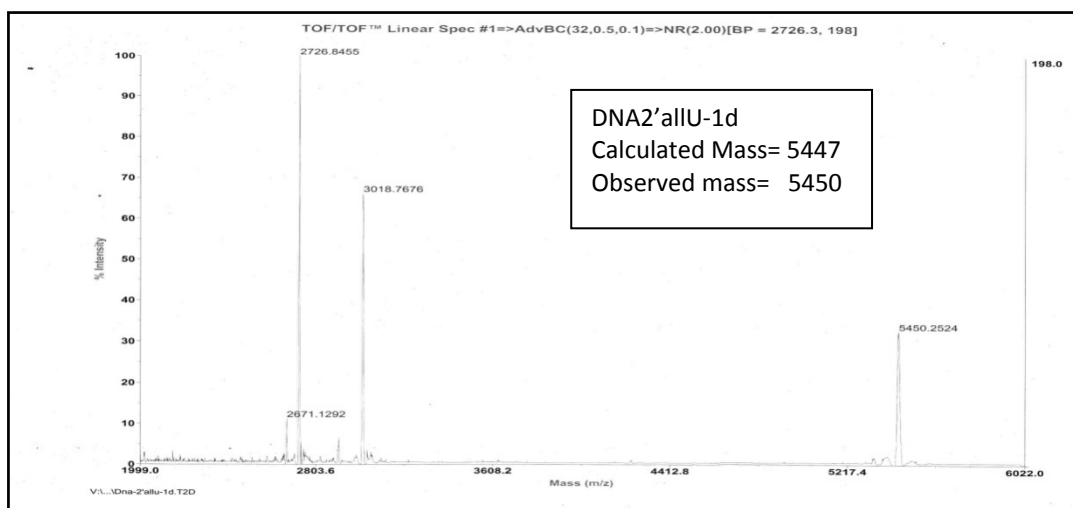


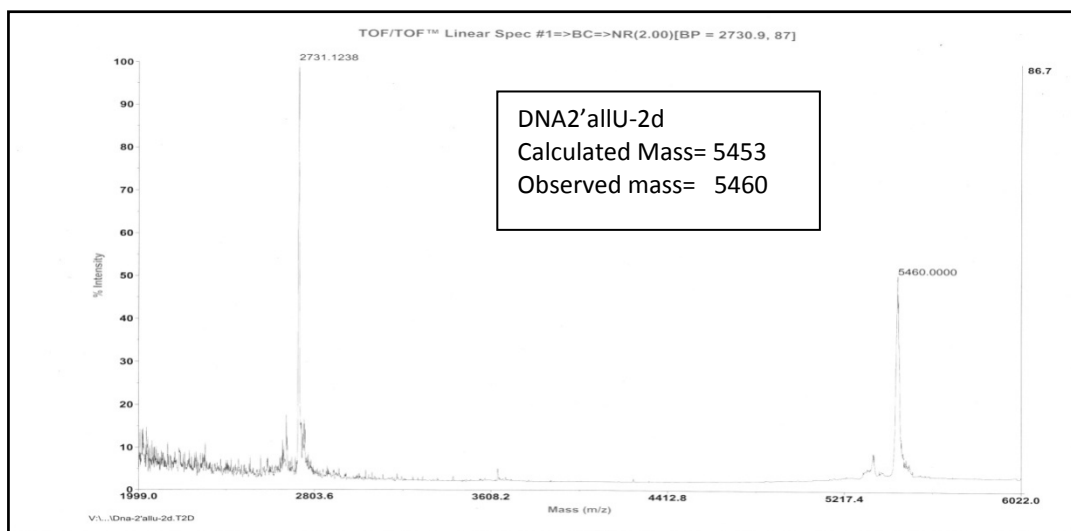
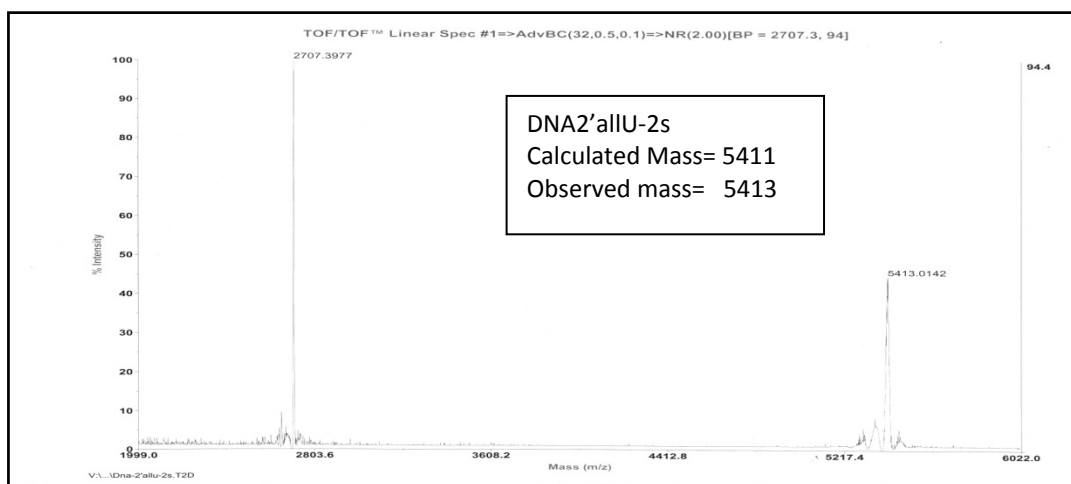
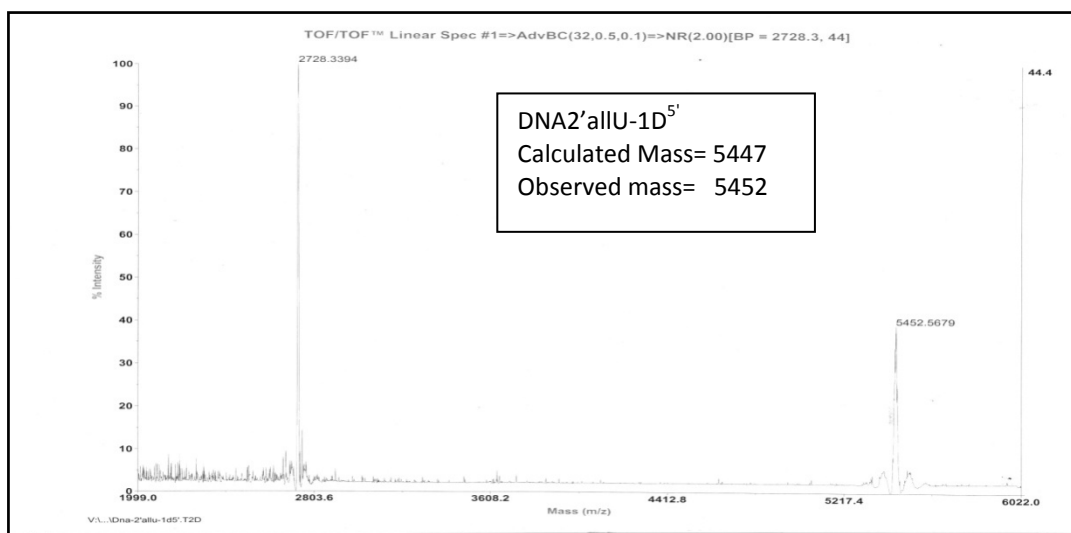


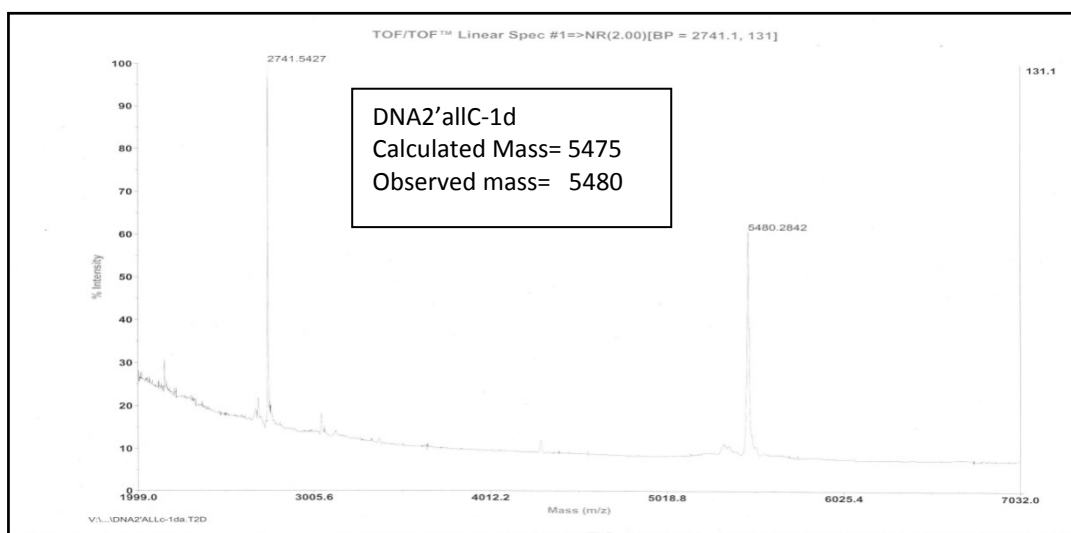
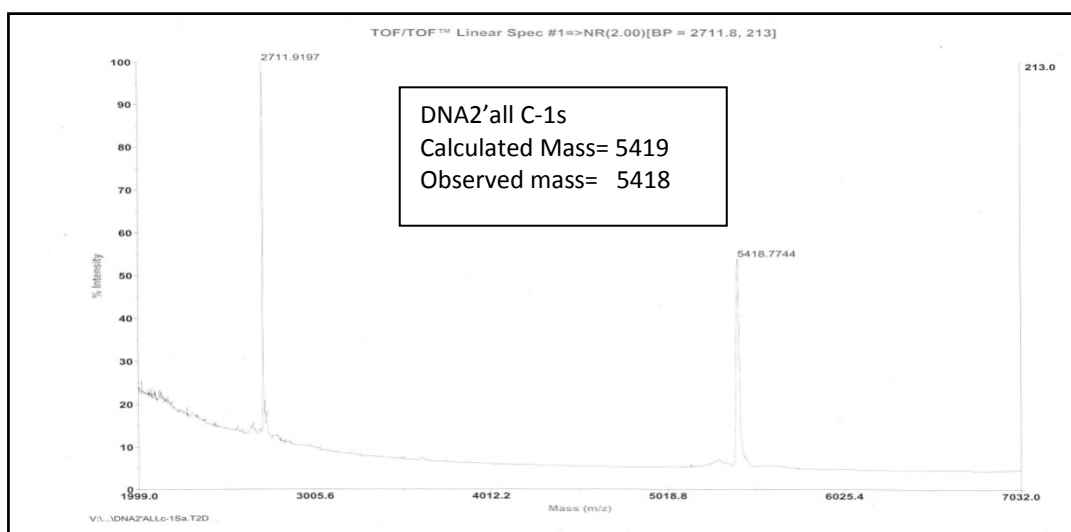
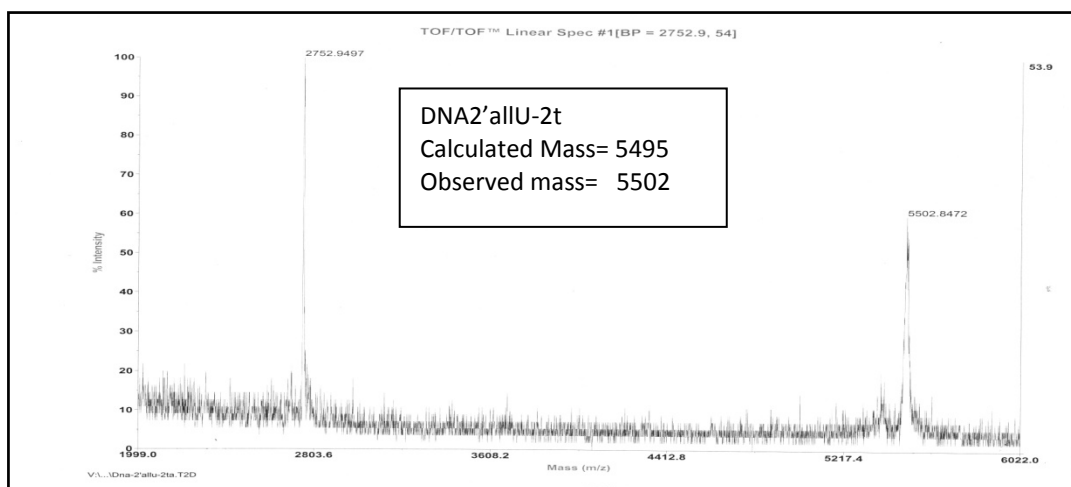


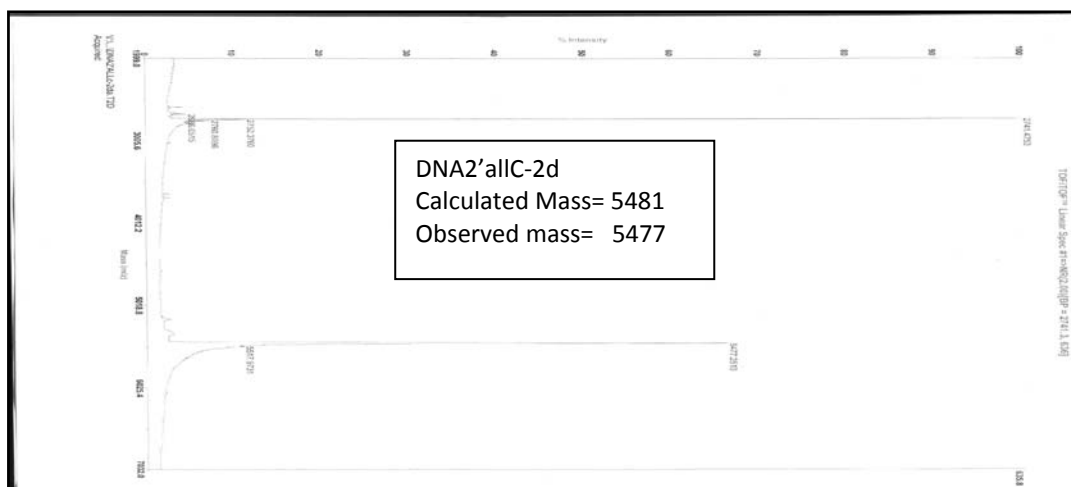
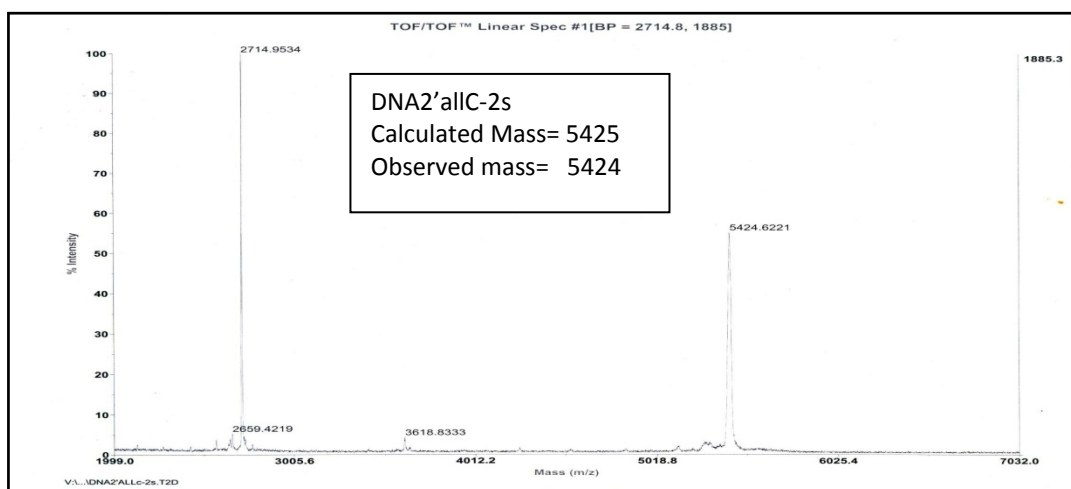
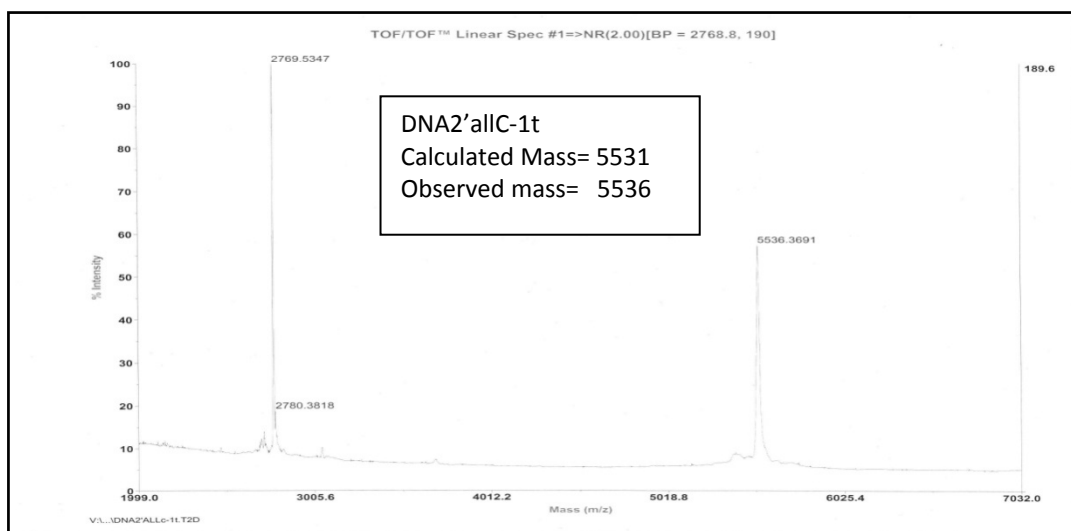


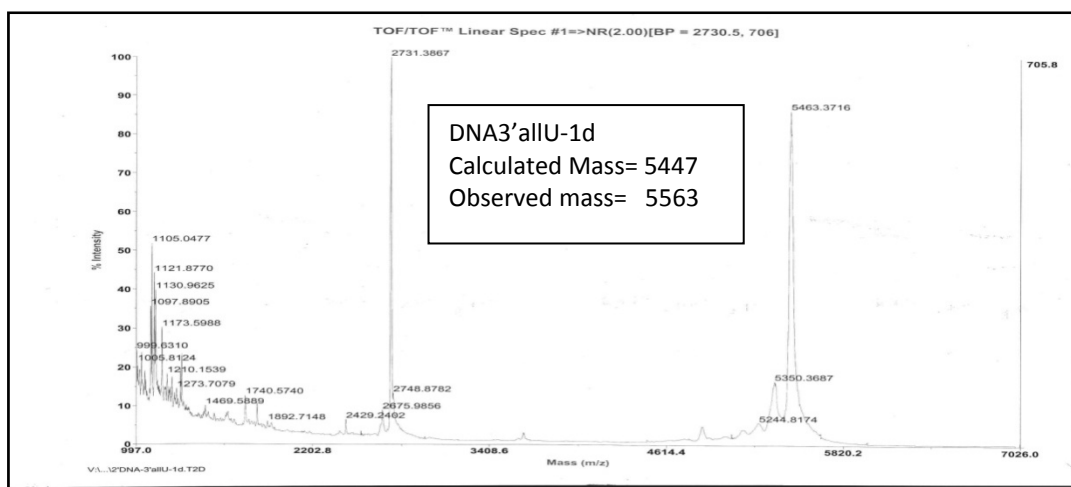
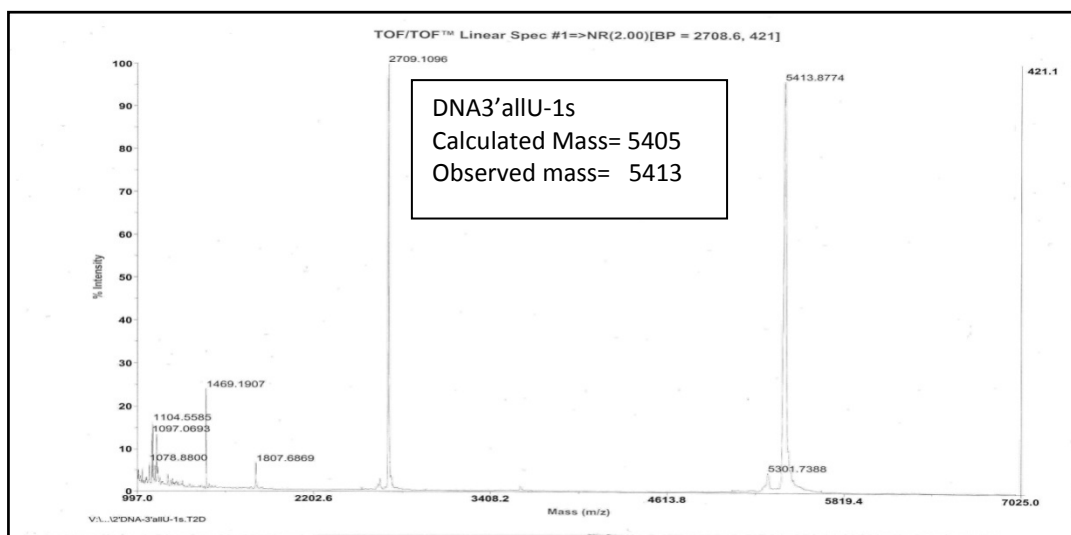
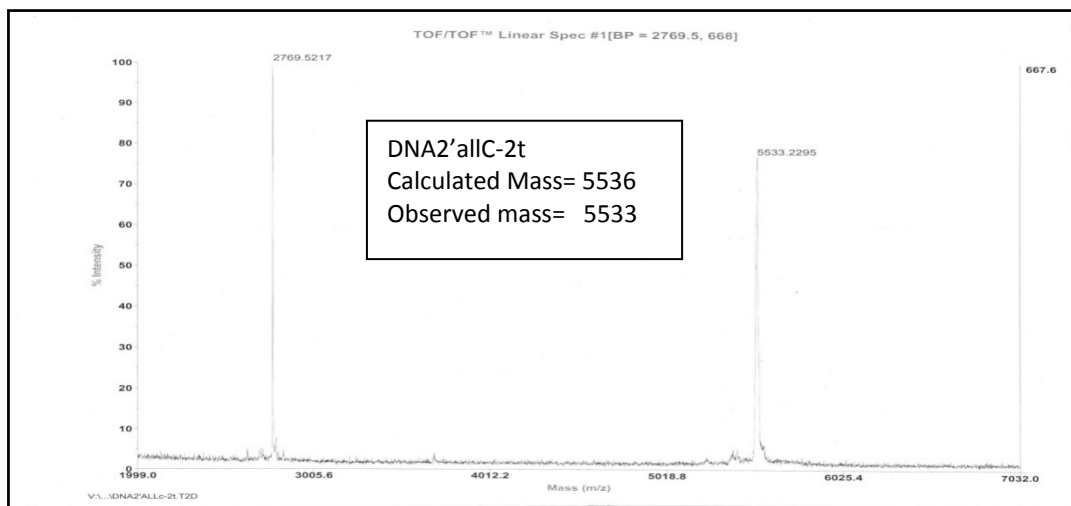


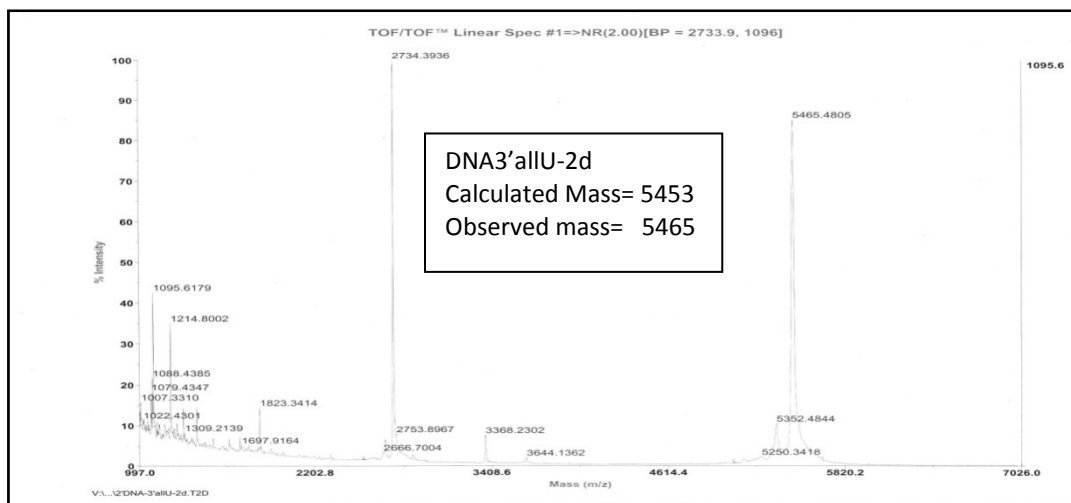
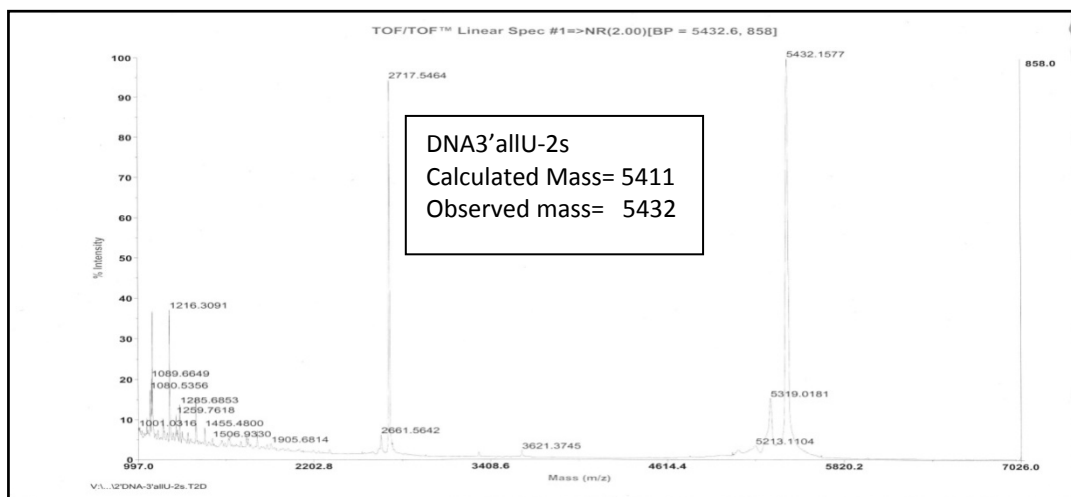
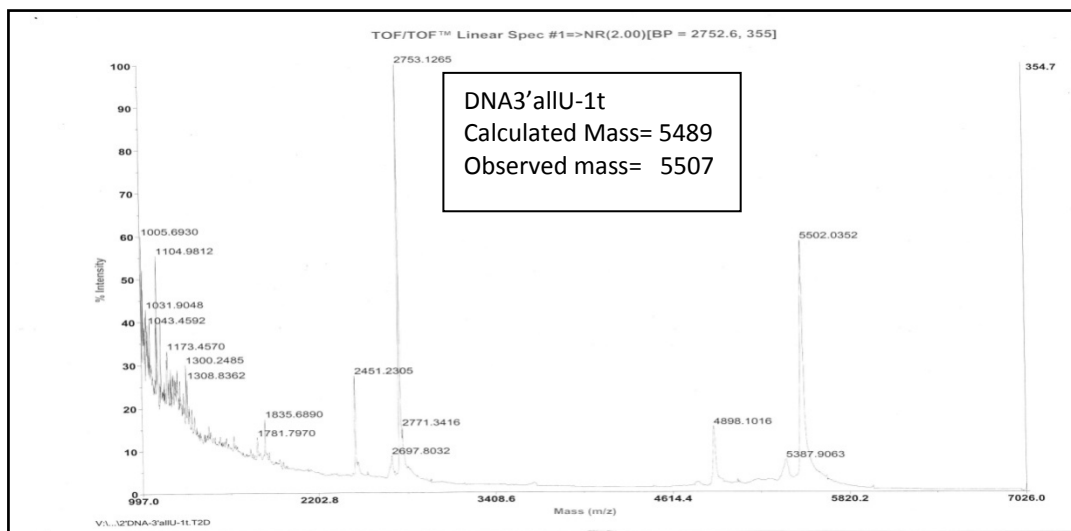


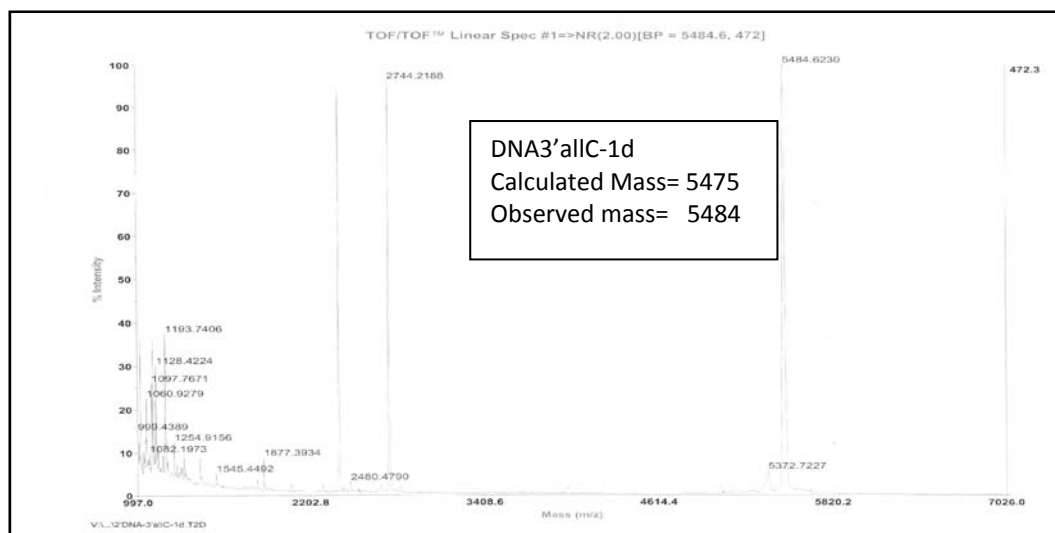
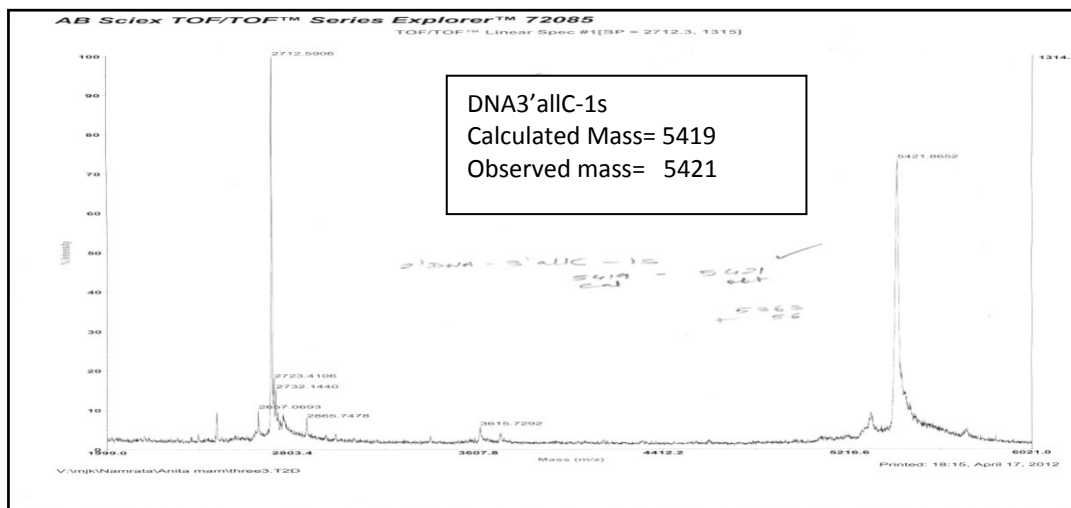
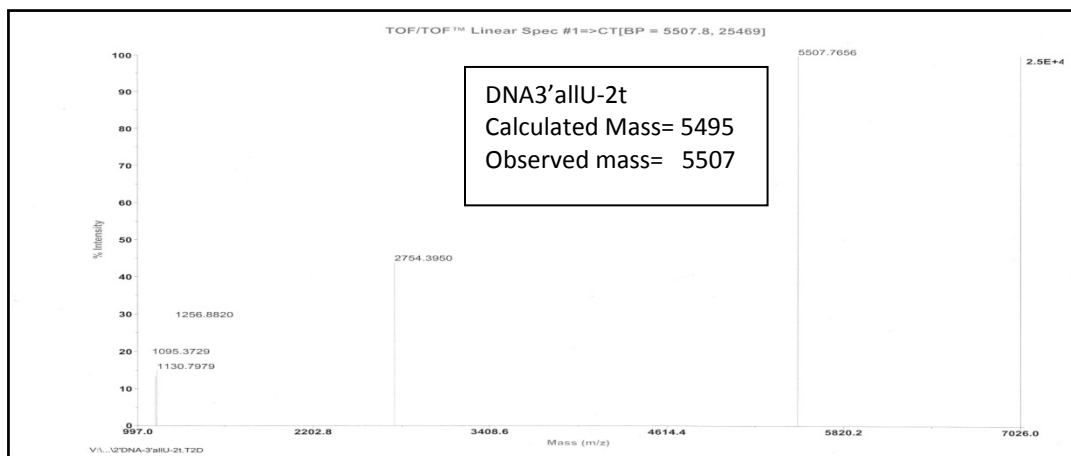


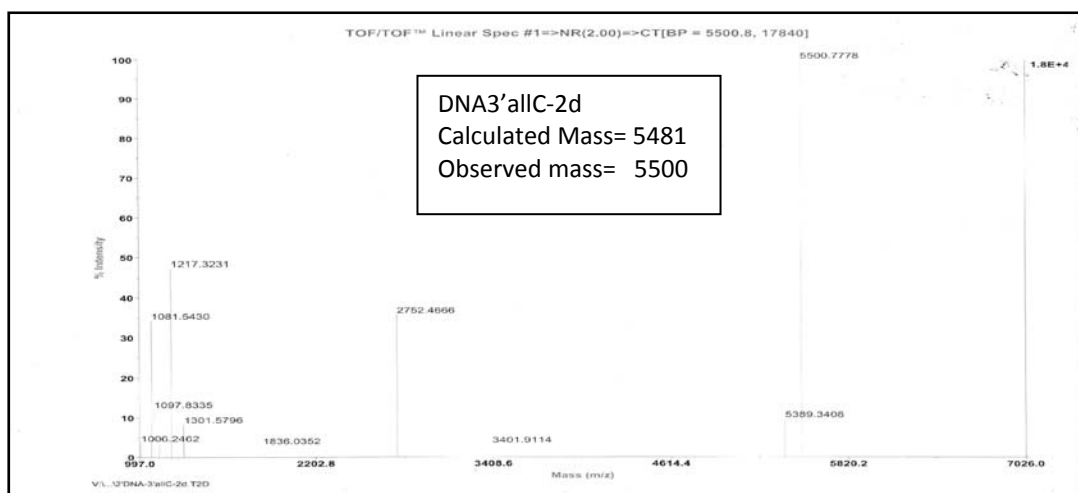
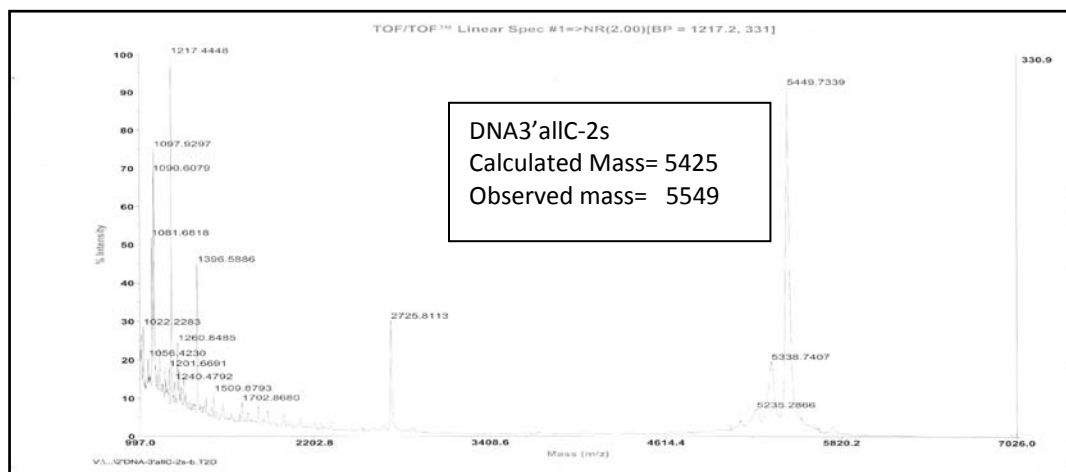
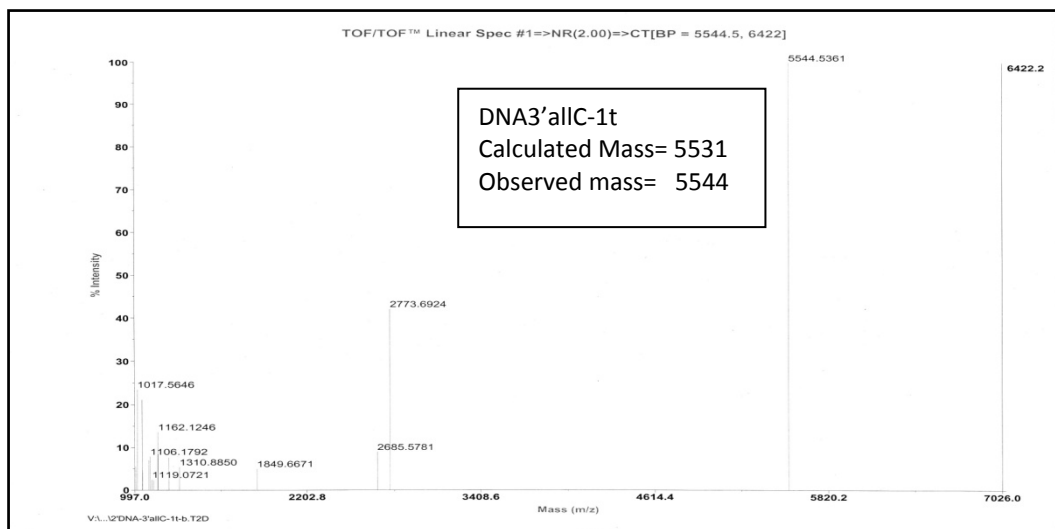


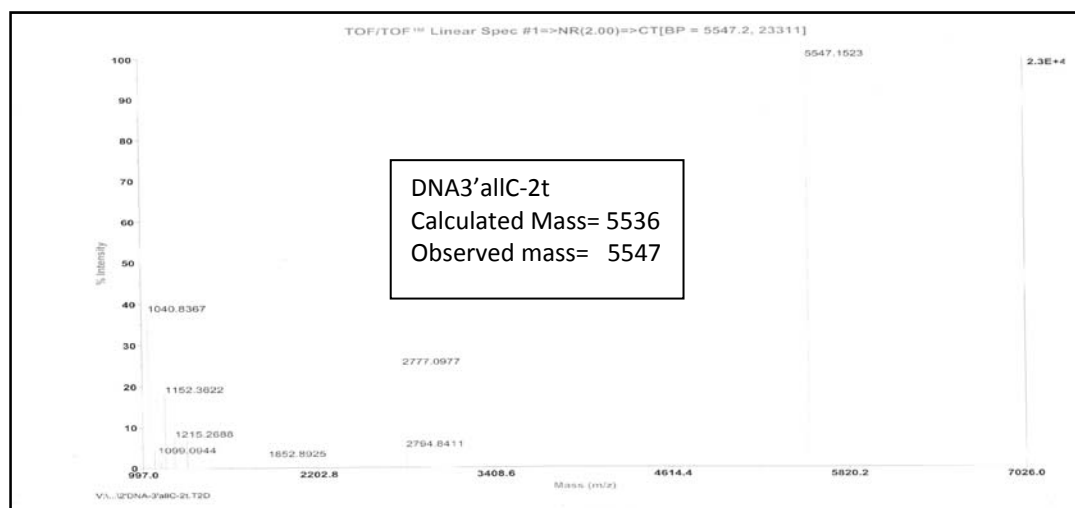












3.6 References

1. (a) Iribarren, A.M., Sproat, B.S., Neuner, P., Sulston, I., Ryder, U. and Lamond, A.I., *Proc. Natl. Acad. Sci. USA.*, **1990**, *87*, 7747-7751, (b) Sproat, B.S.; Iribarren, A.M., Garcia, R.G., Beijer, B., *Nucleic Acids. Res.*, **1991**, *19*,No. 4, 733-738.
2. (a) Stephenson, M. L., Zamecnik, P.C., *Proc. Natl. Acad. Sci. USA*, **1978**, *75*, 285, (b) Zamecnik, P.C., Stephenson, M. L., *Proc. Natl. Acad. Sci. USA*; **1978**, *75*, 280.
3. (a) Dutta, S., Bhaduri, N., Rastogi, N., Chandel, S. G., Vandavasi, J. K., Upadhaya, R. S., Chattopadhyaya, J., *Med. Chem. Commun.*, **2011**, *2*, 206, (b) Chiu, Y-L., Rana, T. M., *RNA*, **2003**, *9*, 1034, (c) Bennett, C. F., Swayze, E. E., *Annu. Rev. Pharmacol. Toxicol.*, **2010**, *50*, 259, (d) Lima, F., Prakash, T. P., Murray, H. M., Kinberger, G. A., Li, W., Chappell, A. E., Li, C. S., Murray, S. F., Gaus, H., Seth, P. P., Swayze, E. E., Crooke, S. T., *Cell* **2012**, *150*, 883.
4. (a) Wang, Z. *Methods Mol. Biol.*, **2011**, *676*, 51, b) Davis, S., Lollo, B., Freier, S., Esau, C., *Nucleic Acids Res.* **2006**, *34*, 2294.
5. (a) Kole, R., Krainer, A.R., Altman, S., *Nat.Rev.Drug Discov.*, **2011**, *11*, 125, (b) Prakash, T.P., *Chem. Biodiversity*, **2011**, *8*, 1616, (c) Kumar, V.A., Ganesh, K.N., *Curr. Topics. Med. Chem.*, **2007**, *7*, 715.

6. Freier, S.M., Altmann, K. H., *Nucleic Acids Res.*, **1997**, *25*, 4429-4443.
7. Stein, C.A., Cohen, J.S., ed., *Oligodeoxynucleotides-Antisense Inhibitors of Gene Expression.*, London: Macmillan Press.,**1989**, 97.
8. (a) Monia, B.P., Lesnik, E.A., Gonzales, C., Lima, W.F., McGee, D., Guinasso, C.J., Kawasaki, A.M., Cook, P.D., Freier, S.M., *J.Biol.Chem.*, **1993**, *268*, 14514-14522. (b) Zang, R., Lu, Z. Zhao, H., Zhang, X., Diasio, R.B., Habus, I. Jiang, Z., Iyer, R.P., Yu, D., Agarwal, S., , *Biochem. Pharm.*, **1995**, *50*, 545-556. (c) Zhao, Q., Temsamani, J., Iadarola, P.L., Jiang, Z., Agarwal, S., *Biochem. Pharm.*, **1995**, *51*,173-182. (d) Baker, B.F., Lot, S.S., Condon, T.P., Cheng-Flournoy, S., Lesnik, E.A., Sasmor, H.M., Bennett, C.F., *J.Biol. Chem.*, **1997**, *272*, 11994-12000 (e). Mckay, R.A., Miraglia, L.J., Cummins, L.L., Owens, S.R., Sasmor, H., Dean, N.M., *J.Biol. Chem.*, **1999**, *274*, 1715-1722. (f). Henry, S., Stecker, K., Brooks, D., Montieth, D., Conklin, B., Bennett, C.F., *J.Pharm. Exp. Ther.*, **2000**, *292*, 468-479. (g) Geary, R.S., Watanabe, T.A., Truong, L., Freier, S., Lesnik, E.A., Sioufi, N.B., Sasmor, H., Manoharan, M. Levin, A.A., *J.Pharm. Exp. Ther.*, **2001**, *296*, 890-897.
9. (a) Inoue, H., Hayase, Y., Asaka, M., Imura, A., Iwai, S., Miura, K., Ohtsuka, E., *Nucleic Acid Res.*, **1987**, *15*, 6131-6148. (b) Mukai, S., Shibahara, S., Morisawa, H., *Nucleic Acids Res. Symp. Ser.*, **1988**, *19*, 117-120. (c) Inoue, H., Hayase, Y., Iwai, S., Ohtsuka, E., *Nucleic Acids Res. Symp. Ser.*, **1988**, *19*, 135-138. (d) Shibahara, S., Mukai, S., Nisihara, T., Inoue, H., Ohtsuka, E., Morisawa, H., *Nucleic Acid Res.*, **1987**, *15*, 4403-4415. (e) Inoue, H., Hayase, Y., Iwai, S., Ohtsuka, E., *FEBS Lett.*, **1987**, *215*, 327-330.
10. Sproat, B.S., Lamond, A.I., Beijer, B., Neuner, P., Ryder, U., *Nucleic Acid Res.*, **1989**, *17*, 3373-3386.
11. Prakash, T.P., Kawasaki, A.M., Wancewicz, E.V., Shen, L., Monia, B.P., Ross, B.S., Bhat, B., Manoharan, M., *J. Med. Chem.*, **2008**, *51*, 2766.
12. Seth, P.P., Siwkowski, A., Allerson, C.R., Vasquez, G., Lee, S., Prakash, T.P., Wancewicz, E.V., Witchell, D., Swayze, E.E., *J. Med. Chem.*, **2009**, *52*, 10-13.
13. Boiziau, C., Larrouy, B., Sproat, B.S., Toulmé, J.J., *Nucleic Acids Res.*, **1995**, *23(1)*, 64-71.

14. Haseloff, J., Gerlach, W.L., *Nature*, **1988**, 334, 585-591.
15. Cech, T., *Curr. Opin. Struct. Biol.*, **1992**, 2, 605-609.
16. Paolella, G., Sproat, B.S., Lamond, A.I., *EMBO J.*, **1992**, 11, 1913-1919.
17. Beigelman, L., Karpeisky, A., Matulic-Adamic, J., Haeberli, P., Sweedler, D., Usman, N., *Nucleic Acids Res.*, **1995**, 23, No.21, 4434-4442.
18. (a) Ruparel, H., Bi, L., Li, Z., Bai, X., Kim, D.H., Turro, N.J., Ju, J., *Proc. Natl. Acad. Sci., USA*, **2005**, 102, 5932-5937.; (b) Oh, G., Nam, Y., Shin, D., Ahn, D-R., *Bull. Korean Chem. Soc.*, **2009**, 30, 2769-2772.
19. Wagner, D., Verheyden, J.P.H., Moffatt, J.G., *J. Org. Chem.*, **1974**, 39, 24.
20. David, S., Thieffry, A., Veyrieres, A., *J. Chem Soc. Perkin I*, **1981**, 1796.
21. Gopalkrishnan, V., Kumar, V., Ganesh, K.N., *Nucleosides Nucleotides*, **1992**, 11, (6), 1263-1273.
22. (a) Divaker, K.J., Reese, C.B., *J. Chem. Soc. Perkin Trans. I*, **1982**, 1171-1176. (b) Xu, Y.Z., Zeng, Q., Swann, P.F., *J. Org. Chem.*, **1992**, 57, 3839-3845.
23. Chang, C.J., Ashworth, D.J., Chern, L.J., Gomes, J.D., Lee, C.G., Mou, P.W., Narayan, R., *Org. Mag. Res.*, **1984**, 22, 671.
24. Krutzfeldt, J., Rajewsky, N., Braich, R., Rajeev, K.G., Tuschel, T., Manoharan, M., Stoffel, M., *Nature*, **2005**, 438, 685.
25. Kang, S.H., Cho, M.J., Kole, R., *Biochemistry*, **1998**, 37, 6235.
26. (a) Koshkin, A., Singh, S.K., Nielsen, P., Rajwanshi, V.K., Kumar, R., Meldgaard, M., Olsen, C.E., Wengel, J., *Tetrahedron*, **1998**, 54, 3607, (b) Obika, S., Nanbu, D., Hari, Y., Andoh, J., Morio, K., Doi, T., Imanishi, T., *Tetrahedron. Lett.*, **1998**, 39, 5401. (c) Braasch, D.A., Corey, D.R., *Chem. Biol.*, **2001**, 8, 1. (d) Vester, B., Wengel, J., *Biochemistry*, **2004**, 43, 13233. (e) Koizumi, M., *Biol. Pharm. Bull.*, **2004**, 27, 453.
27. Giannaris, P.A., Damha, M.J., *Nucleic Acids Res.*, **1993**, 21, 4742-4749.

Chapter 4

Synthesis of 2'-5'-linked thrombin binding aptamer (*iso*TBA), its quadruplex formation, and application as a thrombin inhibitor

G-quartets.³ Aptamers are chemically synthesized oligonucleotides with abilities to bind to small molecules, peptides, proteins with selectivity, specificity and affinity equal or superior to those of antibodies.⁴ A thrombin binding aptamer (TBA), a 15-mer DNA oligonucleotide, 5'-GGTTGGTGTGGTTGG3' was discovered in 1992 by *in vitro* selection.⁵ This aptamer was found to inhibit fibrin-clot formation by binding to the thrombin protein with high selectivity and affinity. The RNA binding selectivity and stability of regioisomeric 2'-5'-linked *iso*DNA towards endonucleases as seen in the earlier work (Chapters 2,3) prompted the synthesis of isomeric TBA oligonucleotides aptamers, to examine their quadruplex forming possibility and anti-thrombin activity which remains unexplored. These 2'-5'-linked G-rich aptamers synthesized (*iso*TBA2 and *iso*TBA3) indeed, did form stable G-quadruplexes, structurally similar to TBA and were found to bind to thrombin. Surprisingly the anti-thrombin activity was also exhibited by both the *iso*TBA sequences proving their functional capability, though less than the TBA aptamer. Additionally, high enzymatic stability (SVPD) towards was observed compared to unmodified TBA.

4.1 Introduction to present work

4.1.1 G-quadruplex formation, structure and topology

G-quadruplexes are formed when four G-rich oligonucleotide strands associate through hydrogen-bonding by means of G-tetrad formation, as discussed in Chapter 1, Section 1.7.1, resulting in a right-handed helical motif or by folding of the single G-rich strand to form stacked G-tetrads.⁶ The stacked tetrads are stabilized by sandwiched monovalent cations co-ordinated to the O6 oxygen atoms of the guanines (Figure 1). As discussed in Chapter 1, Section 1.7.4, G-quadruplexes have been found to occur widely in the genome, mainly in regions that are associated with regulatory activity, such as promoters, telomeres, centromeres, etc. Telomeric repeats in a variety of organisms have been shown to form quadruplexes both *in vitro* and *in vivo* in some cases. The human telomeric repeat (same for all vertebrates) is several repeats of the sequence d(GGTTAG); the quadruplex structure formed is well-established by NMR and X-ray crystal structure

determination. The formation of the quadruplex structure in telomeres has been shown to decrease the activity of the enzyme telomerase which is responsible for maintaining the length of telomeres and is implicated in around 85% of all cancers. Thus this has become an active target for drug discovery.⁷

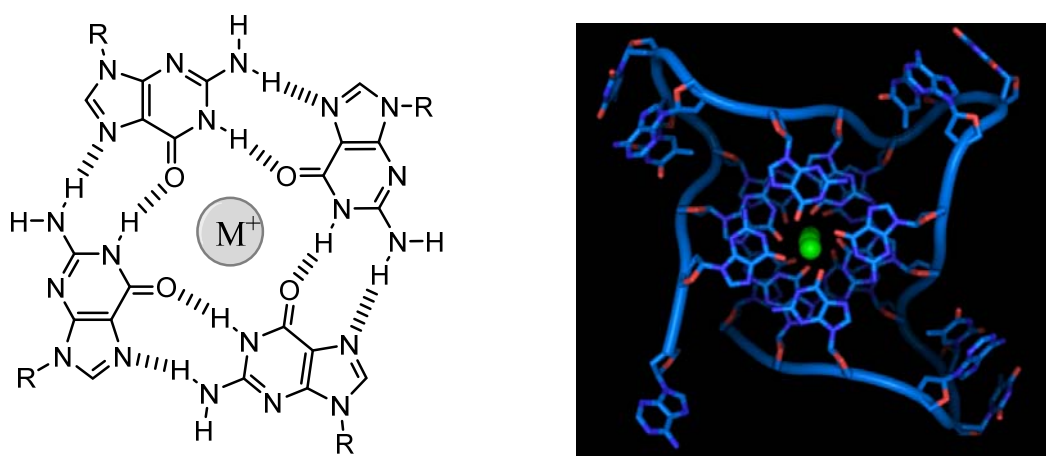


Figure 1. The G-tetrad motif and a G-quadruplex.

A quadruplex-forming sequence can exhibit equilibrium between several different G-tetrad conformations. The biological function and molecular recognition properties may well be associated with one predominant conformation. The relative arrangement of the strands can have different polarities. Strands can be parallel, antiparallel and mixed type. A single intramolecular G-quadruplex structure can be based on loops with different conformations (Figure 2). Both loop length and sequence play a role in determining the folded conformation and thermodynamic stability of a quadruplex-forming sequence.

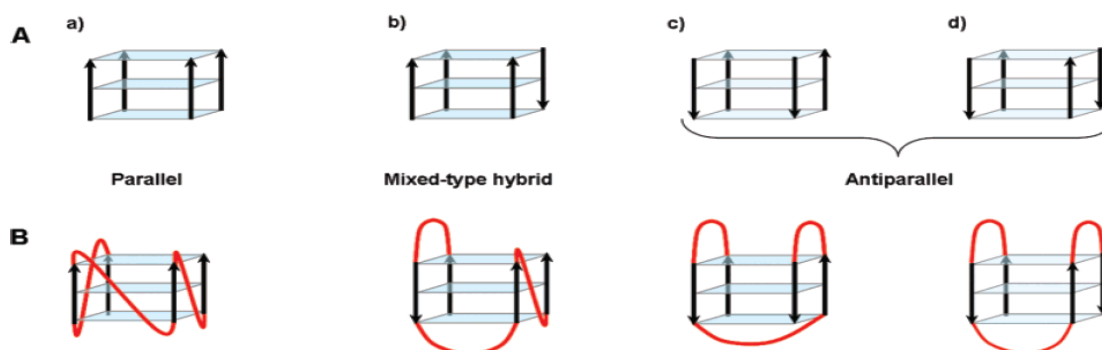


Figure 2: (A) Different arrangements of strand polarity, arrows show 5' → 3' polarity: (a) all strands parallel, (b) three parallel and one antiparallel, (c) two pairs of adjacent parallel strands, and (d) alternating antiparallel strands. (B) Various loop topologies leading to different arrangements of strand polarity. (Bugaut, A. and Balasubramanian, S., *Biochemistry*, 2008, 47, 689-697)

4.1.2 Quadruplex stability dependence on metal ions

G-quadruplexes have been demonstrated to be stabilized by different cations. These include monovalent cations such as Na^+ , K^+ , Li^+ , Cs^+ , etc., and also divalent cations such as Ba^{++} , Ca^{++} , Sr^{++} ,⁸ etc. In addition, non-metal cations such as NH_4^+ ⁹ have also been shown to result in stable G-quadruplexes. Changes in the stabilizing cation have also been exploited as conformation¹⁰ and redox¹¹ switches in literature.

4.1.3 Molecular crowding conditions

A characteristic of the interior of all cells is the high total concentration of macromolecules they contain. Such media are therefore, termed ‘crowded’ rather than ‘concentrated’ because, in general, no single macromolecular species occurs at high concentration, but taken together, the macromolecules occupy a significant fraction (typically 20-30%) of the total volume. This fraction is thus, physically unavailable to other molecules. Molecular crowding is more accurately termed as the excluded volume effect, because the mutual impenetrability of all solute molecules is its most basic characteristic (Figure 3). How much of the intracellular volume is unavailable to other macromolecules depends upon the numbers, sizes and shapes of all the molecules present in each compartment.¹² **Crowding is not confined to cellular interiors, but also occurs in the extracellular matrix of tissues such as cartilage and blood plasma.**

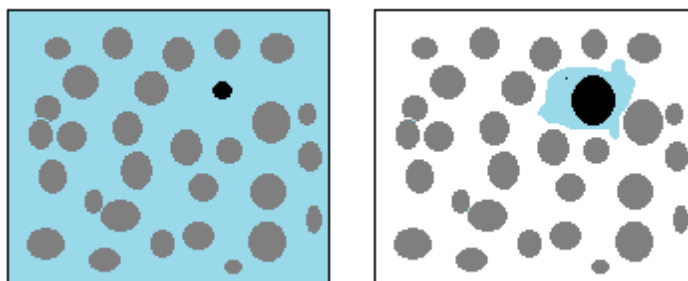


Figure 3. Illustration of the volume of solvent available (blue) for two molecules of different sizes (black spheres) in a compartment containing a high concentration of macromolecules (grey spheres). This reduction in available volume increases the effective concentration of macromolecules in concentrated solutions - an effect known as macromolecular crowding: [\(Wikimedia Commons\)](#)

In principle, it is possible to measure the effects of molecular crowding in the system under study by addition to the solution high concentrations of macromolecules that mimic those found within cells. The ideal crowding agent should have a molecular weight in the range 50000 to 200000, be highly water-soluble and not be prone to self-aggregation; it should have a globular rather than an extended shape to prevent solutions becoming too viscous to handle. It should be easily available in the pure form and importantly, should not itself interact with the system under study, except *via* steric repulsion. Commonly used synthetic crowding agents include Ficolls, dextrans, polyethylene glycol and polyvinyl alcohol.

Crowding could explain why molecular chaperones exist despite the ability of many proteins to assemble themselves. Crowding should favour aggregation because of its effect of increasing the thermodynamic activity of partly folded polypeptide chains. It should enhance the aggregation of slow-folding chains, since fast-folding chains can internalize their hydrophobic surfaces before these can bind to those in other chains. **Crowding should also increase the functional activity of chaperones by stimulating their association with partly folded chains.**

Crowding thus influences macromolecular association and conformation, thus playing a role in all biological processes that depend on non-covalent associations and/or conformational changes. It was very recently shown to increase the robustness of gene expression in artificial cellular nanosystems.¹³

In the context of G-quadruplexes, molecular crowding was found to induce human telomere G-quadruplex formation under cation-deficient conditions.¹⁴ Similarly, TBA was shown to fold into a quadruplex in the absence of stabilizing cations, but in the presence of molecular crowding agents or thrombin.¹⁵ The activity of most G-quadruplex stabilizing ligands have been shown to be noticeably reduced under molecular crowding conditions that mimic the physiological milieu.¹⁶ Recently, however, a G-quadruplex stabilizing ligand was shown to enhance the stability of G-quadruplexes, resulting in an increase in anti-telomerase activity in the presence of molecular crowding conditions.¹⁷

4.1.4 Aptamers or Decoy oligonucleotides: An emerging class of therapeutics.

Numerous nucleic acid ligands also termed decoys or aptamers, have been developed during the past 25 years that can inhibit the activity of many pathogenic proteins. Several properties of aptamers make them an attractive class of therapeutic compounds. Their affinity and specificity for a given protein makes it possible to isolate a ligand to virtually any target and further adjusting their bioavailability expands their clinical utility. Development of aptamers that retain activity in multiple organisms facilitates preclinical development. Thus they may prove useful in the treatment of a variety of human maladies, including infectious diseases, cancer, and cardiovascular disease.¹⁸ Aptamers¹⁹ are usually synthetic oligonucleotides that are specifically selected for binding to a certain target, which may range from small molecules to peptides, proteins, or even whole cells. However, natural aptamers also exist in riboswitches. Their binding affinity and specificity may be equal or even superior to that of antibodies (The reported dissociation constants are in the picomolar to micromolar range), and aptamers are known to be able to differentiate and discriminate between even small structural differences that may exist as a result of the

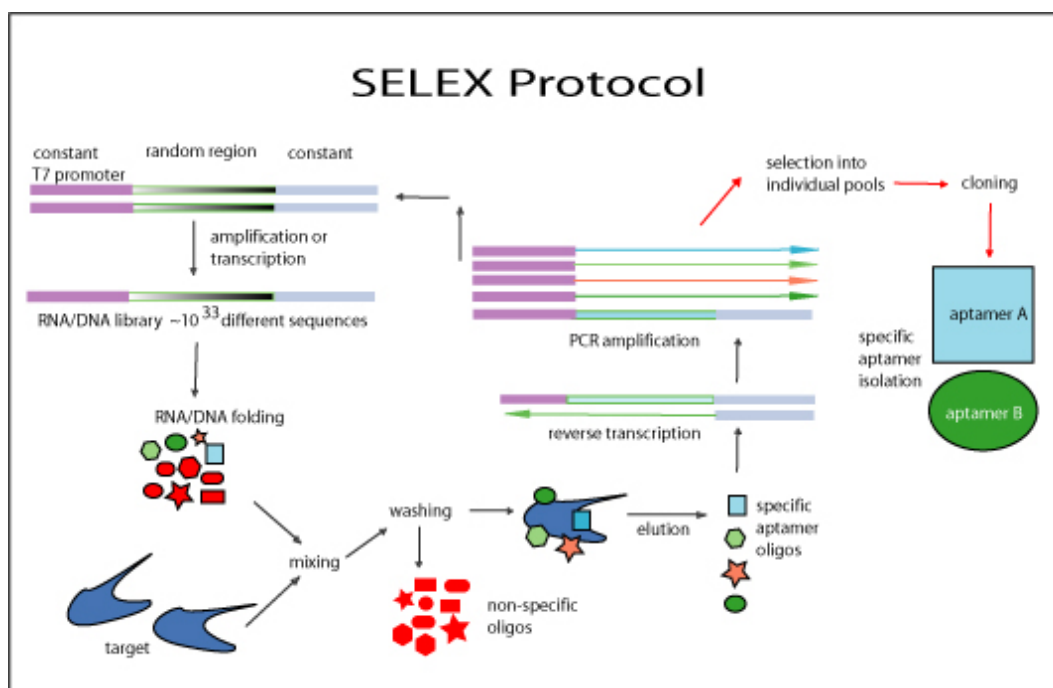


Figure 4. SELEX *in vitro* selection protocol

(<http://www.genelink.com/newsite/products/aptamers.asp>)

presence or absence of a small functional group such as methyl or hydroxyl or even as a result of differing chirality. The word ‘aptamer’ was first coined by Ellington and Szostak²⁰ in 1990. Aptamers were first developed by an *in vitro* selection technique termed SELEX (Systematic *E*volution of *L*igands by *EX*ponential enrichment) independently in the laboratories of Joyce,²¹ Szostak²⁰ and Gold²² in 1990 (Figure 4).

Till date, the sequences and binding characteristics of more than a hundred aptamers against a range of different targets have been published. Aptamers can be used for basic research as well as for clinical purposes, in diagnostics, as well as in therapeutics, as macromolecular drugs.

4.1.5 Spiegelmers

The susceptibility of the DNA/RNA backbone to nuclease attack spurred a search for modifications that could resist nuclease degradation, but would still be amenable to a suitable selection procedure. ‘Spiegelmers’, first developed by Fuerste and co-workers²³ are based on the enantiomeric L-ribose sugars in nucleotides, the name being derived from the German ‘spiegel’ meaning ‘mirror’. They are highly resistant to nuclease degradation and form a relatively new class of potential drugs, some being currently tested in clinical trials. The first step involves the synthesis of the enantiomeric form of the target. For example, in peptides, this would involve the synthesis using D-aminoacids. This is followed by the selection of a natural D-ribose-based RNA against the unnatural enantiomeric form of the target by the SELEX procedure. In the next step, the mirror-image RNA (based on the enantiomeric L-ribose sugars), termed the Spiegelmer, is chemically synthesized, which binds specifically, the natural target (Figure 5). Very recently, the discovery of DNA- and DNA/RNA-mixed Spiegelmers that bind glucagon with a K_d of 3nM were reported,²⁴ as potential therapeutic candidates to attenuate hyperglycemia in type 1 and type 2 diabetes. However the drawback of spiegelmers is that the production of a spiegelmer involves selection of a preliminary oligonucleotide against the synthetic enantiomer of the chosen target, which is not always feasible, and thus the route of chemical modification of oligonucleotide library used in SELEX is more universally applicable.

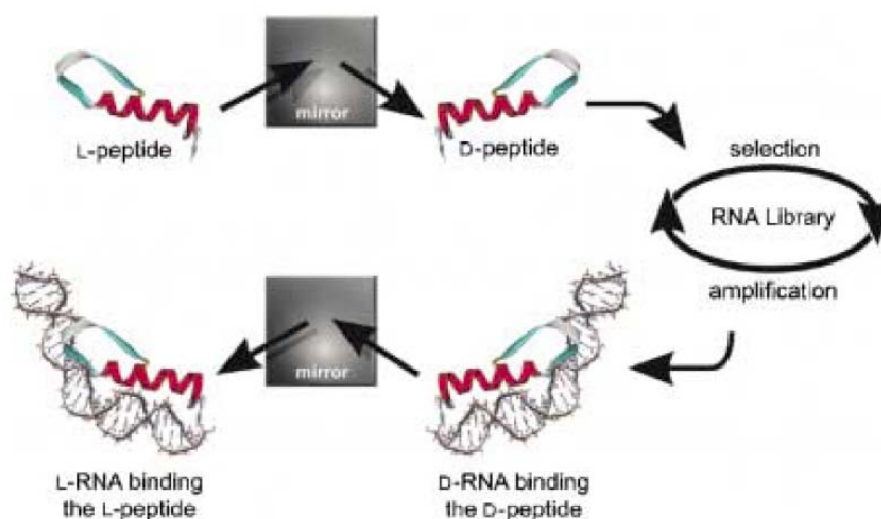


Figure 5. The Spiegelmer technology schematic.²⁵

4.1.6 Thrombin-binding aptamer-TBA: Discovery, structural features, function, modifications with effect on structure and function

Thrombin is a key regulatory enzyme in the coagulation cascade. It is a serine protease produced from prothrombin by the action of factor Xa. Thrombin, in turn, converts fibrinogen into fibrin, which is the building block of the fibrin matrix of blood clots.²⁶

The **thrombin binding aptamer (TBA)** was discovered in 1992 by *in vitro* selection and found to inhibit fibrin- clot formation with high selectivity and affinity. This single-stranded DNA aptamer prolonged clotting time from 25s to 169s in purified fibrinogen and from 25s to 43s in human plasma.⁵ In cynomolgus monkeys, the prothrombin time (PT) increased by 1.7-fold 10min after infusion of the aptamer and returned to baseline 10min after the infusion was terminated.²⁷ In a canine cardiopulmonary bypass (CPB) model, the aptamer-treated group exhibited increases in PT, activated partial thromboplastin time (aPTT), and activated clotting time that subsequently returned to baseline after aptamer infusion ceased.²⁸ This DNA aptamer is being evaluated in preclinical studies by Archemix Corporation in preparation for human clinical trials. Currently the only approved anticoagulant for coronary artery bypass graft is heparin. TBA exhibits a K_D of 2nM for thrombin, 50nM for prothrombin and binding to other serum

proteins or proteolytic enzymes is essentially undetectable.¹⁸ It could be useful as a heparin alternative in cardiovascular surgery. It has the key advantages that it avoids the risk of thrombocytopenia, associated with heparin, and is a specific inhibitor, effective at inhibiting clot-bound thrombin. No significant toxicities nor excessive bleeding intraoperatively has been observed.

The 3D solution structure of TBA was solved by NMR studies^{29, 30} and showed this sequence [d(GGTTGGTGTGGTTGG)] to be an intramolecular antiparallel G-quadruplex, with two G-quartets stacked on each other and linked by two TT loops and one TGT loop (Figure 6).

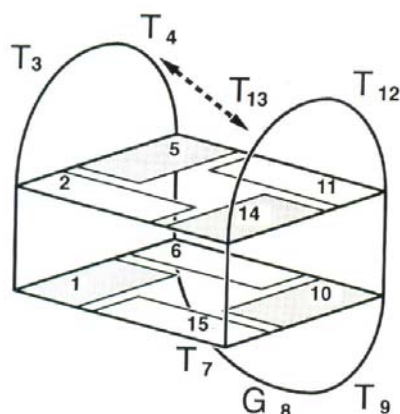


Figure 6. Thrombin binding aptamer.³¹

X-ray crystallographic studies³¹ have shown the importance of the loops in protein recognition and binding. This has prompted a number of studies aimed at improving the anti-thrombin effect of TBA.

4.1.6.1 Modifications in TBA

Single-base substitution studies with unlocked nucleic acids, for example, identified a single position out of 15 investigated, that resulted in enhanced activity.³² Most substitutions with LNA, on the contrary, led to reduction of anticoagulant activity.³³ The effect on quadruplex stability of North-nucleoside in the loops of TBA was reported by Eritja and coworkers.³⁴ The replacement of thymidines in the TGT loop of the TBA quadruplex by uridine (U) and 2'-fluorouridine (FU) induced greater stability to the

antiparallel quadruplex structure determined by UV- T_m experiments and CD spectroscopy. However the presence of North-methanocarbathymidine (NT) in the same positions destabilized the quadruplex structure. Also, the substitution of thymidines in the TT loops by U, FU and NT destabilized the antiparallel quadruplex structure (Figure 7). Thus the changes in sugar conformations of the nucleotides in the loop region of TBA are important in determining the stability of TBA quadruplex structure.

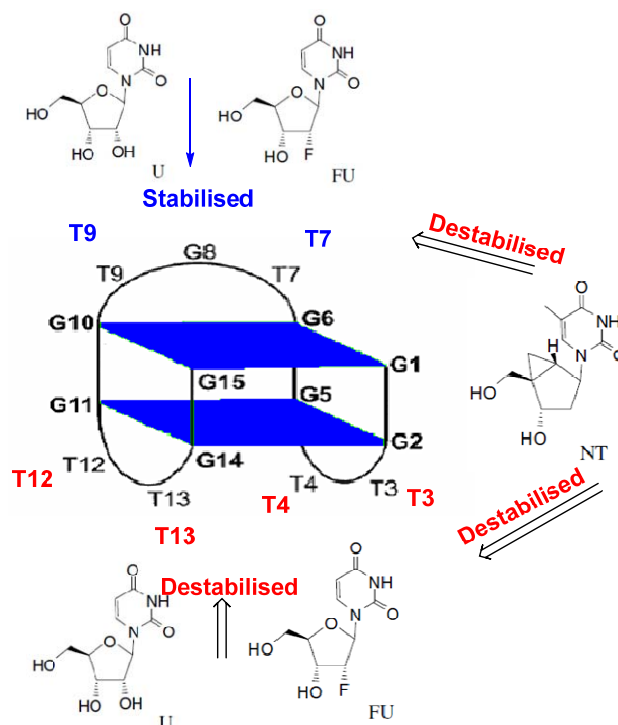


Figure 7. Effect of loop modifications on the stability of TBA.

Phosphorothioates (Figure 8) in the internucleotide linkage of the guanines resulted in reduced stability, but in the TT loop cause increased nuclease resistance, at the same time, retaining the stability and anticoagulant activity.³⁵ A series of 15-mer oligonucleotides with one or more negatively charged phosphodiester groups replaced by a neutral formacetal group (Figure 8) were synthesized and evaluated for their thrombin inhibitory activity *in vitro* and *in vivo*. Replacement of the negatively charged phosphodiester linkage with a neutral formacetal linkage³⁶ was studied with the goal to understand the role of the phosphodiester group in binding to thrombin and which phosphodiester group or groups are critical for the interactions. Another goal was to derive analogues with increased *in vivo*

half life through structural modifications. TBA has a short half- life which makes it an ideal anticoagulant for cardiopulmonary bypass surgeries, where a quick onset of anticoagulation and rapid return to normal clotting value are desirable. However analogues of TBA with an increased *in vivo* half-life could be useful in clinical cases such as deep vein thrombosis where extended anticoagulant effect is necessary. The short half-life of TBA is mainly due to rapid tissue uptake.³⁷ Cellular uptake of oligonucleotide (ODN) occurs mainly through receptor-mediated endocytosis³⁸ and binding of an ODN to the cell surface is mainly based on charge-charge interactions.³⁹ It was found that more than one of the phosphodiester groups are simultaneously involved in the binding with thrombin. For the ODNs containing two non-contiguous formacetal groups, additive results were obtained for the effect of the substitution on the thrombin inhibitory activity. The *in vivo* anticoagulation study in monkeys showed that the ODN containing four formacetal groups shows an increased *in vivo* PT and extended *in vivo* half-life compared to the unmodified ODN, suggesting that replacement of negatively charged phosphodiester groups with neutral formacetal groups may decrease the tissue uptake of the ODN. Modified nucleobases in the form of 4-thio-dU in a position-dependent manner resulted in significant improvements in anticoagulant activity.⁴⁰ Similarly, *isoguanine* nucleobases were used to increase the stability of modified TBA.⁴¹

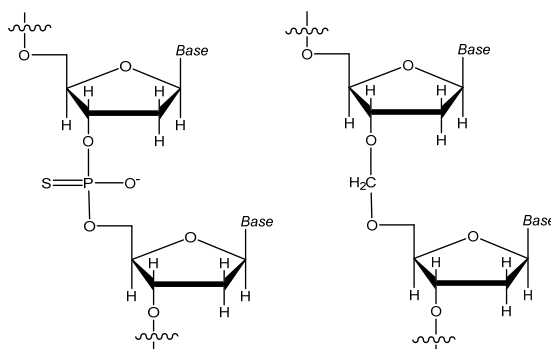


Figure 8. Dinucleotides showing phosphorothioate and formacetal internucleoside linkages.

Inversion of strand polarity⁴² was also shown to have a favourable effect on thermal stability and also thrombin-affinity (Figure 9). However, decreased thrombin inhibition was observed in this case.

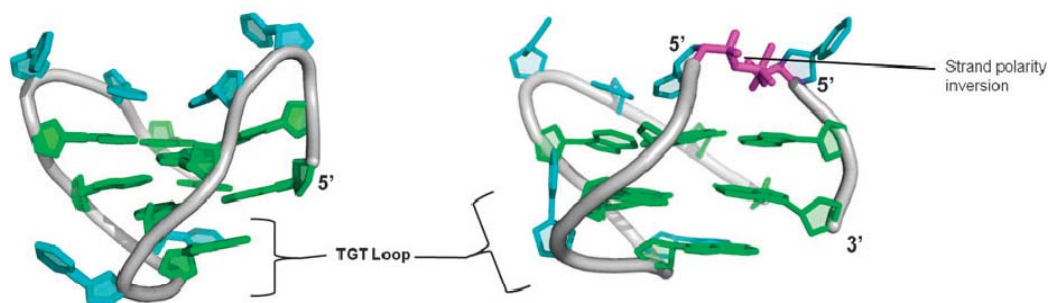


Figure 9. NMR solved structures of thrombin binding aptamer (TBA) and modified TBA with strand-polarity inversion. (Collie, G. W., Parkinson, G. N., *Chem. Soc. Rev.*, 2011, 40, 5867.)

It has also been demonstrated that the thermal stability of TBA is not the only factor influencing anticoagulant activity. Specific TBA-thrombin interactions are equally important, particularly those involving the loop regions.

Backbone modifications of TBA are reported to have profound effects on the structural topology of the resulting quadruplex. The *iso*-sequential RNA (rTBA) was shown to form a multimolecular parallel G-quadruplex,⁴³ in contrast to TBA, which is a unimolecular antiparallel G-quadruplex.^{29,5} A mixed DNA/RNA backbone TBA sequence folded in either DNA-like or RNA-like quadruplex structure, depending on the position of the ribo- or deoxyribo-nucleotides in the sequence.⁴⁴ An RNA-based SELEX process for thrombin-binding yielded a nucleobase sequence completely different from TBA.^{45,46} The nucleobase sequence of the recently reported 3',2'-TNA aptamer for thrombin-binding, although a G-rich sequence,⁴⁷ was also different from TBA. The loop configuration of the quadruplex can also be a deciding factor for various structural topologies with varying loop configurations.^{1b} Thus, it is evident that the backbone is a crucial governing entity for maintaining the functional structural quadruplex topology of the given TBA sequence.

4.2 Present Work

Considering the facts that the regioisomeric 3'-deoxy-2',5'-linked DNA/RNA (*iso*DNA/*iso*RNA, Figure 10) were suggested as plausible genetic material in the past, that they form stable duplexes with themselves and with RNA,⁴⁸ and that they are also able to

take part in template-directed oligomerizations,⁴⁹ the investigation of the quadruplex-forming ability of oligomers bearing this alternative backbone was undertaken.

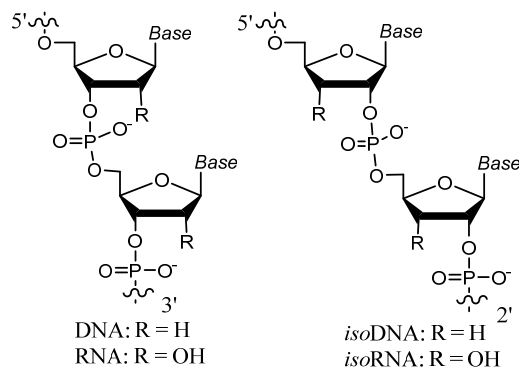


Figure 10. DNA/RNA and *iso*DNA/*iso*RNA structures.

The *iso*DNA backbone was also chosen because (i) the 2',5'-linkages maintain an extended backbone geometry due to the anomeric effect and the O4'-C1'-C2'-O2' *gauche* effect on the substituted sugar leading to the N-type sugar conformations,^{50, 51, 52} (ii) the guanine base orientation could be either *syn* or *anti*,⁵³ (iii) the 2'-5'-linkages are known to form stable loop structures in the hairpin DNA/RNA motifs,⁵⁴ and (iv) the *iso*DNA oligomers are relatively stable to exonuclease degradation.⁵⁵ Further, as aptamers are selected for a particular function, it was proposed to investigate the capability of the *iso*DNA aptamers of carrying out the designated function. The well-documented thrombin-binding aptamer^{5,29,56} (TBA) sequence, 5'-dGGTTGGTGTGGTTGG-3' was chosen as a G-quadruplex-forming model oligomer for the studies presented in this chapter. The structural topology of the 2',5'-backbone in *iso*TBA was studied with reference to the control 3',5'-linked TBA. The effect of the alternative 2',5'-backbone on the anti-clotting ability of the TBA oligomer was investigated. In addition, the effect of modification by including riboU units in the *iso*TBA oligomer on the G-quadruplex formation and activity of the resulting structure was investigated. Thus, the present study has immediate importance for use in cardiovascular surgery and other instances where anti-coagulation is desired, and has the potential to be extended to other biologically and diagnostically/therapeutically important G-quadruplex-forming aptamers.

4.2.1 Chemical synthesis of a 2'-5'-linked, non-genetic, regioisomeric thrombin binding aptamer (*iso*TBA) and a modified *iso*TBA

Using an automated Bioautomation MM-4 DNA synthesizer and commercially available 5'-*O*-dimethoxytrityl-3'-deoxy-2'-phosphoramidites, two sequences, *iso*-TBA-2 and a modified *iso*-TBA-3 were synthesized. Replacement of 3'-deoxythymidine in the TGT loop (T7 and T9 in *iso*-TBA-2) by uridine gave UGU loop-modified sequence *iso*-TBA-3. Longer coupling times were used to ensure efficient coupling. The 3'-5'-linked TBA-1 was synthesized for control experiments. The oligonucleotide sequences synthesized for the study are listed in Table 1.

Table1: Oligomers synthesized, MALDI-ToF mass spectrometric characterization and HPLC retention time.

Sequence code	Sequence	MALDI-ToF Mass		HPLC t_R (min)
		$M_{\text{calcd.}}$	$M_{\text{obsd.}}$	
TBA-1	5'-dGGTTGGTGTGGTTGG-3'	4726	4728	10.05
<i>iso</i> -TBA-2	5'-dGGTTGGTGTGGTTGG-2'	4726	4731	8.45
<i>iso</i> -TBA-3	5'-dGGTTGGUGUGGTTGG-2'	4730	4739	8.74

The replacement of the 3'-5'-phosphodiester linkages in TBA-1 by 2'-5'-phosphodiester linkages gave the 3'-deoxy-2'-5'-oligomer *iso*TBA-2. Replacement of 3'-deoxythymidine in the TGT loop of *iso*TBA-2 by uridine gave UGU loop-modified oligomer *iso*TBA-3. The 3'-OH group would shift the equilibrium towards S-type sugar conformation in this case, and impart rigidity and stability to the loop similar to that imparted by the N-type sugars in DNA.³⁴ The most recent corrected crystal structure of thrombin complexes with TBA⁵⁷ revealed the extended interface between thrombin exosite I and the two TT loops of the G-quadruplex and minimum interactions of thrombin with the TGT loop of TBA. The sugar residues in the TT loop involved in interactions with thrombin and the guanine nucleosides involved in the G-quartet formation, were therefore, not changed in our design.

4.2.2 G-tetraplex formation in the presence of monovalent cations using CD, UV and fluorescence spectroscopy

CD spectroscopy and T_m measurement of the TBA sequences The G-quadruplex formation for the synthesized sequences was studied by CD spectroscopy^{34,58} in the presence of added monovalent cations such as K^+ and Na^+ and their stability was determined as a function of temperature-dependent change in CD amplitude at 295nm (Figures 11, 12, Table 2).

The 2'-5'-linked *isoTBA-2* and *isoTBA-3* and control sequence **TBA-1** were found to exhibit intense maxima at 295nm in the CD spectra in presence of K^+ ions (Figure 11A) which correspond to the previously-described⁶¹ group-III antiparallel G-quadruplex topology for 3'-5'-DNA. The stability of the G-quadruplexes was followed by the change in the amplitude of the CD signal at 295nm with temperature (Figure 11B). The monovalent cations Na^+ and K^+ were necessary for the stability of the quadruplex structure, K^+ being most favoured (Figure 12 A,B). The *isoTBA-2* quadruplex was less stable compared to the control **TBA-1**. These CD signals gave clear indication of the formation of antiparallel folded G-quadruplex in the presence of monovalent cations for *isoDNA* backbone. The replacement of the TGT by **UGU** in the loop region (*isoTBA-3*) improved the stability of the quadruplex structure as seen by a positive change in T_m in presence of K^+ (Table2), showing the influence of loop geometry on quadruplex stability as found earlier for DNA-TBA.³⁴

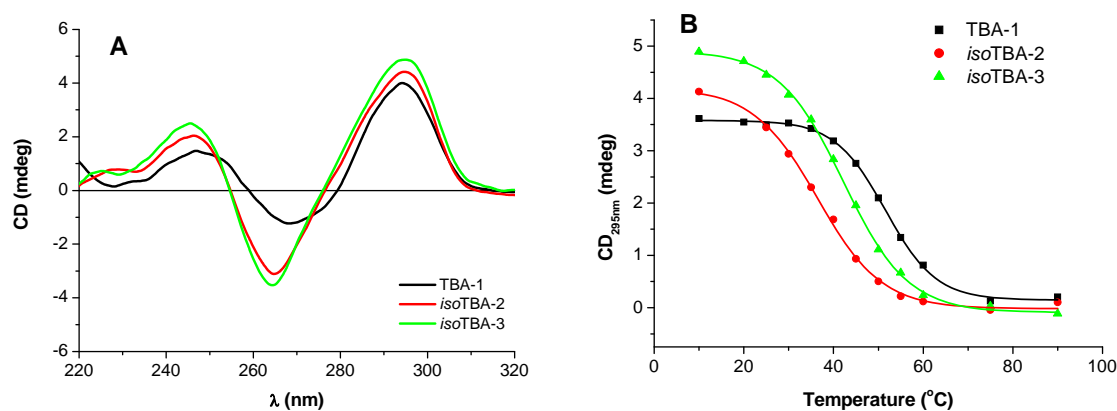


Figure 11. A CD spectra of oligomers **TBA-1**, *isoTBA-2* and *isoTBA-3* in K^+ buffer, B Temperature-dependent changes in CD amplitude at 295nm plotted against temperature.

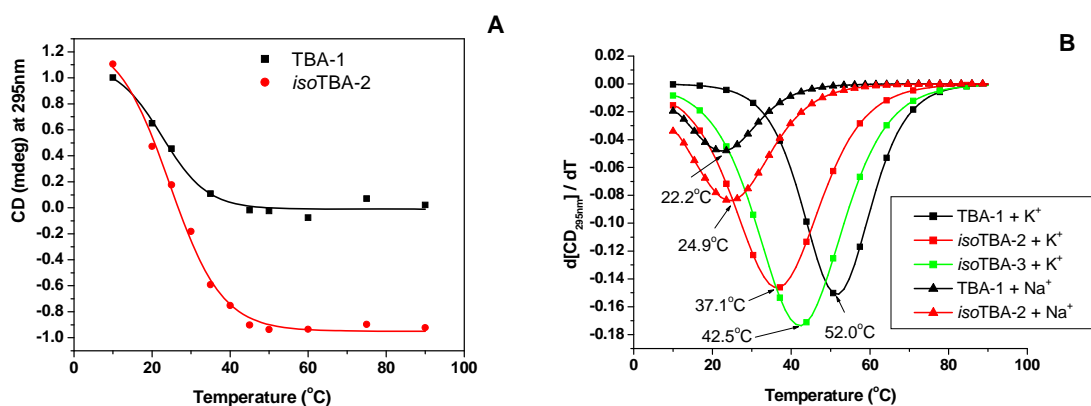


Figure 12. CD- T_m of oligomers **TBA-1**, *isoTBA-2* having a strand concentration of 5 μ M: **A** in 10mM Na-phosphate buffer (pH 7.5) containing 100mM NaCl. **B** The first derivative curves of **TBA-1**, *isoTBA-2* and *isoTBA-3* in K-phosphate and Na-phosphate buffers.

Table 2 Quadruplex melting data of TBA sequences of the study

Sequence code	TBA sequences	T_m °C	
		Na ⁺	K ⁺
TBA-1	5'-dGGTTGGTGTGGTTGG-3'	22.2	52.0
<i>isoTBA-2</i>	5'-dGGTTGGTGTGGTTGG-2'	24.9	37.1
<i>isoTBA-3</i>	5'-dGGTTGGUGUGGTTGG-2'	nd	42.5

Hysteresis Phenomenon determination by CD and UV

The CD hysteresis between the heating and cooling curves (Figure13a) was found to be negligible in all the cases indicating unimolecular folding into G-quadruplex form. These results were further supplemented by UV- T_m and hysteresis measurements (Figure13b).

Comparison of TBA-1 and *isoTBA-2* quadruplexes in the presence of different monovalent ions

The CD spectra of TBA-1 and *isoTBA-2* in the presence of different monovalent ions is shown in Figure14. In contrast to **TBA-1**, which exhibited characteristic CD

signatures of stable quadruplexes in the presence of all the monovalent ions under study, *isoTBA-2* showed the characteristic maximum at 295nm for antiparallel quadruplex formation only in the presence of Na^+ and K^+ ions indicating a subtle difference in the quadruplex structure of the *isoTBA-2*.

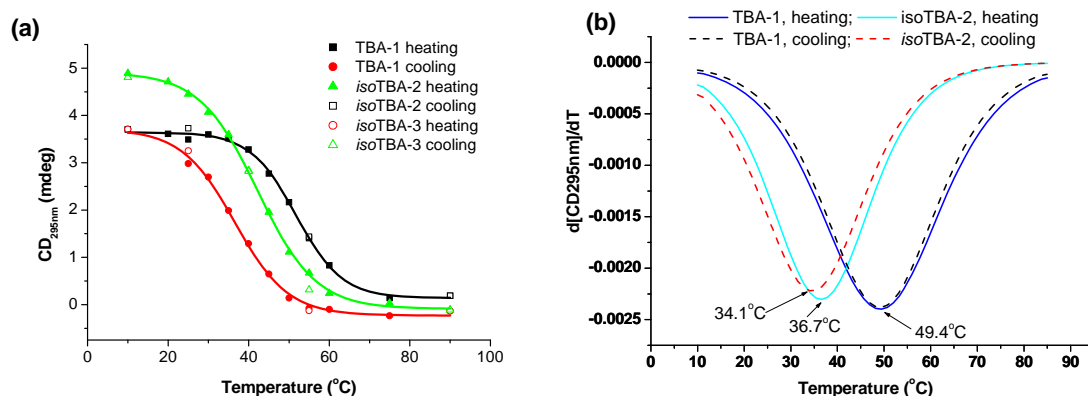


Figure 13. (a) CD hysteresis for **TBA1**, *isoTBA-2*, *isoTBA-3*, (b) UV hysteresis-first derivative plots for **TBA1** and *isoTBA-2*. Strand concentration = $5\mu\text{M}$ in 10mM potassium phosphate buffer (pH 7.5) containing 100mM KCl.

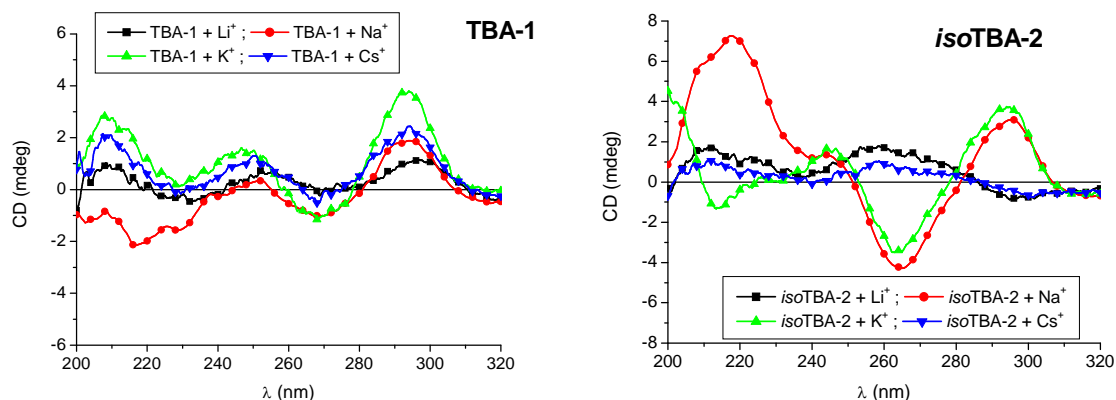


Figure 14. CD spectra of **TBA-1** and *isoTBA-2* at 10°C , in the presence of different cations (Li^+ , Na^+ , K^+ , Cs^+).

Intrinsic Fluorescence of G-quadruplexes

The intrinsic fluorescence of G-quadruplexes⁵⁹ was also used to confirm the formation of G-quadruplexes, in addition to the CD and UV spectroscopic studies discussed above. Accordingly, a significant increase in fluorescence emission was observed at $\sim 330\text{nm}$ to 340nm for **TBA-1** and *isoTBA-2* in the presence of cations, which was minimal with **TBA-1**, and absent with *isoTBA-2*, in the absence of any added cations (Figure 15).

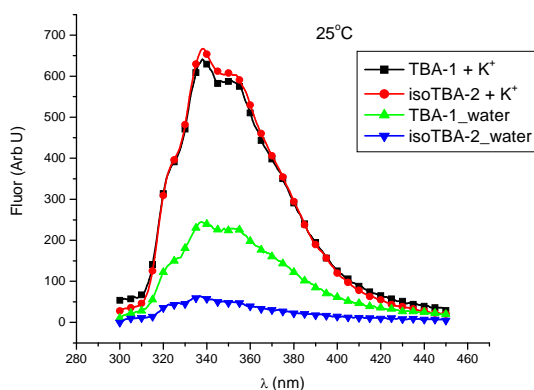


Figure 15. Fluorescence emission spectra of TBA-1 and *iso*TBA-2 in the presence and absence of added cations (K^+) at 25°C.

4.2.3 Thermal Difference Spectra (TDS)

The characterization of G-quadruplexes can be conveniently and rapidly carried out by the thermal difference spectra (TDS), which are the spectra obtained by subtracting the spectra of the folded state from that of the unfolded state at temperatures below and above the melting temperatures (T_{ms}). A comparison of >900 spectra from 200 different sequences⁶⁰ led to the conclusion that the TDS has a specific shape that is unique for each type of nucleic acid structure, that reflects the subtleties of base-stacking interactions that occur within each type of nucleic acid structure. Moreover, it is applicable to both DNA and RNA and from short oligomers to polynucleotides. UV TDS^{60,61} complements CD spectroscopy as a tool for the structural characterization of nucleic acids in solution. Fluorescence TDS⁵⁹ is also similarly useful in characterization of G-quadruplexes.

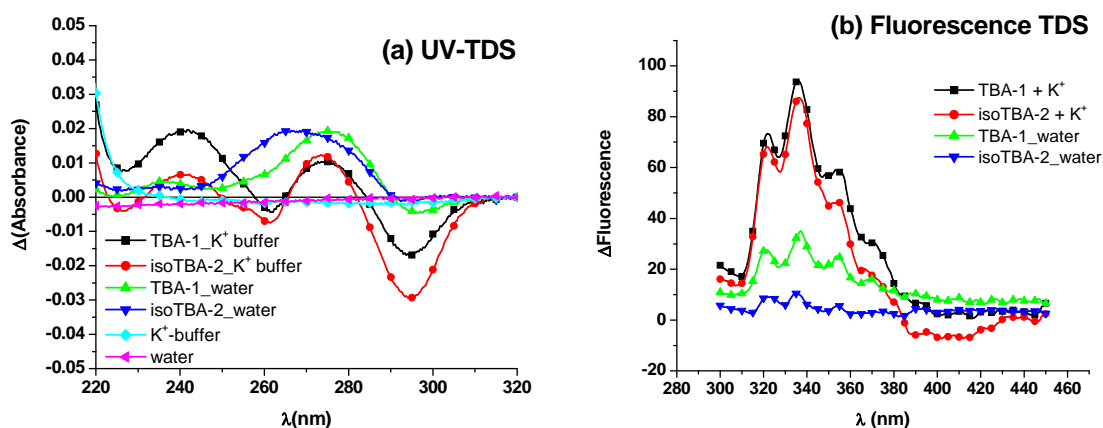


Figure 16. (a) UV-TDS and (b) Fluorescence-TDS of TBA-1 and *iso*TBA-2 in water and in buffer containing K^+ ions.

The TDS of *iso*TBA-2 and TBA-1 (Figure 16) clearly illustrate the formation of G-quadruplexes in buffer containing K^+ ions. TBA-1 also shows some degree of quadruplex structure in water, even in the absence of any added cations, which is not observed in the case of *iso*TBA-2. These studies thus provide yet another proof for the quadruplex structure observed for TBA-1 and *iso*TBA-2 in the presence of cations such as K^+ .

4.2.4 Molecular crowding effects on TBA-1 and *iso*TBA-2

As described in Section 4.1.3, the cell environment is crowded by 40% (w/v) macromolecules⁶² and the structural study of the synthesized oligomers under molecular crowding conditions becomes important to gain insight into the structure possibly assumed by the oligomers in cellular conditions. The CD spectra were recorded for TBA-1 and *iso*TBA-2 in water and in the presence of PEG-200 as a molecular crowding agent.

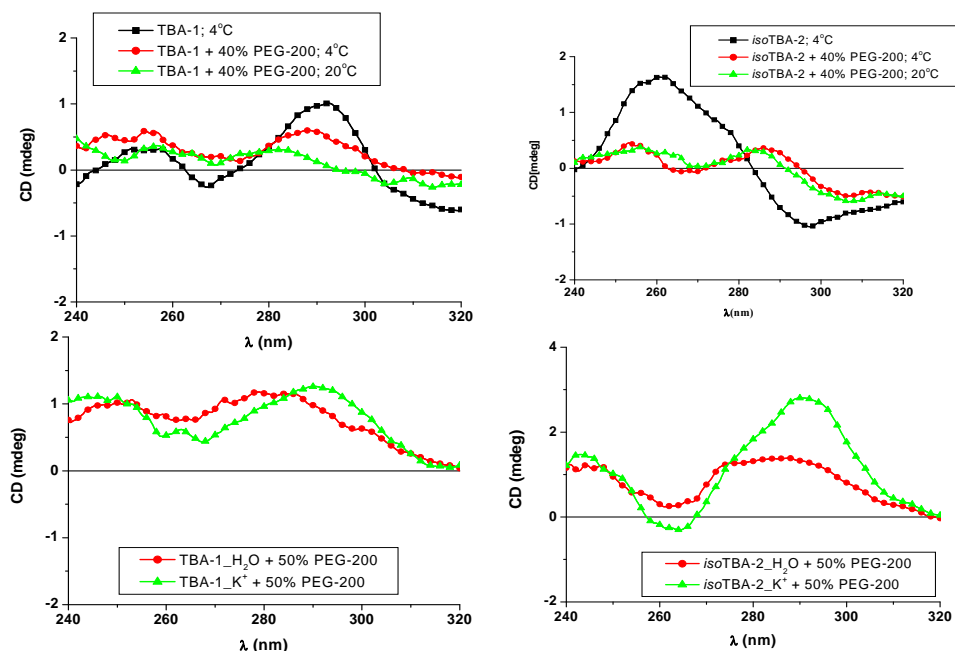


Figure 17. CD spectra of TBA-1 and *iso*TBA-2 (a) without and with the molecular crowding agent, PEG-200, and (b) With PEG-200 in the absence and presence of added K^+ ions.

As seen from the above plots (Figure 17), molecular crowding conditions induced a change in the CD spectrum. For TBA-1, this was observed (Figure 17a) as a decrease in intensity at ~ 295 nm, which showed further decrease with increasing temperature, while for *iso*TBA-2, this was evident as the disappearance of the maximum at 260nm and the

appearance of a maximum $\sim 290\text{nm}$, with only a slight decrease in amplitude with temperature increase from 4°C to 20°C , probably indicating the formation of a stable G-quadruplex. In the presence of K^+ ions, PEG-200 induced a change in the CD maximum from 290nm to $\sim 280\text{nm}$ for TBA-1, while a broad maximum was observed at $280\text{-}290\text{nm}$ for isoTBA-2. This could imply that isoTBA has a greater propensity to fold into a quadruplex form in the presence of the crowding conditions.

4.2.5 Imino proton NMR spectra of TBA-1 and isoTBA-2.

The characteristic chemical shifts of imino proton signals of the eight H-bonds formed between the guanines of each G-quartet of a quadruplex structure were observed between 11.5ppm and 12.5ppm range in the ^1H NMR spectrum as reported³⁴ earlier. The imino proton chemical shifts for isoTBA-2 are comparable with the control TBA-1 and indicate the hydrogen-bonded quadruplex formation (Figure 18). The temperature-dependent changes in the spectra were then recorded. As seen for the CD at 295nm , the ^1H NMR signals between 11.5ppm and 12.5ppm slowly disappeared with increasing temperature due to the loss of quadruplex structure near T_m . In the case of TBA-1 and

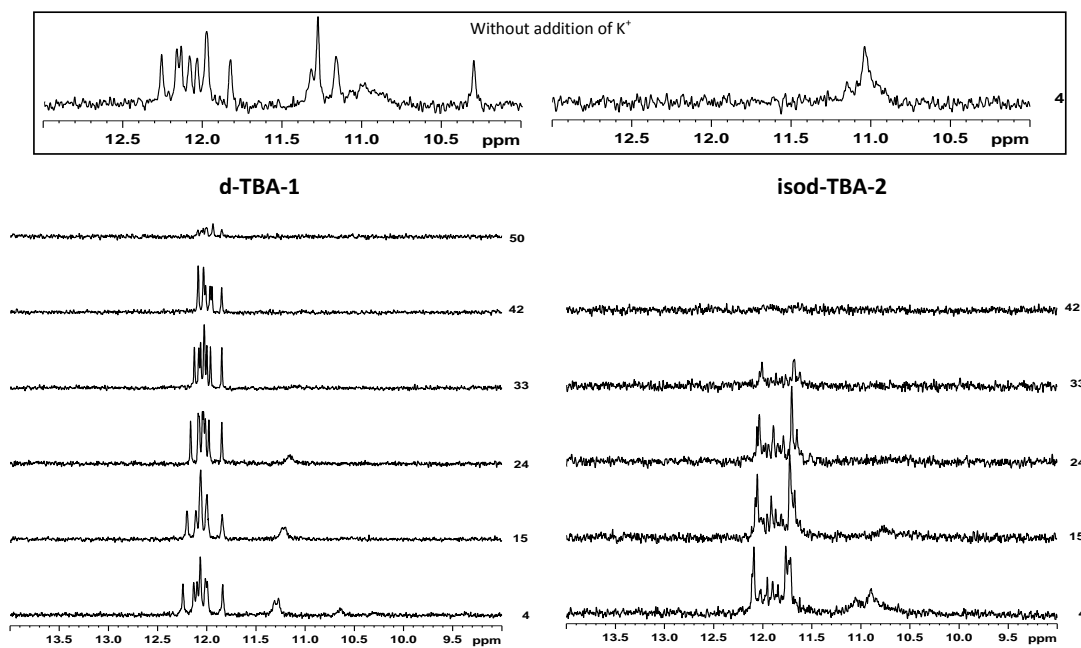


Figure 18. Quadruplex imino proton spectral region for TBA-1 and isoTBA-2 in the presence of K^+ from 4°C to 50°C . Inset shows the imino proton spectral region in the absence of K^+ at 4°C .

isoTBA-2, the NMR signals were observed up to 50°C, and 33°C, respectively (Figure 18). The broad peaks between 10.5-11.1ppm in the **isoTBA-2** and **TBA-1** spectra disappear much below the melting temperature (~20-25 °C) in each case, suggesting that these may not be involved in the H-bonded quadruplex structure. The appearance of characteristic H-bonded imino protons supports the fact that **isoTBA-2** does form a G-quadruplex structure, although less stable (Table 2, T_m 37°C) compared to the 3'-5'-linked **TBA-1** (Table 2, T_m 52°C) quadruplex structure. It is evident from the ^1H NMR signals at 4°C between 11.5ppm and 12.5ppm that **TBA-1** has significant quadruplex structure even in the absence of K^+ whereas **isoTBA-2** is not structured without monovalent cations such as K^+ (Figure 18 Inset).

4.2.6 G-tetraplex formation in the presence of thrombin without added monovalent cations

It has been earlier demonstrated that thrombin can act as a molecular chaperone for the folding of **TBA-1**.^{63,15} It was observed that at low temperature, the quadruplex structure necessary for thrombin-binding was formed, even in the absence of K^+ , but as the temperature was increased, the presence of K^+ was needed to preserve the quadruplex integrity. We performed CD experiments with **TBA-1**, **isoTBA-2** and **isoTBA-3** in the presence of increasing concentrations of thrombin at low temperature .

Thrombin was indeed found to display its chaperone effect^{15,34} on the folding of the G-quadruplex in the oligomers of the present study. In the presence of thrombin, the CD maximum in **TBA-1** (Figure 19a, 19d) was shifted to ~300nm, as previously reported.^{63b} Similar shifts were also reported for strontium ion⁶⁴ and lead ion,^{8d} suggesting that the G-quartet structure is **distinct** from that for potassium ion.^{8b,65} In the case of control **TBA-1**, a CD maximum at 295nm was observed even in the absence of either thrombin or K^+ , revealing the preference of G-quadruplex structure as reported earlier¹⁵ and also as seen by ^1H NMR in the present studies.

We observed increase in the CD signal amplitude upon incremental addition of thrombin, even at the relatively low concentrations of thrombin used in the present study.

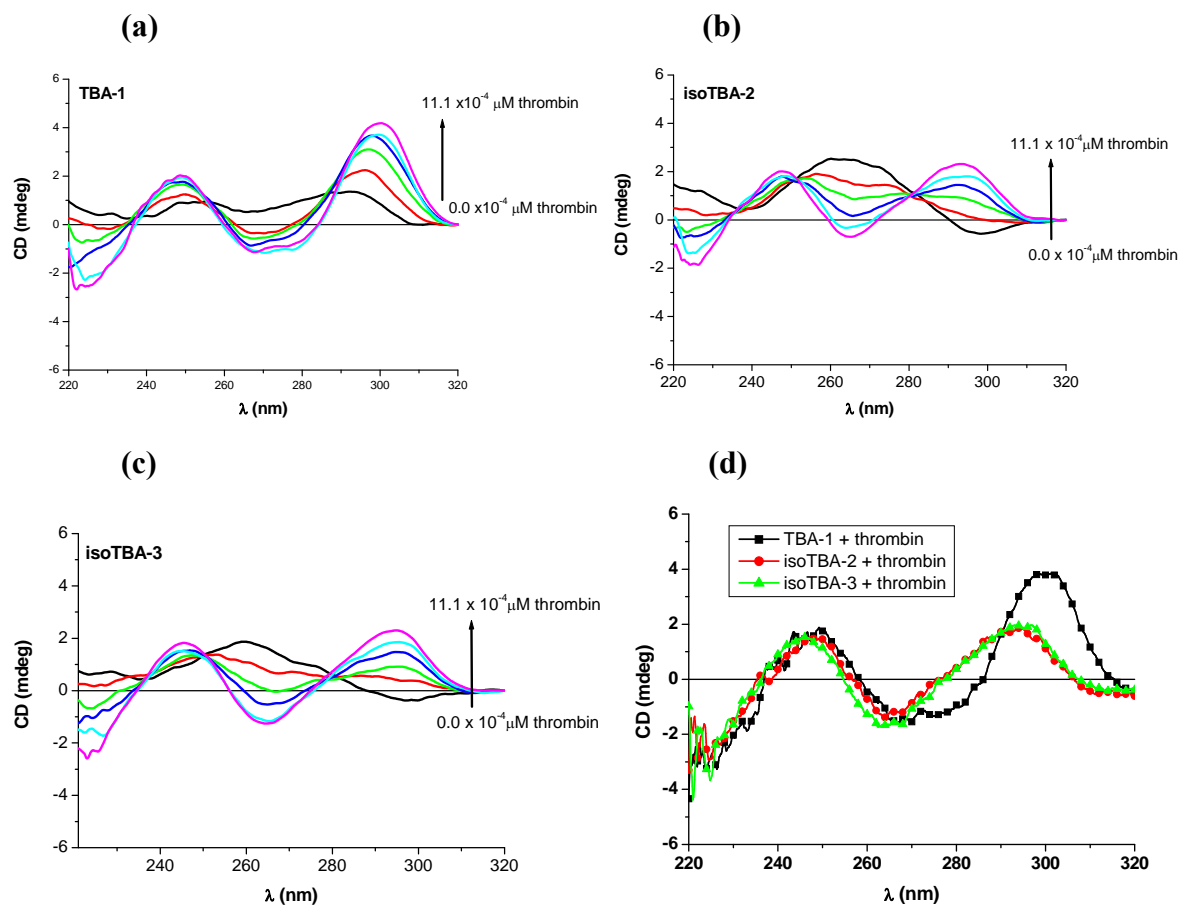


Figure 19. Changes in CD signal at 295nm upon addition of thrombin to (a) **TBA-1**, (b) *isoTBA-2*, and (c) *isoTBA-3*. (d) CD spectra of **TBA-1**, *isoTBA-2* and *isoTBA-3* in presence of thrombin.

In the case of *isoTBA-2* and *isoTBA-3*, the CD band at 295nm and G-quadruplex structure was not evident in the absence of either thrombin or K^+ , a fact also supported by 1H NMR. Upon incremental addition of thrombin, however, the characteristic CD maximum at 295nm emerged for *isoTBA-2* (Figure 19b) and *isoTBA-3* (Figure 19c). Isoelliptic points were observed at 280nm and 255nm in all the cases, indicating the two-state nature of the structural transition.¹⁵ The temperature-dependent stability of the quadruplex structure was followed by recording the CD amplitude at 295nm with increasing temperature. The strength of **TBA-1** G-quadruplex was the highest with $T_m = 22$ °C, followed by *isoTBA-3* ($T_m = 13$ °C) and *isoTBA-2* ($T_m < 10$ °C). The CD signal at 295nm was restored upon addition of K^+ and the quadruplexes were as stable as with K^+ alone at the thrombin concentrations used in this study (Table 3). Changes in CD spectral

amplitudes were not observed when serum albumin¹⁵ was used instead of thrombin in these experiments (Figure 20), confirming the specific role of thrombin in inducing quadruplex structures. These experiments clearly point out the similarity in structural topology of *isoTBA* with *TBA*, necessary for interaction with thrombin.

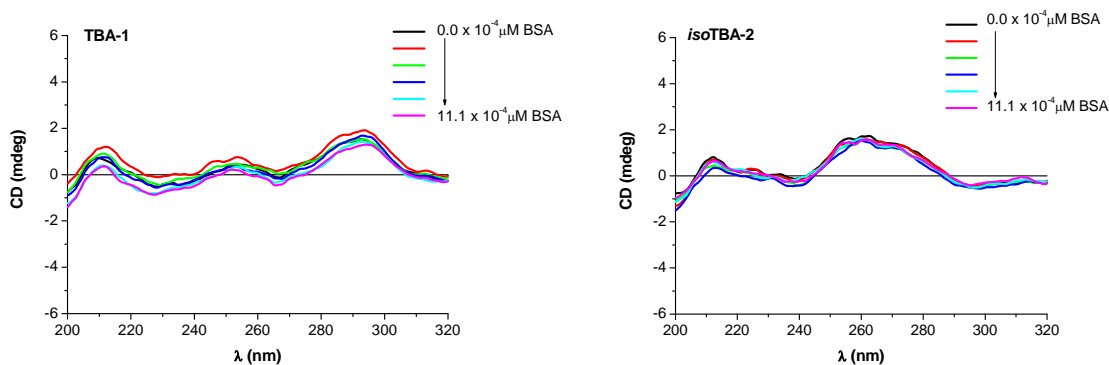


Figure 20. CD spectra of (a) *TBA-1* and (b) *isoTBA-2* with incremental additions of Bovine serum albumin (BSA) at 4°C.

Table 3. CD melting temperatures of the sequences of the study. Values in parentheses indicate the T_m values in presence of added K^+ ions.

Sequence code	TBA sequences	T_m °C
		Thrombin ^a
TBA-1	5'-dGGTTGGTGTGGTTGG-3'	22.2 (52)
<i>isoTBA-2</i>	5'-dGGTTGGTGTGGTTGG-2'	<10.0 (37)
<i>isoTBA-3</i>	5'-dGGTTGGUGUGGTTGG-2'	13.2 (42.5)

4.2.7 Anti-thrombin activity measurements

The inhibitory activity of the aptamers on thrombin-catalyzed conversion of fibrinogen to fibrin (clotting) was investigated by measuring the percent transmittance with time. **TBA-1** slowed down the coagulation with an increased induction time (t_i as coagulation parameter), confirming its reported inhibitory activity (Figure 21).⁶⁶ The induction time for the *isoDNA* oligomers *isoTBA-2* and *isoTBA-3* was considerably less than for **TBA-1**, but more than that in the absence of any aptamer. However the higher

thermal stability of *isoTBA-3* was not effectively reflected in its anti-thrombin activity, as this modified *isoTBA-3* shows a decreased ability to inhibit thrombin. These findings reiterate previous work^{33,67} that thermal stability does not always translate to increased anti-thrombin activity. Thus, the overall quadruplex stability is not a major contributor to the biological activity. These experiments provide conclusive evidence that the *isoTBA* oligomers are indeed capable of not only forming G-quadruplex structures but also hold similarity in structural topology capable of taking active part in the assigned function of the TBA, though less efficiently.

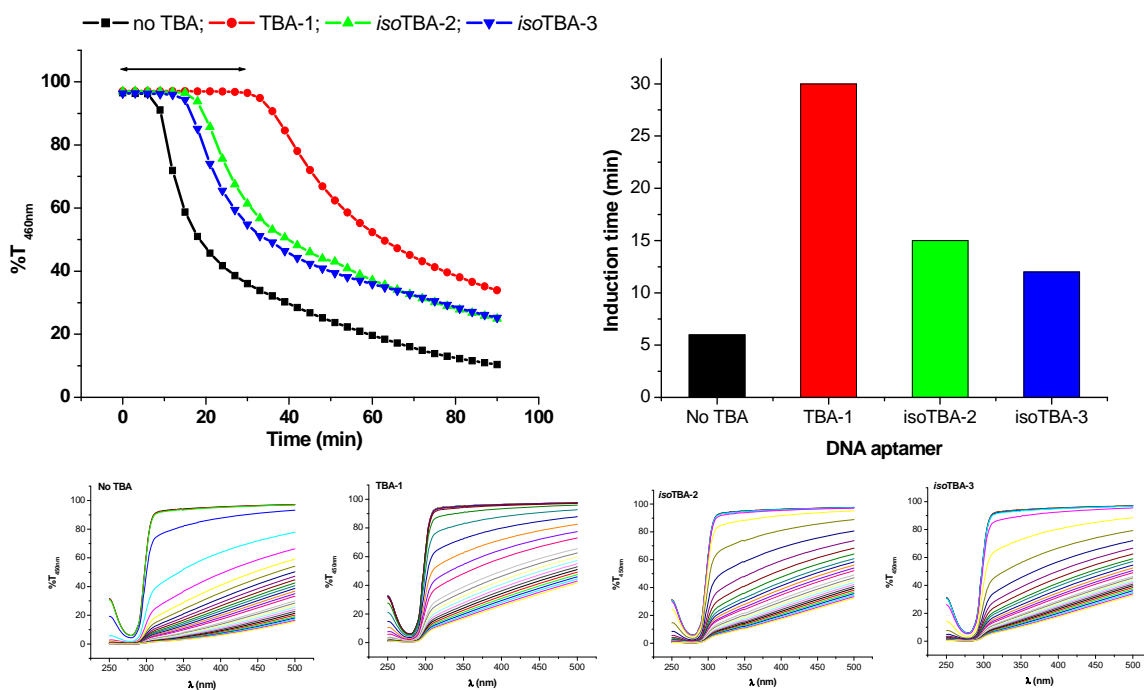


Figure 21. Antithrombin activity measured by % transmittance at 450nm in the presence of TBA-1, *isoTBA-2* and *isoTBA-3* and % transmittance Vs wavelength plots at different time-points of the study. \leftrightarrow indicates induction time as coagulation parameter (t_i).

The thrombin-catalysed fibrinogen clotting experiment was also carried out in the presence of exonuclease (SVPD), when the induction time with TBA-1 was found to be greatly decreased (Figure 22). This underlines the advantages of *isoTBA-2* in terms of its higher half-life, which may prove useful in biological systems.

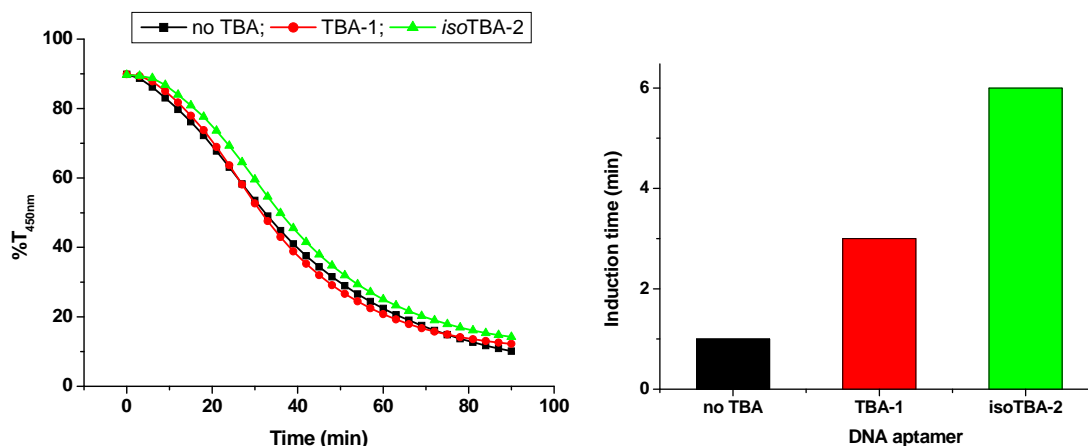


Figure 22. Antithrombin activity measured by % transmittance at 450nm with **TBA-1** and *isoTBA-2* in the presence of SVPD and the corresponding induction time plots.

4.2.8 Stability of aptamers to SVPD

To test the enzymatic stability of the *iso*DNA quadruplex-forming backbone as compared to the 3'-5'-DNA quadruplexes, we exposed these aptamers to SVPD (Figure 23).⁵⁵ The 2'-5'-linked *iso*DNA oligomer *isoTBA-2* was found to be digested much slower compared to the control **TBA-1** the reaction was monitored by HPLC (Figure 23a). The half-life of *isoTBA-2* was found to be ~120min (Figure 23b) while that of **TBA-1** was found to be ~20min at 37°C. The observed higher stability of the *iso*DNA oligomer offers

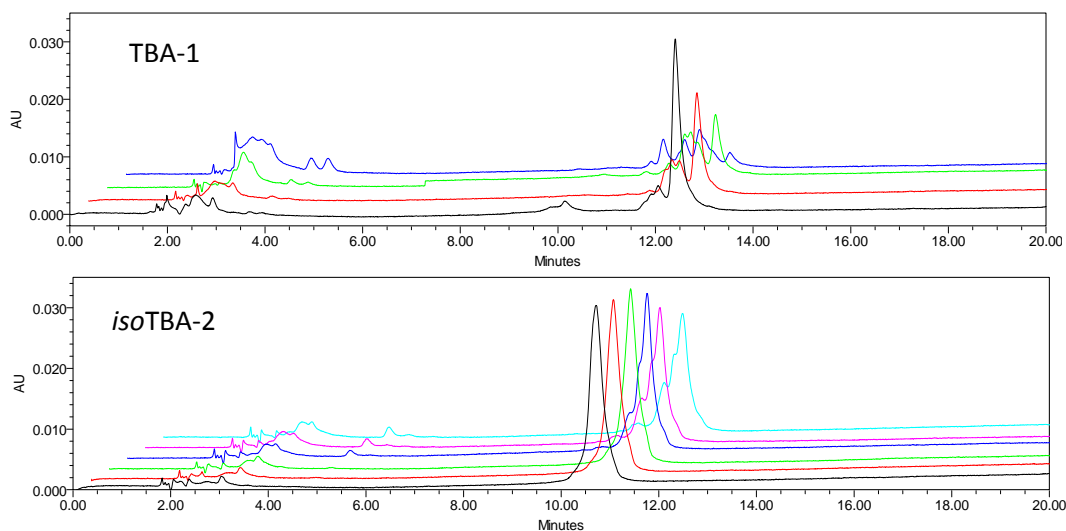


Figure 23a. HPLC chromatograms showing better stability of *isoTBA-2* towards SVPD than **TBA-1**

obvious advantages for applications in biological systems, where the control unmodified oligomer has a relatively low half-life.

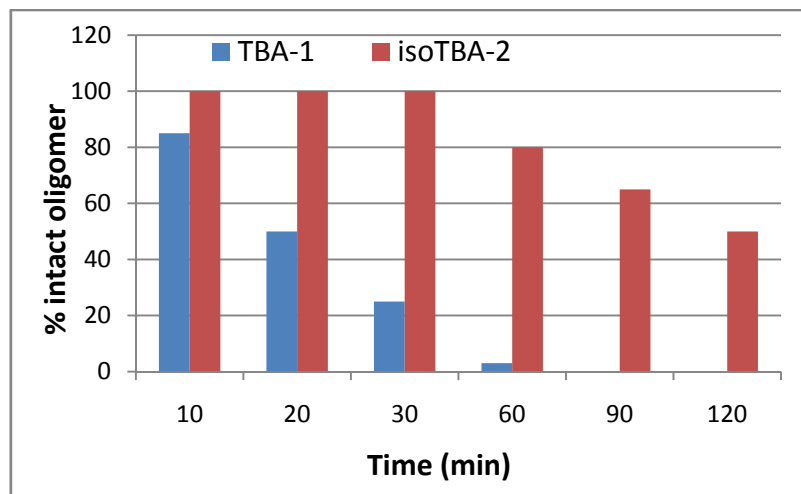


Figure 23b. Stability of the aptamers **TBA-1** and **isoTBA-2** ($7.5\mu\text{M}$) towards Snake venom phosphodiesterase (SVPD) enzyme (0.05mg/mL).

It could therefore, possibly find use in clinical cases such as deep vein thrombosis, as described in Section 4.1.6.2, where prolonged anticoagulant activity is required.

4.2.9 Non-denaturing Gel electrophoresis study

The quadruplex-forming ability of the synthesized oligomers was assessed by non-denaturing polyacrylamide gel electrophoresis. As reference oligonucleotides, two oligomers of differing lengths, viz., 5'-dAACCGATTTCAG-3' (12-mer) and 5'-dCACCATTGTCACACTCCA-3' (18-mer) were used. The TBA and isoTBA oligomers were annealed in buffer prior to loading on the gel. PAGE analysis indicated similar complex formation in the case of **TBA-1** and **isoTBA-2**, evident from their similar mobilities in the gel Figure 24 and Figure 25 shows the mobility of **isoTBA-3** similar to **TBA-1** and **isoTBA-2**. The gels were visualized by UV-shadowing and ethidium bromide staining. Thus, quadruplex formation was also confirmed by PAGE analysis for the oligomers of the current study.

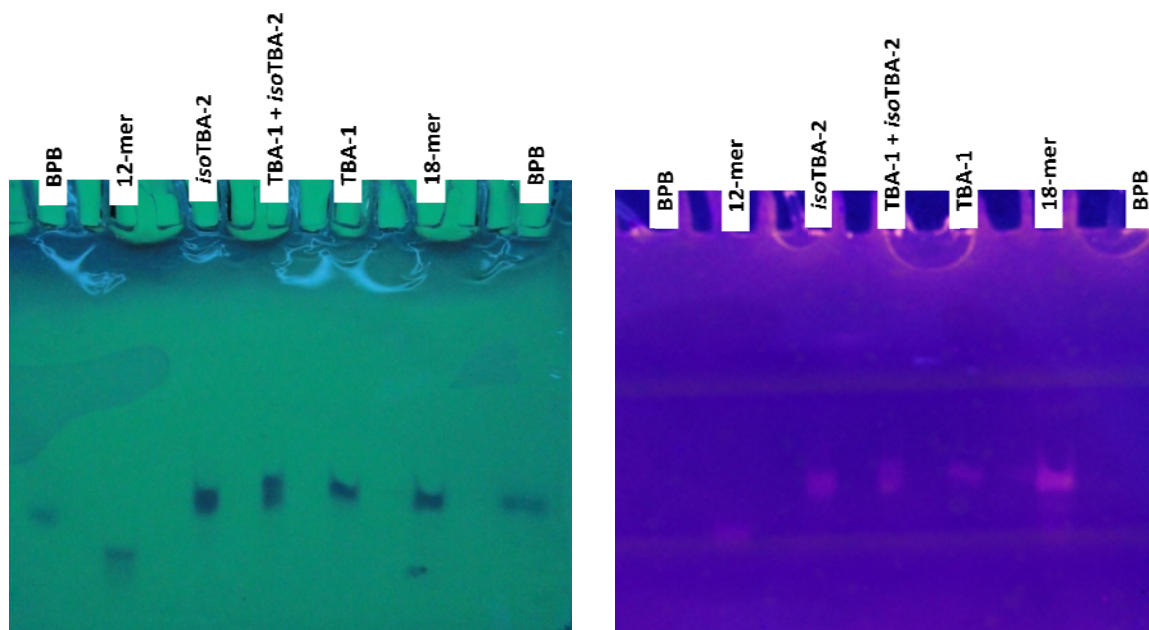


Figure 24. Non-denaturing PAGE analysis showing the relative mobilities of TBA-1 and *isoTBA-2*. (a) visualized by UV shadowing and (b) visualized by ethidium bromide staining.

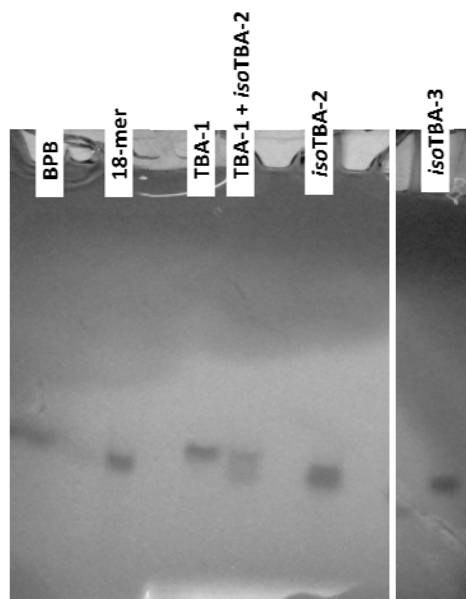


Figure 25. Non-denaturing PAGE analysis showing the quadruplex formation by TBA-1, *isoTBA-2* and *isoTBA-3*, visualized by UV-shadowing.

4.2. 10 Summary

The aptamers studied in this work are the first examples of 2'-5'-linked *isoDNA* sequences *isoTBA-2* and *isoTBA-3* which are able to form G-quadruplexes similar in

structure to the well established TBA aptamer which was used for comparison. The modified sequence **isoTBA-3** in which the thymidines in the 7 and 9 positions of the TGT loop were replaced by uridine resulted in a more stable quadruplex than **isoTBA-2**. Both the *isoDNA* aptamers not only formed quadruplexes in the presence of monovalent cations like Na^+ and K^+ , they exhibited binding to thrombin in absence of cations at low temperature. Additionally, the anticoagulation function ie thrombin inhibition was also exhibited by the *isoDNA* aptamers though with less efficiency than **TBA-1**. However, with an additional property of stability towards nuclease enzyme **isoTBA-2** functioned as a better anticoagulant than **TBA-1**, as seen in the thrombin-catalysed fibrinogen clotting experiment carried out in the presence of exonuclease (SVPD). Finally, the observed higher enzymatic stability of the *isoDNA* oligomer offers obvious advantages for applications in biological systems, where the control unmodified oligomer has a relatively low half-life.

4.2.11 Conclusion

The new findings in this work seem to prove that the 2'-5'-*isoDNA* aptamers are quite similar to the natural DNA aptamer (TBA) both structurally and functionally. Though their functional efficiency is lower compared to the TBA They can form G-quadruplexes, though their functional efficiency is lower compared to the TBA however, with an additional property of stability towards nuclease enzyme can function as a better anticoagulant than TBA. Thus applications in clinical or biological systems are viable where a longer half-life of aptamers is necessary.

4.3 Experimental

Oligonucleotide synthesis

Oligonucleotides both 3'-5' and 2'-5' were synthesized in-house on a Bioautomation Mermade-4 DNA synthesizer employing β -cyanoethyl phosphoramidite chemistry. The 2'-deoxy-3'-phosphoramidites and uridine 3'-*O*-TBDMS CED phosphoramidite (used for modified *isoTBA-3* sequence) were obtained from ChemGenes and 3'-deoxy-2'-phosphoramidites were obtained from Glen Research. Universal columns procured from

Bioautomation were used for 2'-5' oligomer synthesis. Oligonucleotides after post-synthetic treatment were desalted by passing through Pharmacia NAP-5 columns then purified by RP-HPLC on a C18 column using a Waters system (Waters Delta 600e quaternary solvent delivery system and 2998 photodiode array detector and Empower2 chromatography software). An increasing gradient of acetonitrile in 0.1M triethylammonium acetate (pH 7.0) was used.

MALDI-TOF mass

Mass was obtained by MALDI-TOF mass spectrometry. The MALDI-TOF spectra were recorded on Voyager-De-STR (Applied Biosystems). The matrix used for analysis was THAP (2', 4', 6'- trihydroxyacetophenone).

CD spectroscopy

CD spectra were recorded on Jasco J-815 CD Spectrometer equipped with a Jasco PTC-424S/15 peltier system. 2 mm path-length quartz cuvettes were used for a sample volume 500 μ l and strand concentration of 5 μ M in 10mMol Na/K-phosphate buffer (pH 7.5) containing 100mM NaCl/KCl respectively. Oligomers prepared in buffer were annealed by heating at 95° C for 5 minutes then slowly cooling to room temperature followed by refrigeration for 5 to 6 hours before use. For the CD experiments with various cations the respective salts (100mM) were added to Tris buffer. Spectral scans were collected over a wavelength range 200- 320nm at a scanning rate of 100 nm min⁻¹. Three scans were averaged for each sample. CD thermal denaturation of the TBA sequences, Thrombin and BSA binding studies were performed.

Buffers used for CD experiments

Phosphate buffer (pH = 7.2, 100 mM NaCl)

Na₂HPO₄ (110mg,10mM), NaH₂PO₄·H₂O (35.3mg,10mM), NaCl (585mg,100mM) was dissolved in minimum quantity of water and the total volume was made 100 mL. The pH of the solution was adjusted 7.2 with aq. NaOH solution in de-ionised water(DI), and stored at 4°C.

Phosphate buffer (pH = 7.2, 100 mM KCl)

K_2HPO_4 (174mg,10mM), KH_2PO_4 (136mg,10mM), KCl (746mg,100mM) was dissolved in minimum quantity of water and the total volume was made 100 mL. The pH of the solution was adjusted 7.2 with aq. KOH solution in DI water, and stored at 4°C.

Tris-HCl buffer (pH = 7.5)

Tris-HCl (157mg,10mM), was dissolved in minimum quantity of water, the pH was adjusted to 7.5 by adding a few grains of Tris base. and the total volume was made 100 mL.

UV- T_m experiments

Thermal denaturation of the TBA 1,2 and 3 oligomers was performed using a 10 mm quartz cell in a Cary 300 Bio UV-Visible Spectrophotometer Varian. The TBA oligomers 5 μ M concentration were annealed in a 10 mMol potassium phosphate buffer pH 7.5 , 100mMol KCl. The concentration was calculated on the basis of absorbance from molar extinction coefficients of the corresponding nucleobases of DNA/RNA.^{Gait} Absorbance *versus* temperature profiles were obtained by monitoring the absorbance at 295 nm from 10–85°C at a ramp rate of 0.5°C per minute. Both melting and annealing profiles were obtained to check reversibility of the process. A stream of dry nitrogen was gently applied through the sample compartment to prevent condensation of water on the cuvette at low temperatures.

NMR experiments

All the NMR measurements were performed on a Bruker AV 500 NMR spectrometer operating at 500.13 MHz for 1H using a 5mm BBFO probe. Water suppression was achieved by using a standard Bruker watergate W5 pulse sequence with gradients. 2000 transients were collected with an acquisition time of 3.54 sec and a pulse delay of 1 sec. The raw data were processed with a Gaussian function for improvement of signal to noise ratio. Temperature during the measurements was controlled by means of a Bruker BVT 3000 unit. 1H NMR spectra were acquired at 500Mhz using a Bruker-500 NMR spectrometer. HPLC purified and lyophilised TBA-1 and iso-TBA-2 were dissolved in 150

μl of 10mMol K-phosphate buffer pH7.5 containing 100mMol KCl and lyophilized, then diluted in 90% v/v H₂O /10% v/v D₂O to 100 μM . 3mm NMR tubes were used for scanning the spectra. One-dimensional spectra were acquired at 4, 15, 24, 33, 42, 50 °C. The presence of imino protons in the region between 11.5 to 13.5 δ indicate quadruplex formation. One-dimensional spectra of TBA-1 and isoTBA-2 only in 90% v/v H₂O /10% v/v D₂O (100 μM) at 4° C were scanned to show that isoTBA-2 did not form quadruplex in the absence of KCl while TBA-1 does form a quadruplex in H₂O alone.

UV-Transmittance measurements for clotting inhibition assay

Clotting inhibition assay was performed by using Cary 300 Bio UV-Visible Spectrophotometer Varian to measure % transmittance change over time. 0.1NIH unit of thrombin (50 NIH/ml, bovine thrombin, Fibroscreen reagent, Tulip Diagnostics (P) LTD.) was added to the TBA-1, isoTBA-2 or isoTBA-3 aptamers dissolved in water to a concentration of $3.7 \times 10^{-8}\text{M}$ and incubated for 15 minutes at 25° C. This was then added to a 1.0 ml fibrinogen solution ($3.0 \times 10^{-6}\text{M}$, Sigma product No F 3879), in saline (0.85%) and the transmittance was measured at 3.0 minute intervals for 90 minutes.

For the transmittance assay in the presence of SVPD, the requisite aptamer was incubated with SVPD (0.5 μg , $0.6 \times 10^{-4}\text{U}$) in 100mM Tris-HCl buffer (pH 8.5), 15mM MgCl₂, 100mM NaCl at 37°C for 30min, followed by addition of thrombin, incubation for 10min at 25°C, and subsequently added to a 1.0 ml fibrinogen solution ($3.0 \times 10^{-6}\text{M}$, Sigma product No F 3879), in saline (0.85%). The transmittance at was measured at 3.0 minute intervals for 90 minutes.

Snake venom phosphodiesterase stability experiments

Enzymatic hydrolysis of the aptamers TBA-1, isoTBA-2 (7.5 μM) was carried out at 37°C in 100 μl buffer (100mM Tris-HCl (pH 8.5), 15mM MgCl₂, 100mM NaCl) and SVPD (5 μg , $6.0 \times 10^{-4}\text{U}$) aliquots were taken at several time intervals. Each aliquot was heated at 90°C for 2 min to inactivate the nuclease enzyme. The intact oligomer at each time interval was

monitored by RP-HPLC. Percentage of intact oligomer was plotted against time to show the degradation of oligomers with respect to time.

Polyacrylamide Gel Electrophoresis (PAGE)

Preparation of Gel and buffer solutions

1. 5X TBE buffer (500 ml, pH 8.0)

Tris (hydroxymethyl)methyl amine (Tris base) 27g, boric acid 13.75g and EDTA 1.462g was dissolved in 500 ml of deionised water (DI water). The pH was adjusted to 8.0 with tris base or HCl.

2. 1X TBE buffer (500 ml)

100ml of 5X TBE buffer was diluted to 500ml with DI water.

3. 29:1 acrylamide : N,N-methylene bis-acrylamide solution.

29g of acrylamide and 1g of N,N-methylene bis-acrylamide was dissolved in 100ml of DI water.

4. Bromophenol Blue dye (marker dye)

40% of glycerol solution in DI water (V/V) + 0.25% Bromophenol Blue dye solution was prepared.

5. 40% sucrose solution in DI water (w/v).

This solution was mixed with the Bromophenol Blue dye solution and the sample to be loaded in 1:1 ratio, to make the loading solution viscous and heavy for proper loading into the gel wells.

6. 10% ammonium persulfate solution.

50mg ammonium persulfate was dissolved in 500 μ l DI water. Fresh solution prepared just before preparing the gel for casting.

7. 20% acrylamide gel. (19.314% acrylamide + 0.6% cross linker)

To prepare 10 ml gel solution, 6.66 ml of acrylamide (29:1) + 1.27 ml DI water + 2 ml of 5X TBE buffer were mixed and degassed for 15-20 minutes under vacuum. Then 70 μ l of ammonium persulfate was added followed by 4.6 μ l of TEMED (N,N,N',N'-tetraethylmethylenediamine)

8. Gel casting procedure.

The above prepared gel solution after swirling for a minute was immediately poured into the previously cleaned and fixed gel plates. The appropriate gel comb was inserted

for the formation of wells. Then the cast gel was allowed to stand for 40 minutes or more till it was set to a proper polymerised gel.

9. Gel experiment

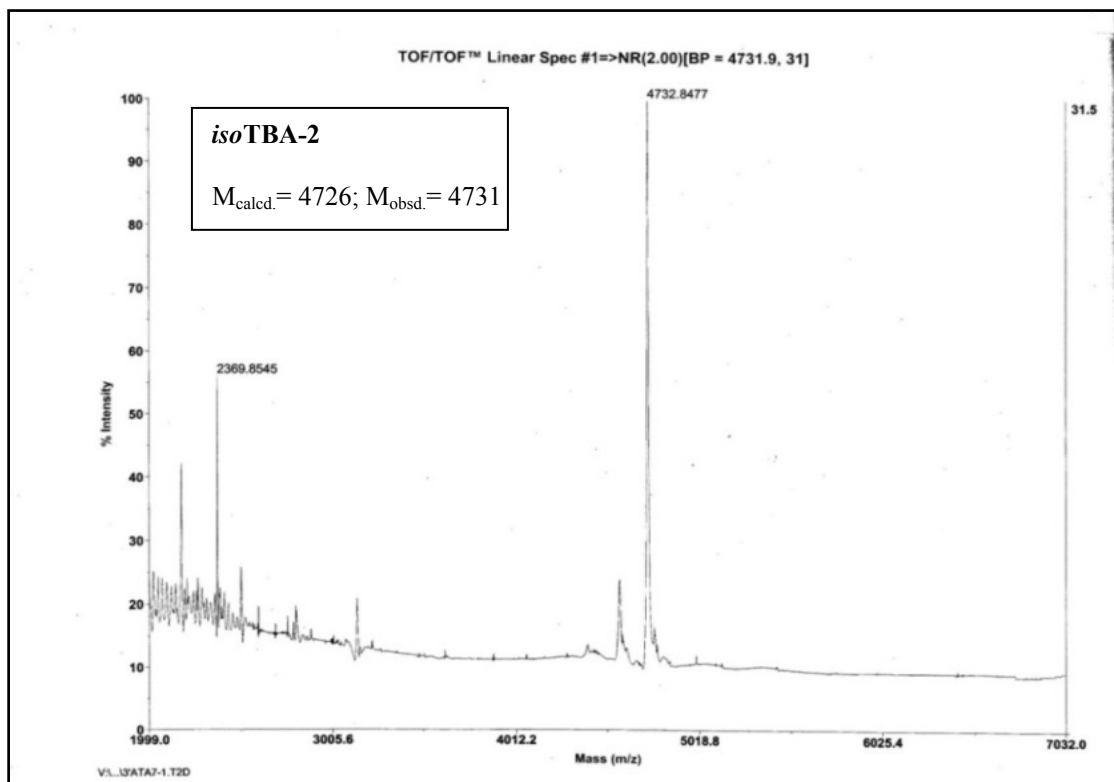
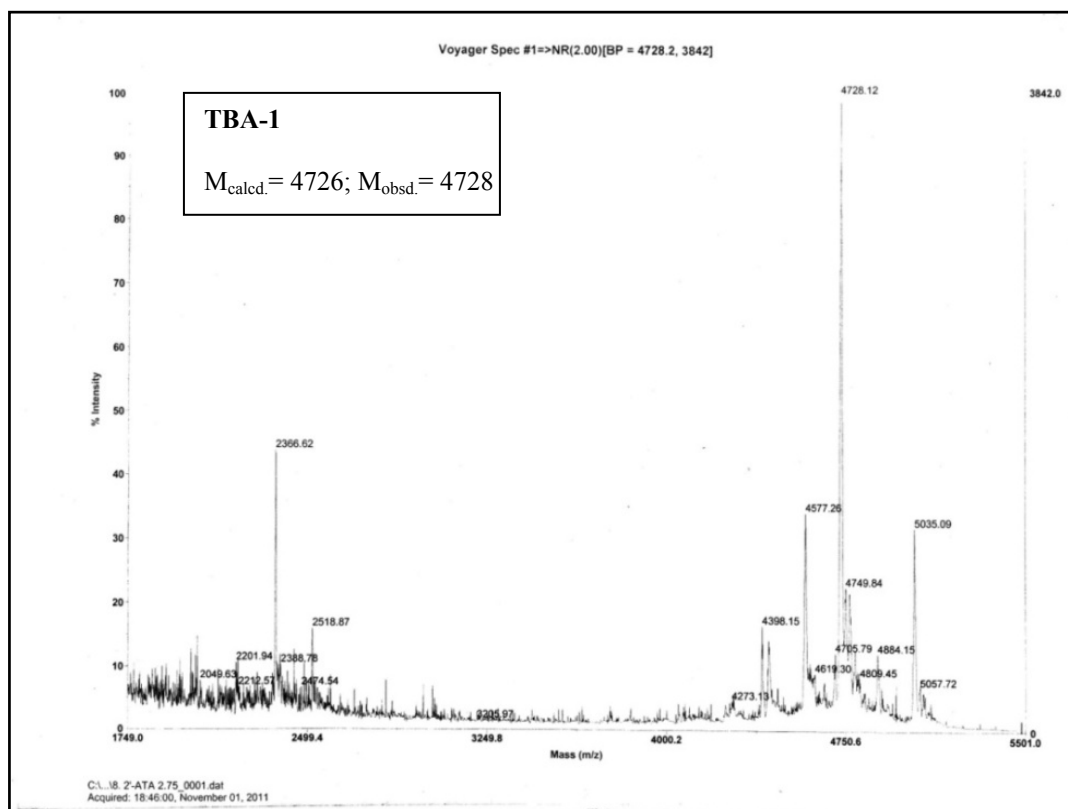
Pre-run: The set gel was rinsed with DI water to remove any excess of unpolymerised gel after the comb was removed. For a pre-run or blank run, the gel plate assembly was placed in the gel run chamber and completely immersed in the 1X TBE buffer. Each well was loaded with 2 μ l of the bromophenol blue dye in 40% sucrose solution(1:1). Then 200V voltage was applied and the gel run was carried out at 4°C for 1hour till the marker dye had travelled down and washed out along with any unpolymerised gel.

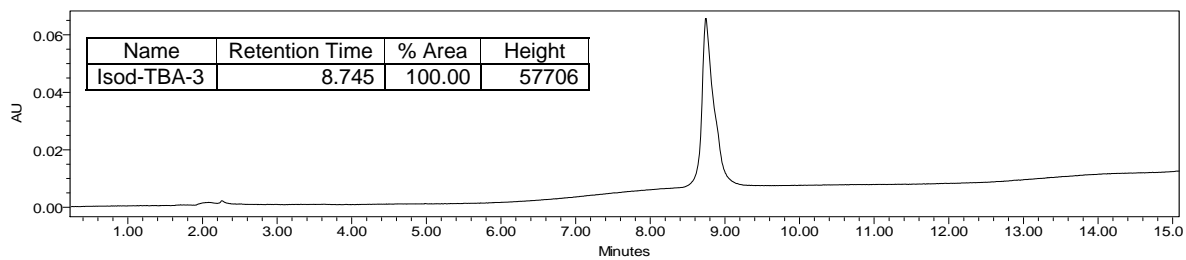
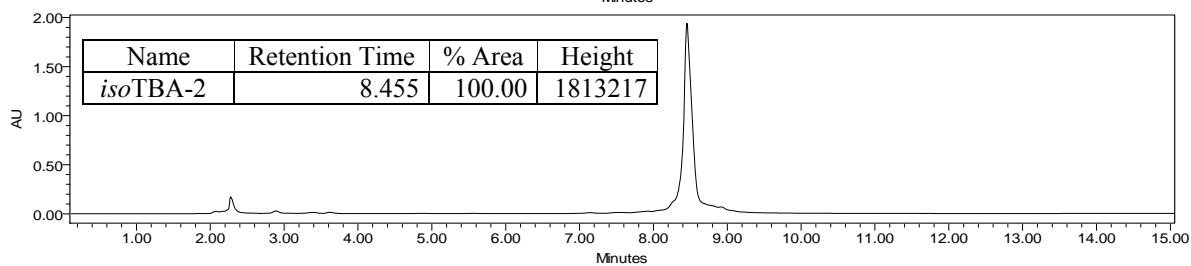
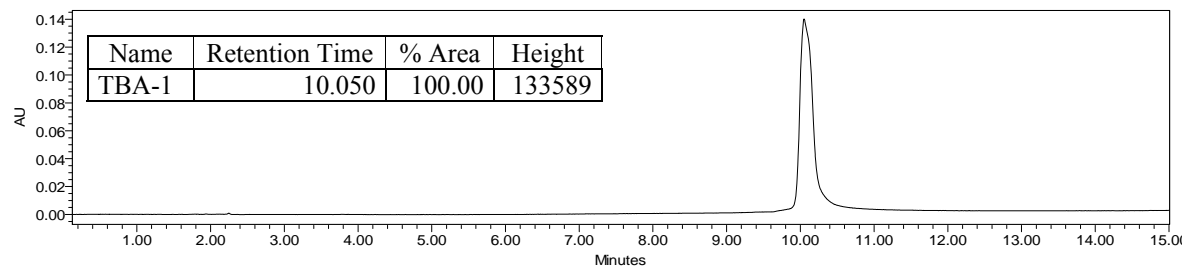
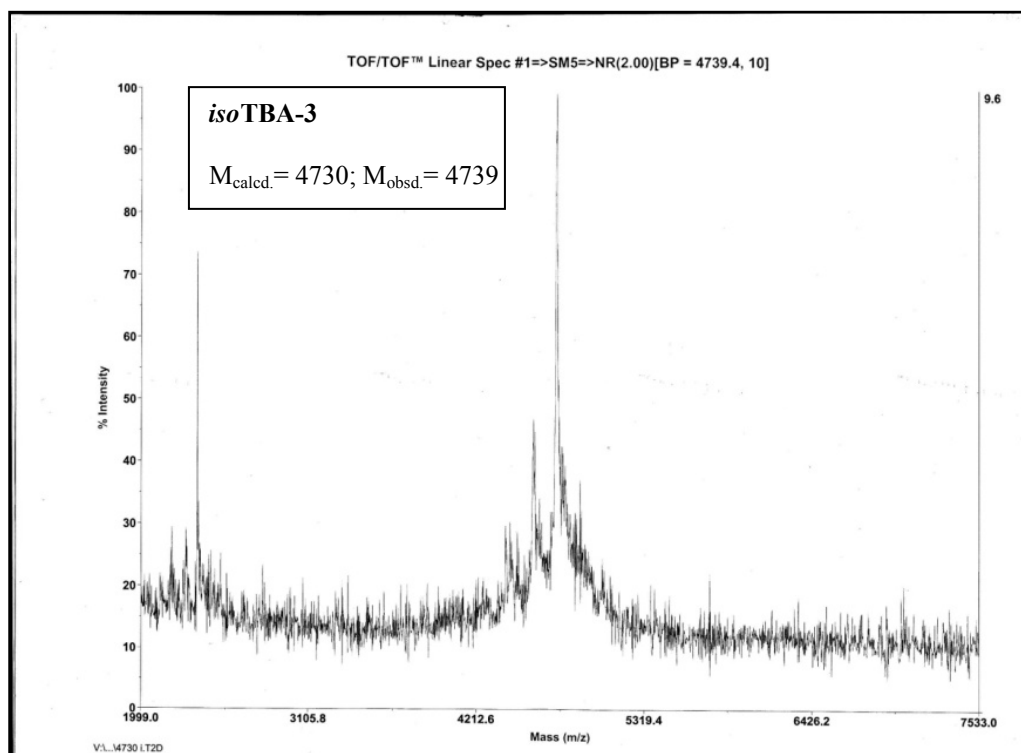
Sample run.: The DNA oligomer control and samples 2 μ l solution (350 μ mol concentration) were mixed with equal volume of the 40% sucrose solution and loaded into the appropriately numbered wells. The marker dye was loaded in the first and last wells to monitor the run. The gel was run with the voltage set at 250V for 30-40 minutes till the marker was visible at 3/4th the gel height.

Gel visualization: The gels after run were washed with DI water and then were visualized by UV-shadowing and ethidium bromide staining.

4.4 Appendix

Compound No.	Page No.
MALDI-ToF spectra of TBA-1	202
MALDI-ToF spectra of <i>iso</i> TBA-2	202
MALDI-ToF spectra of <i>iso</i> TBA-3	203
HPLC spectra of TBA-1	203
HPLC spectra of <i>iso</i> TBA-2	203
HPLC spectra of <i>iso</i> TBA-3	203





4.5 References

1. (a) Johnson, J.E., Smith, J.S., Kozak, M.L., Johnson, F.B., *Biochimie*, **2008**, *90*, 1250–1263. (b) Burge, S., Parkinson, G.N., Hazel, P., Todd, A.K., Neidle, S., *Nucleic Acids Res.*, **2006**, *34*, 5402–5415. (c) Siddiqui-Jain, A., Grand, C.L., Bearss, D.J., Hurley, L.H., *Proc. Natl Acad. Sci. USA*, **2002**, *99*, 11593–11598. (d) Huppert, J.L., Balasubramanian, S. *Nucleic Acids Res.*, **2005**, *33*, 2908–2916. (e) Xu, Y., Kaminaga, K., Komiyama, M., *J. Am. Chem. Soc.*, **2008**, *130*, 11179–11184. (f) Huppert, J.L., *Chem. Soc. Rev.*, **2009**, *37*, 1375–1384.
2. (a) Biffi, G., Tannahill, D., McCafferty, J., Balasubramanian, S., *Nat. Chem*, **2013**, *5*, 182–186. (b) Lam, E Yi Ni., Beraldi, D., Tannahill, D., Balasubramanian, S., *Nature Communications*, **2013**, *4*, article no:1796.
3. (a) Bates, P.J., Kahlon, J.B., Thomas, S.D., Trent, J.O., Miller, D.M., *J. Biol. Chem.*, **1999**, *274*, 26369–26377. (b) Mashima, T., Matsugami, A., Nishikawa, F., Nishikawa, S., Katahira, M., *Nucleic Acids Res.*, **2009**, *37*, 6249–6258. (c) Huppert, J.L., *Philos. Trans. Roy. Soc. Ser. A*, 2007, *365*, 2969–2984. (d) Balasubramanian, S., Neidle, S. *Curr. Opin. Chem. Biol.*, **2009**, *13*, 345–353. (e) Tian-miao, O., Yu-jing, L., Jia-heng, T., Zhi-shu, H., Kwok-Yin, W., Lian-quan, G., *Chem. Med. Chem.*, **2008**, *3*, 690–713.
4. (a) Hesselberth, J.; Robertson, M. P.; Jhaveri, S.; Ellington, A. D. *Rev. Mol. Biotechnol.* **2000**, *74*, 15-25. (b) Haller, A. A.; Sarnow, P. *Proc. Natl. Acad. Sci. U.S.A.* **1997**, *94*, 8521-6. (c) Gebhardt, K.; Shokraei, A.; Babaie, E.; Lindquist, B. H. *Biochemistry* 2000, *39*, 7255-65. (d) Wilson, D. S.; Keefe, A. D.; Szostak, J. W. *Proc. Natl. Acad. Sci. U.S.A.* **2001**, *98* (7), 3750-5. (e) Kawakami, J.; Imanaka, H.; Yokota, Y.; Sugimoto, N. *J. Inorg. Biochem.* **2000**, *82* (1-4), 197-206. (f) Brody, E. N.; Gold, L. *J. Mol. Biotechnol.*, **2000**, *74*, 5-13. (g) Keefe, A.D., Pai, S. and Ellington, A., *Nature Reviews, Drug Discovery*, **2010**, *9*, 537-550.
5. Bock, L. C., Griffin, L. C., Latham, J. A., Vermaas, E. H., Toole, J. J., *Nature*, **1992**, *355*, 564-566.
6. Gellert, M., Lipsett, M. N., Davies, D. R., *Proc. Natl. Acad. Sci., USA*, **1962**, *48*, 2013.

7. Roth, A., Harley, C.B., Baerlocher, G.M., *Recent Results Cancer Res.*, **2010**, *184*, 221-234
8. (a) Kankai, B. I.; Marky, L. A. *J. Am. Chem. Soc.* **2001**, *123*, 10799-10804, (b) Mao, X.A., Marky, L.A. and Gmeiner, W.H., *J. Biomol. Struct. Dyn.*, **2004**, *22*, 25, (c) X. Mao, X., Gmeiner, W.H., *Biophys. Chem.*, **2005**, *113*, 155. (d) Smirnov, I.V. and Shafer, R.H., *J. Mol. Biol.*, **2000**, *296*, 1. (e) Smirnov, I.V., Kotch, F.W., Pickering, I.J., Davis, J.T., Shafer, R.H., *Biochemistry*, **2002**, *41*, 12133. (f) Vairamani, M., Gross, M.L., *J. Am. Chem. Soc.*, **2003**, *125*, 42. (g) Wang, K.Y., Kumar, S., Pham, T.Q., Marathias, V.M., Swaminathan, S., Bolton, P. H. *J. Mol. Biol.*, **1996**, *260*, 378.
9. Trajkovski, M.; Šket, P.; Plavec, J. *Org. Biomol. Chem.* **2009**, *7*, 4677-4684.
10. De Rache, A.; Kejnovská, I.; Vorlíčková, M.; Buess-Herman, C. *Chem. Eur. J.* **2012**, *18*, 4392-4400.
11. Diculescu, V. G.; Chiorcea-Paquim, A.-M.; Eritja, R.; Oliveira-Brett, A. M. *J. Nucleic Acids* **2010**, *2010*, 841932.
12. Ellis, J. R. *Trends in Biochem. Sci.* **2001**, *26*, 597-604.
13. Tan, C.; Saurabh, S.; Bruchez, M. P.; Schwartz, R.; LeDuc, P. *Nat. Nanotech.* **2013**, *8*, 602-608.
14. Kan, Z.; Yao, Y.; Wang, P.; Li, X.; Hao, Y. Tan, Z. *Angew. Chem. Int. Ed. Engl.* **2006**, *45*, 1629-1632.
15. Nagatoishi, S.; Tanaka, Y.; Tsumoto, K. *Biochem. Biophys. Res. Commun.* **2007**, *352*, 812-817.
16. a) Arora, A.; Balasubramanian, C.; Kumar, N.; Agrawal, S.; Ojha, R. P.; Maiti, S. *FEBS J.* **2008**, *275*, 3971-3983, (b) Chen, Z.; Zheng, K. W.; Hao, Y. H.; Tan, Z. *J. Am. Chem. Soc.* **2009**, *131*, 10430-10438.
17. Agarwal, T.; Pradhan, D.; Géci, I.; El-Madani, A. M.; Petersen, M.; Pedersen, E. B.; Maiti, S. *Nucleic Acid Ther.* **2012**, *22*, 399-404.
18. Nimjee, S.M., Rusconi, C.P. and Sullenger, B.A., *Annu. Rev. Med.*, **2005**, *56*, 555-583.

- 19.(a) W. James in *Aptamers in Encyclopedia of Analytical Chemistry* (Ed.: R. A. Meyers), Wiley, Chichester, UK, **2000**, 4848-4871.; (b) *The Aptamer Handbook*. Edited by S. Klussmann. (2006) WILEY-VCH Verlag GmbH & Co. KGaA, Weinheim.
20. Ellington, A. D.; Szostak, J. W. *Nature* **1990**, *346*, 818-822.
21. Robertson, D. L.; Joyce, G. F. *Nature* **1990**, *344*, 467-468.
22. Tuerk, C. Gold, L. *Science* **1990**, *249*, 505-510.
- 23.(a) Klussmann, S.; Nolte, A.; Bald, R.; Erdmann, V. A.; Fuerste, J. P. *Nature Biotechnology* **1996**, *14*, 1112., (b) Nolte, A., Klussmann, S., Bald, R., Erdmann, V. A., Fuerste, J. P., *Nature Biotechnology* **1996**, *14*, 1116.
24. Vater, A.; Sell, S.; Kaczmarek, P.; Maasch, C.; Buchner, K.; Pruszyńska-Oszmialek, E.; Kolodziejcki, P.; Purschke, W. G.; Nowak, K. W.; Strowski, M. Z.; Klussmann, S. *J. Biol. Chem.* **2013**, *288*, 21136-21147.
25. Eulberg, D.; Klussmann, S. *ChemBioChem.* **2003**, *4*, 979-983.
26. Coughlin, S. R., *Nature*, **2000**, *407*, 258-64.
27. Griffin, L. C., Tidmarsh, G. F., Bock, L. C., Toole, J. J., Leung, L. K., *Blood*, **1993**, *81*, 3271-76.
28. DeAnda Jr., A., Coutre, S. E., Moon, M. R., Vial, C. M., Griffin, L. C., Law, V. S., Komeda, M., Leung, L. L., Miller, D. C., *Ann. Thorac. Surg.*, **1994**, *58*, 344-350.
29. Wang, K. Y.; McCurdy, S.; Shea, R. G.; Swaminathan, S.; Bolton, P. H. *Biochemistry* **1993**, *32*, 1899-1904.
30. Schultze, P., Macaya, R. F., Feigon, J., *J. Mol. Biol.*, **1994**, *235*, 1532-1547.
31. Macaya, R. F., Schultze, P., Smith, F. W., Roe, J. A., Feigon, J., *Proc. Natl. Acad. Sci. USA.*, **1993**, *90*, 3745.
32. Pasternak, A., Hernandez, F. J., Rasmussen, L. M., Vester, B., Wengel, J., *Nucleic Acids Res.*, **2010**, *39*, 1155-1164.
33. Bonifacio, L., Church, F. C., Jarstfer, M. B., *Int. J. Mol. Sci.*, **2008**, *9*, 422-433.
34. Aviñó, A., Mazzini, S., Ferreira, R., Gargallo, R., Marquez, V. E., Eritja, R., *Bioorg. Med. Chem.*, **2012**, *20*, 4186-4193.
35. Zaitseva, M., Kaluzhny, D., Shchyolkina, A., Borisova, O., Smirnov, I., Pozmogova, G., *Biophys. Chem.*, **2010**, *146*, 1-6.

36. He, G.-X., Williams, J.P., Postich, M.J., Swaminathan, S., Shea, R.C., Terhorst, T., Law, V.S., Mao, C.T., Seouka, C., Coutré, S., Bischofberger, N., *J. Med. Chem.*, **1998**, *41*, 4224-4231.
37. (a) Shaw, J.-P., Fishback, J. A., Cundy, K. C., Lee, W. A., *Pharm. Res.*, **1995**, *12*, 1937-1942, (b) Lee, W. A., Fishback, J. A., Shaw, J.-P., Bock, L. C., Griffin, L.C., Cundy, K. C., *Pharm. Res.*, **1995**, *12*, 1943-1947.
38. (a) Loke, S. L., Stein, C. A., Zhang, X. H., Mori, K., Nakanishi, M., Subasinghe, C., Cohen, J. S.; Neckers, L. M., *Proc. Natl. Acad. Sci. U.S.A.*, **1989**, *86*, 3474-3478. (b) Yakubov, L. A., Deeva, E. A., Zarytova, V. F., Ivanova, E. M., RYTE, A. S., Yurchenko, L. V., Vlassov, V. V., *Proc. Natl. Acad. Sci. U.S.A.*, **1989**, *86*, 6454-6458.
39. Beck, G. F., Irwin, W. J., Nicklin, P. L., Akhtar, S., *Pharm. Res.*, **1996**, *13*, 1028-1036.
40. Mendelboum Raviv, S., Horváth, A., Aradi, J., Bagoly, Z., Fazakas, F., Batta, Z., Muszbek, L., Hársfalvi, J., *J. Thromb. Haemostasis*, **2008**, *6*, 1764-1771.
41. Nallagatla, S. R., Heuberger, B., Haque, A., Switzer, C., *J. Comb. Chem.*, **2009**, *11*, 364-369.
42. (a) Martino, L., Vimo, A., Randazzo, A., Virgilio, A., Esposito, V., Giancola, C., Bucci, M., Cirino, G., Mayol, L., *Nucleic Acids Res.*, **2006**, *34*, 6653-6662, (b) Pagano, B., Martion, A., Randazzo, A., Giancola, C., *Biochem. J.*, **2008**, *94*, 562-569.
43. Joachimi, A., Benz, A., Hartig, J. S., *Bioorg. Med. Chem.*, **2009**, *17*, 6811-6815.
44. Tang, C-F., Shafer, R. H. *J. Am. Chem. Soc.*, **2006**, *128*, 5966-5973.
45. Jeter, M.L., Ly, Linda V., Fortenberry, Y, M., Whinna, H. C., White, R. R., Rusconi, C. P., Sullenger, Bruce A., Church, F. C., *FEBS Letters*, **2004** *568*, 10-14.
46. White, R., Rusconi, C., Scardino, E., Wolberg, A., Lawson, J. Hoffman, M., Sullenger, B. *Mol. Ther.*, **2001**, *4*, 567-573.
47. Yu, H., Zhang, S., Chaput J. C., *Nature Chemistry*, **2012** *4*, 183-187.
48. (a) Usher, D. A., McHale, A. H., *Proc. Natl. Acad. Sci. USA*, **1976** *73*, 1149-53, (b) Sheppard, T. L., Breslow, R. C., *J. Am. Chem. Soc.*, **1996**, *118*, 9810-9811. c) Prakash, T. P., Jung K.-E., Switzer, C. *Chem. Commun.*, **1996**, 1793. d) Jung K.-E. and C. Switzer, *J. Am. Chem. Soc.*, **1994**, *116*, 6059-6061.
49. Prakash, T. P., Roberts, C., Switzer, C., *Angew. Chem. Int. Ed. Engl.*, **1997**, *36*, 1522-1523.

50. Polak, M., Manoharan, M., Inamati, G. B., Plavec, J. *Nucleic Acids Res.*, **2003**, *31*, 2066-2076.
51. Premraj, B. J., Raja, S., Bhavesh, N. S., Shi, K., Hosur, R. V., Sundaralingam, M., Yathindra, N., *Eur. J. Biochemistry*, **2004**, *271*, 2956-2966.
52. Wodak, S. Y., Liu, M. Y., Wyckoff, H. W., *J. Mol. Biol.*, **1977**, *116*, 855-875.
53. Kumar, A., Katti, S. B., Rosemeyer, H., Seela, F., *Nucleosides and Nucleotides*, **1996**, *15*, 1595-1601.
54. Hannoush R. N., Damha M. J., *J. Am. Chem. Soc.*, **2001**, *123*, 12368-12374.
55. Erande, N., Gunjal, A. D., Fernandes, M., Gonnade R., Kumar V. A., *Org. Biomol. Chem.*, **2013**, *11*, 746-757 (2013).
56. (a) Avino, A., Fabrega, C., Tintore, M., Eritja, R., *Current Pharmaceutical Design*, **2012**, *18*, 2036-2047. (b) Tucker, W.O., Shum K.T. and Tanner, J.A., *Current Pharmaceutical Design*, **2012**, *18*, 2014-2026.
57. Krauss, I. R., Merlino, A., Randazzo, A., Novellino, E., Lelio M., Sica F. *Nucleic Acids Res.*, **2012**, *40*, 8119- 8128.
58. Karsisiotis, A. I., Hessari, N. M., Novellino, E., Spada, G. P., Randazzo, A., da Silva M. W., *Angew. Chem. Int. Ed.*, **2011**, *50*, 10645 –10648.
59. Dao, N. T.; Haselsberger, R.; Michel-Beyerle, M.-E.; Phan, A. T. *FEBS Lett.*, **2011**, *585*, 3969-3977.
60. Mergny, J.-L.; Li, J.; Lacroix, L.; Amrane, S.; Chaires, J. B. *Nucleic Acids Res.* **2005**, *33*, e138.
61. Mergny, J.-L.; Phan, A. T.; Lacroix, L. 1998, *FEBS Lett.* **1998**, *435*, 74-78.
62. Zimmerman, S.B. and Trach, S.O., *J.Mol. Biol.*, **1991**, *222*, 599-620.
63. Baldrich E., O'Sullivan, C. K., *Analytical Biochemistry.*, **2005**, *341*, 194–197.
64. Kankia, B.I., Marky, L.A., *J.Am.Chem.Soc.*, **2001**, *123*, 10799-10804.
65. (a) Mondragón-Sánchez, J.A., Liquier, J., Shafer, R.H., Taillandier, E., *J. Biomol. Struct. Dyn.*, **2004**, *22*, 365-373.
66. Uehara, S., Shimada, N., Takeda, Y., Koyama, Y., Takei, Y., Ando, H., Satoh, S., Uno, A., Sakurai K. *Bull. Chem. Soc. Jpn.*, **2008**, *81*, 1485–1491.
67. Collie, G.W. and Parkinson, G.N., *Chem.Soc.Rev.*, **2011**, *40*, 5867-5892.